On advanced daylighting simulations and integrated performance assessment of complex fenestration systems for sunny climates

THÈSE N^{O} 6425 (2014)

PRÉSENTÉE LE 27 NOVEMBRE 2014

À LA FACULTÉ DE L'ENVIRONNEMENT NATUREL, ARCHITECTURAL ET CONSTRUIT
LABORATOIRE D'ÉNERGIE SOLAIRE ET PHYSIQUE DU BÂTIMENT
PROGRAMME DOCTORAL EN GÉNIE CIVIL ET ENVIRONNEMENT

ÉCOLE POLYTECHNIQUE FÉDÉRALE DE LAUSANNE

POUR L'OBTENTION DU GRADE DE DOCTEUR ÈS SCIENCES

PAR

Chantal BASURTO DÁVILA

acceptée sur proposition du jury:

Prof. A. Berne, président du jury
Prof. J.-L. Scartezzini, Dr J. H. Kämpf, directeurs de thèse
Prof. M. Bodart, rapporteuse
Prof. R. Compagnon, rapporteur
Dr S. Hostettler, rapporteuse

ÉCOLE POLYTECHNIQUE
FÉDÉRALE DE LAUSANNE

Suisse
2014

The best way to light a house, is God's way.

-Frank Lloyd Wright-

To my sister Lupita, you are always in my mind.

Acknowledgements

First of all, I want to thank my family for their support during the long process that the fulfilment of such project represents. I have a special gratitude to my parents Félix and Teresa for their unbreakable trust and strength which have always given me that extra energy when is needed. To my brother Ricardo, which leadership and intelligence has always been an example for me, and for his invaluable advice and help especially at the beginning and end of this thesis. A special thought to my grandmother who turns 100 years old this year.

I would like to express my gratitude to the Consejo Nacional de Ciencia y Tecnologia (CONACYT) in México for granted me with a scholarship during the four years of my PhD studies. I would like to thank as well to the Swiss Federal Office of Energy (SFOE) and to the Velux Foundation for providing the additional financial support for the fulfilment of this Thesis.

Thanks to Professor Scartezzini, for giving me the opportunity of being part of LESO-PB in the first place, for his trust and guidance during the process and his invaluable support at the end of my studies. I would like to express my very great appreciation to Dr. Jérôme Kämpf for taking in charge the co-direction of this thesis, for the unconditional way of sharing his knowledge and his unique friendly way of being strict; likewise for the enjoyable working environment he creates. Thanks to Dr. Mirjam Münch for the time and knowledge shared while the completion of one of the studies part of this work, as well to Dr. Bernard Paule for his invaluable advice.

I want to thank to my thesis committee for accepting being part of the jury, Dr.Prof. Raphäel Compagnon, to Dr.Prof. Magali Bodart, Dr.Sc. Silvia Hostettler and to the President of the Jury Dr. Prof. Alexis Berne.

This work could not have been possible without the approval of the responsible authorities in both Universities in México, who let me spend long days in their offices taking measurements, pictures, and so on. Thanks to Ing. Efren Mazatàn, director of academic services in the ITESM campus Zacatecas where the office room (Building B1) is located, as well to Lic. Mirella Mireles, responsible of the library, and colleagues for their cooperation. In Building B2: the Autonomous University of Zacatecas (UAZ); thanks to the director of the Institution Dr. Raul Delgado Wise, and very special thanks to the personnel in this building for their unconditional help beyond any expectations, to the secretary Mrs. Olivia and to Don Héctor who was always around whenever I need, and of course to all the staff and security guys in both buildings who were also always available to help.

Thanks to Eng. Julien Tharin for his work with the gonio-photometer; to Dr. Anothai Tanachareonkit for allowing us using part of her thesis work, to Pierre Loesch for his help with the luxmeters, thanks to Laurent Deschamps and IT colleagues for their support during these years. My special thanks are extended to Barbara Smith and Suzanne L'epplatanier for their unvaluable support and eternal smiles.

I am particularly grateful for the assistance given by the RADIANCE community, online and in the workshops, of course to Dr. Greg Ward, Dr. Andrew McNeal who provide immense distance-help with the XML files, Dr. German Molina, Lars O. Grobe and Dr. David Geisler-Moroder who kindly replied many of my questions. I acknowledge the contribution of Carsten Bauer during the workshop 2012 which advice led to the implementation of one of the studies part of this thesis.

Thanks also due to Dr. Ian Edmonds, Dr. Helmut Müller and B.Sc. Pauline Ludwig for providing further information regarding the Complex Fenestration Systems employed in this Thesis.

To all my LESO friends and colleagues, who some of us have recognized as family, for their help and support but overall for filling the Lab with the warmth atmosphere of their friendship, charm and joy. Thanks to Dr. Apiparn Borisuit for her help with the measurements in the experimental modules and general support over the years, to Olivia Bouvard for her help in the correction of the Résumé. To those who left too early: Raquel P.Gagliano, Maria Papadopoulou, Marja Edelman, Lenka Maierova. Half way: Urs Wilke, Vahid Nik, Diane Perez. And those who stayed until the end: Nikos Zarkadis, Silvia Coccolo, Govinda Upadhyay, Nahid Mohajeri, Antonio Paone, André Kostro, Stefan Mertin, Andreas Schueler, Dasaraden Mauree. Thanks to all of you who shared the time in LESO with me.

Very special thanks to my lecturers of the Master Programme in Wismar Germany for their academical support and encouraging, Prof. Dr. Thomas Römhild, Prof. Dr. Detlev Gerich, B.A. Annuka Larsen. I owe my gratitude to Arch. Marcus Patton and Arch. John Gilbert for their orientation and words back in 2005. Additional thanks to Arch. J. Tamés y Batta in the UNAM for his availability to use his office during the planning stage of this thesis project.

Lastly, I would like to give a very special mention to five special people, without whom I couldn't have even start this trip. Fist, to Daniele Capodicasa for his unconditional support; to Enrique Cedeno, Beatriz Leon, Thamal Udamulla and Irina Shuta, who were there in the right place at the right moment in such a benevolent way, Thank you!

Lausanne, 12th October 2014

Abstract

The inclusion of daylight in buildings represents several benefits: its use not only signifies a reduction in the building energy consumption through the compensation of electric lighting, it also has positive effects in the execution of human activities. Through its spectral composition, it contributes to create a better interior atmosphere for visual comfort, leading to a better performance on working tasks. It also influences biological human cycles, which has an impact on human alertness, mood and well-being. Compared with electric light, its intensity and dynamic variations have a stimulating effect by providing a connection with the exterior environment.

However, for buildings located at low latitudes (between 23°N and S), the inclusion of daylight implies the admission of sunrays, which affect the visual comfort and perception of the indoor environment by altering the interior luminance distribution increasing the risk of glare. An additional unfavourable effect is the increment of the interior thermal loads which represent a risk of overheating for the occupants. In those regions, common practices such as: the reduction of the window size, the use of tinted glazing and solar protection are usually applied to buildings in the search of overcoming such problems. However, the use of such strategies also implies a reduction of the admission of daylight inducing the use of electric light, which is incongruent in countries with large amounts of this natural resource. The use of Complex Fenestration Systems (CFS) may represent a solution given their characteristics: daylight redirection and direct solar rays protection. The latter would contribute to control the admission of solar gains while maintaining a good visual interior environment. However, the appropriate selection of CFS requires a careful evaluation of their features and performance regarding their suitability to the building location.

This thesis explores the potentiality of using CFS to improve the interior daylight distribution in buildings located at low latitudes while maintaining a satisfactory visual and thermal interior environment for the occupants. In order to do this, the existing daylight situation of two office rooms located in the central-north of México (Zacatecas 22° 783' N., 102° 583' W, Altitude: 2543m) were monitored from 2011 to 2013. Illuminance and luminance were measured on periods of the year that are crucial for the interior luminous environment (summer and winter solstices together with spring equinox), in order to characterize the existing daylighting situation and to study the dispersion of results obtained using a virtual model which reproduces the features of both offices.

The performance of five CFS was then tested using computer simulations in order to assess their suitability to the local sky conditions. For this, three main factors were taken into account: the improvement of the interior daylight distribution, the risk of glare and overheating. The effects of the CFS in a room regarding such conditions were simulated using RADIANCE and Energy Plus using BTDF data (Bidirectional Transmission Distribution Function that characterizes the CFS's lighting transmission properties) assessed by the use of a gonio-photometer. The assessment was performed first during the winter and summer solstices as well as spring equinox and secondly then on annual basis. The latter was done in order to take into account the daylight variation characteristics of two locations with prevailing clear sky conditions. The results obtained allow determining the CFS that better contributes to a better interior luminous environment in each building without compromising the thermal and visual comfort of the occupants.

Keywords

Daylight, Daylighting Optimization Strategies, Complex Fenestration Systems, Building Performance Simulation, Radiance and EnergyPlus, Bidirectional Transmission Distribution Function, Thermal Comfort, Visual Comfort.

Résumé

L'utilisation de la lumière naturelle dans les bâtiments représente des avantages connus. Son utilisation signifie une réduction de la consommation d'énergie finale à travers la compensation de l'énergie électrique, elle a aussi des effets positifs dans l'exécution des activités humaines. A travers sa composition spectrale elle contribue à créer une meilleure atmosphère intérieure pour le confort visuel, conduisant à une meilleure performance des activités de travail. Son utilisation a aussi une influence dans les cycles biologiques humains, ayant un impact sur l'attention l'humeur et le bien-être. Comparé avec la lumière artificielle, son intensité et variations dynamiques ont un effet stimulant du fait de leur connexion avec l'environnement extérieur.

Cependant, dans les bâtiments qui sont situés en basses latitudes (entre 23°N et S) l'inclusion de la lumière naturelle signifie l'admission des rayons du soleil, qui affecte le confort visuel et la perception de l'environnement intérieur en modifient la distribution intérieur de la luminance ce qui augmente le risque d'éblouissement. L'autre effet défavorable est l'augmentation des charges thermiques internes qui représentent un risque de surchauffe pour les occupants. Dans ces régions, les pratiques courantes afin de surmonter ces problèmes sont la réduction de la taille de la fenêtre, l'utilisation de vitrages teintés ou d'éléments de protection solaire. En revanche, de telles stratégies signifient aussi la réduction de l'admission de la lumière naturelle impliquant l'utilisation de la lumière artificielle, ce qui est incohérent dans les pays disposant de cette ressource naturelle en grande quantité. L'utilisation des systèmes de fenêtrage complexes (acronyme CFS) pourrait représenter une solution grâce à ses caractéristiques : la redirection de la lumière et la protection des rayons solaires directs. Le dernier, pourrait contribuer à contrôler l'admission des gains solaires en gardant un bon environnement visuel intérieur. Cependant, le choix de CFS exige une évaluation minutieuse de leurs propriétés et performances pour déterminer de sa pertinence en fonction de l'emplacement du bâtiment.

Cette thèse examine la possibilité d'utiliser CFS pour ameliorer la distribution interior de la lumiere naturelle dans les bâtiments situes en basses latitudes tout en conservant un environnement intérieure visuelle et thermique confortable comfortable pour les occupants. Pour ce faire, la situation existante de deux bureaux situés au centre-nord du Mexique (Zacatecas 22° 783' N., 102° 583' W, Altitude: 2543m) a été étudiée de 2011 à 2013. Les niveaux d'éclairement et de luminance ont étés mesurés durant des périodes de l'année qui sont décisives pour les niveaux d'éclairage intérieur (solstice d'été, hiver et l'équinoxe de printemps) avec l'objectif de caractériser la situation existante de la lumière naturelle intérieure et de faire calibrer un modèle virtuel qui reproduit les caractéristiques de ces deux bureaux. La performance de cinq CFS a été testée en utilisant la simulation par ordinateur pour évaluer leur aptitude par rapport aux conditions du ciel local. Trois facteurs principaux ont été pris en compte: l'amélioration de la distribution intérieure de la lumière, l'augmentation du risque d'éblouissement et celui de surchauffe. Les effets des CFS dans un bureau par rapport à ces conditions ont êtes simulés en utilisant RADIANCE et Energy Plus avec l'utilisation de BTDF data (Bidirectional Transmission Distribution Function). Qui évalué avec l'utilisation d'un gonio-photomètre, caractérise les propretés lumineuses des CFS. L'évaluation a d'abord été effectuée durant l'équinoxe de printemps et les solstices d'hiver et été, puis en base annuelle. Le dernier était fait pour prendre en compte les variations de la lumière naturelle qui caractérisent les emplacements avec une prédominance de conditions de ciel clair. Les résultats obtenus permettrait de déterminer le CFS qui contribue le mieux à fournir une ambiance intérieure lumineuse sans compromettre le confort thermique et visuel des occupants.

Mots-clés

Lumière naturelle, Stratégies d'optimisation de la lumière naturelle, Systèmes complexes de fenêtrage (CFS), simulation de performance énergétique des bâtiments, Radiance, Energy Plus, Bidirectional Transmission Distribution Function, Confort Thermique, Confort Visuel.

Contents

List of Figures

List of Tables

Chapter 1 Introduction

Sun and architecture in the ancient times in México

The sun was an important element in the ancient worlds in the Mesoamerican region (Pre-Columbian societies extended from central México to northern Costa Rica). In Ancient México, the Aztecs (Post-Classic period c. VIII to XVI) studied acutely astronomy and meteorology and used the calendar to facilitate their farming, but the sun also held a religious and mythical meaning; they believed in the sun as the leader of heaven, for them the sequence of day and night represented the defeat of the night by the sun. In Aztec cosmology the ages were determined by suns, which final was marked by cataclysms, they believed that the history of the universe was ruled by principles taking turns in an alternated way [1]. The calendar stipulates that the world collapsed four times: the first sun was destroyed by tigers, the second sun was destroyed by a hurricane, the third sun was destroyed by rain and fire and the fourth sun was destroyed by a flood; at the end of the fourth sun it is believed that the Aztecs gods gather to create a new age to put the sun in motion and start the history of the new era, which would require the sacrifice of one of them. That fifth sun began the ancient city of Teotihuacan (600-150 B.C.) which means 'the place where gods were born' and that is characterized by monumental pyramidal structures with symbolic meaning from which the largest one is dedicated to the Sun [2]. The city of Teotihuacan is astronomically aligned; the front wall of the Sun's Pyramid is exactly perpendicular to the point on the horizon where the sun sets on the equinoxes. An aerial view of Teotihuacan is shown in Figure 1.1.

Figure 1.1 Aerial view of the sun's pyramid in Teotihuacan, México.

The Mayans (Pre-Classic period c. 2000 BC to AD 250) were astronomers; they used the sky as a method of measuring the passage of time, to benefit the agriculture and as a religious aspect that derived into astrology. For them, the movement of constellations and other objects across the sky represented a connection between celestial and human events. The Mayans conception of the universe was multi-layered, where the earth lay between thirteen levels of heavens and nine layers of the underworld. The first layer would be water (the oceans), the next would be moon and clouds, then stars, the fourth is the sun (Tonatiuh), then Venus, then the comets, winds and storms, the blue heaven is in the eight layer, thunder is nine, ten, eleven and twelve is white, yellow and red respectively and finally the 13^{th} layer where the dual (male-female) creator lives. K'iin is a Mayan word that means equally: day, sun and time. For the Mayans, the most important aspect in the sky was the sun, recognized as the life giver on earth.

Many Mayan buildings are aligned to correspond to astronomical events, one good example is the pyramid Chichen-Itza or recognized as 'El Castillo' (the castle). It was dedicated to the god Kukulkan (Quetzalcoatl or the feathered serpent). The temple has 365 steps (one for each day of the year), in the spring and autumn equinoxes while the sun goes down, the shadow of the pyramid step's creates a visual effect in the shape of a serpent, as the sun sets it descends to eventually join the head of the serpent made of stone at the base of the pyramid, as shown on Figure 1.2 where it can be seen the event of the descending serpent is accomplished [2, 3].

Figure 1.2 The pyramid of Chichen Itza, showing the accomplished event of the 'descending serpent' occuring during the Equinoxes.

Sun and architecture in modern times in México

The mythic and religious meaning of the sun was dissipated during the time of the Spanish Colony. Today, the main significance of the sun is as a source of energy and it's translated socially mainly through its interaction with architecture. The latter, varies in form depending on the region, in the center and north of México, the architecture is highly representative of the period of its construction (Colonial Period and Spanish Baroque), and responds functionally to the requirements of the environment by presenting different characteristics, such as: a reduced size of windows for the protection of a warm exterior environment as it can be the north state of Nuevo León (Figure 1.3), with arcades or galleries for sun and rain protection for the central and northern regions (Zacatecas, Guanajuato, San Luis Potosi, Sonora) which examples are shown in Figure 1.4; deep walls and interior wood fins in the center and northern regions; as well as modern elements for solar protection as is shown in Figure 1.5; for the southern and pacific regions such as Michoacán and Puerto Vallarta, the vernacular architecture presents different characteristics such as slopped roofs and overhangs (Figure 1.6).

Figure 1.3 Windows; Nuevo Leon, México

Figure 1.4 Arcades; Nochistlàn, Zacatecas (left) and Alamos, Sonora (right)

Figure 1.5 Solar shading in historical buildings in Puebla, Méx

Figure 1.6 Overhangs, Pàtzcuaro Michoacan (left), Puerto Vallarta (right).

1.1 Context

The sun as an energy resource

Solar energy is a costless, abundant resource that can be exploited to satisfy human needs through the use of active or passive technologies. Active solar systems refer to the use of photovoltaic or solar thermal collectors; their use implies the use of mechanical equipment to collect heat or produce electricity. Passive use of the sun's energy refers to the collection and transport of light and heat by natural means such as radiation, conduction and natural convection with the objective of heating and illuminating buildings [4].

The availability and intensity of this natural resource varies crosswise the earth depending on several factors. First, the angle between the sun and earth is inconstant due to the orbit's elliptic shape, thus the elevation of the sun varies according to locations. In the same way, the earth's surface covered by the incident solar irradiance varies according to the earth's axial tilt, which in view of its daily rotation leads to periodic variations of solar global irradiance and daylight hours [5]. The solar constant outside of the earth's atmosphere in the form of direct irradiance is 1396 W/m^2; while passing through the atmosphere, a fraction remains in the form of direct radiation while the rest is altered by scattering and absorption. About 35% is reflected back into the space while another portion is propagated in a scattered way reaching the earth in the form of diffuse radiation; air molecules, water vapor, carbon dioxide and ozone absorb 10-15%. Then, additional variations across the regions are mainly due to the effect of clouds and water vapor due to their dissimilar and changeable distribution [4].

A graphical representation of the solar irradiance distribution before and after reaching the earth is shown in Figure 1.7, where the effect of the atmosphere on the solar irradiance at the earth surface (right) can be compared with that occurring at the top of the atmosphere (left) [5].

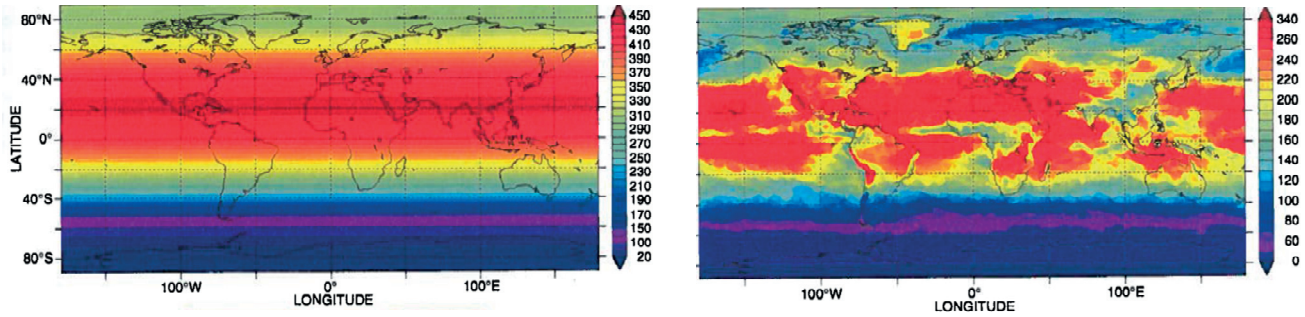

Figure 1.7 The effect of the atmosphere on the distribution of the global solar irradiance at the earth's surface (right) compared with that at the top of the atmosphere (left). The data represents monthly mean of August 2009 (W/m2) [5].

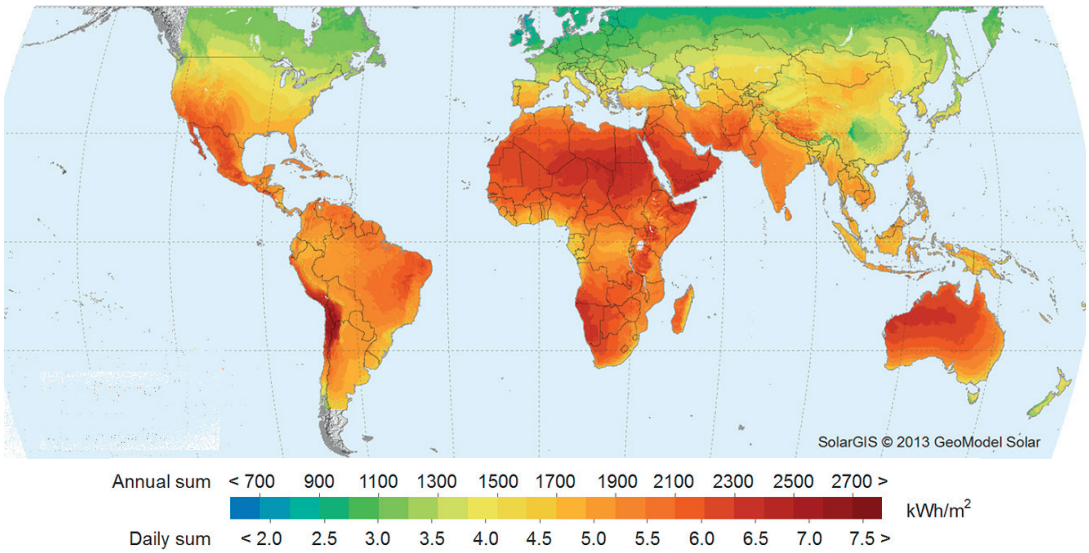

Figure 1.8 Global Horizontal Irradiation, which represents an annual and daily long term average [6].

In México, assessments of solar energy have been implemented since 1990, mainly with the use of pyranometers and piranographs, as well as using satellite for radiation mapping [7]. These assessments of hourly radiation levels over the Mexican territory show that the region counts with huge solar energy resources, especially in the north-west areas near the tropic of cancer (Chihuahua and Sonora) [8]. Measurements of Global Horizontal Irradiation show that this region receives a maximum of 30 MJ/m² during the summer time. Another zone receiving high levels of direct normal irradiation is located in the centre-north (Durango and Zacatecas), which receives about 28-30 MJ/ m² from February to May.

The annual average solar irradiation in México corresponds to 5.2 kWh/m²/day. To provide a reference point, the Sahara Desert counts with 6.2 kWh/m² solar resources, while Germany receives 2.4 kWh/m²/day [9]. A global map illustrating this data is presented in Figure 1.8, where red represents the highest irradiation levels and blue depicts the lowest levels. Figure 1.9 depicts the annual number of clear sky days around the world; clearly, an extensive part of the Mexican territory has a high annual number of clear sky days [10]. Average annual Global Horizontal Irradiation (kWh/m²) in Mexico (left, 1999-2012) and Switzerland (right, 2004-2010) are shown in Figure 1.10 [11].

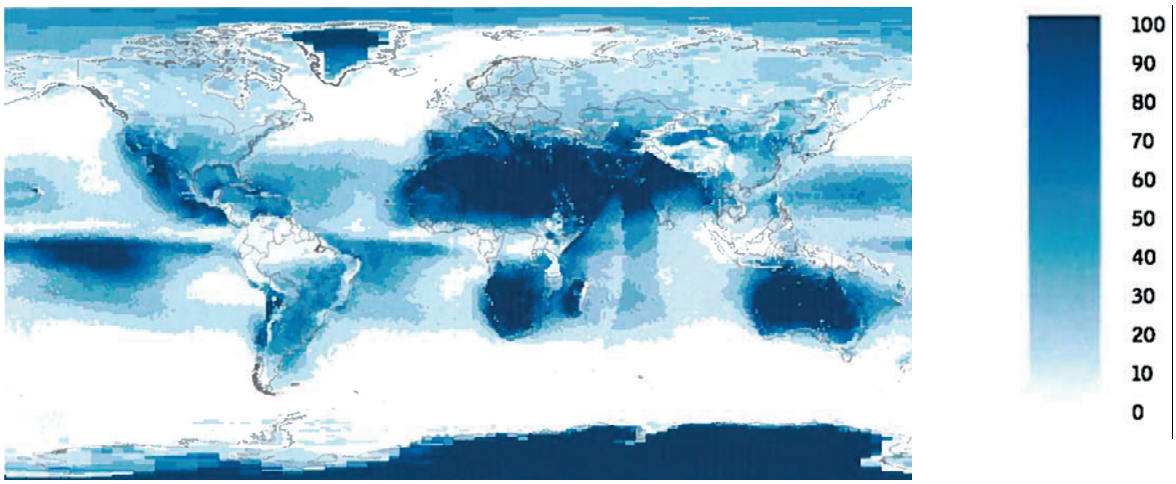

Figure 1.9 Annual number of clear sky days, showing higher number of clear sky days with a darker blue color [10].

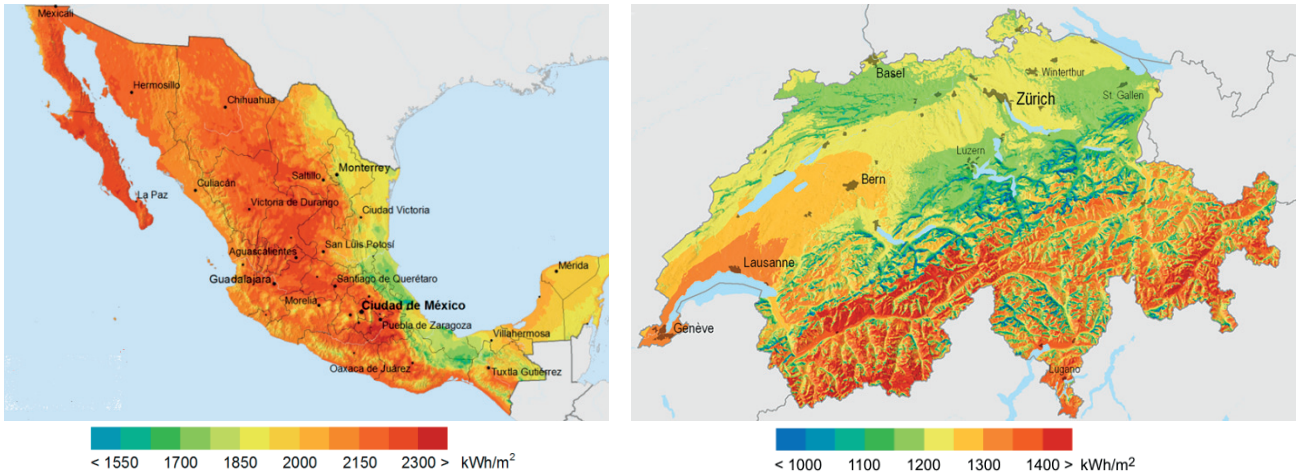

Figure 1.10 Global Horizontal Irradiance (kWh/m²) showing the comparison between those received in México (left) and Switzerland (right) [6].

Despite of the extensive availability of solar energy in México, this resource has been insufficiently exploited, although there has been some progress in recent years. For instance, the installed capacity of photovoltaic systems increased in 10 years from 7 to 15 MW generating 8000 MWh/year for electricity, pumping and refrigeration [12]. For comparison, Germany produces 19340 GWh/year of electricity generated by photovoltaic systems, currently leading the installed capacity worldwide [13]. Further steps need to be taken in order to take advantage of the vast solar resources in México, by expanding the installed capacity of active solar systems and by improving building codes and regulations that stimulate and promote the use of solar energy as a renewable resource through the application of passive solar systems.

Energy consumption in Buildings

According to the International Energy Agency (IEA), buildings represent 32% of total final energy consumption [13]. Across countries, different measures have been implemented to mitigate the impact energy consumption from buildings, such as establishing regulatory and incentive schemes to ensure that energy efficiency is an important factor considered during the building design [10]. These measures have also led to the creation of high-energy performance building initiatives (HEPB) [14], (e.g., passive buildings, positive energy building), as well as the creation of the concept of the Zero Energy Building (ZEB) and, more recently, the Net Zero Energy Building (NZEB), which refers to a building with very low energy demand, primarily supplied by renewable sources.

Regarding the renewable resources or technologies available within the building footprint to provide energy to a NZEB at the site are the use of natural ventilation, solar hot water, evaporative cooling and daylighting [15]. The benefits of sustainable buildings can be reduced operating costs , healthy and comfortable working environments, environmental benefits, and maintenance costs [16]. The construction of NZEB buildings would represent important energy savings, but it also involves important challenges in the transition from concepts to real projects, especially considering the cost that its implementation represents [17].

Another important issue to consider is that new buildings will have limited impact in total energy consumption since they embody a small fraction of the total building stock. On the other hand, retrofitting existing buildings represents a more significant potential for energy savings. In order to smooth such transition, a project called *Towards Net Zero Energy Solar Buildings* has been implemented in an international agreement by several countries in Europe, Asia, Australia, the United States and Canada. The focus point of this agreement, Energy Conservation in Buildings and Community Systems (ECBCS), is the study and development of methodologies and solutions towards the implementation of NZEB, including the assessment of energy performance in different climates and across different building types [13].

Energy consumption in Buildings in México

In México, non-residential buildings represent about 16% of the total energy consumption [9]. It has been estimated that electricity represents 27% of the energy use in residential buildings from which 40% is mainly used for lighting in temperate climates while cooling is the main use in warmer climates (44%). Despite of the lack of official information regarding the use of air conditioning in non-residential buildings through the country, the results of a study that took in to account public buildings larger than 1000 m^2 showed that almost 80% count with air conditioning. Only in México City, more than 69% of air conditioning systems were found, a substantial amount for a city which weather conditions is considered as non-extreme. It has been estimated an increment of the total energy consumption for non-residential buildings of 144% by 2030 if no action is taken in the direction of designing more efficient buildings in México [9]. Unfortunately, most of the existing sustainable building regulations are focused on dwelling construction, which application is unconstrained and no explicit regulations are applied for the construction of non-residential buildings. Even if existing mandatory initiatives include clauses for building energy efficiency they only consider the use of electric lighting. When it comes to the effort of designing sustainable non-residential buildings, their conception is based on international regulations such as the Energy Star from United States (which unfolds in México through the imported materials), or the LEED building certification [18].

A study carried-out in 2007 to evaluate the whereabouts of green building in North America recognized the regulations lag in México and concluded with the recommendation of six actions to promote the construction of sustainable buildings. Four of those are related to the implementation of official norms and regulations to introduce the principles applicable to sustainable buildings [19], although the reception to such recommendations has been impermanent over the years. As an example, the first recommended action was to introduce the concept of sustainable building in the National Plan of Development (NDP), in which the last dated 2013 ([20] Objective 4.4), includes general mentions about the protection of the natural resources, the development of ecological zoning, the use of advanced technology for energy efficiency and the promotion of environmental education [20]. However, no specific reference was found for the development of sustainable building regulations, which would impulse the use of renewable energies. Perhaps the initiative should emerge from regional government authorities.

1.2 Problem statement

The passive use of solar energy in buildings implies its exploitation for heating and illumination. The latter (subject of this Thesis), invokes the use of the solar radiation in its direct and indirect components, which refers to the sun light scattered while passing through the earth's atmosphere. The latter can be briefed in a concept known as daylight.

It is known that the intensive use of daylight in buildings represent several advantages. Besides of being a resource that is readily available, it provides a sufficient level of illumination to perform working activities during most of the day, which implicates a decrease in the use of artificial light and thus a reduction in electricity consumption [21, 22]. Its spectral composition often leads to higher visual comfort, when compared to electric light, which has a positive effect in the task performance [23]. Moreover, there is an illuminance and spectrally dependent photo biological impact of light on the human circadian timing system, which strongly regulates hormonal rhythms, alertness and performance throughout a working day [24, 25].

However, because of its characteristics (predominantly sunny and clear sky conditions) in buildings located at low latitudes the admission of daylight also implies the inclusion of sun rays which increases the risk of glare and the interior cooling loads causing the occupants discomfort. In order to mitigate those effects, the typical strategies applied in those regions are for instance the reduction of the window size, the use of tinted glazing or window blinds. The use of such strategies, have as a consequence a reduction the interior daylighting levels provoking the use of artificial light, which in turns increases the final energy consumption. In order to achieve an optimal interior daylight performance in buildings, its inclusion must take into account a thorough assessment of the local climate conditions, the building orientation, the window configuration and the glazing properties. The latter by itself, has the ability of increasing or decreasing the daylight provision and heat gains inside the building, since the admittance of visible light and solar radiation through glazing can be controlled according to its properties: transmittance, reflectance, absorptance and emittance. For instance, standard single pane windows are a source of heat loss and gains, while the use of tinted glazing reduce the admission of daylight and the view to the exterior [16]. In the last years, several improvements have been applied to windows and glazing in order to improve its performance in energy efficiency, such as the spectrally selective low-E coatings that keep out most of the solar heat gain but transmit most of the daylight, and the design and manufacturing of Advanced Daylighting Systems.

1.3 State of the art

Advanced Daylighting Systems are based on the principles of transmission, reflection and refraction of sunlight and diffuse daylight. They can be integrated in the building envelope and improve the daylight interior environment by bringing diffuse daylight and sunlight deeper in the room reducing the use of artificial light and, therefore, the electricity consumption. Some examples of Advanced daylighting systems are: Light shelves, Anidolic systems [26] and also Complex Fenestration Systems (CFS) e.g. louvers and blinds, prismatic panels and films, laser-cut panels, holographic films. CFS are advanced window systems that can be installed or attached to glazing, they have a double function as solar shading and daylight redirection. Their use represents a solution in buildings to control the admission of solar gains whilst contributing to maintain a good visual environment. Besides the mitigation of the final energy demand, the application of CFS represents also benefits for the users by allowing a more even redistribution of direct sunlight, improving the interior visual environment and providing optimal interior thermal conditions, especially in buildings located at low latitudes, where weather conditions are predominantly sunny and warm over the year.

Over the years, the research on Advanced Daylighting Systems has been mainly focused on locations with overcast prevailing weather conditions, in order to improve the interior luminous conditions given the low exterior illuminance levels that characterize these locations during the year [26, 27]. A good example is the Anidolic Daylighting System (ADS), developed at LESO-PB, EPFL [26], which is based on the principle of non-imaging optics and that was designed mainly to collect and redistribute the diffuse component of daylight. The assessment of three different versions of Anidolic Systems was carried-out under overcast and clear sky conditions and their performance showed an overall improvement on the work plan illuminances and daylight factor compared to a standard façade [26]. This system has also been tested in different locations under different weather conditions, performing well in those with predominantly overcast skies [28, 29]. However, when tested in locations with higher luminous conditions, the results showed increased illuminance levels although an increment in the risk of glare was observed [30, 31].

The daylighting strategies applied to buildings located at low latitudes differ from those located at high latitudes, given that as the daylighting levels increase in the room, the risk of overheating and glare rises substantially which compromises the visual and thermal comfort of the occupants. Thus, in buildings located at low latitudes the challenge is to minimize the admission of the direct solar rays in order to prevent alterations to the interior environment. Therefore, there is also an interest in developing a system that can control the admission of sunrays without compromising the admission of diffuse daylight. Hence, the use of light shelf has been proposed by several studies (Figure 1.11) to be used in high luminous climates, because of its double function: to redirect the daylight in the depth of the room while acting as a solar protection (in the case of south orientated buildings) [30, 32-34]. An innovative evolution of the light shelf system was proposed by I. Edmonds and P.J.Greenup named the Lighting Guiding Shade (LGS), which is an adaptation of an external shade to work as an non-imaging optical system that redirects light deep into the room [35]. Such a system consists of an external shade with a diffusing glass aperture, formed from an upper planar and a lower parabolic reflector to direct diffuse light through the interior space. An illustration is presented in Figure 1.12.

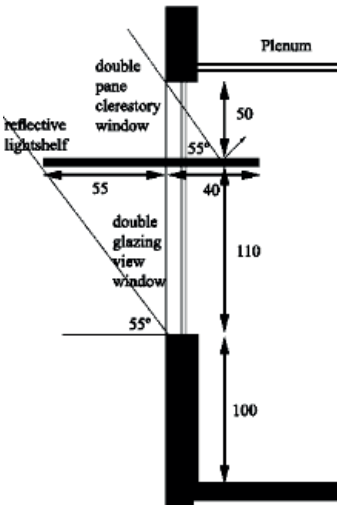

Figure 1.11The design and components of an exterio r light shelf [30].

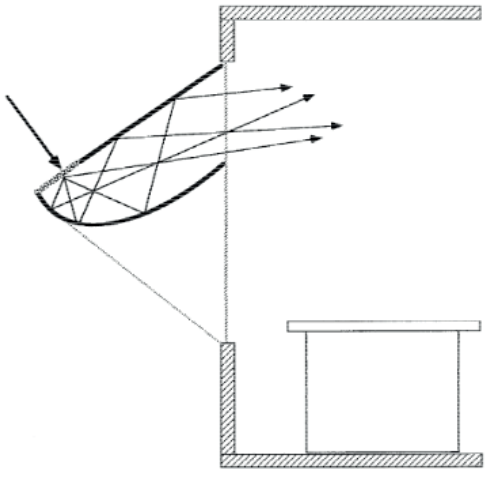

Figure 1.12 A section that shows the functioning of LGS developed by Ian Edmonds [35].

However, the use of such systems implies substantial investments not only because of the expensive materials that are needed for its design (especially in the case of the LGS) but also because of the expertise required for the installation of the device. Other lighting redirecting devices with more simplistic characteristics have also been proposed for high luminous climates, an example is the lasercut panel (LCP). The LCP deflects the light when passing through a thin acrylic material with internal parallel laser cuts that work as internal mirrors redirecting the daylight upwards and transforming the ceiling into a secondary light source [35]. With LCP, the light coming from higher angles is strongly redirected upwards, which would increase its efficiency in low latitudes with the appropriate orientation of the building. The CFS used for the development of this thesis would aim at having similar characteristics: reducing the cost of the system and making the installation of the device easier.

In the preceding sections it was discussed the differences that the inclusion of daylight in buildings implies for those located at high or low latitudes. Accordingly, the selection of an appropriate CFS to be used in buildings located at low latitudes implies not only the assessment of the daylight distribution indoors, but also a visual and a thermal comfort assessment to determine the risk of glare and overheating that the inclusion of daylight might. The performance of CFS in a building is often assessed by the use of computer simulations, in order to overcome the difficulties that performing on-site evaluations in full scale buildings represent, such as: the availability of a testing facility, materials and equipment transportation as well as the CFS installation. For this study, the RADIANCE ray-tracing programme represents the best alternative due to its accurate prediction of lighting environments which comprehend the accuracy of numerical results and the generation of renderings as identical representations of real scenes [36].

A brief survey of RADIANCE based studies that assess the performance of Advanced Daylighting Systems in luminous climates was carried-out in order to establish their similarities to the present study and to determine the latter's novelty. As a result, six studies were found pursuing related objectives: an improved interior daylight environment for buildings located in sunny climates [30, 33, 34, 37-39]. However, as discussed before, a daylighting strategy applied to buildings in those regions implies not only the assessment of the improved interior daylight distribution, but also the thermal and visual comfort of the occupants. The review show that such studies regularly include the assessment of only one of such relevant aspects; few combine two, while is barely found one that includes the three of them. From the studies found which contemplate the optimization of the interior daylight environment as main goal, four included the assessment of the visual comfort [30, 37-39], and none considered the assessment of the thermal comfort of the occupants. However, two studies were found that couple the daylight and thermal aspects assessment, although they present fundamental differences to the present study. The first one, even if includes visual comfort estimation results, its main objective is the assessment of solar shading devices and focuses on the methodology proposed to solve the difficulties found when carring-out parametrical studies [40], while the second study is based in a middle latitude location focusing its research on testing of different façade configurations [41].

An important difference to those studies is the use of CFS, which is included in only one of the studies considered in the review [38], although its objective is not to compare the daylight improvement capabilities of CFS but to assess the performance of only one CFS. The most similar found to the present study [30], considers the comparison of three advanced daylighting systems in a prevailing clear sky conditions location, and includes the assessment of the interior daylight distribution and the visual comfort of the occupants. However, it differs in the use of an interfaced version of RADIANCE (which might limit the modelling capabilities of the software), and in that the sky is simulated using first the standard CIE skies and secondly averaged compiled data, which might also convey certain inaccuracies in the results.

Thus, the present study can be distinguished from those targeting a similar objective, first in that it aims to achieve an improved daylighting interior environment in buildings located in sunny climates by the use of CFS. Therefore it contemplates the assessment of the improved daylight distribution in-sync with an estimation of the interior thermal and visual comfort of the occupants. Additionally, one of the objectives of this study is to perform a realistic evaluation, thus simulations being referenced to existing buildings is a remarkable characteristic of this study. On-site monitoring practices are not frequently employed due to the difficulties that it implies, such as: the availability of the necessary equipment, the availability of a disturbance-free area to monitor, technical and logistics support and so on. As for instance a similar approach was found in only two of the six studies considered in the review [30, 37].

Furthermore, a focal aspect of the present study is the computer based approach for the assessment of the aforementioned relevant aspects to the inclusion of daylight in sunny climate locations. Such, represents an innovation in daylighting simulations since it includes the evaluation of the annual interior daylight distribution and the thermal comfort with the use of CFS. The former, represents a recently included RADIANCE capability which relies in the use of the bi-directional scattering distribution function (BSDF) data, and allows the prediction of the interior daylight distribution through CFS in annual basis. The latter, allows the simulation of the thermal effects of CFS in a room by creating a CFS input file for energy plus using the software Window 7; a procedure available since the use of the Window 6 version (2010), and the Energy Plus 7.2 version (2012). A leading edge synthesis of the simulation approach employed in this study is explained as following.

1.3.1 Simulation of the daylight propagation through CFS

1.3.1.1 Computer tools for daylight assessment in buildings

The daylighting performance of buildings can be assessed using real scale or testing facilities; another option is to perform the assessment using scale models, which require the use of special equipment such as a Sky Simulator and/or an Heliodon [42, 43]. However, the use of computer simulation represents a very convenient alternative, given that it facilitates the evaluation process by minimizing possible difficulties related to the physical installation of the CFS on the façade (in the case of performing tests on real buildings or mock-ups), and/or do not require sophisticated equipment such as an Artificial Sky or Heliodon, as would be the case when testing scale models.

Computer simulations for the lighting performance assessment were first used in the 1970s to create 3D shapes and shadows, even though they only became common in the 1990s with the introduction of personal computers [43]. Today, they are widely used in the building and engineering fields to assist the design process and to assess the building's performance, as shown in a study published in 2006, outlining that 79% of users working with daylight are using computer simulations [44]. Lighting simulation can be divided into two main areas, the first one is the photorealistic rendering and the second one is the physically based visualization or predictive rendering, which offers an accurate prediction of reality [45, 46]. Photorealistic rendering is characterized by creating very attractive renderings although not representative of the reality, few examples of photorealistic software are 3Ds Max, Architect 3D and Artlantis. Nonetheless, a recent study has proved the reliability of using 3Ds Max for simulating design related daylighting in cases of comparable complexity to the ones tested in such study [47].

The daylighting simulation tools use computer algorithms to solve the light distribution within or outside buildings; those used in the prediction of daylight can be classified in three types: direct calculations, view dependant algorithms (ray-tracing technique) and scene-dependent algorithms (radiosity method). The view-dependent algorithms are then divided according to the direction of the rays' computation (backward tracing or forward tracing), while the scene-dependent algorithm are not able to deal with specular reflections. The algorithms that combine both ray-tracing and radiosity are considered as the more efficient ways of calculating the global illumination [45]. A graphical description of the different lighting simulation approaches is shown in Figure 1.13.

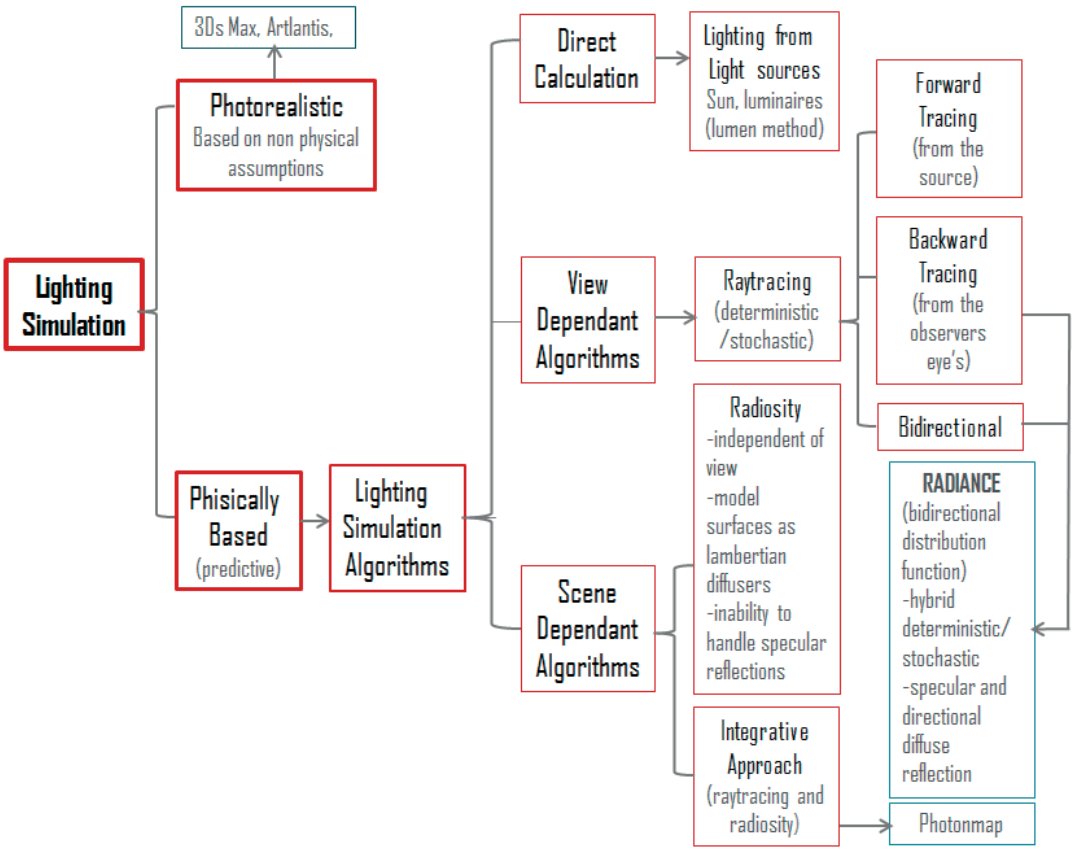

Figure 1.13 Description of the most relevant existing lighting simulation approaches synthetized in a graph [36, 45].

The most accurate programme for lighting simulation nowadays is RADIANCE. The programme uses a method that combines backward ray-tracing and bidirectional transmission distribution functions [45] hence, it performs effectively the calculation of specular and directional-diffuse components [36]. Its main advantage over other existing lighting simulation software is that it has almost no limitations on the geometry or the materials that can be simulated and that it is distributed as an open source. Its main disadvantage is the complexity of handling the software due to a lack of a user interface. As a solution to the latter, other daylighting simulation software are using RADIANCE as a simulation engine. An overview of the most relevant ones is listed as follows:

a) DAYSIM

Radiance based daylighting software that calculates annual illuminance values based on local climatic data. It uses a weather data file for annual calculations as well as the CIE standard skies for calculating the daylight factor. It allows the calculation of annual glare risks and electric lighting energy demand for dynamic systems and switchable glazing. Dynamic facades systems such as standard venetian blinds can be modelled; however, the use of BSDF data has not been implemented yet in the programme's capabilities [48].

b) LIGHTSOLVE

It offers the possibility to make the pre-design phase of a lighting project more accessible for architects as it allows the exploration of different design options [45]. It predicts illuminances on yearly basis using a time segmentation method, which averages hourly typical meteorological year data over periods during which weather conditions are similar. The software bases its calculations on the ASRC/CIE Perez model [49], and can be adapted to a wide range of climate zones [50].

c) DIAL+

DIAL+ is an advanced daylighting design tool. It performs the assessment of lighting, cooling and ventilation in buildings using standard windows and external blinds. It allows the calculation of the daylight factor, daylight autonomy and the electricity demand of office rooms. Advanced fenestration systems such as blinds, overhangs and fins can be accounted for by selecting and dimensioning inbuilt available options [51].

d) DIVA for Rhino

DIVA is a Rhino plug-in for daylighting and energy modelling in buildings. It allows the assessment of environmental performance including climate-based daylighting metrics, annual and individual time step glare analysis and single thermal zone energy. The use of shading devices and controls is implemented in the programme and RADIANCE materials type can be used including BSDF data. However, climate-based simulations and annual glare calculations cannot be carried-out using BSDF files [52].

e) GERONIMO

It is user-friendly, free of charge software for architects and lighting designers, which is able to perform CFS daylighting calculations for different sky types (overcast and clear skies). The rendering engine of GERONIMO is the backward ray-tracing software RADIANCE. The advantage of GERONIMO is that it avoids the classical command-line usage of RADIANCE offering a simple interface that can be adapted to the user's skills [53, 54].

f) Relux Pro (Relux Informatik 2010)

It is a free of charge software, used mainly for electric lighting calculations, although daylighting and energy calculations can also be performed. A convenient characteristic of Relux is that photometric data from luminaire manufacturers is linked to the programme. Relux simulations are mainly based on the radiosity method; however, an enhanced version of RADIANCE has been implemented in Relux Pro that allows ray-tracing calculations for renderings and lighting analysis. This makes CFS simulations possible, nonetheless only four monitored CFS are currently available in the EPFL/LESO-PB database [45, 55].

Other Non-Radiance based software for lighting simulations:

a) Dialux (DIAL GmbH 2010)

Mainly used for indoor and outdoor electric lighting, it has the possibility to import photometric data directly from luminaire manufacturers. Some capabilities for daylight calculations are available using the German standard DIN 5043 and CIE Publication 110. Dialux is a free-of-charge software [45].

Even if some of the mentioned daylighting calculations software can perform very accurate simulations, only three of them can be used to describe the daylight distribution through CFS within buildings (Geronimo, DIVA for Rhino and ReluxPRO) and few of them, such as DAYSIM and LIGHTSOLVE, allow performing annual simulations. However, not all of them can account for light reflecting systems including specular materials, and none of them use Bidirectional Scattering Distribution Functions (BSDF) to describe the performance of a Complex Fenestration System for climate-based annual calculations. Therefore, the assessment of daylight strategies in two office rooms was carried-out using RADIANCE without recurring to an interfaced version, in order not only to calculate the daylighting distribution in presence of a CFS, but also to assess daylighting performance throughout the year.

1.3.1.2 Simulation of the daylight propagation through CFS using RADIANCE

In order to simulate the daylight propagation through CFSs, it is first necessary to determine their photometric properties, such as the visible transmittance and reflectance. Such properties can be assessed using a gonio-photometer which is a computer controlled mechanical device that measures the characteristics of planar materials using either a scanning or a video method [56]. The bi-directional gonio-photometer available at the Solar Energy and Building Phyiscs Laboratory (LESO-PB) of EPFL uses advanced digital imaging technics (CCD video camera) and is based on light incident directions following the 145 sky subdivisions of Tregenza [56-58]. These subdivisions define the incident and emerging light directions pertaining to the so-called called Bi-directional Transmission Distribution Functions (BTDF) [56, 57, 59], stored in the corresponding format officialised by IEA Task 21 [60]. BTDF data are useful to represent graphically the distribution of daylight fluxes in a plot diagram in order to visualize the daylighting performance of advanced daylighting systems.

RADIANCE performs the lighting simulation using inbuilt materials such as glass, plastic, metal, light, dielectric (refracts and reflects radiation and is transparent), trans-material (for materials transmitting and reflecting light in diffuse and specular components). BRTDfunc which is the most general material provides input for specular, directional diffuse, and diffuse refraction and transmission [36]. The primitive *prism2* is a RADIANCE material that supports only two emerging lighting directions for a single incident beam direction; it is mainly used to simulate sharp redirecting CFS such as lasercut panels, holographic film and prismatic films [36, 61, 62].

In order to use BTDF data to simulate the daylight distribution in rooms using CFS, a RADIANCE procedure named BTDF2*prism2* was designed as initial step. It determines the two prevailing emerging directions from BTDF data and translates them into the required *prism2* input data [61]. However, given that the primitive *prism2* allows only two emerging lighting directions, in appearance the lighting flux is modelled as a direct component in the simulation results [61]. However, since the adaptation of BTDF2*prism2* in 2004, some improvements have been applied to RADIANCE that allow the rendering of the diffuse and direct components of daylight on the inner surface of a CFS, taking into account all input and output directions defined by the monitoring resolution of the bidirectional gonio-photometer. These improvements started with the development of the programme Window 6, which allows the modelling of complex fenestration systems storing their transmission properties in an XML file [63].

To be able to use the BTDF data generated by the gonio-photometer, it is necessary to transform the data which is described using the IEA Task 21 format into the new XML format that takes multiple lighting redirections into account. A programme named *btdf2radiance* was created for this purpose, which generates the BTDF data as a rectangular matrix considering the 145 Tregenza's sky zones as input directions and each 5° in azimuth and elevation including the zenith to make a total of 1297 zones [64] as output directions.

Two new Radiance procedures reproduce the CFS properties using BTDF data stored in the XML format. A first procedure uses the pre-process *Mkillum* to simulate the daylight distribution on the basis of BTDF data [36]: the programme converts the BTDF data, assigned to a polygon in the virtual model, into a 'secondary light source'. Subsequently, it generates the corresponding candlepower distribution, which corresponds to a particular daylighting condition including external obstructions, weather, and so on. A second procedure uses the *bsdf* material function which models directly the transmitted daylight distribution from the BTDF data without the use of *Mkillum* [65].

1.3.1.3 RADIANCE use for daylight annual simulations using CFS

The essential way of assessing daylight in buildings is by calculating the DF, a metric that by definition is derived from illuminance measurements obtained under overcast sky conditions (See Section 2.3). The daylight factor approach is a fundamental way of predicting the daylight distribution in a room, given that it represents an interior daylight condition derived from the lowest external illuminance levels. However, daylight being a dynamic natural source, its potential for building energy savings depends on the external weather conditions, as well as the design and orientation of the building. Therefore, assessing the performance of daylight by considering only a constant daylight factor would lead to an inaccurate interpretation. Thus, in order to obtain a realistic daylight evaluation in a building it is important to consider the daily and seasonal variations of the sky luminance distribution.

The two simulation processes mentioned in Section 3.3 (mkilllum and *bsdf*) are not directly applicable to carry-out accurate annual simulations using CFS, given that they only allow simulating specific outdoor conditions; in the case of mkillum, the CPU time required to perform the simulation of the exterior environment and the related inter-reflections is prohibitive. A solution to this problem was found by using a Daylight Coefficient approach [65].

The 'Daylight Coefficient' approach (DC method) was introduced by Peter Tregenza and M. Waters [66] in 1983: it assumes that daylight illuminance on a given location depends on two independent factors: i) the luminance distribution of the sky and ii) the form and material of the surrounding surfaces [66]. This method represents an effective way to speed-up the process of predicting interior daylighting illuminance when considering several different outdoor daylighting conditions (e.g. such as different sky types). An attempt to apply the DC method to innovative daylighting systems with the aid of computer programming can be tracked already in 1992 [67]; in this study the calculation was split in two parts: i) the daylight flux coming from the sky and ii) the daylight component reflected from the interior surfaces in the room. The DC method has also been tested using computer simulations with Test Reference Years (TRY) [68]; others suggested the use of new standard daylighting coefficient models independent from the building location and orientation [69]. The first step for carrying-out annual simulations of CFS started with the development of a method to model solar gains through CFS. This method was introduced by Klems in 1993 [70]: it relies on the use of the measured bidirectional transmittance and reflectance properties of each layer of a fenestration system obtained with a scanning radiometer. It employs a matrix calculation method to produce a solar heat gain coefficient at the end [70-72]. The result of the monitoring is the directional-hemispherical transmittance of the fenestration system and the layer-by-layer absorption; it is designated by the Bidirectional Scattering Distribution Function (BSDF) [70-72].

The use of BSDF monitored data of CFS to simulate their annual performance in a room using RADIANCE was made possible by the introduction of the *rtcontrib* tool, the latter is used to associate the transfer of the light flux from the sources to their final destinations (a window or a monitored value) [65]. A method based on the Daylighting Coefficient method was created as a result of the introduction of two new RADIANCE tools: genklemsamp and klems_int.cal, which assist to determine the daylight coefficient by sampling rays based on the Klems subdivision of the sky vault. This new RADIANCE method is called "The Three-phase method" [71].

The Three-phase method performs the daylighting calculations by dividing the transfer of the lighting flux from the sky to the monitoring sensor in the room into three phases: i) from the sky vault to the exterior of the window, ii) the light transmission through the fenestration element and finally iii) from the fenestration to the interior space. A matrix describing the light flux transferred between the elements represents each phase of the method. At the end, the matrices are multiplied by the input of a given sky condition [65, 73]. An evolution of the Three-Phase Method is the Five-Phase Method, in which the calculation is performed by separating the direct solar component from the diffuse sky component and the internal reflections in order to compute the distribution of the direct solar component in a more accurate way [74]. In order to do this, simulations according to the three-phase method must be carried-out first, after which the direct solar contribution is calculated and subtracted from the results obtained in the first instance; a more accurate direct solar contribution is than calculated and added to the results in the final stage.

1.3.2 Visual Comfort assessment using RADIANCE

For the assessment of lighting quality in a room, the most important aspect to consider is the risks of glare. IESNA defines glare, as the sensation produced by luminance within the visual field that is greater than the luminance to which the eyes adapt to cause annoyance, discomfort, or loss in visual performance. IESNA identifies two types of glare: Disability glare which results in a reduced visual performance and visibility, and **Discomfort glare** which does not necessarily interfere with visual performance [75]. In general, glare is caused by a high or non-uniform luminance distribution within the visual field, or a high contrast of luminance between the glare source and its surroundings, a situation that might often happen when a room is lit by daylight [76].

Several studies based on the subjective perception of glare led to the suggestion of different glare indexes. Many of them were developed as a result of studies carried-out under artificial light conditions, such as:

a) Visual Comfort Probability (VCP)

VCP was developed to evaluate discomfort glare due to small artificial light sources, and therefore cannot be used to predict discomfort glare from windows given that the source of glare in daylighting situations is usually larger and the eyes adaptation to the source is higher reducing the glare sensation [76]. It is described in a range of 0 to 100% as the relative fraction of people who would feel comfortable under similar lighting circumstances [77].

$$VCP = 279 - 110\,[log10]\sum_{i=1}^{n}\left[0.5Ls, \frac{i(20.4\omega s,i+1.52\omega_{s,i}^{0.2}-0.075)}{Pi*E_{avg}^{0.44}}\right]n^{-0.092} \quad (1.1)$$

b) CIE Glare Index (CGI)

The CGI was developed in 1983 by the technical committee of the Commission Internationale de l'Eclairage (CIE) led by Einhorn. It includes the contribution of the glare source to the adaptation of the observer when describing the luminous environment of the room, which is expressed by the direct vertical illuminance at the eye [10] [77]39].

$$CGI = C1 * \frac{log10C2\left(1+\frac{Ed}{500}\right)}{Ed+Ei}\sum_{i=1}^{n}\frac{L_{s,i}^{2}\omega s,i}{P_i^2} \quad (1.2$$

c) Unified Glare Rating (UGR)

UGR is a simplification of the CGI. It was developed to evaluate glare sensations for artificial lighting systems, with restrictions regarding the size of the solid angle of the source. It uses the same numerical scale as CGI, any value above 28 corresponding to an intolerable glare sensation and below 13 to an imperceptible glare sensation [77, 78].

$$UGR = 8 * low_{10}\frac{0.25}{Lb}\sum_{i=1}^{n}\frac{L_{s,iw_{s,i}}^{2}}{P_i^2} \quad (1.3)$$

The problem of using glare indexes that were developed for artificial lighting lies with the size of the daylight source which implies an eye adaptation that would reduce the potential glare sensation [10]. There is no established standard way to predict glare sensations for daylighting environments, however different ways for prediction of glare disturbances under daylighting conditions have been proposed such as:

a) Daylight Glare Index (DGI)

It is a modified version of the glare index recommended by the Illuminating Engineering Society (IES). The glare formula was created for large area glaring sources as windows; its use was recommended for daylight conditions. Validation studies of this index show that the correlation between glare from windows and predicted glare is not as strong as in the case of artificial lighting[79, 80]. It was developed from studies conducted under daylight conditions; however, this is why interior specular reflections and direct light were not considered in Hopkinson's studies [77] [81]. In DGI a value greater than 31 will result as intolerable glare while less than 18 suggest glare as 'barely perceptible'[77].

$$DGI = 10 * log_{10}0.48\sum_{i=1}^{n}\frac{L_{s,i}^{1.6}\omega_{pos\,s,i}^{0.8}}{L_b+(0.07\omega_{s,i}^{0.5}L_{s,i})} \quad (1.4)$$

b) New daylight Glare Index (DGIN)

Dveloppedby Nazzal, the DGIN is a modification of the DGI proposed by Hopkinson. The DGI requires data such as the mean exterior luminance, the dimensions of the window, and its distance from view locations. The results are validated using those of the DGI method and also shares the same limitations, specular and luminance sources are not considered [77, 82].

$$DGI_{N=8*log_{10}}0.25\sum_{i=1}^{n}\frac{L_{exterior,i}^{2}\Omega_{z,i}}{L_{adapt}+0.07(\sum_{i=1}^{n}\omega_{s,i}L_{window,i}^{2})0.5} \quad (1.5)$$

c) Daylight Glare Probability (DGP)

DGP is a function of the vertical eye illuminance as well as of the glare source luminance, its solid angle and its position index. The simplified DGP neglects the influence of peak glare sources; the simplified DGP uses the illuminance values for the vertical eye illuminance and a simplified image to retrieve a DGP value [78, 80]. For DGP the first half of the equation uses the vertical eye illuminance (Ev) as input while the latter half performs an evaluation of visual contrast by comparing the source luminance versus the scene luminance and the position of the glare source. Intolerable glare corresponds to a value greater than 0.45 and as imperceptible for results lower than 0.3 [77].

$$DGP = 5.87 * 10^{-5} E_v + 9.18 * 10^{-5} log_{10} 2 \left(1 + \sum_{i=1}^{n} \frac{L_{s,i}^2 \omega_{s,i}}{E_v^{1.87} P_i^2}\right) \quad (1.6)$$

1.3.2.1 Glare indexes calculation

Currently it is possible to predict the risk of glare by the way of computer simulation. In RADIANCE, this can be done with the use of *evalglare*, a glare evaluation tool assuming the existence of a low correlation between the current glare indexes and the subjective evaluation of glare by occupants. The programme uses an HDR fish eye rendering to identify the glare sources using three different thresholds based on: i) a fixed luminance value, ii) a multiplier of the average view field luminance, and iii) a multiplier of the average task luminance [83].

1.3.3 Computer tools for building thermal analysis using CFS

Thanks to a brief survey carried-out among the existing simulation software performing the assessment of thermal comfort in buildings, the following outcome was obtained:

a) DIVA for Rhino

It allows the assessment of the Single Thermal Zone Energy and Load Calculations using Energy Plus. The calculation is performed by creating thermal layers in the virtual model. As output, it generates the monthly energy consumption, hourly heating and cooling energy consumption[52]. However, in order to perform a thermal calculation using DIVA, climate-based simulations (which include any shading and lighting calculations) should be carried-out first; therefore the use of DIVA becomes inconvenient for the purposes of this PhD thesis, since BSDF files cannot be used to perform climate-based calculations using DIVA.

b) DIAL +

It allows the calculation of the solar gains as a function of the glazing properties and the shading devices, indoor temperature (dynamic calculation, hourly step), the annual number of overheating hours and the cooling and heating needs for the room [51]. Special daylighting systems like external and internal blinds can be created using the software tools, advanced daylighting systems with redirecting characteristics are built-in the system however those known as sharp redirecting systems are impossible to model with this software. The use of BTDF data to simulate the daylight propagation through CFS in a room is not available in Dial + software.

c) Energy Plus and Open Studio

It is a building energy simulation non-interfaced software created with the Fortran programming language, it is based on the features of previous energy simulation programmes such as BLAST and DOE-2 [84]. It assists architects and designers in the optimization of the building design to reduce the use of energy and water. Energy Plus models heating, cooling, lighting, ventilation and water use. The assessment of the different variables in E+ is performed in a simultaneous way in the intention that the simulation performs as a real building. Regarding the modelling of windows, E+ has a library of more than 200 glazing systems, it allows the calculation of the solar energy absorption using advanced fenestrations such as controllable window blinds or electro chromic glazing [85]. The daylight simulation through CFS and its thermal effects is possible using BSDF data generated by the Window 7 software. In order perform thermal simulations in E+ a glazing system created with the use of Window 7 software is converted into an 'idf' file which is the input file of Energy Plus.

1.4 Research objectives

The objective of this thesis is to improve the interior daylight distribution based on the use of CFS for buildings located at low latitudes characterized by prevailing clear sky conditions. Such approach, would lead to an integral balanced solution between an improved distribution of daylight indoors and the thermal and visual comfort of the occupants. This thesis aims to prove that the use of CFS contributes not only to improve the distribution of daylight but also to mitigate the unfavourable effects that its inclusion in buildings located at low latitudes might cause. Thus, the use of CFS would contribute to maintain an interior environment that provides satisfactory visual and thermal conditions for the occupants. The application of such method, benefits of the available resources in terms of equipment and local weather data, aiming to obtain a solution that closely represents the existing situation and thus could be implemented in realistic conditions. Based on the previous assumptions, the development of this thesis presents the following characteristics:

a) As overall approach, it intends to consider a situation close to reality; therefore the applied daylighting strategy is based on the case-study of two existing buildings.
b) The computer simulations were carried-out based on real weather data obtained from a local meteorological station, in order to perform simulations that more closely approximates the reality.
c) The computer tool selected to carry-out the simulations was the lighting simulation programme RADIANCE in its original form, in order to broaden the simulation possibilities regarding materials and daylight modelling capabilities.
d) The proposed solution does not include major modifications to the existing buildings, such as the size of the window, the interior design of the building or the distribution of the working spaces; as such it only includes CFS.

1.5 Hypothesis

In the precedent sections the benefits that the admission of daylight in buildings would represent in terms of energy efficiency, human health and productivity were examined. However, they also consider the disadvantages that the inclusion of daylight may represent for buildings located at low latitudes. Because of its dual function (daylight redirection and solar shading) the use of CFS represents a solution to improve the interior daylight distribution while maintaining a comfortable visual and thermal interior environment. Efforts to develop Advanced Daylight Systems for high luminous climate locations have been carried-out in the last decades, as well as the assessment of the performance of CFS in different climates in order to determine its suitability to different sky conditions. However, in order to succesfully achieve an improved interior daylight environment that includes the use of CFS in buildings located in predominantly clear sky conditions an integral evaluation that comprises the assessment of the thermal and visual comfort of the occupants is required.

The main hypothesis of this thesis implies that an improvement of the interior daylight distribution is feasible in buildings located at low latitudes without compromising the visual and thermal comfort of the occupants. The latter can be achieved through a controlled use of daylighting and passive solar gains by applying a daylighting strategy based on CFS.

Such hypothesis intends to be demonstrated as follows:

Chapter 2: Daylight Assessment of Buildings
Monitoring of the existing interior daylight situation of two office rooms located in the centre-north of México following two main objectives: first, to establish their physical characteristics and particularities regarding the current daylight situation indoors and secondly, to create a virtual model representing the two offices by adopting their characteristics. The representativity of the existing situation by the virtual models is explored as a previous step to the assessment of the performance of different CFS using computer simulations.

Chapter 3: Assessment of the improved interior daylight situation using CFS: Solstices and Equinox Assessment
Among numerous available, five CFS are pre-selected to be tested in the two office rooms. The computer based assessment of the daylighting improvement in the two office rooms using the pre-selected CFS is carried-out under different sky conditions. The assessment includes the interior daylight distribution, as well as the thermal and visual comfort of the occupants for three different critical days regarding the inclusion of daylight in buildings: Winter and Summer Solstice and Spring Equinox.

Chapter 4: Annual Assessment of the improved interior daylighting environment using CFS
Annual climate-based estimation of the performance of the CFS in the office rooms using computer simulations, which includes the assessment of the interior daylight distribution as well as the thermal comfort of the occupants. The overall assessment of the CFS performance in the two office rooms is implemented using a multi-criterion analysis leading to the selection of the outstanding CFS best suitable for each office room.

Chapter 2 Daylight assessment of buildings

The ideal way to assess daylight propagation through a CFS in a room would be to perform detailed on-site evaluations in a full-scale room. However, this comprises several difficulties, such as: the unavailability of a testing facility, materials and equipment transportation, as well as the installation of the CFS on the facade. An alternative is to perform the assessment using computer simulations based on virtual models. The latter was selected as assessment method giving the difficulties of carrying-out testing using CFS in México. In order to do that, two rooms were selected as a first step as subjects of the daylight evaluation study; as a second step a short-term daylighting on-site monitoring was performed during the periods of the year that are considered as critical for daylighting: spring equinox as well as winter and summer solstices. The monitored data was also used, aside from the assessment of the existing daylight situation for the calibration of virtual models employed to assess the daylighting performance by the way of computer simulations.

2.1 Building Location

Due to the planning convenience, the selection of the building was carried-out in the center-north of México (Zacatecas 22°783' N., 102° 583' W, Altitude: 2543m), which location can be seen in Annex 2.1. In the Köppen climate classification such region is located in the group BS (See Figure 2.1), which would correspond to a Dry semi-arid steppe. It presents an average temperature of 18°C and a maximum average temperature of 31°C which occurs mainly in May [86], while the low average annual rainfall is below 800mm. Due to the climate change it is expected an increase temperature between 1.0 and 1.4°C by 2020 and a decrease of the annual rainfall between 0 and 5%. The region counts with 12h per day of daylight, an annual average sunshine of 2676 hours per year thus 7.3 average sunlit hours per day, which would correspond to a 61% of sunny daylight hours in a year [9, 87].

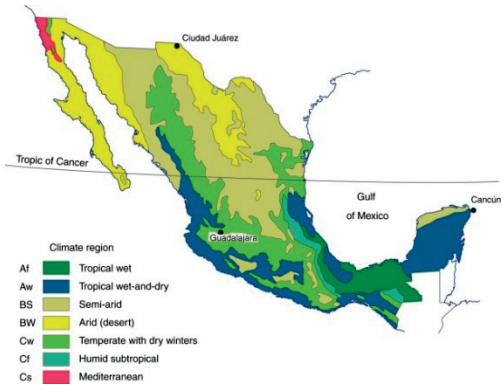

Figure 2.1 The Köppen climate classification across the Mexican territory [9, 88].

2.2 Building Selection

The selection of the office room was made in order to analyse interior working environments with high desk illuminance requirements for difficult visual tasks, with regular occupancy patterns and constant activities during all day long. The aim was to study an office room that would represent the characteristics of a typical office in central México. However because of the different opportunities that were offered, two office rooms located in different buildings were selected. The first one is a typical office room located in a building representative of the period of its construction (1995). However, despite its modern exterior features, the characteristics of its design lead to insufficient daylighting provisions in the interior. The second building is of recent construction (2005) its architectural design took into account the building orientation, thus it presents a better interior daylighting situation and was selected to explore possible improvements by the application of advanced daylighting strategies. A detailed description of the two office rooms is presented as follows:

a) Building B1: Tecnologico de Monterrey Campus Zacatecas (ITESM)

The ITESM is a private university in Mexico counting with 31 campuses along the country; it offers high school, undergraduate, and postgraduate courses. The office room selected is the administrative office of the library located in building CC1, where the computer rooms, auditorium and the administrative offices of the campus are also located. The architecture's style is identified as contemporary–modern; however, despite its exterior appearance, the characteristics of the building do not contribute to an enough daylight propagation in the interior spaces.

Figure 2.2 Exterior views of building CC1 on the university campus; the office room is located on the second level.

As an approximation, more than 50% of the facade's building is glazed, without exterior solar protection the admission of the sun rays was intended to be controlled using tinted reflective glass whose transmission is ranging from 9 to 30% according to the manufacturer (10–15% according to data collected on-site). The latter provides very low illuminance levels especially for overcast sky conditions, as can be seen in the picture shown in Figure 2.5.

Two exterior views of building CC1 are presented on Figure 2.2, the window of the office room can be found on the second level left (See Annex 2.1). The orientation of the office room is south-west; hence direct sunlight is admitted into the room until late afternoon. In winter and spring, when clear sky conditions occur, the use of internal blinds for sun shading are necessary from about 15h00, reducing the admission of daylight as shown in Figure 2.5 (pictures taken at 16h00 and 18h00) and in Figure 2.6, suggesting that the daylighting conditions inside might cause overheating and glare disturbance for the occupants. A second window orientated north-east leads to an atrium space with a round-shaped dome of coloured glass which is covered permanently by a black opaque fabric to protect the interior space from rain and from incident sun rays. The ensemble (glass and fabric) allows about 8-10% of daylight flux to be transmitted inside the atrium area. Pictures showing the round-shaped dome and the atrium from different perspectives are given in Figure 2.3 and 2.4.

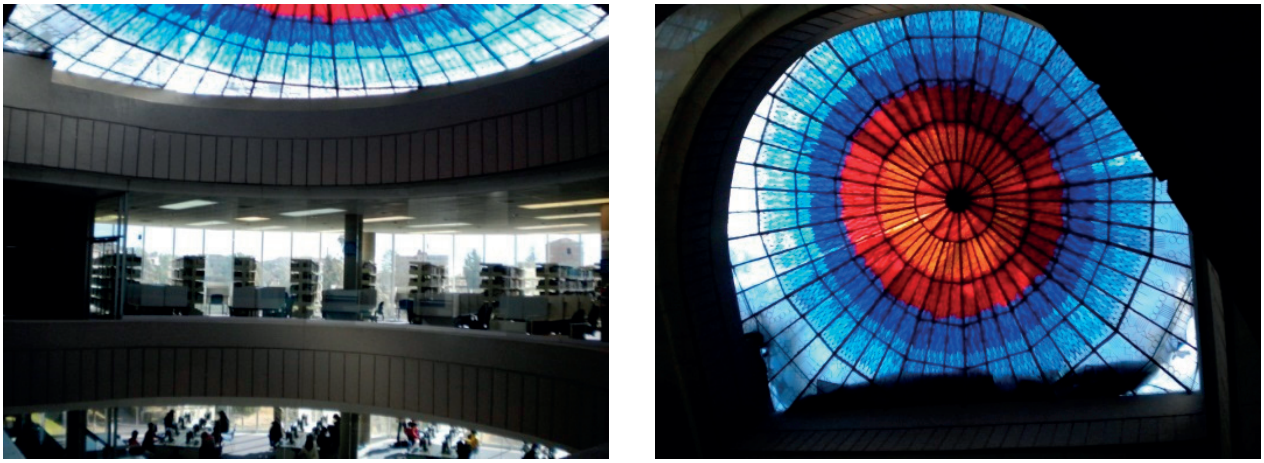

Figure 2.3 Front view of the interior of the library and the atrium area in Building B1 (left) and the dome from the ground floor (right).

Figure 2.4 View of the interior of the office room to the atrium (left) and of the roof dome covered with black fabric (right).

The dimensions of the office room are 4.45m x 7.30m x 3.2m (a detail of the floor plan and room's dimensions can be found in Annex 2.2). Three working spaces are distributed into the room, as well as a small area for social time in the middle of the room; a small glazed-room covered with vertical blinds is used as archive. The external window is 2.0m large by 3.2m high (Window to Wall Ratio of 45%) while the window leading to the atrium has a flag shape of 3.85m width and 3.0m height (Window to Wall Ratio of 27%). A view from the hall-atrium towards the cubicles for the students can be seen in Figure 2.7, the office is located at the right in the view. The photometric properties of the interior surfaces were collected on-site, and shown in Table 2.6.

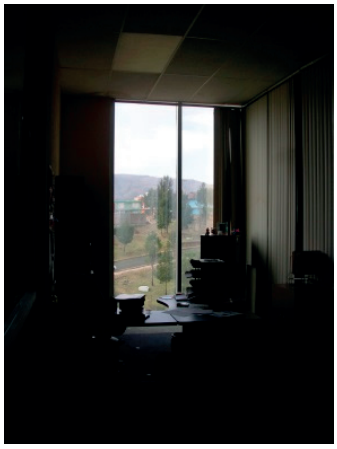

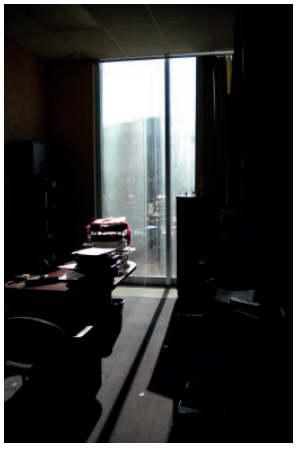

Figure 2.5 Interior views of the existing daylighting situation in the office room in different sky conditions, Ovecast Sky (left) in December 16h00, Clear sky in January 16h00 (centre) and March 18h00 (right).

Figure 2.6Interior view of the B1 office room from the side window to the back of the room, February 5th 2011, 17h55

Figure 2.7 View of the two cubicles located outside the B1 office room which window can be seen at the right side.

b) Building B2: Universidad Autónoma de Zacatecas (UAZ), Unidad Académica de Estudios del Desarrollo

The Autonomous University of Zacatecas is the main public university in the city; its administration is run with public funds but is independent from the government regarding academic programmes and internal decisions. The office room is located in a research complex devoted to social and human studies. Designed in 2005 by local architects, its style is regional–contemporary, adapted to the surrounding orographic environment. An exterior view of the building complex is shown in Figure 2.8 (left), while the exterior view of the building where the office room is located is shown in the picture on the right. In the latter, the window of the office room can be found on the second level at the centre (See Annex 2.1).

Figure 2.8 Exterior view of the whole building complex (left) and exterior view of the building where the office is located (right).

The orientation of the office room is southeast, and its dimensions are 4.17m x 5.25m x 2.6m (See Annex 2.2). As a single person office, only one working space can be found as well as a small round table for occasional meetings. The architectural design contributes to a sound admission and distribution of daylight into the room. The external façade is fully glazed façade (Window to Wall Radio of 90%) with two main sections divided by a column; the window panes are slightly tilted around the z axis (and not located in the same plane), as illustrated in Figure 2.10. An external overhang of 0.8m width is part of the architectural design of the building and intended for sun protection. However, the admission of sunrays from the morning until the late afternoon forces the occupants to use internal solar blinds in order to avoid glare, as is shown in Figure 2.9 (left - December 20th at 10h00) and (right - January 26th 13h30). Figure 2.11 shows a view of the back of the office room with a glass door which leads to a corridor with a window orientated to the West, allowing the admission of daylight for a short time in the evening. The monitored interior material properties are specified in Table 2.6.

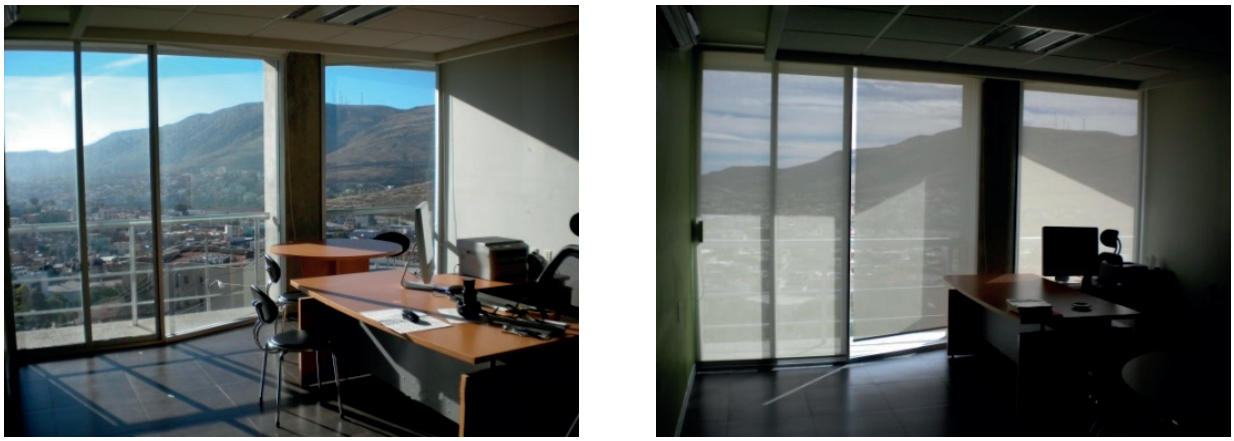

Figure 2.9 Interior view of the office room in winter at 10h00 under clear sky conditions (left) and with the internal fabric blinds for sun protection at 13h30 (right).

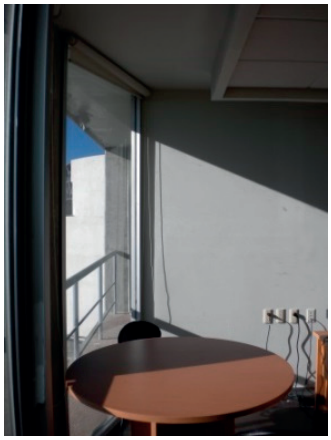

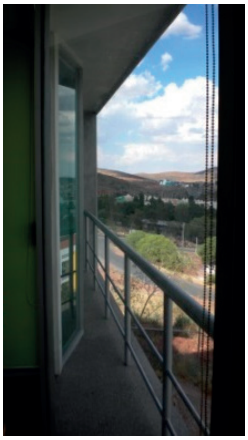

Figure 2.10 Side views of the window facade pointing at different directions and showing the diagonal position of the glazing.

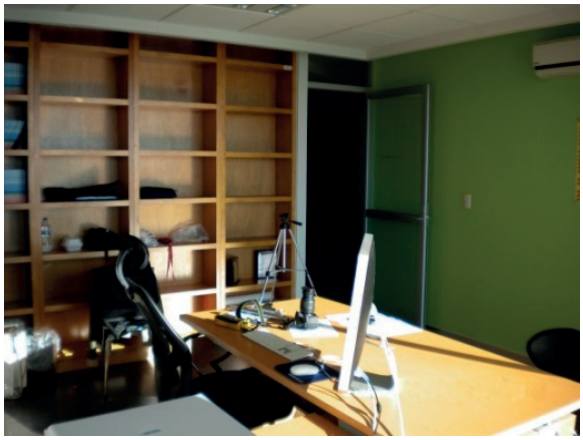

Figure 2.11 View of the back of the office room in Winter at 9h00 showing the interior furniture distribution.

After the selection of the two office rooms, the next step is to assess their existing daylight conditions. Such evaluation is done by the assessment of the interior illuminance and luminance distribution. The former is a quantifiable evaluation that is performed with the use of a Lux meter, while the surface's luminance balance can be assessed with the use of a luminance meter or with the use of images. The detailed procedure of the performed assessment is explained in the following Section.

2.3 Photometric Calibration

Due to the unavailability of monitoring equipment in Mexico, two lux meters Chauvin Arnoux C.A. 811 were borrowed from the Laboratory of Solar Energy and Building Physics (LESO-PB), their measurement range spans from 20 to 20,000 lux with a relative accuracy of ± 18% (under light sources other than incandescent lamp). Numbers assigned in the laboratory (1384 and 1386) were used to identify them for the sake of calibration and used during the building monitoring. In order to ensure that accurate results would be taken on the site, the two lux meters were calibrated using as reference a more accurate device: a Spectroradiometer Specbos 1201, JETI Technische Instrumente GmbH Jena, Germany.

Measurements for the calibration were taken at the exterior of the laboratory from 9h00 to 18h00 during three different days under different sky conditions: overcast, intermediate and clear skies. The spectroradiometer and the lux meters were placed at the same height while horizontal illuminance and luminance values were obtained with the spectroradiometer connected to a laptop. Correction factors were determined empirically that way to convert the data obtained on-site using the two luxmeters into values that would have been obtained using the precision spectroradiometer. Illustrations of the procedure can be seen in Figures 2.12 to 2.15.

A special device appropriate for travel was designed to assess on-site luminances. This consisted of a tube of 38cm with an aperture of 3° (2cm diameter) covered inside with a black foil; the tube was adapted to be placed on the sensor of the lux meter. Aside from the spectroradiometer a luminance meter (LS-110 Minolta) was also used as a reference device for the sake of calibration. The measurements were taken by directing the tube toward a white diffusing paper attached to a wall; the operation was repeated every hour from 9h00 to 18h00 (Figure 2.15). The results of the lux-meters calibration for luminance and illuminance obtained for the three different sky conditions are shown in Table 2.1. The graphs of the results are shown in Figure 2.16 which shows that the lux meter 1384 is characterized by a better correlation for lower values of illuminance, while the calibration of the lux meter 1386 (for luminance measurements) shows a more linear fit, especially under clear and overcast sky conditions. The error bars were defined according to the relative accuracy of the lux meters (18%).

	Illuminance Luxmeter1384	**Illuminance Luxmeter1386**	**Luminance Spectroradiometer (lux meter1386)**	**Luminance Minolta (lux meter1386)**
Overcast Sky	1.150710	1.154401	0.000141	0.000129
Intermediate Sky	1.249917	1.338562	0.000095	0.000845
Clear Sky	1.285518	1.510098	0.000123	0.000126

Table 2.1Correction factor obtained for the two lux meters Chauvin Arnoux C.A. 811 for illuminance and luminance measurements.

Figure 2.12 Lux meters and reference spectroradiometer positioned for the calibration

Figure 2.13.Lux meters and reference spectoradiometer placed at the exterior of LESO-PB.

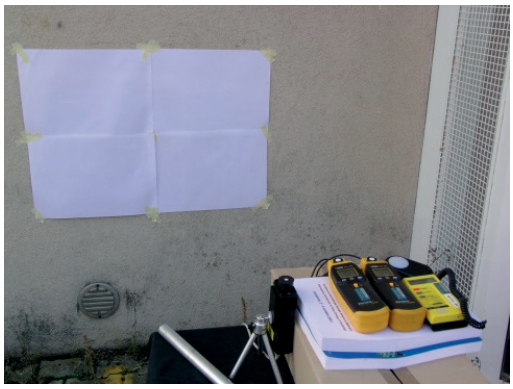

Figure 2.14 Luxmeters and spectoradiometer set-up for calibrations.

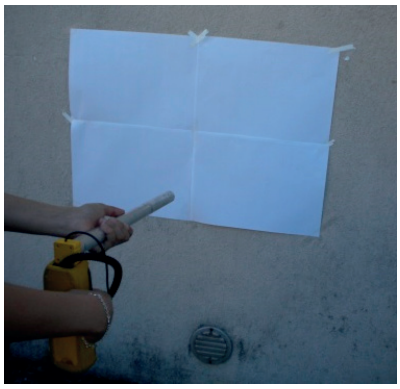

Figure 2.15 A view of the method employed for the lux meters and its black tube for luminance calibration.

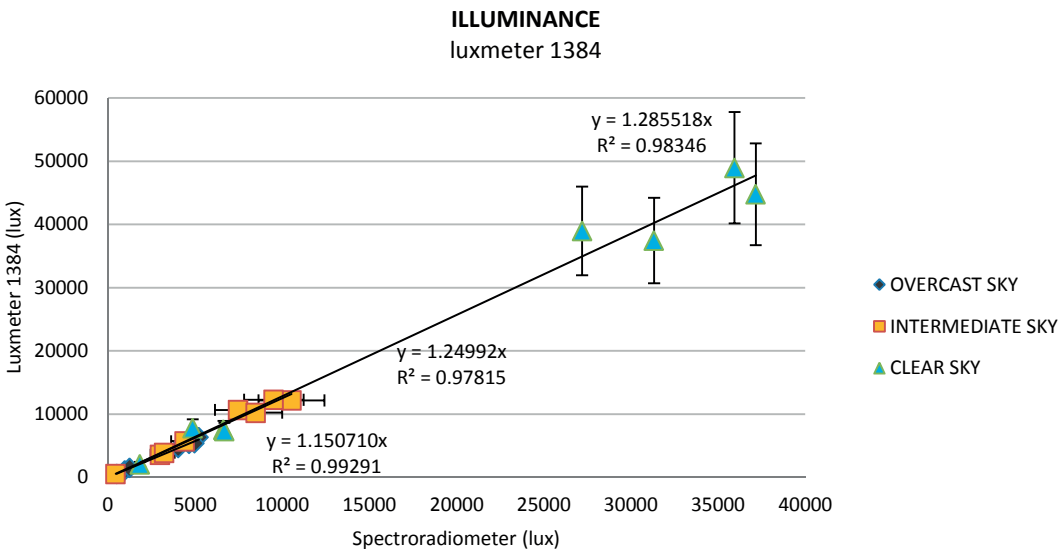

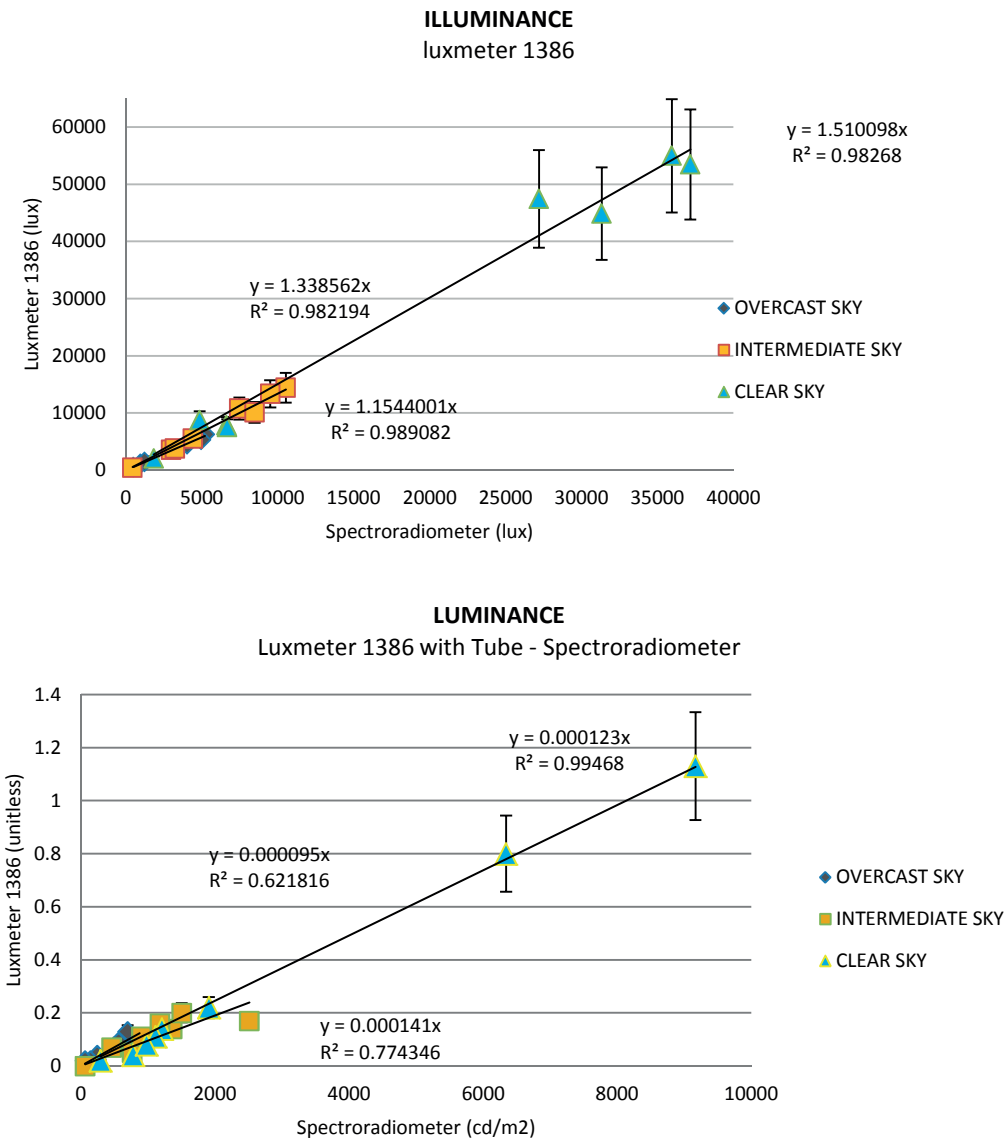

Figure 2.16 Graphs of the linear correlation obtained for the calibration of the lux meters using the spectroradiometer as reference device.

2.4 Daylight On-site Monitoring

In order to identify the limitations and particularities of the current daylighting situations in both office rooms, an on-site daylighting performance assessment was carried out at different periods of the year from 2011 to 2013: spring equinox, and winter and summer solstices. Reliable monitored data was collected using several sets of measurements; those were required in order to become familiar with the monitoring procedure and to achieve the collection of data for different sky conditions (overcast, intermediate and clear). Local meteorological conditions only offered a few hours of overcast sky, therefore the data monitoring had to be rescheduled more than once in order to achieve reliable data sets. Those that were finally used to compare with the simulations results based on virtual models were obtained at the dates listed in Table 2.2.

	Building B1	Building B2
Winter Solstice	December 20th 2013	December 17th 2013
Spring Equinox	March 21th 2013	March 20th 2013
Summer Solstice	June 21th 2012	June 20th 2012

Table 2.2 Dates at which the monitored data used to compare the simulation results was obtained.

Light, as defined by the Illuminating Engineering Society of North America (IESNA), is related to the human visual perception: 'light is radiant energy that is capable of exciting the human retina and creating a visual sensation' [75]. A sound interior daylighting condition is obtained when different aspects related to human vision interact together in a way that a high level of visual performance is allowed [89]. In order to evaluate the daylight condition in an interior space, its performance regarding quantitative and qualitative aspects are assessed. The former refers to the daylighting provision that allows the perception of the surrounding environment, while the latter refers to the possibility of perceiving such environment without disturbances. The lighting quality in working spaces has been mainly assessed under artificial lighting conditions. Nevertheless, such studies have helped to identify the main factors influencing the perception of the environment as well as their interaction that may lead to the creation of a sound interior visual environment. In a study dealing with the lighting quality of working spaces, three main factors were identified: visual capability, visual comfort and visual perception [90]. By their constant interaction, they influence the light conditions by affecting the task performance, the competence, mood and motivation to perform a visual task, hence the feeling of health and well-being [90, 91]. In order to improve the mutual interaction of the three main aspects and thus the quality of daylight in a room, an optimized distribution of the two main photometric variables work plane illuminance (lx) and luminance (cd/m²) – is commended.

2.4.1 Workplane Illuminance

Illuminance is defined as the density of the luminous flux incident on a surface, which is the quotient of the luminous flux by the area of the surface when the latter is uniformly illuminated [75]. A method for determining sufficient illumination levels for task performance which takes into account visibility as a physiological process was published by the Comission Internationale de l'Eclairage (CIE) [92]; later such definitions were complemented with studies of performance related to visual efficiency [91, 93]. Different authorities in the lighting field established recommendations regarding the minimum lighting levels for performing different human activities: Illuminating Engineering Society of North America (IESNA) recommends maintaining illuminance levels at or below 500 lx on the horizontal working plane [75, 94]; others recommend maintaining the horizontal workplane illuminance in the range of 300-500 lx [95, 96]. In order to perform a better quantifiable assessment of the daylighting distribution in a room two metrics related to illuminance were firstly used in this PhD thesis:

a) Daylight Factor –DF- (%)
It is the ratio of the indoor illuminance on a given plane by the simultaneous outdoor global illuminance measured on a horizontal plane for an unobstructed overcast sky assumed to be characterized by a Moon and Spencer luminance distribution [75]. Direct sunlight is excluded from both interior and exterior illuminance measurements [81, 97]

b) Illuminance Ratio -IR- (%)
It is the ratio of the horizontal workplane illuminance measured in the interior space by the global horizontal illuminance measured outside in the absence of obstructions. In contrast with the daylight factor, illuminance ratio include measurements taken under clear and intermediate sky conditions [27, 98].

2.4.2 Room Surfaces Luminance

Luminance describes the physiological effect of light on the eye. It indicates the brightness of an illuminated or luminous surface as perceived by the human eye [99]. Its measurement unit is the one of a luminous intensity per unit area, e.g. candela per square meter (cd/m²). The recommended luminance values for interior surfaces are given in Table 2.3.

Walls	50–100 cd/m^2
Ceiling	100–300 cd/m^2
Working plane	100–300 cd/m^2

Table 2.3 Recommended luminance values for interior spaces [96].

A way to assess the luminous distribution in a room is by comparing the ratio between the luminance of an object and its immediate background, which is called luminance contrast or luminance ratio [75]. In spaces illuminated by daylight, the contrast between the area next to the window and the back of the room are often a source of discomfort glare. In order to avoid visual disturbances to the occupants, the luminance ratio between different areas in the visual field should be kept within a range. The corresponding recommendations are listed in Table 2.4. However, even if such recommendations refer mainly to artificially lit environments, they can be also applied to daylit spaces in order to provide a reference scenario.

	Recommended Value	Maximal Value
Between workplace and the paper	1:3	1:3
Between screen and workplace	1:5	1:10
Between the screen and surroundings	1:15	1:40

Table 2.4 Recommended Luminance ratios [97].

In order to perform the assessment of the current daylight situations in the two office rooms, the following data was collected on-site: indoor and outdoor illluminance (lx), luminance of interior surfaces (cd/m²), building orientation, hourly sun position (azimuth and elevation), sky luminance (cd/m²) and interior material photometric properties (glazing transmittance and soil and wall reflectance, etc.). Table 2.5 shows details of the on-site collected data, the equipment used as well as the sky conditions during the measurements period.

	Variable/Unit	Instrument	To determine	Sky conditions
a	Interior and exterior illuminance (lx)	Lux meter ChA 1384 & 1386	Daylight factor (%) Illuminance ratio (%)	Overcast, Intermediate and Clear
b	Interior surface luminance (cd/m2)	Lux meter ChA 1384 with black tube	Luminance ratio, Reflectance of interior surfaces (walls, ceiling, floor) (%)	Overcast
c	Glazing transmittance (%)	Lux meter ChA 1384 with black tube		Overcast
d	Building orientation	Compass		
e	Hourly sun position	Sundial		Clear
f	Sky luminance (cd/m2)	Lux meter ChA 1384 and with black tube		Overcast, Intermediate and Clear

Table 2.5 Parameters of the on-site monitored data, including the monitoring instrument, calculated metrics and sky conditions.

The working office hours in Mexico are typically from 9h00 to 14h00 and from 16h00 to 20h00. However, measurements of the indoor photometric variables were carried-out at hourly time steps from 9h00 to 18h00, a time-frame when daylight is usually available. The interior and exterior illuminances were monitored simultaneously using the two calibrated lux meters, for which a transceiver portable radio was employed in order to obtain simoultaneous interior and exterior illuminance lectures, a time-lapse of about 10min occurred between the first and the last lecture corresponding to the last measurement point inside the room. The DF (in case of overcast sky conditions) and the IR (for intermediate and clear sky conditions) were then calculated, such difference was estimated by visual observation, the sky condition was considered as overcast when no shadows were projected in the surrounding environment and the sun covered by the clouds was not visible in the sky. The indoor illuminance was monitored using a grid of points placed at 1.0m distance from each other, starting at 0.2m from the window and at 1.0m from the adjacent wall at the standard height of the working surface (0.75m) (such practice replicates similar procedures performed in previous studies [43]), for a total of 25 measurement points for B1 and 20 for B2. Additional measurement points were placed every 0.2m in the centre of the room in order to obtain a detailed profile of the daylight distribution. A description of the on-site measurements layout of the two buildings is shown in Figure 2.17.

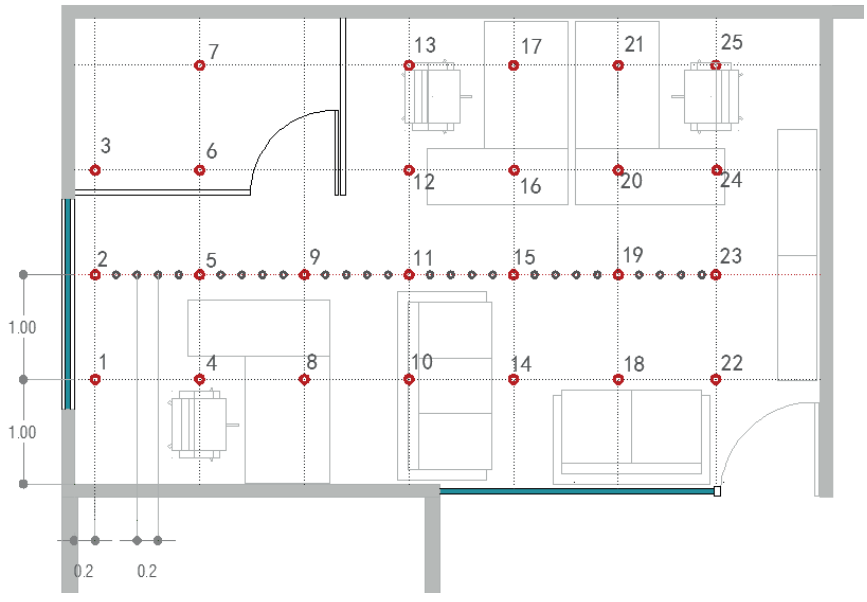

a)

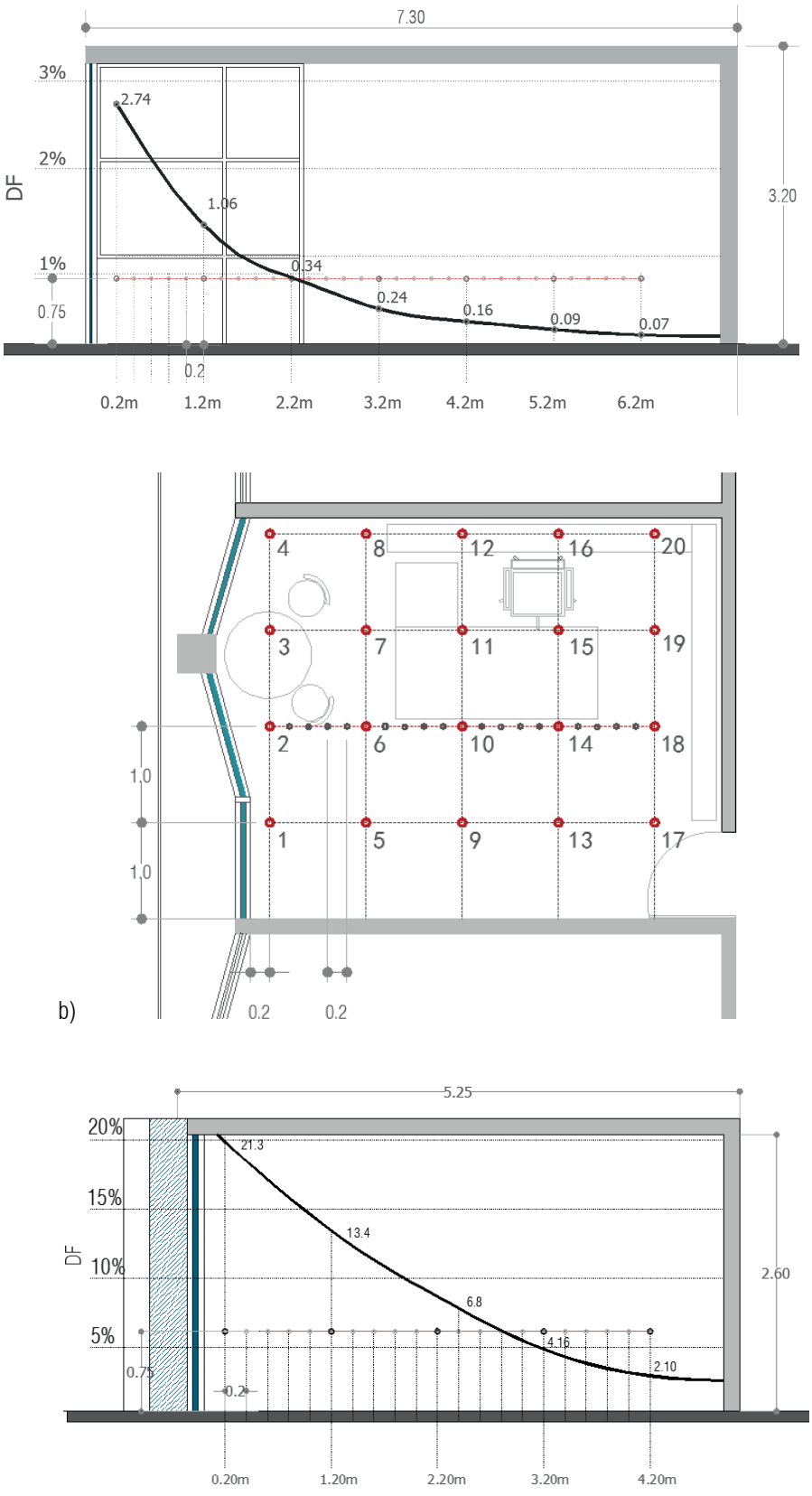

Figure 2.17 Grid points placement in a top view of room of Building B1 (a) and B2 (b) for the monitoring of the illuminance distribution, the room's section with the DF profile is also shown.

In a next step, pictures of the monitored scene were taken each hour from different viewpoints in order to visualize the dynamic evolution of the interior daylight distribution to assist in the calibration of the virtual model. The photographies were shot using Nikon S-230 digital camera, which was available on-site during the first monitoring sets. At the beginning of 2013 a Nikon 5100 digital camera was also available which allowed higher quality pictures to be taken using different exposures (necessary to create HDR images), a fisheye lens of 46-52mm focal-length was used to capture views of the sky and of the room.

In order to determine the luminance ratio among the different interior surfaces located within the occupant's visual field, luminance (cd/m²) were monitored using the 'adhoc' designed luminance meter (see Figure 2.15), such measurements were taken from the occupant's position at each working place pointing to the interior surfaces located within the occupan'ts visual field as it is shown in Figure 2.18 for Building B1 (a) and for B2 (b). The latter was also used to assess the bi-hemispherical reflectance (ρhh) of the interior surfaces (floor, walls, and ceiling) by measuring simoultaneously their luminance and the vertical illuminance on the surfaces under overcast sky conditions [97, 100]; white and grey diffusive papers (Lambertian type) were used as reference using the following equations:

$$\boldsymbol{\rho} = \pi \ (\mathrm{L}) \ / \ \mathrm{E} \tag{2.1}$$

$$\rho 1 = \left(\frac{Lsurface}{Lwhite}\right)$$

$$\boldsymbol{\rho} 2 = \boldsymbol{\rho} gray \left(\frac{Lsurface}{Lgray}\right)$$

$$\boldsymbol{\rho} hh = \frac{(\boldsymbol{\rho} 1 + \boldsymbol{\rho} 2)}{2} \tag{2.2}$$

Where:
L is the measured surface luminance (cd/m²)
E is the measured vertical illuminance (lx)
$\boldsymbol{\rho}$ Is the reflectance of the corresponding surface.

The bi-normal transmittance of glazing was also determined using the 'adhoc' device, by measuring the luminance normal to the glazing pane as well as the luminance behind the glass in both offices [100], as explained in the following formula:

$$\tau \, nn = Lin/Lout \tag{2.3}$$

a)

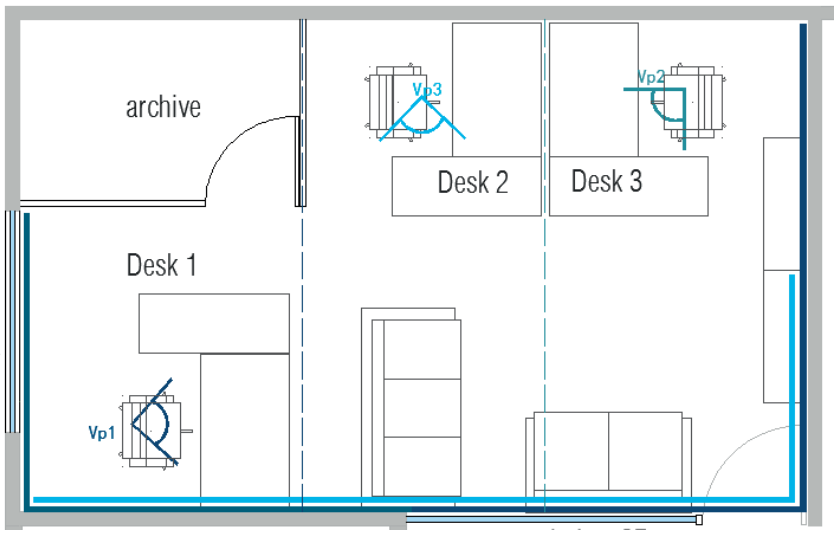

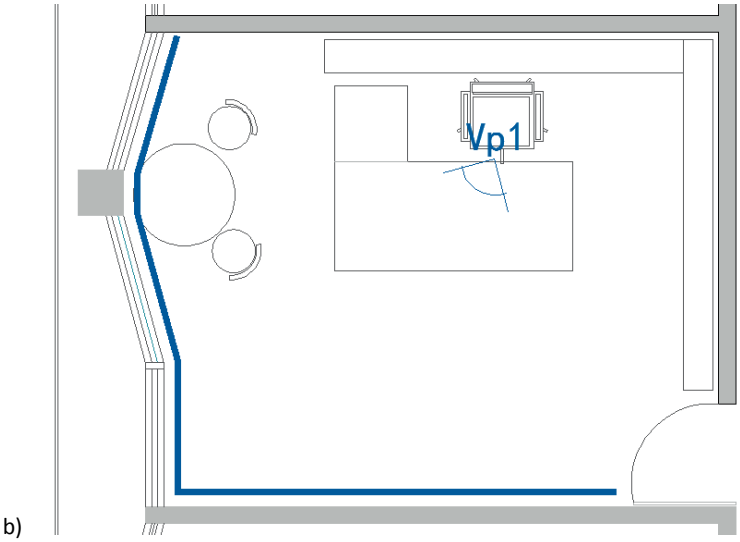

b)

Figure 2.18 Floor plan of B1 (a) and B2 (b) indicating the view point positions in each working space, highlighted in color to correspond each view point.

The monitored data was used first to input the photometric properties of the surface materials of the two office rooms in a virtual model, the latter was then calibrated using the monitored work plane illuminance data. The correspondence between the existing rooms and their virtual models was assessed by comparing the monitored DF and the IR profiles into the rooms with those obtained with RADIANCE simulations. The whole procedure is explained in the following Section.

2.5 Virtual model calibration

2.5.1 Sky virtual models

IESNA defines daylight as the part of the energetic spectrum of electromagnetic radiation within the visible waveband that is emitted by the sun and received at the surface of the earth [75]. Sunlight represents the direct component of daylight while the diffuse component reflected by the sky is the result of scattering and absorption in the earth's atmosphere [81]. The illumination produced by the sky depends on its luminance which varies according to climate and geo-physical variables, such as the sun position, cloudiness and/or air pollution. The sun and sky luminance distribution can be used to determine the solar irradiance and illuminance, therefore a precise knowledge of the sky luminance pattern is crucial for the daylighting simulation if one wants to perform accurate predictions of daylight fluxes indoors. Standard sky models have been created to classify and reproduce the spatial luminous distribution of daylight, the simplest model being the uniform luminance sky distribution which implies a sky of constant luminance over the sky vault covered with thick clouds where the sun is not visible. However, the occurrence of such sky has been considered unrealistic [81]. The CIE adopted accordingly as Standard Overcast Sky a model proposed by Moon and Spencer in 1942, which better approximates the luminance distribution of overcast skies with relative gradation from dark horizon to bright zenith [101, 102]. The luminance distribution that represented sky conditions close to a perfectly clear sky was suggested by Kittler in 1967 and adopted by the CIE as the standard model for clear skies [103-105]. These standards represent the luminous characteristics of two extreme sky conditions; however they fail to represent the constant changes observed in the majority of sky conditions. Additional sky models were proposed to account for the luminance distribution occuring in between overcast and clear skies [49, 106-110]. The CIE adopted as Standard General Sky the model suggested by Kittler, Darula and Perez that incorporates 15 standard relative luminance distributions as a result of different combinations of five geometrical parameters; this model covers the spectrum of all the possible sky distributions existing in nature [111-114]. However, its use requires data which is only available in a few countries, such as the measured luminance of arbitrary sky elements (cd/m²) and the global and diffuse horizontal illuminance (lux). Nonetheless most meteorological stations around the world record data of global horizontal irradiance which is a measure of the total energy flux (W/m²) incident on a horizontal surface. The way of obtaining luminous values from radiation data is to use the daylight luminous efficacy which is defined by the quotient of the luminous flux by the radiant flux [75]. Luminous efficacy of daylight is difficult to evaluate due to the constant daylight variations, given that it depends on solar altitude, cloud cover and water vapour in the atmosphere [81]. However, some studies have determined a luminous efficacy of diffuse radiation ranging between 84 and 173 lm/W; while for direct radiation it was established between 50 and 120 lm/W (for a solar altitude greater than 10°) [81].

Different luminous efficacy models using the global solar irradiance as an input have been proposed to model clear sky conditions [115, 116] as well as for other sky types [117].

In the RADIANCE lighting software the sun and the sky vault are treated as light sources distant from the local scene. The virtual sky is steady state, modelled as a 180° light source providing the effect of a distant dome while the sun is represented as a changeful source with a very narrow angular diameter. In order to generate the virtual sky and characterize its brightness, two RADIANCE function routines are used: a) Gensky and b) Gendaylit.

a) Gensky

Gensky produces the sun and the sky brightness distribution using the CIE Standard Sky Models which correspond to overcast, clear or intermediate skies. The geographic location is given as an input specified in degrees of longitude and latitude to generate the diffuse daylight component of the sky vault as well as the direct sunlight component, while the meridian angle is given to establish the time zone. The month, date and hours are required to generate the sky conditions. The latter can be better characterized using available data of global horizontal illuminance with the –b (zenith radiance) and –B (horizontal diffuse irradiance) options. If data of the sun radiance is available it can also be provided using the –r option, or the –R option for horizontal direct irradiance. If no parameters are specified, *gensky* generates the sky luminance distribution using the standard functions [36]. Particular sky conditions need to be specified using the variables +s/-s (with or without sun), +i/-i (for intermediate skies) and –c for overcast sky conditions.

b) Gendaylit

Gendaylit produces the sky description based on the Perez All-Weather model [49] using input data from the meteorological local conditions such as: direct normal and diffuse horizontal irradiance (W/m²), direct-normal and diffuse horizontal illuminances (lm/m²) or directly using the Perez parameters (epsilon, delta). In order to create the sky description, the geographical location of the site, the date and local standard time are required as input, or the sun position can be directly given by providing the coordinates of the sun azimuth and elevation. By using the input parameters, gendaylit automatically determines the sky luminance distribution, there is only a need to specify the presence or absence of the sun by using the +s or –s option. The output can also be defined as visible radiation (W/m²/sr), solar radiation (W/m²/sr) or luminance (lm/m²/sr).
Among the two available RADIANCE sky generators, the *gendaylit* was selected to reproduce the sky luminous distribution of the location site in the virtual model, given that it describes the sky features closer to reality by using the direct and diffuse component of solar irradiance as input. The data of global horizontal irradiance (W/m²) was obtained from the closest local meteorological station to the site of the two buildings (an approximate distance of 5km). Then the global-to-direct irradiance Perez conversion model [118] was employed to transform global horizontal irradiance data (Igh; W/m²), to diffuse horizontal (Idh) and beam normal irradiances (Ibn). The geographical location of the site was given by providing directly the sun position in azimuth and elevation degrees, measured on-site at hourly time steps using a sundial [119] during the monitoring. Aside from the RADIANCE sun-generating functions, these monitored data (altitude and elevation) was also double checked using the CitySim program for urban energy planning which uses the equation of time to calculate the sun's coordinates [120].

2.5.2 Virtual room models

Two virtual models that reproduce the characteristics of each office room were created using Google SketchUp a program for architectural 3D modelling. Data collected on-site such as the interior surfaces properties (reflectance, transmission), the building dimensions and placement of the interior furniture were used to create a virtual model. Exterior views of the two virtual models are shown in Figures 2.19 (B1) and 2.20 (B2), interior views are illustrated in Figures 2.21 (B1) and 2.22 (B2).

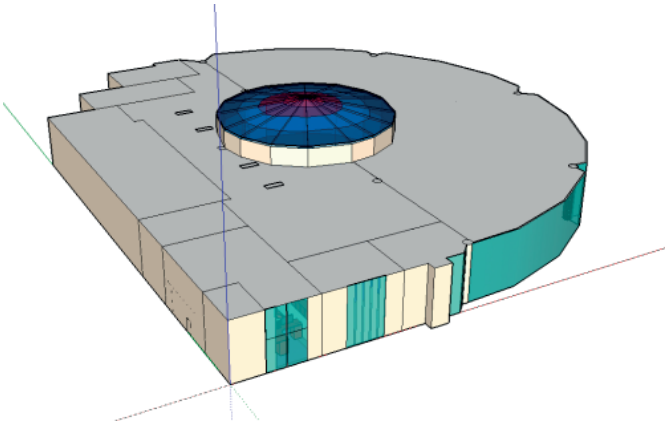

Figure 2.19 Perspective view of the virtual geometric model of Building B1.

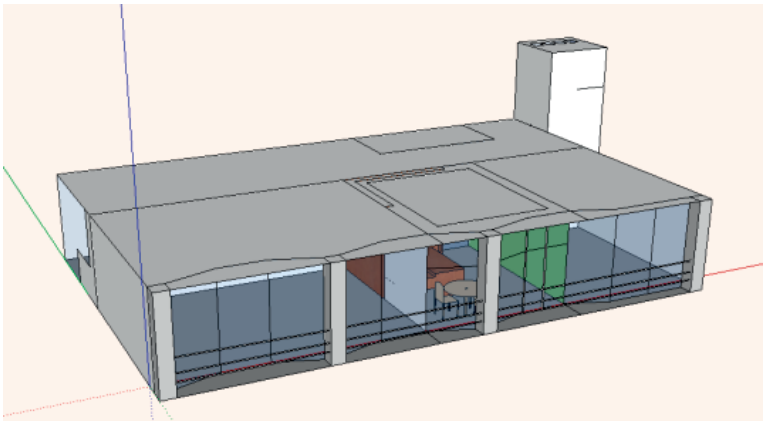

Figure 2.20 Perspective exterior view of the geometric model of Building B2.

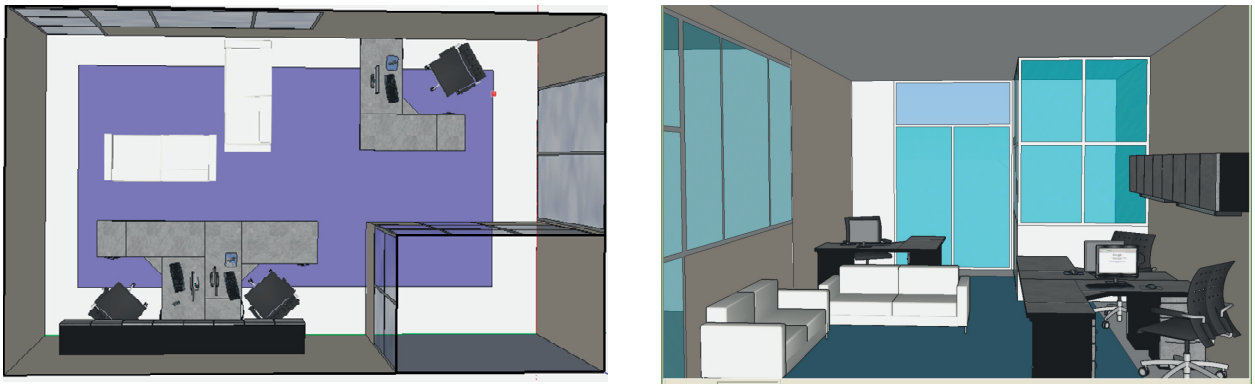

Figure 2.21 Top view of the virtual model of B1 (left) and front view from the back of the office's room (right).

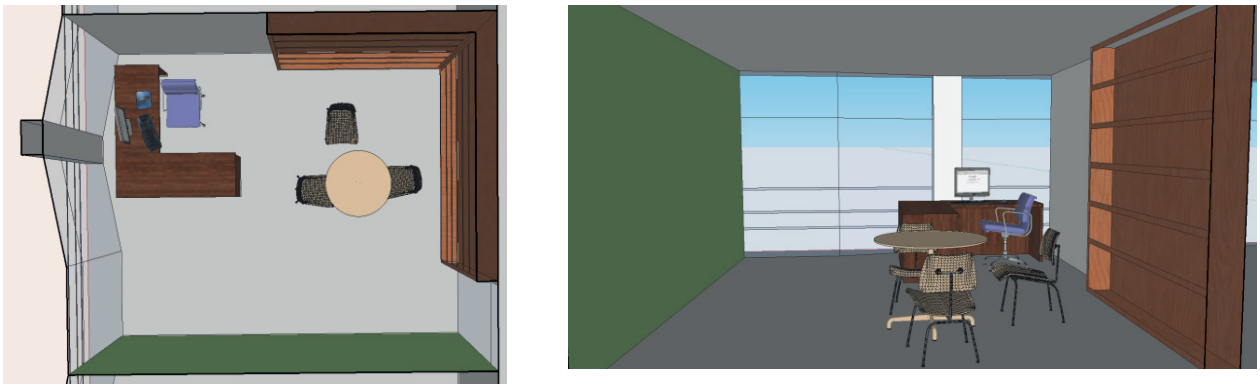

Figure 2.22 Top view of the virtual model of B2 (left) and inside view from the back of the office room (right)

Once that the virtual models were characterized in accordance with the monitored rooms, they were exported to the RADIANCE format using the RADIANCE exporter script for Sketchup [121]. As a following step, computer simulations were carried out using the virtual models to obtain exterior and interior illuminance, which were used to calculate the DF and the IR values, to compare them later with those obtained by monitoring. In order to do this, measurement points were placed in the virtual model reproducing the grid of measurement points placed in the two existing office rooms (Figure 2.17). Additionally, renderings of the interior of the virtual model were generated from different viewpoints in order to visually describe the simulated interior daylight situation and to compare them with the pictures taken during the on-site monitoring process.

The first comparison of the DF and the IR simulated values with the corresponding monitored data showed substantial differences mainly in the Building B1 (library office). Such discrepancies were first attributed to mistakes in the values allocated to the model parameters in order to to fit to the real situation. Therefore, in order to obtain a better agreement of the virtual model with the real building, several model parameters were adjusted such as: the geographical orientation of the office rooms, the transmission factor of the exterior glazing and the reflectance factors of the interior material surfaces; these properties had to be adjusted several times according to the data collected during the different on-site measurements campaigns in México. The final values of the interior material properties used in the virtual model are shown in Table 2.6.

		B1		B2		
Interior Room Surface	**Parameter**	**Monitored Data**	**Virtual Model**	**Interior Room Surface**	**Monitored Data**	**Virtual Model**
Internal wall	Reflectance (%)	0.51	0.51	White wall	0.705	0.705
White ceiling		0.75	0.75	Green wall	0.51	0.519
Floor (blue carpet)		0.10	0.10	White ceiling	0.78	0.78
Floor (grey carpet)		0.13	0.3	Floor (grey)	0.40	0.4
External glazing (SW window)	Transmittance (%)	0.12-0.15	0.13	External glazing	0.68	0.74
Internal glazing (NE window)		0.65	0.71	Internal glazing (door-up)	0.60	0.65
				Internal glazing (door-down)	0.50	0.55

Table 2.6 The monitored interior material properties of B1 and B2 and those applied to the virtual model.

Additional problems were found during the calibration procedure of the virtual model, attributed to discrepancies in the weather data delivered by the local meteorological station in Mexico; the latter were corrected. It was also observed that unbalanced values between the Idh (Diffurse Horizontal Irradiance W/m^2) and Ibn (Direct Normal Irradiance W/m^2) variables were found when using Maxwell model to transform the Igh into these varaibles, especially under clear sky conditions. This suggested that the the Maxwell model is not appropriate for transforming Igh data for predominant clear sky conditions. In order to overcome this problem, the global-to-direct irradiance Perez conversion model [118] was used to obtain the Ibn and Idh irradiance components; the later were then used to determine the sky luminance distribution at the location site using the *gendaylit* sky generator, based on the Perez All-Weather model [49] as explained in Section 2.5.1. After applying these modifications, the simulation results showed a better convergence with the monitored data. Once the calibration of the virtual models was satisfactory enough, they could be confidently used to simulate the daylight interior environment of the two offices for different periods of the year. In order to obtain accurate simulation results, appropriate values were given to the RADIANCE simulation parameters, as listed in Table 2.7.

	Illuminance Calculation	**Image Renderings**
Ambient bounces (-ab)	9	6
Ambient resolution (-ar)	128	64
Ambient accuracy (-aa)	0.1	0.1
Ambient divisions (-ad)	16384	4096
Ambient super samples (-as)	4096	1024
Direct jittering (-dj)	0.9	0.9
Direct certainty (-dc)	0.17	0.17
Direct subsampling (-ds)	0.01	0.01
Direct pretest (-dp)	4096	4096

Table 2.7 RADIANCE simulation parameters for the calibration of the virtual models, for illuminance calculation and image renderings.

2.6 Simulation results

Comparisons of simulated and monitored DF and IR profiles in the office rooms were used to assess the pertinence and robustness of the virtual models. Renderings of interior views were also generated and compared with pictures taken on-site. A relative error of 18% was estimated for the on-site monitored data and applied during the comparison with the simulation results; it is the range of accuracy of the Chauvin Arnoux Luxmeters for light sources other than incandescent lamps [122].

In Building B1, a significant difference was observed between these profiles, especially between 9h00 to 12h00, which evidences the difficulties encountered to accurately simulate a daylighting flux entering from the SouthEast window (which leads to the atrium space) as shown in Figure 2.4. Due to the building orientation, the room is mainly illuminated in the morning by a daylight flux crossing the atrium through the SE window. This area is partially lit by the round-shaped dome as well as by a Southwestern window located in two cubicle glazed rooms that are constantly used by students (See Figure 2.7). Achieving accurate predictions of the daylight flux coming from the dome was difficult since a translucent black fabric permanently covers it, which replication in the virtual model was challenging. In the two cubicles the manipulation of the vertical blinds during the day was difficult to handle with, and might have led to imprecision for the virtual model. Nevertheless, a better correspondence was found between the monitored and simulated DF and IR profiles from 13h00 to 18h00. The close fit of the profiles during this time of the day suggests that the calibration of the virtual model was reasonably fulfilled and that reliable results could be obtained from the computer simulations used for parametric studies (focusing on differential results and not on absolute values). In the case of Building B2, the modelling of the office room presented fewer difficulties, however discrepancies were still observed among the two profiles, especially for the area close to the window. The latter occurred mainly when comparisons were carried-out at the summer solstice under predominantly intermediate sky conditions, which might be explained by modelling difficulties of the sky luminance distribution (high variables compared to clear skies). A better correspondence was obtained at the winter solstice and spring equinox, when monitoring was performed under prevailing clear-sky conditions. The relative errors MBE (Mean Bias Error) for each of the time steps presented in this section were calculated to show the differences between the on-site monitoring and the simulation results relative to the distance from the window. Virtual model calibration results can be discussed as follows:

2.6.1 Calibration under overcast sky conditions

a) **Building B1:** The comparison of the monitored and simulated DF profiles of B1 office room is shown in Figure 2.24. The DF profile presents a close fit between the monitored and the simulations in the area close to the window. A significative difference can be observed between the monitored data and the simulations in the centre of the room from a distance of 1.0m to 3.0m from the window which might be explained by the presence of some obstacles interfereing with the daylight transport in this area of the room; however, the profile shows a closer fit at a distance of 4.0m to the back of the room. The corresponding renderings are shown in Figure 2.25, while a view of the existing situation is shown in Figure 2.23. The MBE (Figure 2.24) show that a maximum difference of 120% is found in the central area of the room while at the back of the room the maximum difference would correspond to 68%. The MBE of the correlation is 56%.

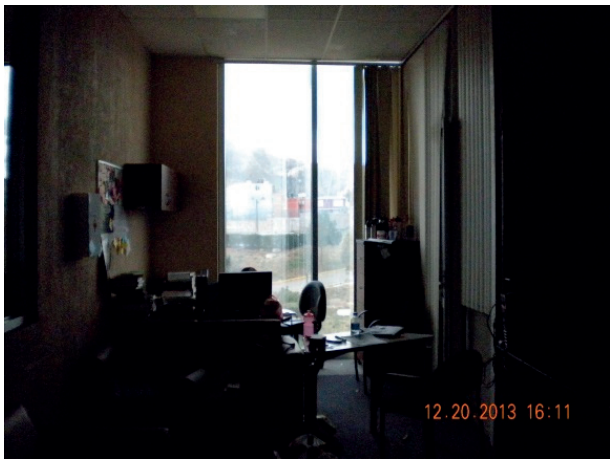

Figure 2.23 Interior view of B1 under overcast sky conditions (20th december 2013, 16h00 LT)

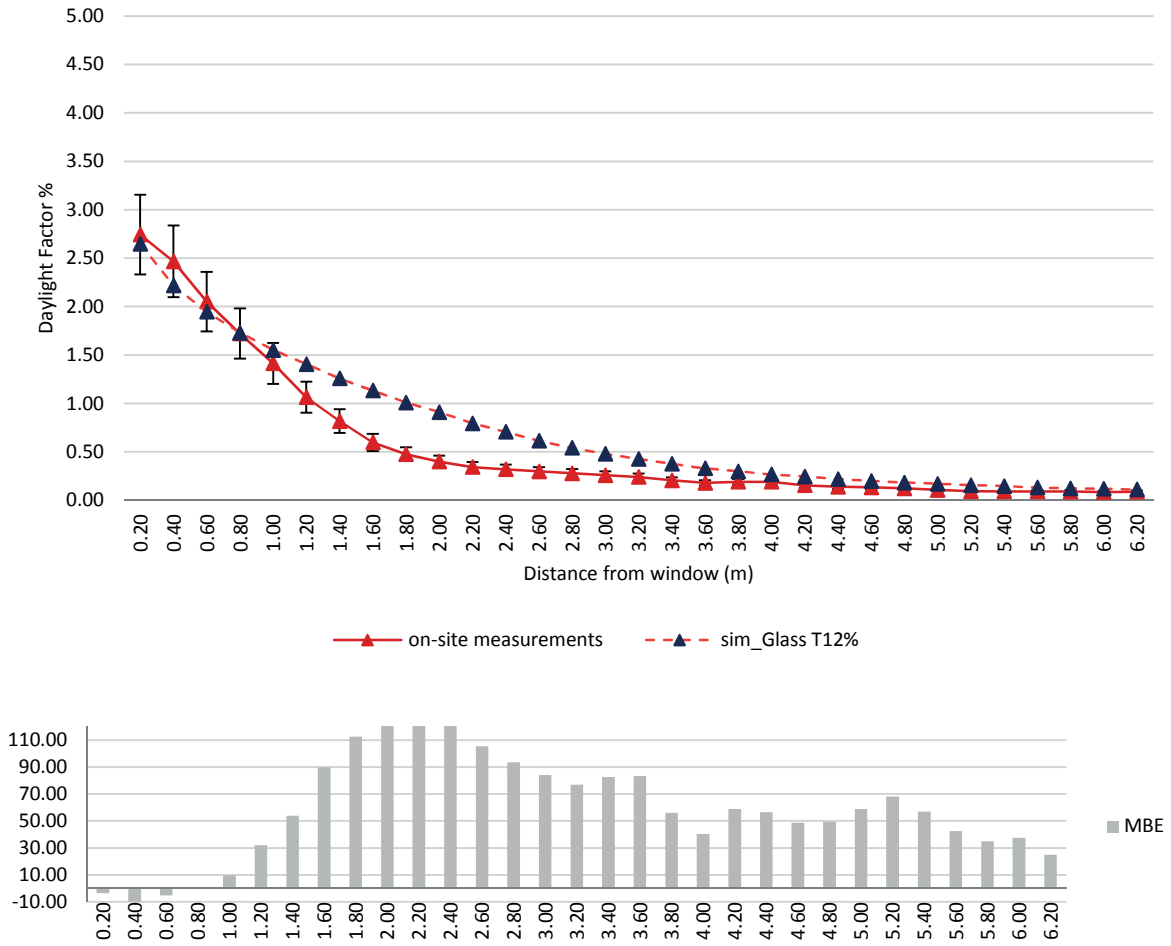

Figure 2.24 Comparison of the simulated DF profile with the monitored data for Building B1, the MBE relative to the distance from the window are shown below.

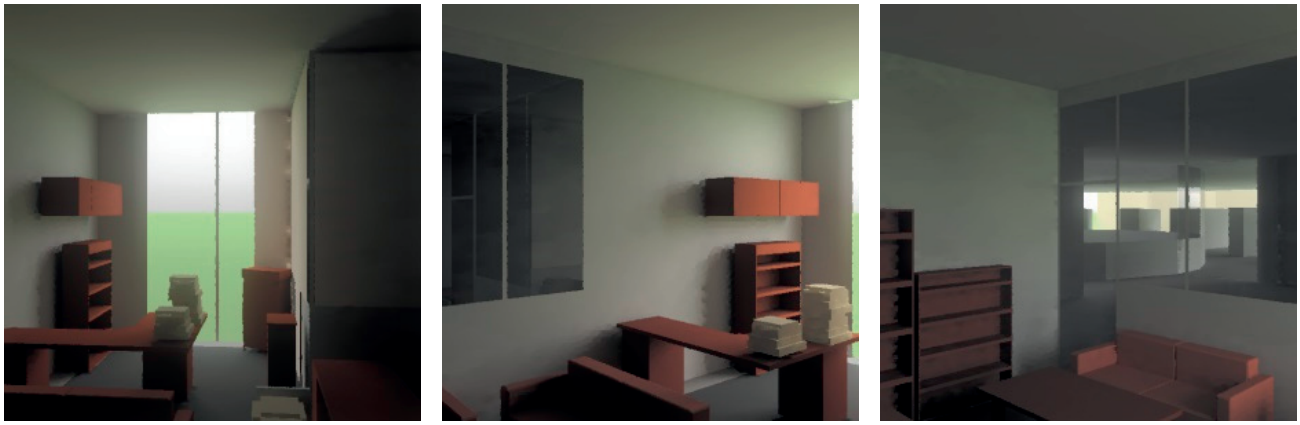

Figure 2.25 Renderings of interior views from the back (left) and the side (centre and right) of the office room located in B1.

a) **Building B2:** The monitored DF of B2 office room shows a similar profile to the one by simulations, the relative difference is close to 2% in the area next to the window, the profile coinciding almost exactly in the middle and at the back of the room (Figure 2.27). A view of the interior of the room is shown on Figure 2.26, while the computer renderings are illustrated on Figure 2.28. The MBE shows a maximum error of 52% at 2.0m distance from the window, while negative errors are found through the room with a maximum of -8% at 1.2m from the window. The Averaged MBE of the correlation is 4%.

Figure 2.26 Interior view of B2 office room under overcast sky conditions (January 27th 9h30 LT).

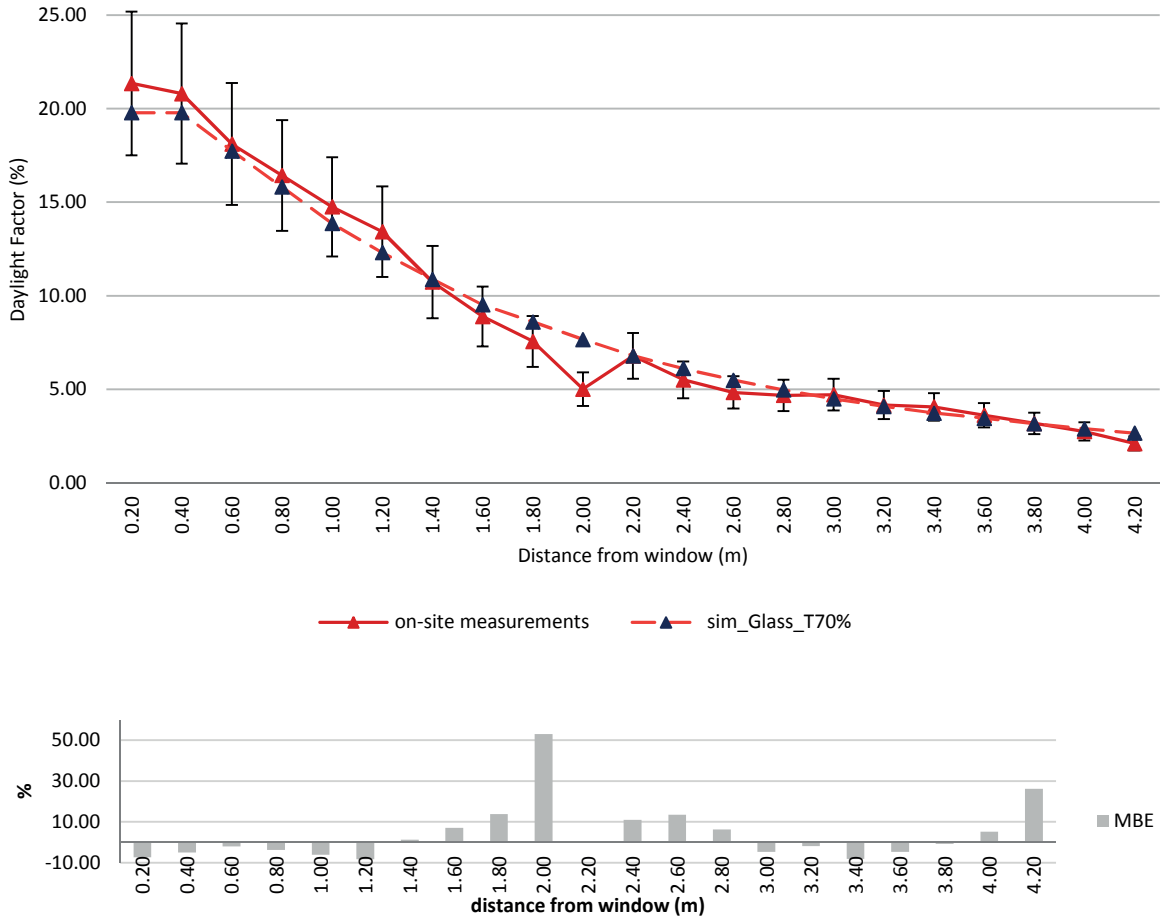

Figure 2.27 Comparison of the simulated DF profile with the monitored data for the B2 office room, the MBE and RMSE are shown below.

Figure 2.28 Renderings of the interior views from the back of the virtual model of the Building B2 office room under overcast sky conditions.

2.6.2 Calibration under clear and intermediate sky conditions

The comparison of the illuminance ratio profiles (IR profiles) obtained with the RADIANCE simulations with monitored data are presented for the three days during which the room was monitored: spring equinox, and winter and summer solstices. The room was monitored from 9h00 to 18h00, a total of 30 hours of monitored data were created for each building from which rendered scenes were generated and compared with reality; however due to space limitations only the the results for the hours 15h00 or 17h00 in the case of B1, and for 9h00 or 12h00 in the case of B2 will be presented. Those are the times where the sun is facing directly on the room's facade, representing the most critical moments during the day regarding the indoor daylight conditions.

2.6.2.1 Summer solstice

Building B1: The comparison of the IR profiles for summer solstice (June 21st 2012, 15h00 LT) for intermediate sky conditions is shown in Figure 2.30. An absolute difference of 1.2% IR can be observed when comparing both results in the area next to the window; a better correspondence is found between the profiles through and at the back of the room. The picture of the monitored room is shown in Figure 2.29 in order to compare with the renderings obtained with the simulations. In Figure 2.31, a view of the simulated room from the back of the room is shown first (left), the SE wall is shown next and the atrium space seen through the SE window, a picture of the back of the room from the exterior window is shown on the right. The MBE also shown in Figure 2.30 shows that high differences are found mainly at the back of the room, whith the highest difference found at 4.2m with 110% difference between the simulation and the on-site measurements. The MBE of the correlation is 102%.

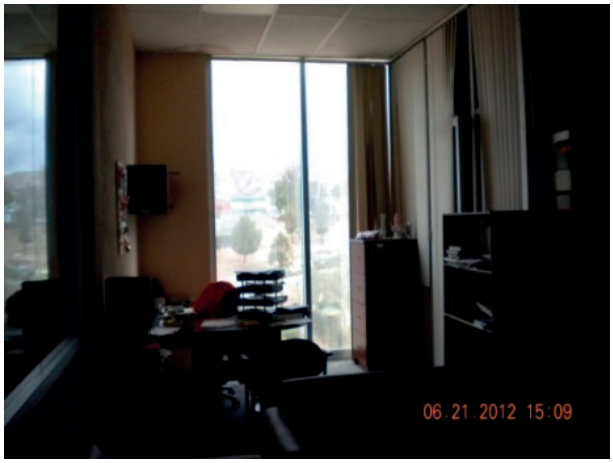

Figure 2.29 Interior view of the B1 monitored room under intermediate sky conditions (June 21st 2012, 15h00 LT).

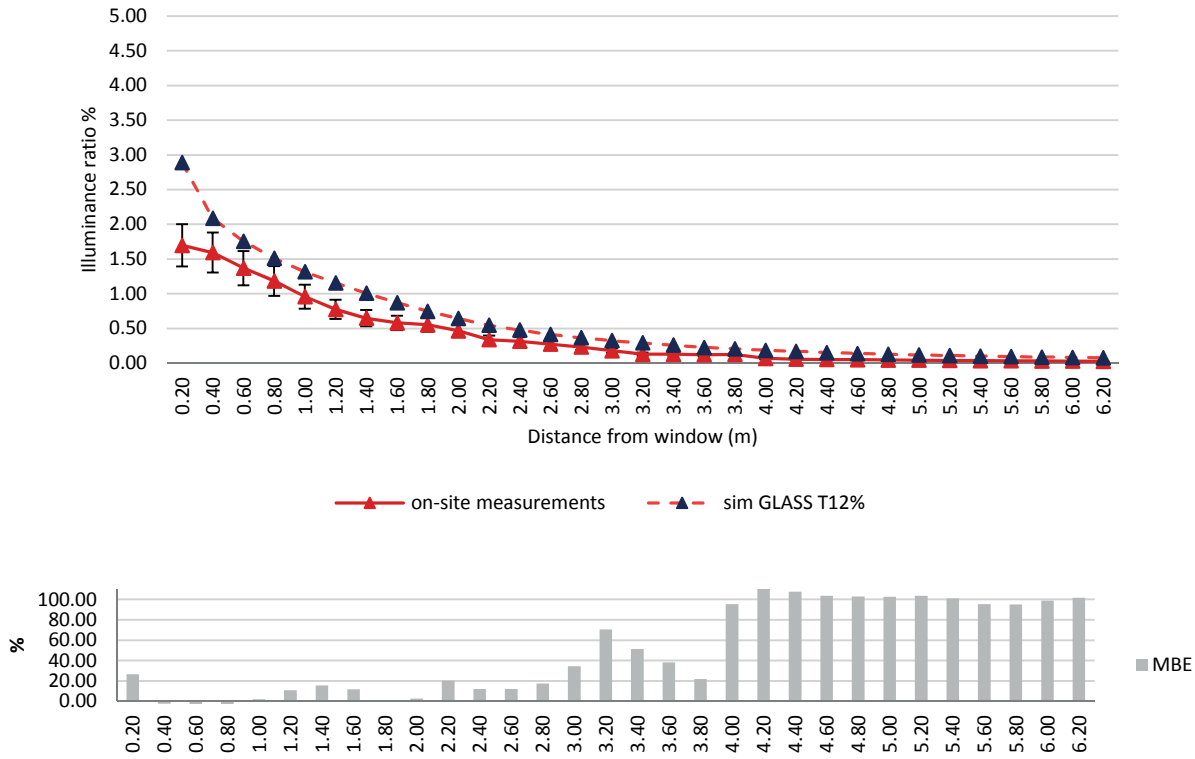

Figure 2.30 Comparison of the simulated IR profile with monitored data for B1 in summer solstice (June 21st 15h00 LT), below the graphs showing the MBE corresponding to the calibration results for summer solstice 15h00.

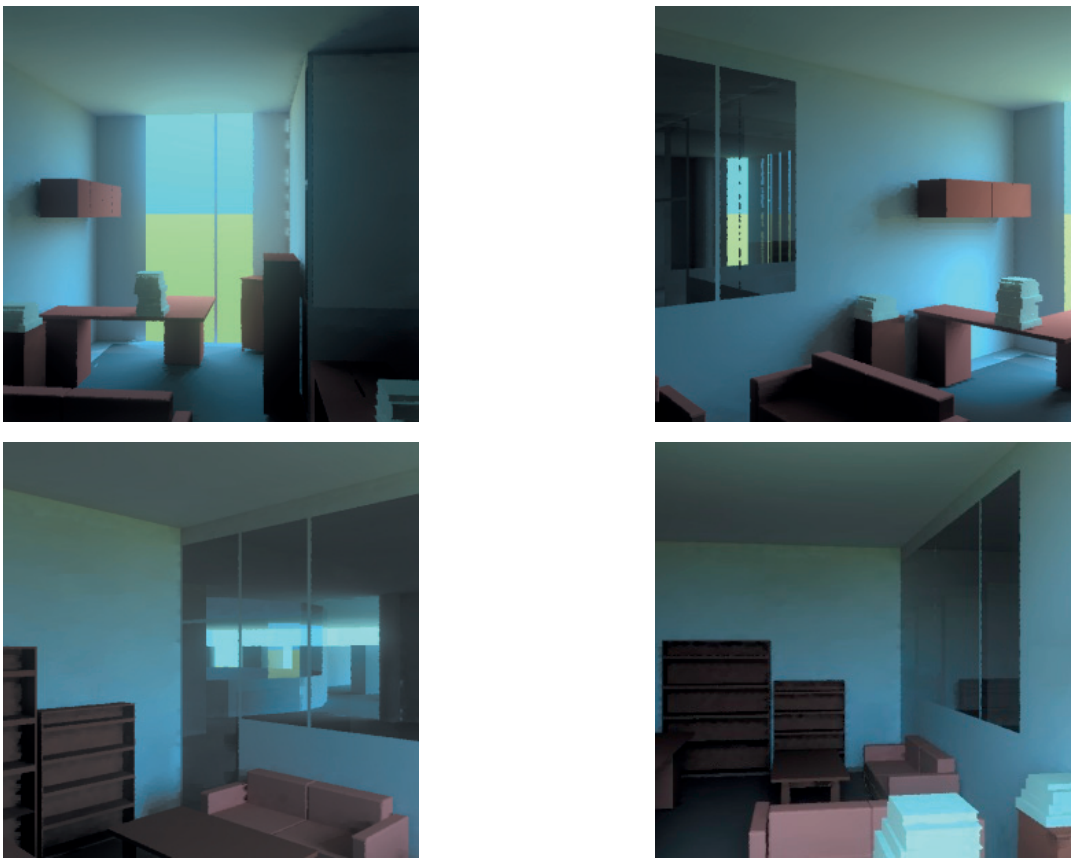

Figure 2.31 Renderings of the interior views of the virtual model of B1 office room at summer solstice under intermediate sky conditions (June 21st 15h00 LT).

Building B2: The results obtained for summer solstice (June 20th, 2012, 12h00 LT) when comparing the IR profile of the monitored room with simulations (Figure 2.33), show a maximal absolute difference of about 3% close to the window, however the simulated IR profile follows a similar curve through the room fitting to the monitored profile at 1.6m distance from the window. A view of the current situation is shown in Figure 2.32; the generated renderings are given in Figure 2.34. The MBE shown in the graph below indicates that the highest difference is found in the area next to the window with 46%, negative values of maximum -22% are found mainly at the back of the room. The MBE of the correlation is 7%.

Figure 2.32 Interior view of the B2 monitored room under intermediate sky conditions (June 20th 2012, 12h00 LT).

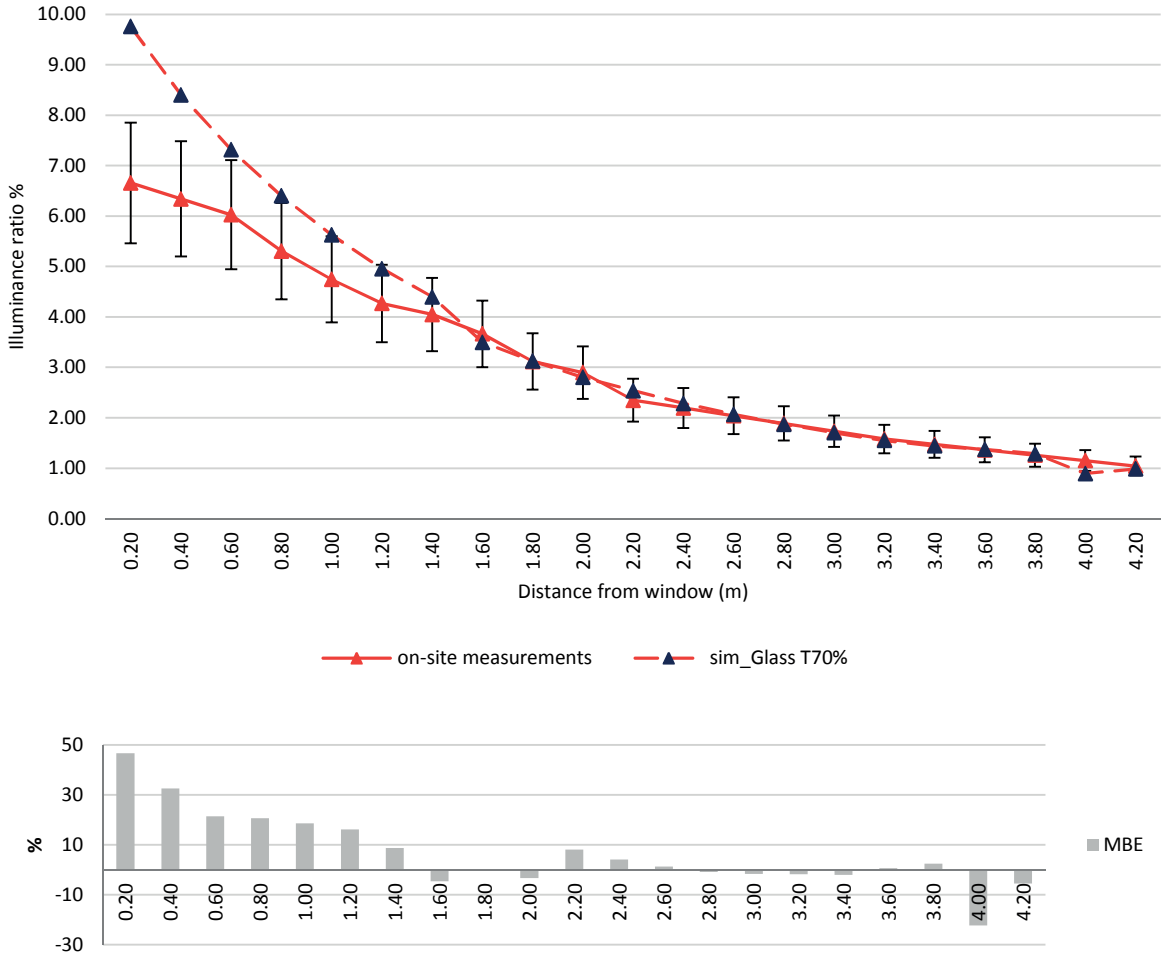

Figure 2.33 Comparison of the simulated IR profile with monitored data for the B2 office room in summer solstice (June 20th 2012, 12h00 LT), the corresponding MBE is shown in the graph below.

Figure 2.34 Renderings of the interior views of the virtual model of B2 in summer solstice under intermediate sky conditions (June 20th 2012, 12h00 LT).

2.6.2.2 Spring equinox

Building B1: The IR profile monitored on spring equinox (March 21st 2012, 17h00 LT) shows an absolute difference of about 1.0% at maximum close to the window where simulation values are larger than the monitored data. After a distance of 0.8m from the window both IR profiles fit very well. A picture view of the current situation is shown in Figure 2.35. The IR profiles results are given on Figure 2.37, the renderings on Figure 2.36. The MBE shows that the highest differences are found at a distance of 0.6m where a steep difference in the correspondance between the profiles is observed due to the effect of the sun and shadow patterns projected inside the room, a better fit is found ath the center and back of the room with a maximum MBE of 28%. The MBE of the correlation is 6%.

Figure 2.35 Interior view of the B1 monitored office room under clear sky conditions (March 21st 2012, 17h00 LT).

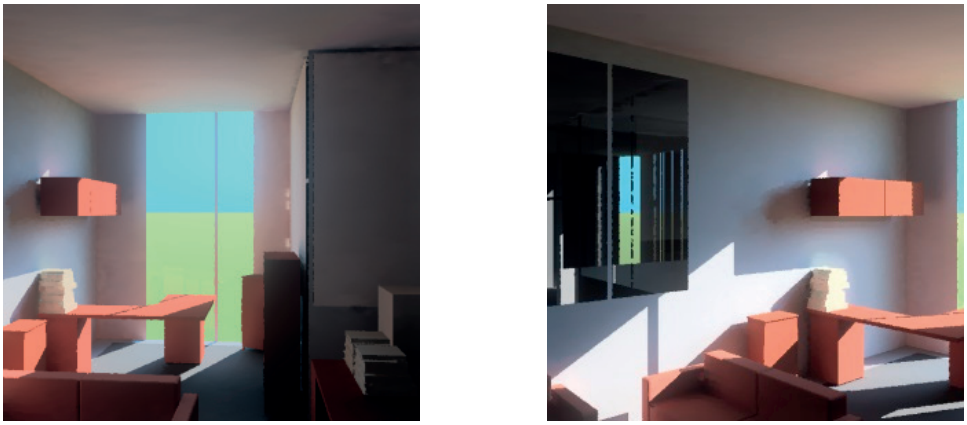

Figure 2.36 Renderings of interior views of the virtual model in B1 in spring equinox under clear sky conditions (March 21st 2012, 17h00 LT).

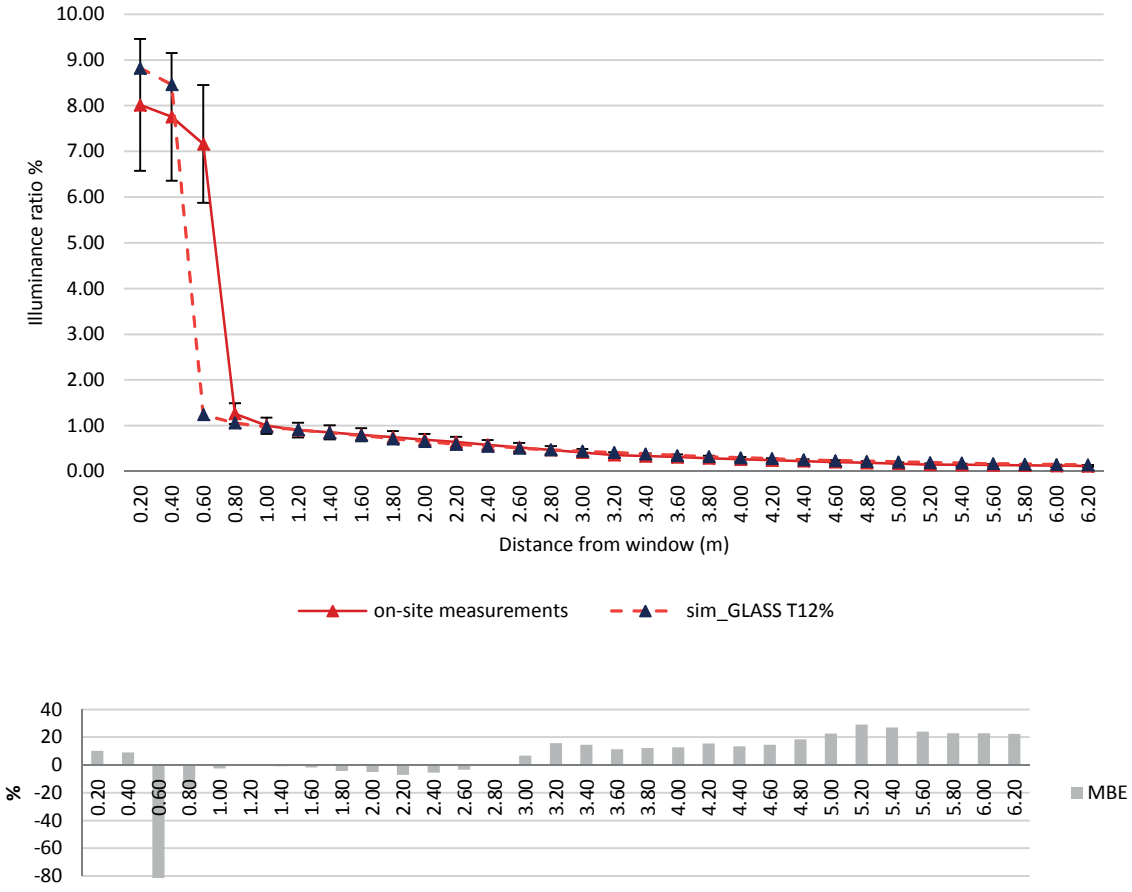

Figure 2.37 Comparison of the simulated IR profile with monitored data for B1 in spring equinox under clear sky conditions (March 21st 2012, 17h00 LT), the MBE graph is shown below.

Building B2: The comparison of the IR profiles of the Building B2 office room at spring equinox (March 20th, 2012 at 9h00 LT), shows a difference of 20% maximal discrepancy in the area next to the window. IR values differ in a rather significant way from 0.8m to 1.6m which might be due to the sun-shadow patterns from the window frame projected through the interior space; both profiles coincide at the end of the room. A view of the existing room is shown in Figure 2.38. The IR profiles results are shown on Figure 2.39, and renderings in Figure 2.40. The MBE indicates the higher differences at the center of the room, which discrepancies might be due to the light and shadow patterns inside the room. The MBE of the correlation is 79%.

Figure 2.38 Interior view of B2 under clear sky conditions (March 20th 2012, 9h00 LT).

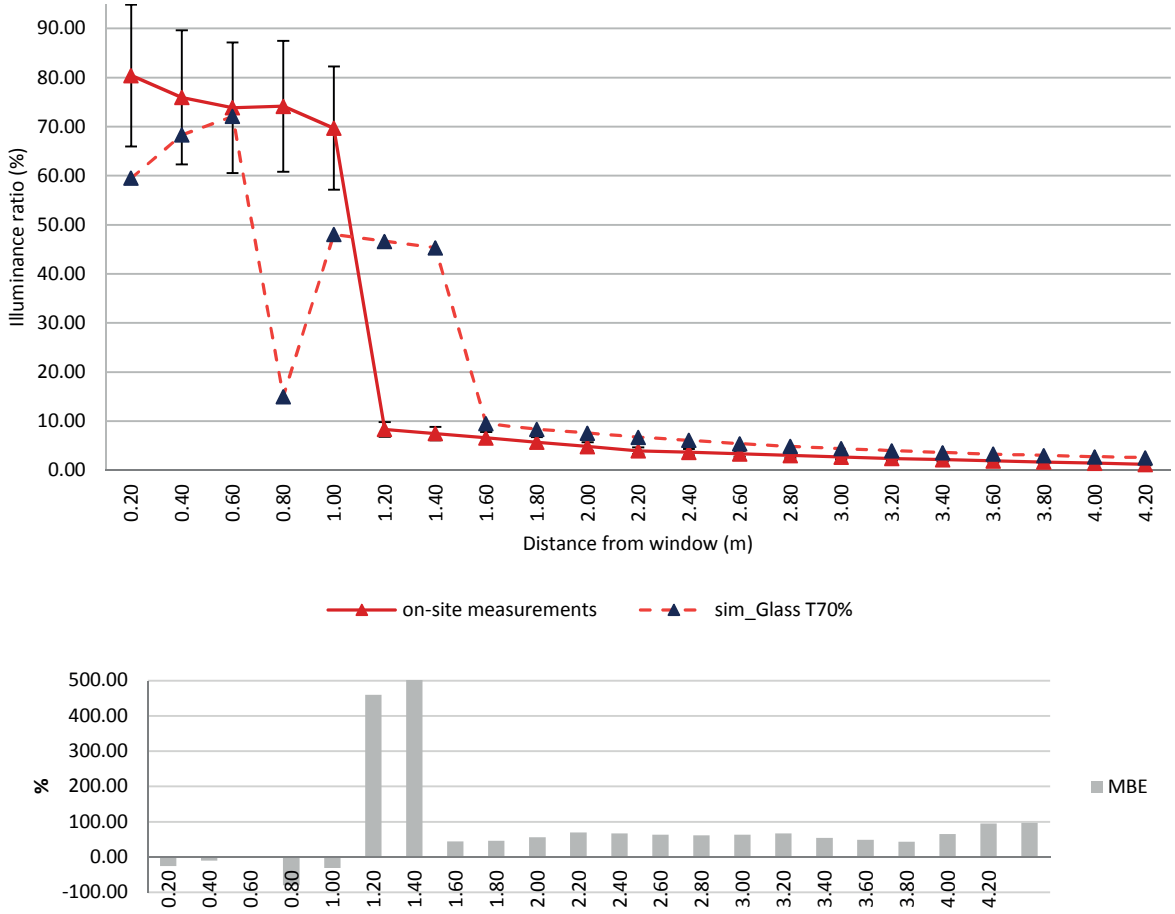

Figure 2.39 Comparison of the simulated IR profile with monitored data for B2 in spring equinox under clear sky conditions (March 20th 2012, 9h00 LT), the relative errors MBE are shown below.

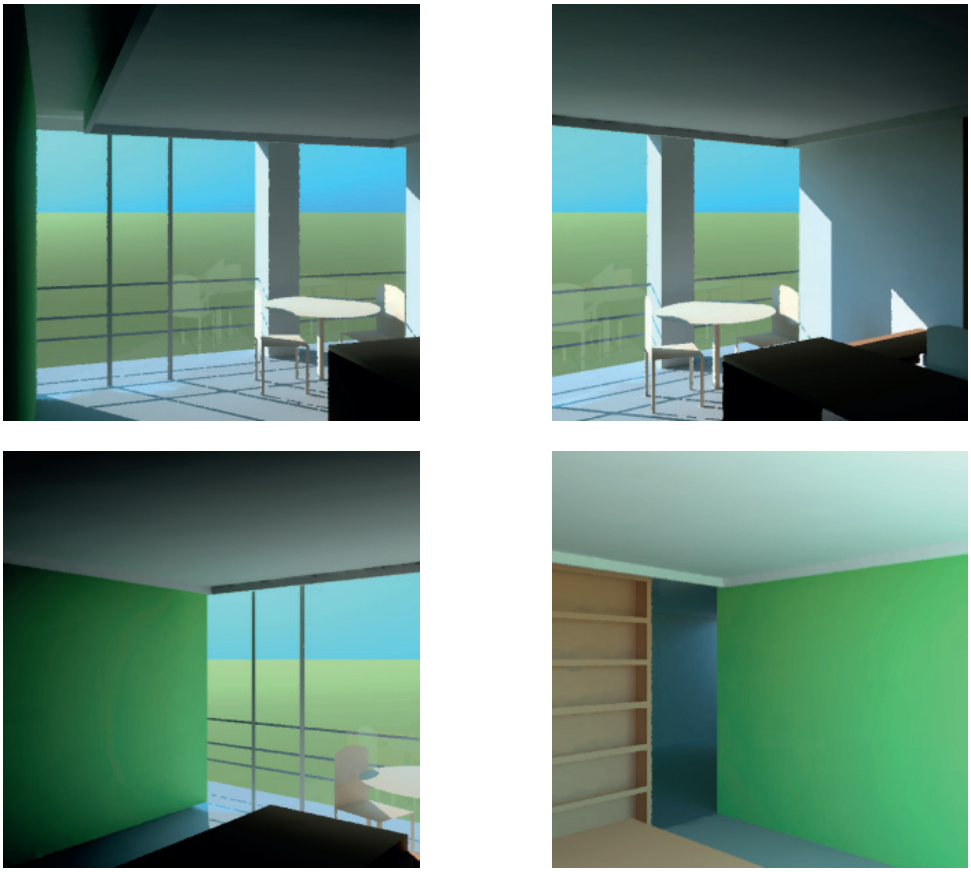

Figure 2.40 Renderings of the interior views of the virtual model in B2 in spring equinox under clear sky conditions (March 20th 2012, 9h00 LT).

2.6.2.3 Winter solstice

Building B1: The comparison of the IR profiles obtained at the winter solstice (December 20th, 2013 at 15h00 LT) in the Building B1 office room show an absolute difference of 1.6% next to the window. A discrepancy is also observed between the two profiles in the middle of the room, with a difference of 1.7% at a distance of 1.2m from the window, and reduced to 0.47% at a distance of 4.2 from the window. A view of the current room is shown in Figure 2.41. The IR profiles are given in Figure 2.42, and renderings in Figure 2.43. The MBE shows that the higher differences are found in the center area of the room, where the simulation exceeds the monitoring for a maximum of 216% in some areas at the center and back of the room. The MBE of the correlation is 125%.

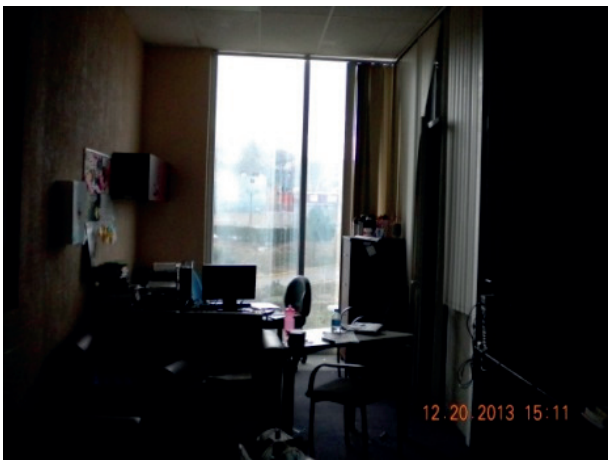

Figure 2.41 Interior view of B1 office room in winter solstice under intermediate sky conditions (December 20th at 15h00 LT).

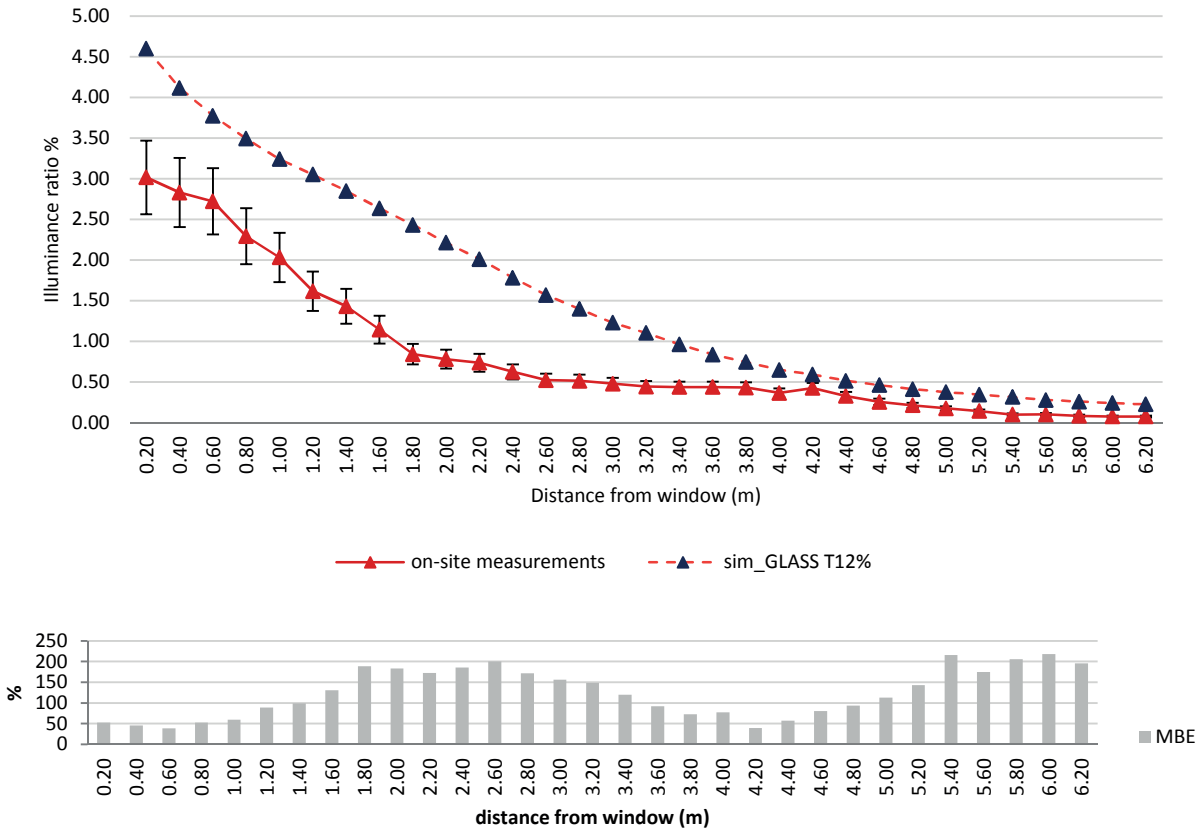

Figure 2.42 Comparison of the simulated profile with monitored data for B1 office room in winter solstice under intermediate sky conditions (December 20st 2013, 15h00 LT), the MBE graph is shown below.

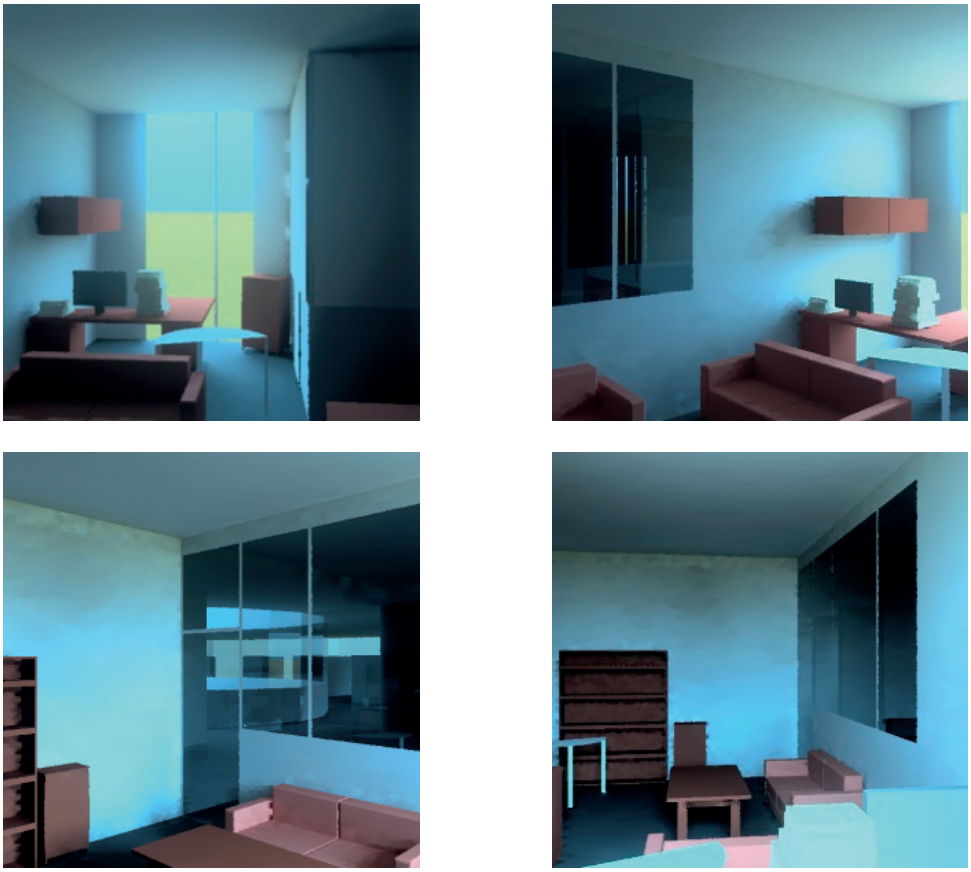

Figure 2.43 Renderings of interior views of the virtual model of B1 in winter solstice under intermediate sky conditions (December 20st 2013, 15h00 LT).

b) Building B2: The IR profiles observed at the winter solstice (December 17th 2013 12h00 LT), monitored in the office room and simulated with RADIANCE, fit closely with a very small difference of about 6% next to the window. Small discrepancies are observed from 1.2m to 1.6m distance from the window; a closer match is found at the end of the room. The view of the current room is shown on Figure 2.44. The IR results are given in Figure 2.45, and renderings on Figure 2.46. The MBE shows that the higher differences between the on-site and the simulation results are found from a distance of 1.0m to the back of the room, with the highest value of 143%. The MBE of the correlation is 100%.

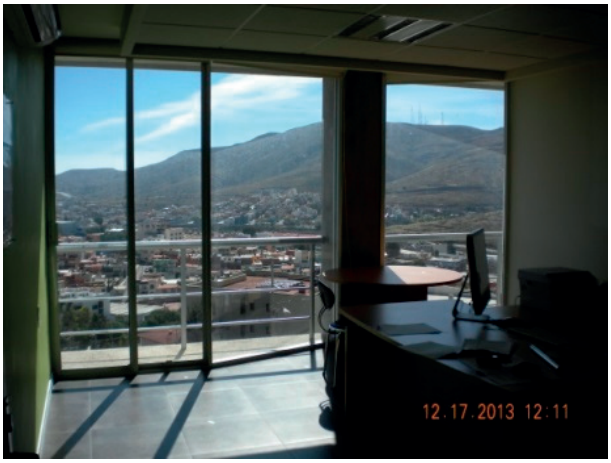

Figure 2.44 Interior view of B2 office room at winter solstice under clear sky conditions (December 17th 2013, 12h00 LT).

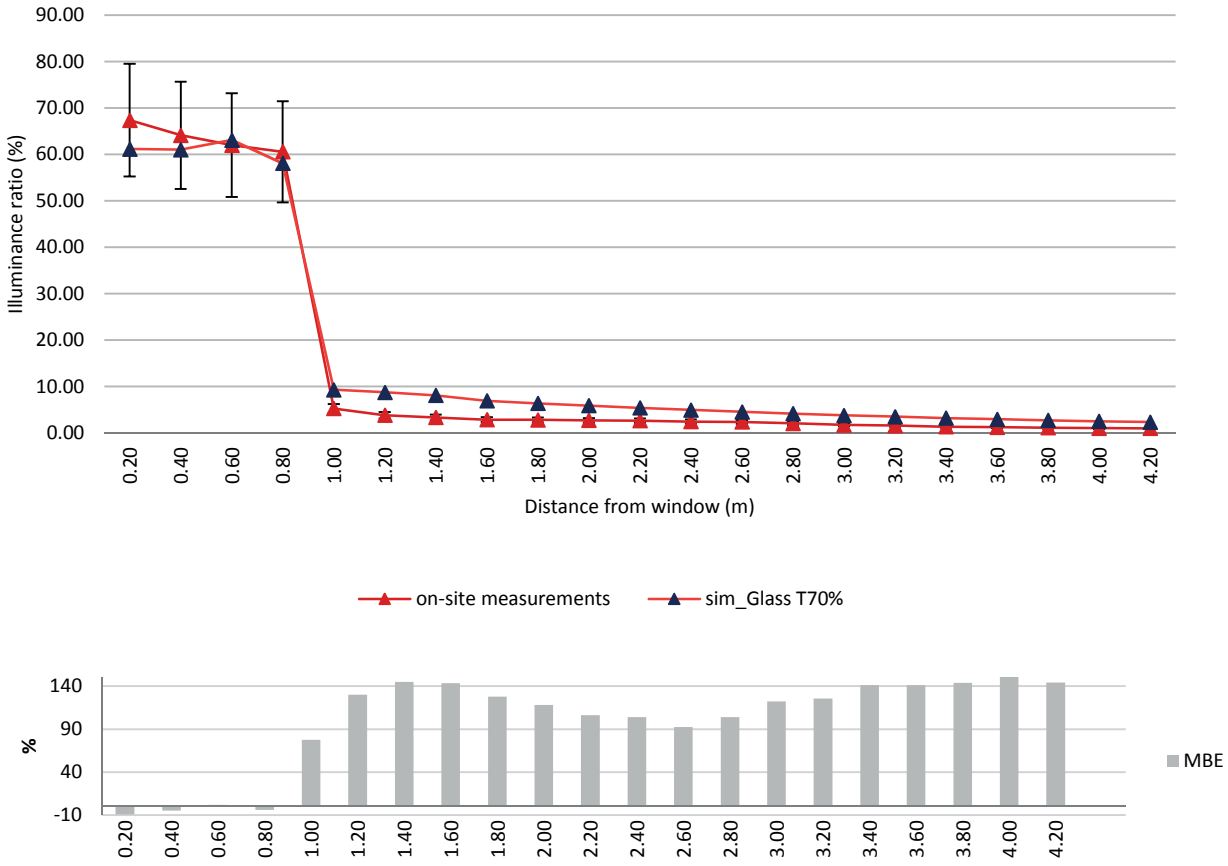

Figure 2.45 Comparison of the simulated IR profile with monitored data for B1 office room in winter solstice under clear sky conditions (December 17th 2013, 12h00 LT), the MBE graph showing the relative errors is shown below.

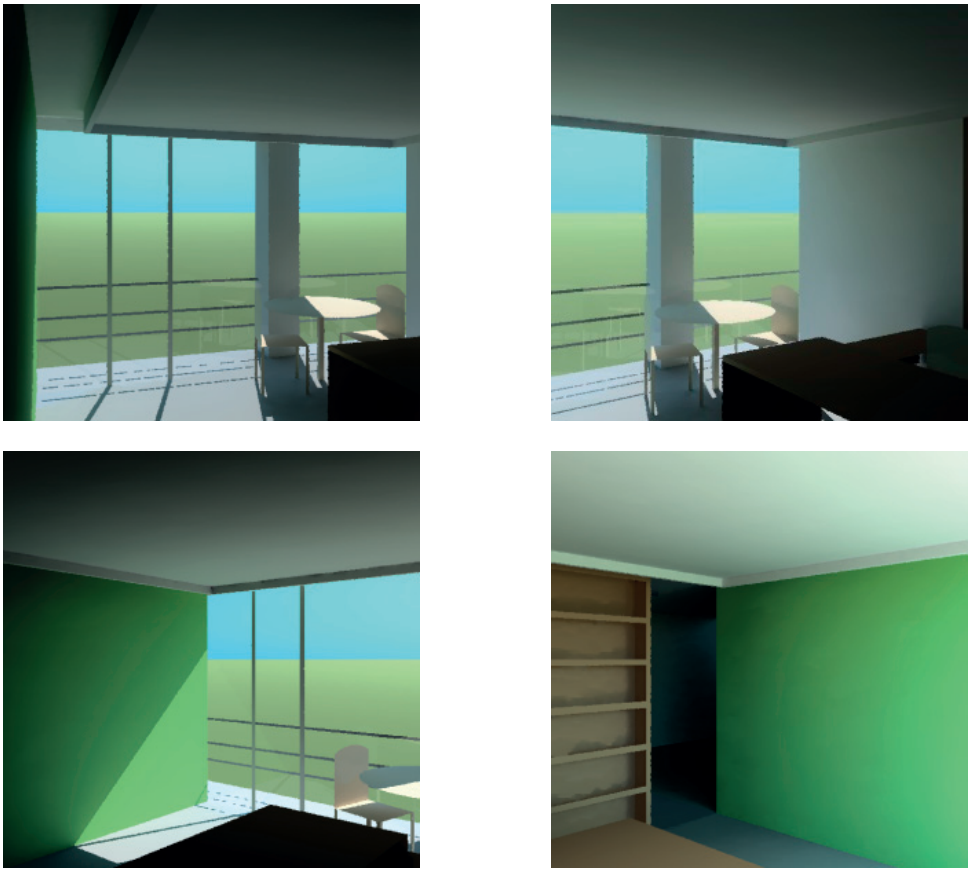

Figure 2.46 Renderings of interior views of the virtual model B2 in winter solstice under clear sky conditions (December 17th 12h00 LT).

2.6.3 Correspondence of the simulations vs. measurements

After the calibration of the virtual models, the next step would be to carry out computer simulations of the office rooms equipped with CFS in order to assess their performance and select the optimal one for the sake of improving the interior daylight distribution in the two office rooms. More than 900 figures (30 hours multiplied by 31 measurement points for each time step) were considered for Building B1 in order to compare on-site measurements and computer simulations results, in the case of Building B2 more than 600 figures were considered (30 hours by 21 measurement points).

In order to explore the representativity of the current daylighting situations by the virtual models the correspondence between the on-site monitored data and the simulations was assessed by expressing all the figures according to logarithmic scale (base 10) in order to smoothen the range variations observed on the DF and IR profiles for different sky conditions (mainly due to the different sky luminance distribution occurring in reality and differing from the simulated skies). Despite of the shallow correspondence found in some of the compared daylight situations, the array of data 'simulations vs measurements' show a similar trend which suggest the presence of a systematic error, as it can be observed in Figure 2.47, where a graph showing the correlation between the interior monitored data and the simulations results for Building B1 (930 figures) is shown, while the correlation between the exterior monitored data and the simulations results is shown on Figure 2.48.

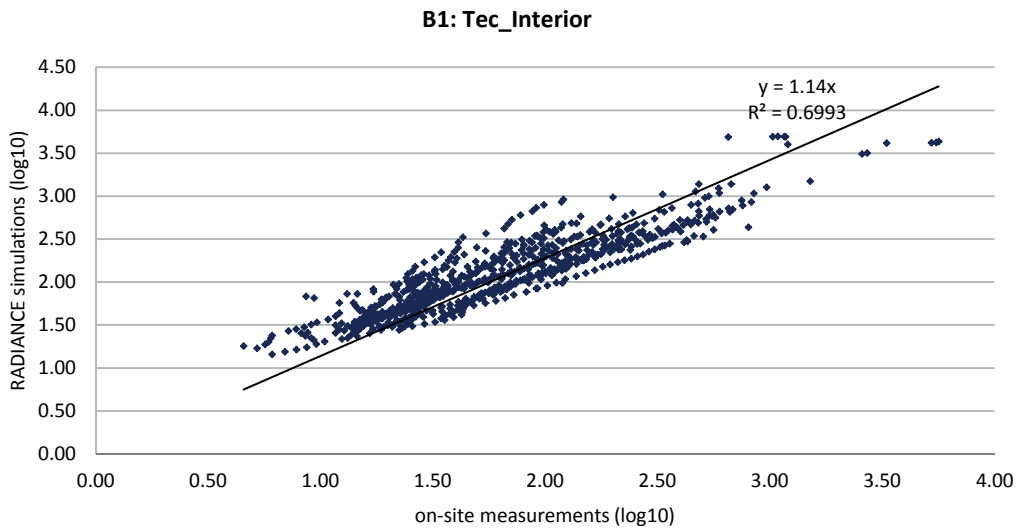

Figure 2.47 Correlation observed between the interior monitored illuminances and the simulations for Building B1.

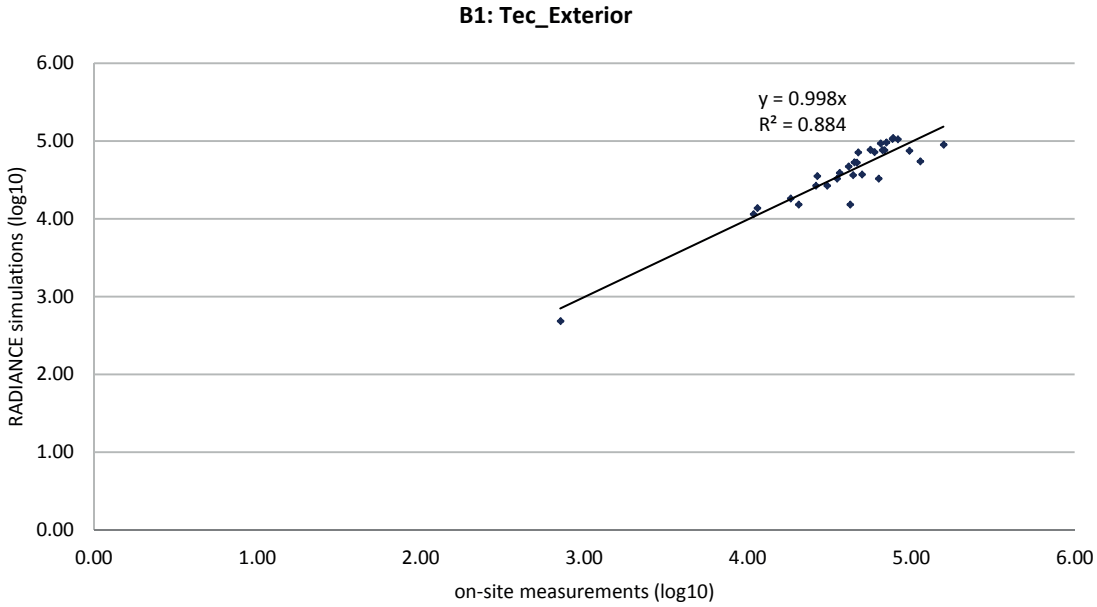

Figure 2.48 Correlation observed between the exterior monitored illuminances and the simulations for Building B1.

The correspondence of the 630 figures comparing the interior on-site monitored and the simulation results for Building B2 is shown in Figure 2.49, where it can be observed that a higher correspondence between the virtual models and the reality was achieved in this case. Likewise, the correspondence between the exterior results (simulations and the monitored data) is presented in Figure 2.50 where a better fit is also observed.

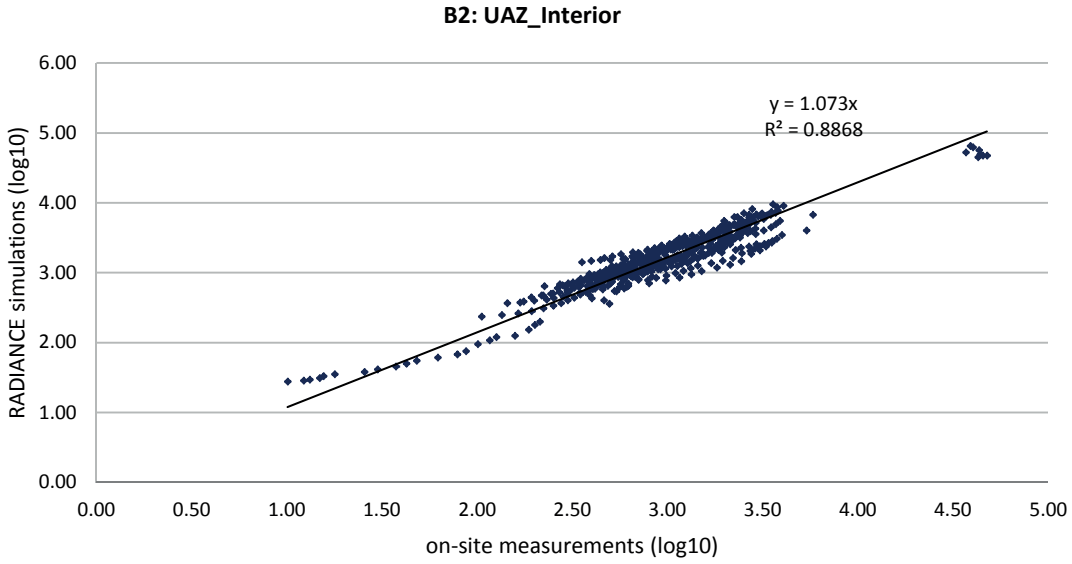

Figure 2.49 Correlation observed between the interior on-site monitored illuminances and the simulations for Building B2.

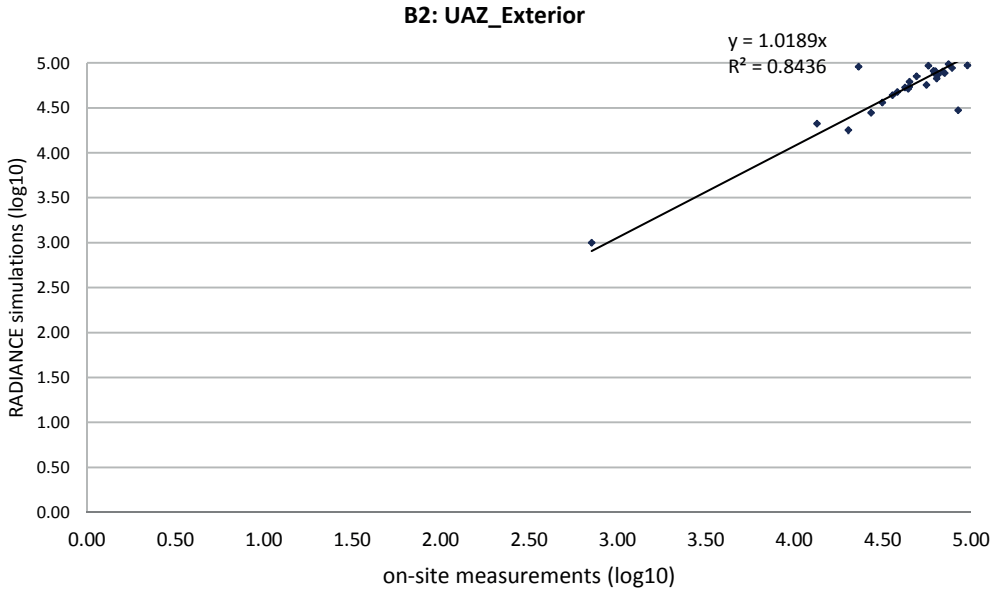

Figure 2.50 Correlation observed between the exterior on-site monitored illuminances and the simulations for Building B2.

2.6.4 Conclusions

-The general trend of the virtual models regarding the DF and IR profiles can be considered as acceptable.
-Excellent fits are generally observed between monitored and simulated profiles in the second half of the rooms where the internal component of daylighting (mainly reflections on the floor and the walls) is predominant.
-Larger discrepancies are observed for both profiles close to the window (especially for Building B1) where the sky-vault component of daylighting strongly impact on the on-site monitoring; solar blinds, furniture, decorative items and even users in the office room must not be understimated and certainly explain some of the observed discrepancies.
-Despite of the existence of some discrepancies between the virtual models and the reality, it is believed that the use of computer simulation to assess the performance of daylighting systems in a comparative way (not in absolute terms) is sound enough.

2.6.5 Luminance mapping

The luminance of the interior surfaces was monitored in the two office rooms using the specially designed photometric device described in Section 2.3. The assessment of the indoor environment quality related to the daylight presence in the room was carried-out by the way of luminance ratios (e.g. similar to luminance contrast); a comparison with the existing recommendations (See Section 2.4.2). Raw data obtained with this device were converted into luminance values (cd/m²), using the conversion factor that was determined by their calibration (Section 2.3). The results obtained from such assessment were used in order to assess the existing interior luminous situation in the two office rooms; no further evaluation was performed by comparing or reproduced the interior situation in virtual models.

Building B1: The luminances of the Building B1 office room were monitored under overcast sky conditions on the February 2nd at 9h00 LT. Due to the low glazing transmission of the side window (estimated 10–15%) low values were observed even in the area close to the window, likewise no records were obtained for the dark areas back into the room due to the poor sensitivity of the 'adhoc' device. Similar difficulties were encountered in the B1 office room for the illuminances monitoring (see Section 2.6). Three working spaces are located in the office room: Desk 1 next to the window, Desk 2 in the middle of the room and Desk 3 at the back of the room. Due to the dark interior environment, it was only possible to monitor data to calculate the luminance ratio for Desk 1 and Desk 2. Given the position of Desk 3 which was at a considerable distance from the sidewindow, data were only retrieved for the adjacent wall, and nil was obtained for the working place and/or the paper task. The results are presented on the pictures of Figure 2.51.

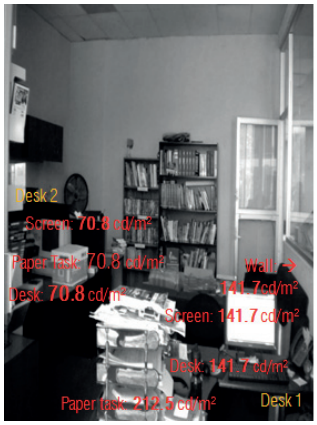

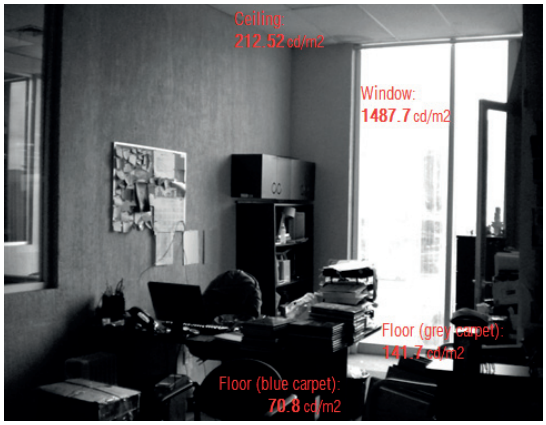

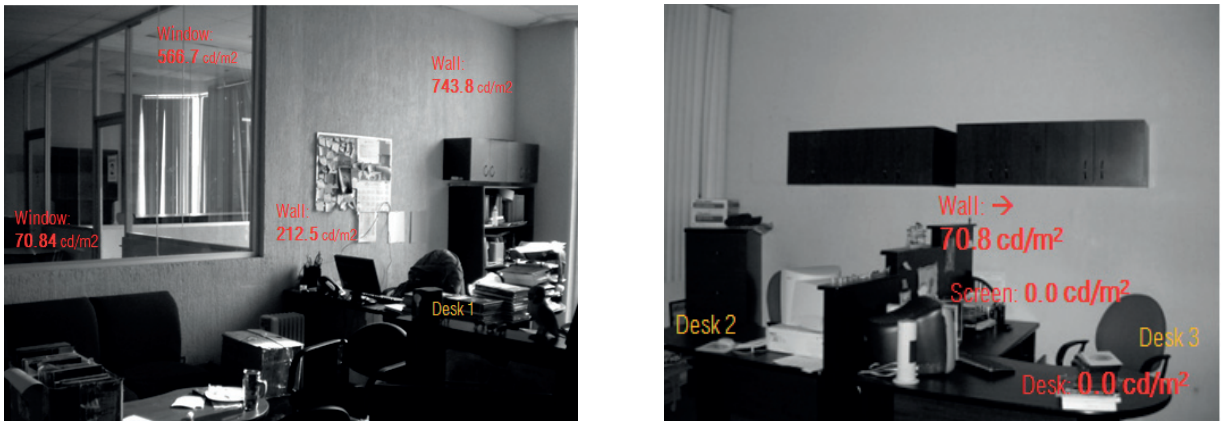

Figure 2.51 Monitored luminance values of the surrounding areas to the working spaces measured under overcast sky conditions.

The luminance ratio were then compared with the international recommendations applicable to working environments [96]. Table 2.8 show that the observed luminance ratios were too low found even for the work place next to the window, e.g. a luminance ratio of 1:3 is recommended between the workplace and the paper task (see Section 2.4.2), and only 1:1.5 for the desk next to the window and 1:1 for the desk in the middle of the room were monitored. A luminance ratio of 1: 5 is recommended between the screen and the work, a ratio of 1: 1 was found for both workplaces. However, given the particular features of the building envelope characterized by very low glazing transmission and the poor sensitivity of the 'adhoc' device used for the luminance monitoring, the use of a precision luminancemeter is commended in this case especially under overcast sky conditions.

	Recommended value	**Desk 1**	**Desk 2**	**Desk 3**
Workplace vs Paper Task	1 : 3	1 : 2	1 : 1	-
Screen vs Workplace	1 : 5 (no more than 1:10)	1 : 1	1 : 1	-
Screen vs Surroundings Ceiling	1 : 15 (no more than 1:40)	1 : 1.5	1 : 3	-
Screen : Wall		1 : 1	1 : 1	-
Screen : Window		1 : 10	1 : 21	-
Screen : Floor (grey carpet)		1 : 1	1 : 2	-
Screen : Floor (blue carpet)		1 : 0.5	1 : 1	-

Table 2.8 Luminance ratio of the interior surfaces for Building B1 office room measured under overcast condtions.

Building B2: The luminance of the interior surfaces was monitored on January 27th at 9h00 Local Time (LT) under overcast sky conditions. Due to the characteristics of the building (SE orientation and a WWR of 90%) the office room is sufficiently lit most of the time. However, the on-site monitoring suggests that high luminance contrast can occur especially when the sun faces the facade at a low elevation i.e. in the early hours of winter and spring time. A large luminance ratio was observed between the screen and the surrounding areas, especially close to the window area, with a luminance ratio of 1:64 when the maximum recommended is 1:40. The screen vs. wall ratio is also slightly high, exceeding by 2 the recommended proportion. It was also observed a low proportion workplace to paper-task of 1:1.6 was almost half the value of the recommended 1:3. The monitored luminances are illustrated on Figure 2.52 the luminance ratios are shown in Table 2.9.

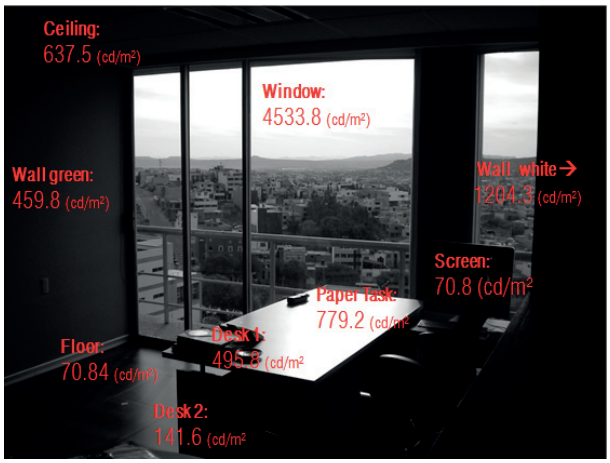

Figure 2.52 Monitored luminance values of the interior surfaces in Building B2 office room under overcast sky conditions.

	Recommended value	Desk 1
Workplace vs. Paper Task	1 : 3	1 : 1.6
Screen vs. Workplace	1 : 5 (no more than 1:10)	1 : 7
Screen vs. Surroundings Ceiling	1 : 15 (no more than 1:40)	1 : 9
Screen : Wall white		1 : 17
Screen : Wall green		1 : 6.5
Screen : Window		1 : 64
Screen : Floor (grey carpet)		1 : 1

Table 2.9 Luminance ratio between the interior surfaces in office room Building B2 measured under overcast sky conditions.

2.7 Summary

The on-site monitoring of the two office rooms was performed in order to assess the existing interior daylight situation and to calibrate a virtual model that would be used to evaluate the performance of CFS through RADIANCE simulations. Measurement campaigns were regularly performed on-site using two lux meters which were previously calibrated in order to obtain reliable data. Secondly an assessment of the luminance distribution was made using an 'adhoc' photometric device, which was also calibrated using a precision luminance meter as reference. Even if the calibration of the virtual models of the office rooms showed some discrepancies with the monitored data, especially in Building B1 as it is explained in Section 2.6, the comparison of the simulated and monitored data was sound enough to justify a further use of the simulation models. It must be emphasized moreover that their use to carry out computer simulations of the daylight flux distribution through CFS in office rooms implies a more differential approach to be employed (by computer simulation results f.i.) than absolute values of daylighting metrics, this requires less stringent constraints for the virtual models.

Chapter 3 Daylight improvement using Complex Fenestration Systems

The optimal peformance of CFS in a building would be the result of a comprehensive assessment in regards to its adequacy to the local sky conditions. Therefore, given the vast range of CFS available on the market, its selection must be based on the valuation of its suitability to the location according to its features. As a result of a performance assessment that took into account different parameters such as visual comfort and performance, visual amenity, energy saving potential The International Energy Agency (IEA) categorized different CFS according to their function, features and application [123]. They were classified into two main groups: with and without shading devices. This classification also includes recommendations of systems primarily used for diffuse skylight and/or for direct sunlight. An excerpt of such classification is presented in Table 3.1.

1. SHADING SYSTEMS	**2. DAYLIGHTING SYSTEMS WITHOUT SHADING INCLUDED**
A. Primary using diffuse skylight	**A. Diffuse light guiding systems**
1. Prismatic panels	1. Light shelf
2. Prismatic and venetian blinds	2. Anidolic integrated system
3. Sun protecting mirror elements	3. Anidolic Ceiling
4. Anidolic Zenithal Opening	4. Fish system
5. Directional selective shading system with concentrating holographic optical	5. Zenith light guiding elements with HOEs
6.Transparent shading system with Holographic Optical Element (HOE) based on total reflection	
B. Primary using direct sunlight	**B. Direct light guiding systems**
1. Light guiding shade	1. Laser cut panel
2. Louvres and blinds	2. Prismatic panels
3. Light shelf for redirection of sunlight	3. HOEs in the skylight
4. Skylight with laser cut panels	4. Sun directing glass
5. Turnable lamellas	
6. Anidolic Solar Blinds	**C. Scattering systems**
	D. Light transport
	1. Heliostat
	2. Light pipe
	3. Solar tube
	4. Fibres
	5. Light guiding ceiling

Table 3.1 IEA classification for Daylighting Advanced Systems according to their functionality, features and application [123] .

Daylighting systems with shading are designed to protect the area near the window from direct sunlight and redirect daylight (diffuse and/or direct) into the interior of the room; those without shading are designed to redirect daylight to areas away from a window and may be able or not to block direct sunlight [123]. Thus, in the selection of the appropriate CFS it is important to define beforehand the aim of the daylighting strategy, in which important parameters should be included, such as site daylighting conditions, daylighting objectives and strategies considered in the architectural design.

3.1 Daylight improvement approach for buildings located at low latitudes

An adequate daylighting strategy takes into account the climatic and daylighting characteristics of the building location. For buildings located at low latitudes, it aims to improve the interior daylight distribution to avoid the degradation of the visual perception while maintaining a pleasant thermal environment for the occupants. In order to attain that, the strategy proposed in this PhD thesis points to the selection of a CFS that contributes to avoid the penetration of sun rays in summer, whilst allowing a higher admission of daylight in winter and supports an angular lighting redirection reducing the risk of glare.

Therefore, the daylighting approach considered in this doctoral thesis proposes the use of CFS characterized by a rather easy installation in buildings compared to other Advance Daylight Systems (as explained in Section 1.3). Such strategy also implies the assessment of the thermal and visual comfort of the occupants, in order to evaluate the risk of glare and overheating that the penetration of daylight may bring to the interior of the room. However, such approach does not include significant modifications of the current characteristics of the building, such as window size or configuration, or the reflectance of the interior surface materials. Regarding the glazing visible transmission, in the case of Building B1 the actual value ranging between 10-15% (set to 12% in the virtual model), was increased up to 80% (corresponding to a clear double glazing) in order to allow more daylight to enter the room as a first step to the improvement of the interior luminous conditions. For Building B2, the glazing transmission in the existing room is ranging between 68-70% (set to 70% in the virtual model), which provides a sufficient daylight flux inside the room; in order to avoid non-essential modifications to the building features in this case the existing glazing transmission was preserved.

3.2 Preselection of the CFS

In order to reach such objectives, the first step was to narrow down the number of CFS being tested in the virtual models, by carrying-out a pre-selection. The latter was based firstly on the classification of the CFS according to their functionnalities and to their efficiency already demonstrated in sun light conditions [123], and secondly on their performance relative to the requirements of the daylighting improvement approach established in Section 3.1. The first step towards their performance evaluation was to generate a diagram that represents the daylight propagation through the CFS using their Bidirectional Transmission Distribution Function (BTDF data [61, 124]), which was monitored by the way of a bidirectional gonio-photometer [56, 57]. These diagrams contribute to predicting the transmitted daylight flux on the façade of the room and the daylight redirection which assist in the prediction of the risk of glare at a certain time and date of the year. They were generated according to the sun position in the considered location according to its latitude and longitude (as well as to the building orientation) on three different days: winter and summer solstices and spring equinox at 9h00, 12h00, 15h00 and 17h00. Simulations were also carried-out using the software GERONIMO [54] by placing the CFS in the upper part of the window of two virtual models at the same times and dates, in order to obtain the corresponding visualization of the interior luminous environment. The BTDF data of nine CFS currently available at LESO-PB were considered in the pre-selection stage: Lasercut panel [125], Optical Lighting Film 3M (SOLF) for indoor and outdoor installation [126], Light Louver, Lumitop [127], three new versions of Lumitop developed at the Technical University of Dortmund (TUD) named CFS1, CFS2 and CFS3 [128], and a microstructured prismatic film, which is a recent version of the Optical Lighting Film 3M (SOLF) [129, 130]. Pictures of some of the CFS samples are presented in Figure 3.1.

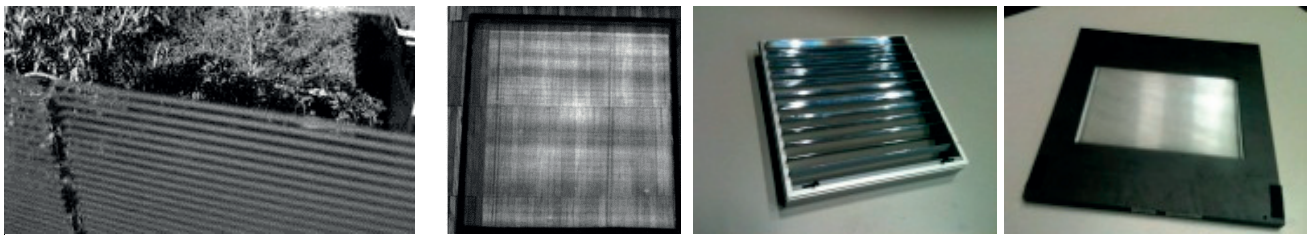

Figure 3.1 CFS considered in the pre-selection, from left to right: Lasercut panel, prismatic Film 3M (SOLF), Light Louver and one sample of the TUD version of Lumitop.

In order to generate the diagrams that describe the daylight propagation through the CFS, a rotation matrix was calculated first, in search of determining the coordinates of the sun's position with respect to the building orientation, and, secondly, to adjust the coordinates system of the BTDF data from the gonio-photometer (which is based on an international agreement issued from IEA Task 21 [123]) to the coordinates system used in RADIANCE 4.0 since the introduction of the *mkillum* routine (that is able to read XML files containing BTDF data [64]). A wider explanation of such improvements is provided in Section 1.3.1.

3.2.1 Results

a) Building B1

Due to the orientation of the building's façade (53° South West), sunrays are impinging on the façade from about 12h00 during winter solstice and spring equinox, and from about 15h00 during summer solstice (see Annex 2.3). Thus, diagrams of the daylight propagation through CFS were generated only for those hours. Firstly, a visual assessment of the daylight distribution into the room was carried out by comparing the renderings generated by the program GERONIMO; a second assessment was done by comparing the daylight flux entering the room according to the transmission of the CFS at the corresponding simulation times. The rendering generated by GERONIMO using the laser cut panel (LCP) in spring equinox at 12h00, 15h00 and 17h00 are presented in Figure 3.2. The corresponding diagram of the daylight distribution is also shown on the same figure as well as the relative fraction of the transmitted light flux for each time step. The daylight distribution in the office room using Film 3M exterior is presented in Figure 3.3. However, due to space restrictions only results of two CFS are shown for Building B1.

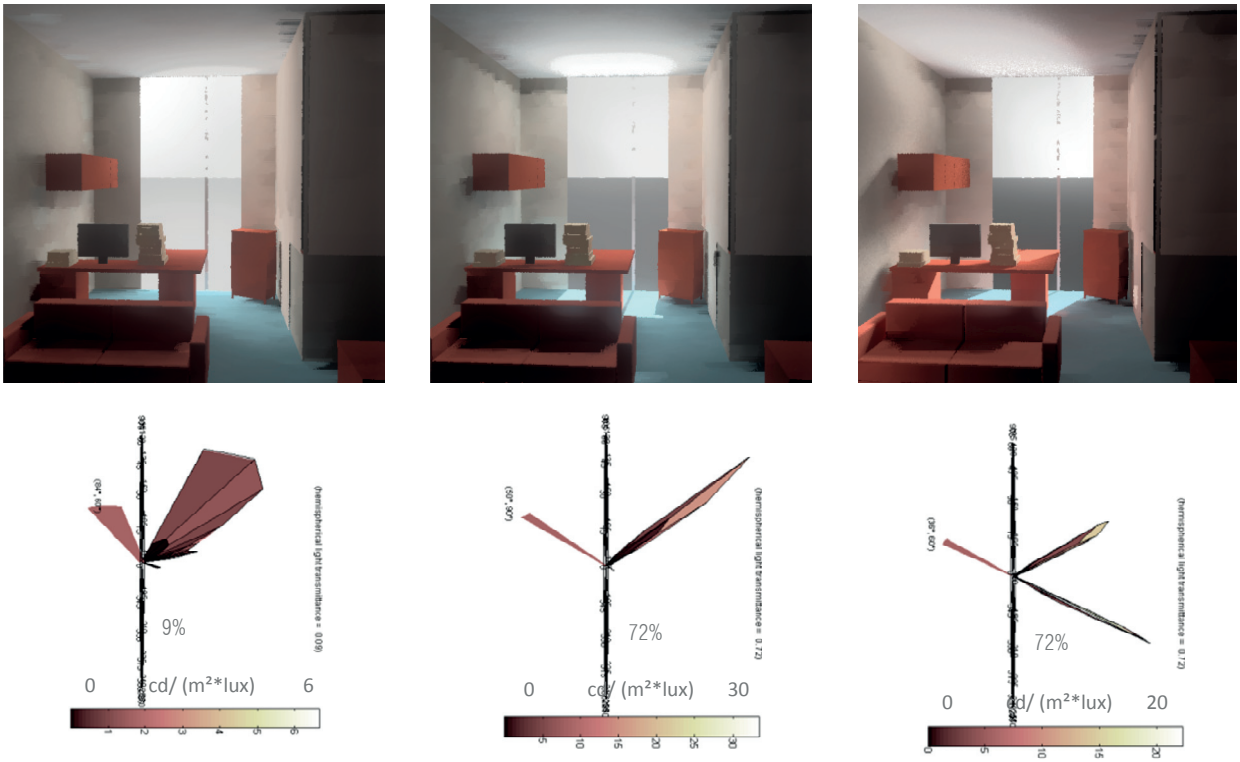

Figure 3.2 Simulated daylight distribution through LCP using the programme GERONIMO on spring equinox at 12h00 (left), 15h00 (centre) and 17h00 (right), the corresponding light distribution diagrams are shown below indicating the light transmission (%) and the scale of the diagram corresponding to the incident light and the light output (cd/ (m²*lux), which due to the small size is shown in text.

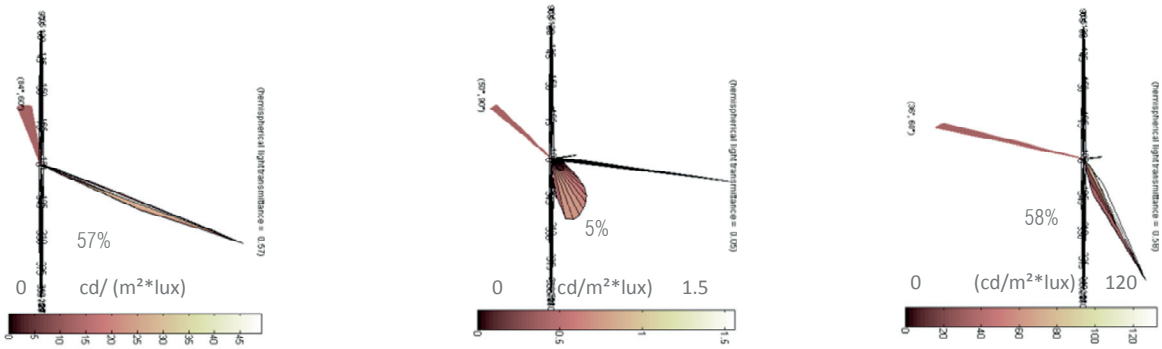

Figure 3.3 Simulated daylight distribution through Film 3M-Exterior on spring equinox at 12h00 (left), 15h00 (centre) and 17h00 (right) the corresponding light distribution diagrams are shown below indicating the light transmission (%) and the scale of the diagram corresponding to the incident light and the light output (cd/(m²*lux)).

The results show that at 17h00, the daylight flux is redirected downwards when using the Film3M-Exterior (Figure 3.3), while when using LCP the daylight flux points upwards and slightly downwards too (Figure 3.2), which might suggest that using the LCP rather than the Film3M exterior for Building B1, is more appropriate. In a second step, the daylight flux transmitted through the CFS was compared for the nine considered CFS, during the winter and summer solstices and the spring equinox. In this way, it was possible to identify the CFS that maximize daylight flux entering in the room during winter time and preventing the sun rays from entering into the room during summer time. The transmitted fraction of the daylight flux for the different CFS is shown in Table 3.2. The optimal results for the daylight improvement in the rooms are highlighted in green, while the values highlighted in orange are those that coincide less, while those that are not coinciding at all were not accentuated.

CFS	Winter Solstice				Spring Equinox				Summer Solstice			
	9	12	15	17	9	12	15	17	9	12	15	17
1 **LCP**		0.44	0.72	0.8		0.09	0.72	0.72			0.46	0.65
2 **Film3M int**		0.62	0.56	0.37		0.27	0.77	0.56			0.67	0.7
3 **Film 3M ext**		0.15	0.58	0.88		0.57	0.05	0.75			0.59	0.1
4 **Lumitop**		0.25	0.5	0.43		0.0	0.48	0.50			0.18	0.41
5 **Light Louver**		0.37	0.49	0.19		0.49	0.46	0.49			0.43	0.53
6 **CFS1**		0.54	0.75	0.75		0.11	0.63	0.72			0.62	0.61
7 **CFS2**		0.79	0.89	0.77		0.55	0.80	0.86			0.69	0.88
8 **CFS3**		0.75	0.86	0.86		0.31	0.66	0.86			0.65	0.73
9 **Film 3M new**		0.63	0.89	0.87		0.17	0.67	0.88			0.46	0.79

Table 3.2 Transmitted fraction of the solar flux for the 9 different CFS in B1, in Spring Equinox, Winter and Summer Solstice at 9h00, 12h00, 15h00 and 17h00. The figures that better agree with the proposed strategy are highlighted in green; those in orange coincide less while those that are not coinciding are not accentuated.

a) Building B2

The considered façade of buiding B2 is orientated 34° South East; therefore, daylight fluxes diagrams were generated from 9h00 to 17h00 at the winter solstice, from 9h00 to 15h00 at spring equinox, and from 9h00 and 12h00 at summer solstice. The daylight distribution in Building B2 using Lumitop during the winter solstice at 9h00, 12h00 and 15h00 as well as the the corresponding transmitted daylighting fluxes are shown in Figure 3.4.

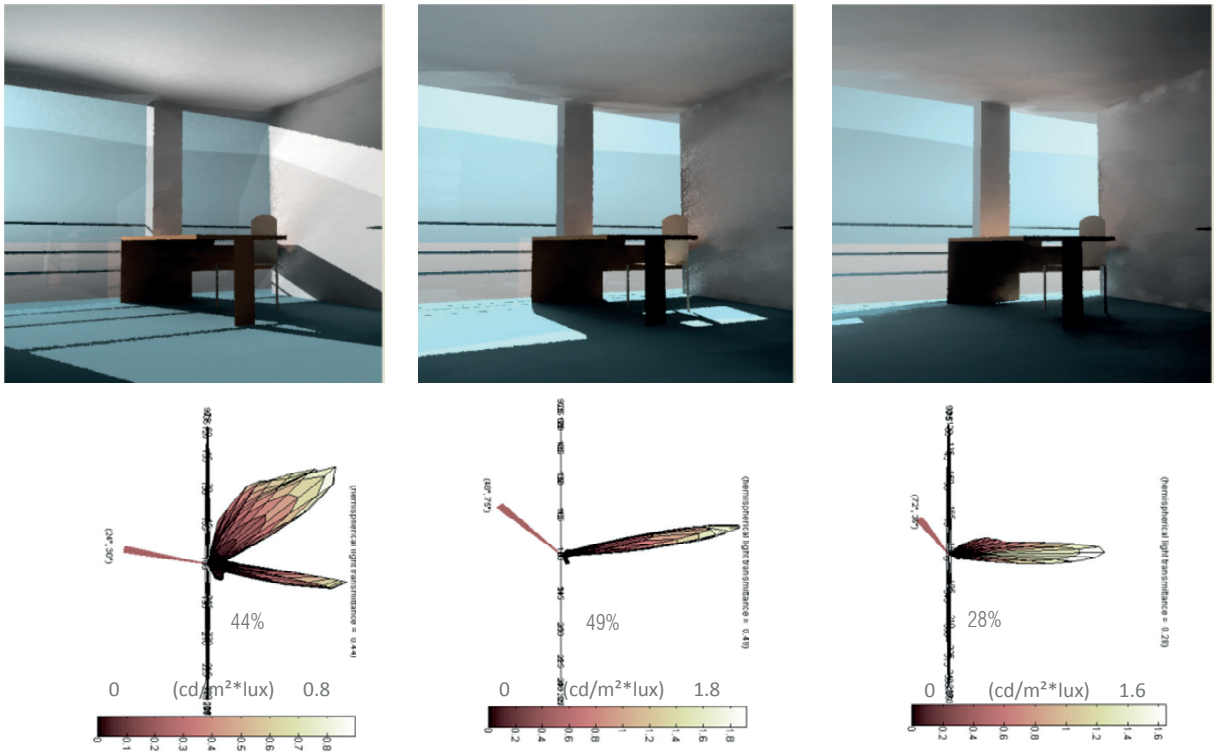

Figure 3.4 Simulated daylight distribution in office room B2 using Lumitop for winter solstice at 9h00 (left), 12h00 (centre) and 15h00 (left).

In order to compare the results of Building B2, the daylight distribution simulated using the improved version of Lumitop (TUD-CFS3), are presented on Figure 3.5, along with the diagrams including the relative fraction of the transmitted daylight flux.

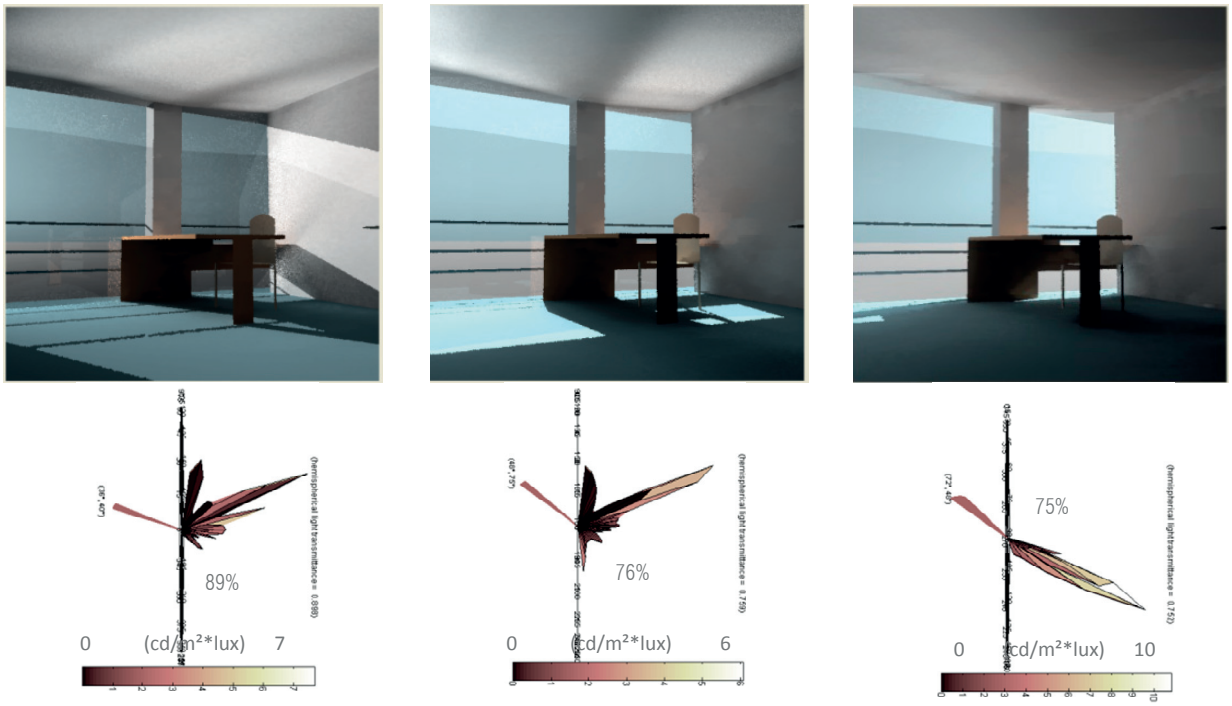

Figure 3.5 Simulated daylight distribution in room B2 using the improved version of Lumitop-CFS3 for winter solstice at 9h00 (left), 12h00 (centre) and 15h00 (left).

From the renderings generated with GERONIMO, it can be observed that at 12h00 (centre) the daylight flux is slightly redirected upwards to the ceiling when using the CFS3 (Figure 3.5) as shown by the corresponding diagram, while when using Lumitop (Figure 3.4) the daylight is mainly redirected to the back of the room, as is illustrated by the diagram. The comparison of the transmitted daylighting fluxes through the five CFS considered in Building B2 is listed in Table 3.3.

CFS	Winter Solstice				Spring Equinox				Summer Solstice			
	9	12	15	17	9	12	15	17	9	12	15	17
1 **LCP**	0.78	0.71	0.48	0.17	0.71	0.67	0.09		0.52	0.09		
2 **Film3M int**	0.09	0.74	0.50	0.0	0.45	0.74	0.25		0.04	0.27		
3 **Film 3M ext**	0.84	0.04	0.09	0.0	0.18	0.25	0.57		0.02	0.57		
4 **Lumitop**	0.44	0.49	0.28	0.01	0.47	0.37	0.0		0.23	0.23		
5 **Light Louver**	0.42	0.48	0.45	0.06	0.43	0.47	0.45		0.35	0.453		
6 **CFS1**	0.79	0.63	0.49	0.002	0.61	0.61	0.16		0.41	0.11		
7 **CFS2**	0.86	0.82	0.78	0.04	0.73	0.77	0.27		0.57	0.55		
8 **CFS3**	0.89	0.76	0.75	0.067	0.77	0.82	0.28		0.21	0.31		
9 **Film 3M new**	0.83	0.85	0.63	0.015	0.8	0.67	0.23		0.31	0.17		

Table 3.3 Relative fraction of daylight flux transmitted through the 9 CFS considered in Building B2, for Spring Equinox, Winter and Summer Solstices at 9h00, 12h00, 15h00 and 17h00.

3.2.2 Conclusions

The pre-selection of the CFS was made according to the daylighting approach applied in this study for buildings located in prevailing sunny climates: allowing a higher admission of daylight in winter, a reduction of sun rays penetration in summer and an angular lighting redirection that can contribute to reduce the risk of glare. According to the results obtained it was possible to observe that for Building B1, the Lumitop-CFS2 and the new version of Film 3M allow a larger daylight flux to enter into the room during winter time while the laser cut panel and the Lumitop-CFS1 provide also a sound daylighting transmission. During summer time the light louver and Lumitop allow a lower daylight penetration into the room, while the LCP, the new Film3M and the Film 3M exterior are not performing badly according to the proposed strategy. In the case of Building B2, during winter solstice, two of the three CFS created by the University of Dortmund: CFS2 and CFS3 and the new version of Film 3M allow more daylight flux to enter the room, while the LCP and the CFS1 perform also in a sound way. For summer solstice, Film 3M interior, Lumitop, CFS3 and the new Film 3M allow a daylight flux to enter the room during summer solstice, while CFS1 and LCP also showed to be a sound option.

The CFSs that showed the optimal performance during this pre-selection procedure in both buildings were accordingly selected for the suggested daylighting strategy. This include: the Lasercut panel[125], the new version of prismatic Film 3M (OLF), and the three CFS Lumitop types from the Technical University of Dortmund (TUD): CFS1, CFS2 and CFS3[128]. A detailed description of these CFSs can be found in Annex 3.1.

3.3 Simulation of daylight propagation through CFS using RADIANCE

3.3.1 Verification of the computer modelled daylight propagation through CFS

In order to establish confidence in the new RADIANCE simulation procedures (Section 1.3.1.2), a comparison was carried-out using the virtual model of an office module located on the EPFL campus. The simulation results obtained using the new procedures were compared with those obtained using the primitive *prism2* issued from a previous study at the LESO-PB [43]. In the latter, the daylighting features of a testing module located on the EPFL campus in Lausanne, Switzerland (Lat. 46°5' N, Long. 6°6' E, elevation 396m) were monitored and compared with those obtained under an artificial sky and those issued from computer simulations. Such study was presented in the international conference Clima 2013.

The characteristics of the module are those of an office room (dimensions: 6.5m x 3.05m x 2.65m) equipped with a conventional double glazing. The interior material properties, such as the surfaces reflectance (floor 16%, walls 82%, and ceiling 80%) and glazing transmittance (80.5%) were reproduced in a virtual model in order to carry out computer simulations. Indoor and outdoor illuminance was than measured at a height of 0.8m under overcast and clear sky conditions at 10h00, 13h00 and 17h00. The double glazing was considered first, then two different CFS: a laser cut panel (6mm single acrylic with 4mm parallel cuts) and a 3M brand optical lighting film (SOLF).

In the previous study, a total of six different cases were analysed from which two were used to perform this verification. First, the data monitored in the testing module under real sky conditions, then the simulation results using the primitive *prism2* function, in which the sky was reproduced using the CIE standard skies (Type 1 for the overcast sky and Type 12 for the clear sky) [131]. The results were compared with those obtained for three different cases: a) by applying the primitive *prism2* in an improved RADIANCE version and by using the two new RADIANCE procedures; b) the first procedure which uses the pre-process *mkillum* and c) the second procedure called *bsdf* material function which models directly the transmitted daylight distribution without the use of *mkillum*[65]. In order to assess the daylighting distribution in the office room close to the window, additional simulation points were considered at each 10 cm up to a 2 m distance from the window and each 20 cm from that point to the back of the room. Digital renderings of the module were also generated in order to visualize the indoor daylight propagation when applying the CFS. The CPU time taken to carry-out each simulation was also considered in order to compare the convenience of using each procedure. Parameters similar to those used for the simulations carried-out in the previous study were applied for the present RADIANCE simulations in order to achieve highly accurate illuminance calculations (-ab 9, -aa 0.1, -ad 26315, -ar 128). The daylighting performance was assessed using the daylight factor (DF) in case of overcast sky conditions and the illuminance ratio (IR), in the case of clear sky conditions. However due to space restrictions only the results obtained under clear sky conditions are presented in this document.

3.3.1.1 Results

a) Simulations under clear sky conditions using Laser Cut Panel

From the simulations performed under clear sky conditions, the results obtained at 13h00 are presented since they show more discrepancies than those carried-out at 10h00 and 17h00. A comparison of the IR profile is illustrated on Figure 3.7, showing that a detailed profile was obtained from the present simulations (*prism2*, mkillum and *bsdf*), thanks to the additional points considered in the virtual model. Larger IR values are observed next to the window, where the sun rays fall on the floor after passing through the upper and lower windows of the module. When using the primitive *prism2* larger values are shown for the direct contribution of the lower window, while in the case of the upper window the levels decreased as a daylight fraction is redirected to the ceiling when passing through the laser cut panel. A comparison of the renderings is shown on Figure 3.6, the rendering obtained with *prism*2 (left) shows the light flux projected on the floor as the contribution of the upper window, which is not shown when using the other two procedures (center and right). This is due to the new RADIANCE simulation procedures (*bsdf* and mkillum) which allow a detailed daylight rendering thanks to multiple lighting redirections and supports the calculation of the daylight propagation through the CFS in a diffused way (therefore is more evenly distributed). The IR profiles for the present simulations are very close to the monitored one through the rest of the room. The CPU time for the *prism2* was about 2h and with the mkillum procedures about 21 hours, for the *bsdf* procedure was about 5 minutes due to the modifications of the simulation parameters (in this case: -ab 5, -ar 32, -aa 0.2, -ad 512, -as 256).

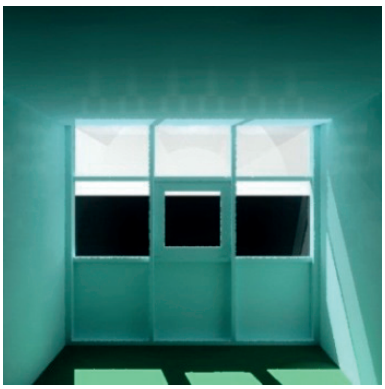

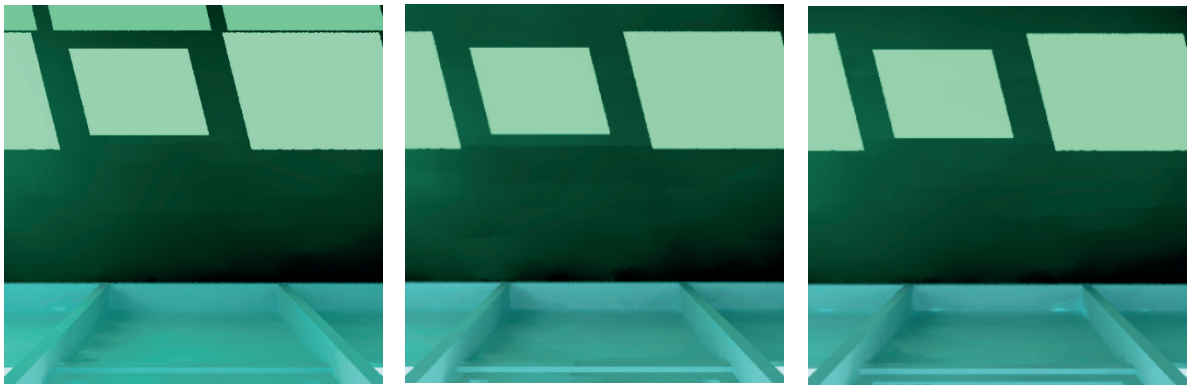

Figure 3.6 Interior view of the virtual model under clear sky conditions using Lasercut Panel. On the left the simulation using *prism*2, the mkillum procedure is shown at the center and the *bsdf* procedure in the right picture. The corresponding views from the top showing the light projected in the floor after passing through the CFS are shown below.

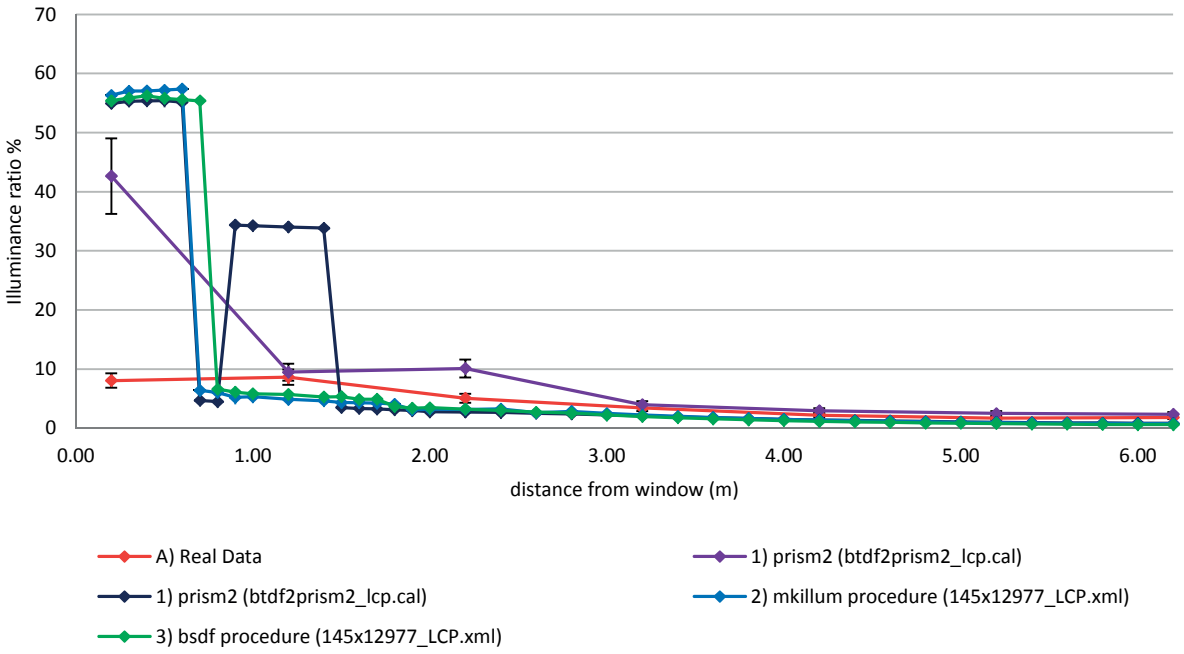

Figure 3.7 Results of simulations using LCP comparing the IR profile obtained with different RADIANCE procedures under clear sky conditions.

b) Simulations under clear sky conditions using the 3M Film (SOLF)

The IR deduced from the simulations obtained using a prismatic 3M optical lighting film (SOLF) carried out for clear sky conditions at 13h00 are illustrated on Figure 3.9, while the renderings are shown on Figure 3.8. It can be observed that IR values larger than 50% can be observed next to the window for the simulations using *prism2*, mkillum and *bsdf* procedures; they are due to the sun-rays impinging on the floor when passing through the lower window of the module. When using an SOLF film the light is directed according to two directions, the largest intensity being redirected slightly downwards and to the back of the room while a lower intensity is redirected down next to the window. Therefore, larger IR values can be observed at the back of the room, which are due to the contribution of the upper window equipped with the SOLF Film. When using the mkillum and *bsdf* procedures, lower IR values are observed at the back of the room, due to the daylight diffusive propagation simulated by these procedures. A difference appears when comparing the IR values of the present simulations at 0.2 m from the window with the monitored data. The former shows an IR value larger than 50% while the latter results are lower than 10%, which is due to the shadowing of the breast wall at the first measurement point. The CPU simulation time using *prism2* was equal to 2 hours; with the mkillum procedure it took 28 hours, while when using *bsdf* it took about 10 minutes. The RADIANCE simulation parameters in this last case were the following: -ab 5, -ar 32, -aa 0.2, -ad 512, -as 128 (As shown in Table 3.5).

Figure 3.8 Interior view of the virtual model in the testing module equipped with the 3M Film (SOLF) under clear sky conditions. The picture on the left shows the simulation using prism2, the mkillum procedure is shown in the centre and the bsdf procedure in the right picture. The corresponding views from the window side to the back of the room are shown in the pictures below.

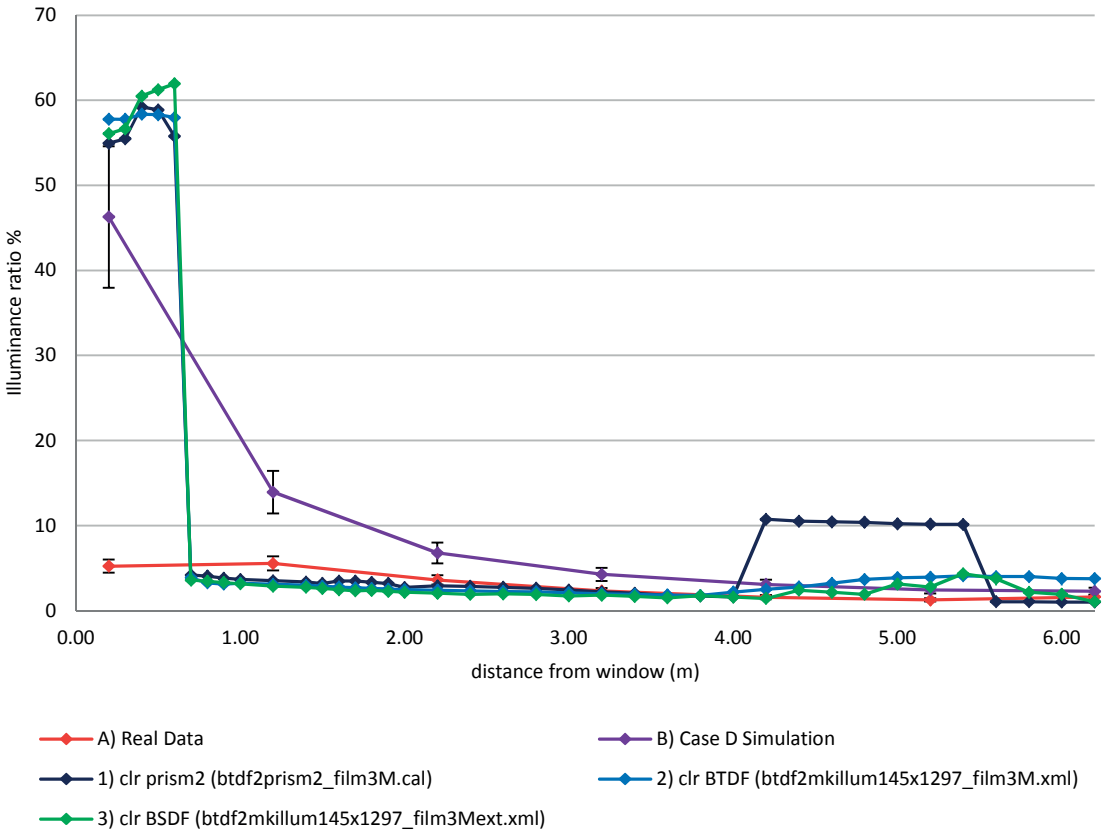

Figure 3.9 Simulations involving the 3M Film (SOLF) comparing the DF profile obtained with different RADIANCE procedures under clear sky conditions.

As a result of this study, it was found that the use of the *bsdf* procedure using low RADIANCE parameters would provide comparable results to those obtained when using medium and high RADIANCE simulation parameters, while the former could be obtained in a reduced CPU time. In order to corroborate this, the MBE were calculated taking into account the simulations carried-out in clear sky conditions (10h00, 13h00 and 17h00). For this, simulations were carried-out with the *bsdf* procedure using different RADIANCE parameters, shown in Table 3.4. The MBE were calculated using as a reference the results obtained with the high quality radiance parameters (c), the differences found between those and the low quality simulation (a) and the medium quality simulation (b) are shown in Figure 3.10 for the simulations using LCP, and 3.11 when using the Film 3M. In the case of LCP (Fig 3.10), they show that when using low simulation parameters a minimum value of -2.55% and a maximum of -39% MBE can be achieved (MBE -23%), while when using medium quality parameters the difference ranges from 17% to -26% (MBE -12%). In the case of the Film 3M (Figure 3.11) the differences range between 47% and -66% (MBE -12%) when using low quality parameters, while when using medium quality parameters they are within 70% and -50% (-0.37%). Such results show that in the case of LCP a low quality simulation would represent a noticeable range of error therefore its use might not be favoured, even considering the short CPU time required to complete the calculation. However, the use of medium simulation parameters show a moderate range of error (within average 12%), thus its use would be recommended in view of the CPU time that carrying-out the simulations using high quality parameters takes (See Table 3.5). However different results were found when using Film 3M, where the medium quality parameters showed higher range of error (37%) compared with the low quality parameters (12%). Thus, these results are useful to deduce that using simulation parameters within a 'medium' quality range would represent an option in view of the CPU time required when using high quality parameters. The former, represents a choice since it would produce results within an acceptable range of error while obtained during a reasonable CPU time.

RADIANCE parameters		
a)	Low quality parameters	ab 5, aa 0.2, ad 512, as 256, ar 32,
b)	Medium quality parameters	ab 6, aa 0.1, ad 2048, as 512, ar 64,
c)	High quality parameters	ab 9, aa 0.1, ad 26315 ar 128

Table 3.4 RADIANCE parameters used to carry-out the simulations in order to compare their differences when using the *bsdf* procedure.

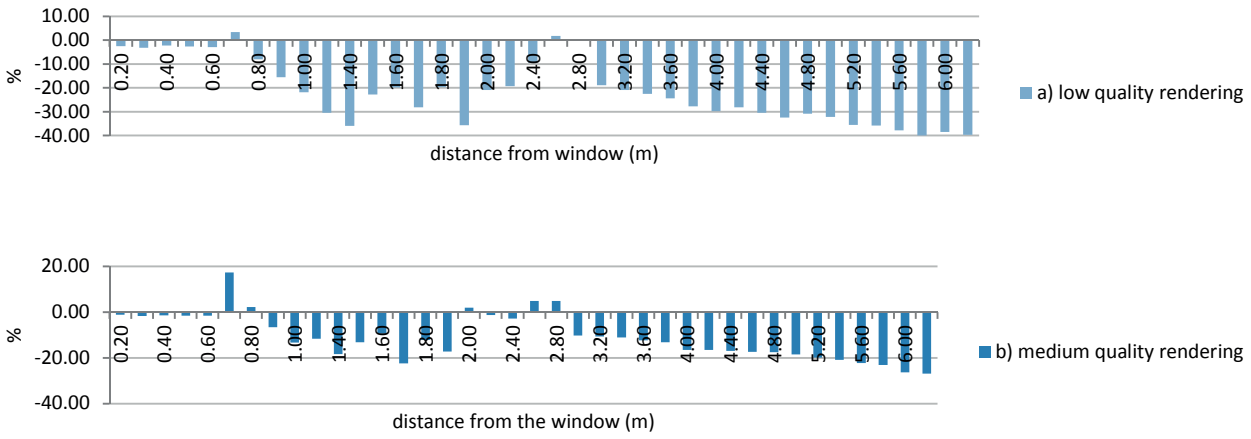

Figure 3.10 MBE of the comparison between the low and medium quality RADIANCE parameters when using LCP, using as reference the results obtained when using the high quality paramters.

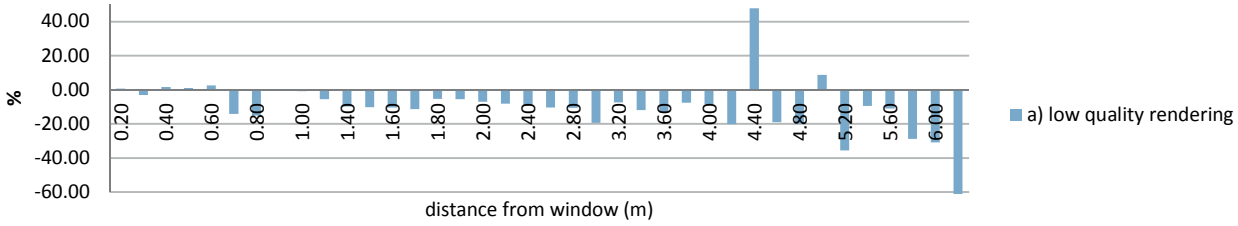

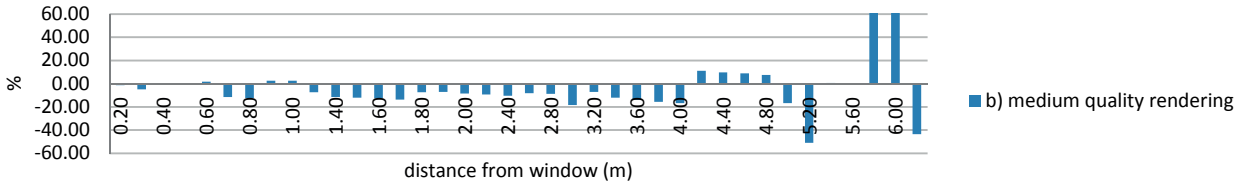

Figure 3.11 MBE of the comparison between the low and medium quality RADIANCE parameters when using Film 3M, using as reference the results obtained when using the high quality parameters.

CPU Time		LCP		Film 3M	
RADIANCE procedure	**Simulation parameters**	**Overcast sky**	**Clear sky**	**Overcast Sky**	**Clear Sky**
prism2	High quality parameters	50 min	<2h	40 min	<2h
mkillum		20h	21h	20h	28h
bsdf	Low quality parameters	~2min		~3min	
	Medium quality parameters	~ 8 min	~ 10 min	~ 10 min	~ 20 min
	High quality parameters	~ 96h	~ 96h	~ 96h	~ 96h

Table 3.5 CPU time of the simulations carried-out under overcast and clear sky conditions using the three RADIANCE procedures, when using LCP and Film 3M with different RADIANCE parameters.

3.3.1.2 Conclusions

The present comparison was carried-out using an improved *prism2* routine as well as the new RADIANCE procedures (mkillum and *bsdf*) in order to compare the results obtained to establish confidence in the use of the new procedures. The IR profiles of the currently performed simulations show higher differences in the area next to the window due to the additional measurement points included to perform the present simulations. It can be observed in the results shown in Figure 3.7 and 3.9 that when using *prism2* higher IR are obtained in the window area and back side of the room (LCP and Film 3M resepectively) compared to the use of the other procedures, which is due to the way how *prism2* simulates the propagation of daylight through the CFS. The latter is the reason for which the *prism2* routine as a simulation procedure has not been considered in this doctoral thesis (see Section 1.3.1). When using *prism*2 the emerging lighting flux is being modelled only in two directions, reproducing the daylight propagation in an unrealistic way. However, it can be concluded that one can rely on the new RADIANCE procedures (mkillum and *bsdf*) for daylighting simulations of CFS in a single room. Regarding the selection of using the mkillum or the *bsdf* procedures, this verification lead to the following observations: when the *bsdf* procedure was used with the same rendering parameters employed in the the previous study; the CPU time is considerably increased. However, when these values were reduced, no significant difference was observed when comparing the results with those obtained in the previous study, while the CPU time was substantially lower. This suggests that the *bsdf* procedure has more impact on the CPU time than on the improvement of the simulation results. In the case of visualizations using the *bsdf* procedure, the CPU time is larger than when using the mkillum procedure, making necessary to adjust the RADIANCE parameters in order to obtain a reasonable CPU time, which has an impact on the quality of the rendering. This suggests that privileging the use of the mkillum procedure is commended when renderings are required.

Both procedures (mkillum and *bsdf*) use the BTDF data stored in an XML file to simulate the daylight distribution through the CFS. However, the two procedures are significantly different in the way they perform the simulation. The *bsdf* procedure uses the *bsdf* material function which models directly the transmitted daylight distribution without the use of *mkillum* to model the way daylight passes through the CFS. On the other hand, the *mkillum* procedure requires a pre-process that takes into account weather conditions and exterior obstructions to generate the CFS candle power distribution; such calculation is performed from the centre of the polygon assigned to the BTDF data. When assessing the daylighting performance of CFS in a room, the accuracy of the results generally relies on the simulation parameters that drive the lighting calculation in the computer model, but also on the BTDF data resolution assigned to the polygon mimicking the CFS. Therefore, when using the *bsdf* procedure the polygon resolution is significant, especially in an urban context where exterior obstructions are usually present. A study was carried-out in order to investigate the impact that the polygon resolution assigned to the BTDF data representing the CFS might have on the simulation accuracy in the presence of exterior obstructions. The latter proposes that the use of a subdivided polygon would lead to more precise calculations. The corresponding methodology is presented as follows.

3.3.2 Simulating daylight propagation through CFS in an urban context using a variable sample subdivision scheme

As a common practice, the BTDF data is applied to a single polygon representing the full pane of a window in virtual models. However, when using the mkillum procedure, the calculation of the daylight distribution through the CFS is performed from the center of the polygon, taking into account its full area assigned to the BTDF data. Therefore, when a combination of light and shadow falls over such polygon, the calculation is performed taking into account the entire polygon as if it was fully lit or fully shadowed. In such case, inaccurate results might be obtained when the shadows of adjacent buildings are projected on the building's façade.

In order to determine the accuracy of the simulated daylight propagation through CFS in presence of external obstructions, a daylighting situation involving the virtual model of Building B2 (whose characteristics are specified in Section 2.3) was created. In that, exterior obstructions would partly project a shadow over the entire polygon representing the window (winter solstice at 11h50). Three buildings, placed 7.0m away from the façade in order to create shadows in the office room, were included in the model. Simulations were then carried-out using firstly the mkillum procedure [64], and secondly using the *bsdf* material function [65], in order to compare the results of the two RADIANCE procedures.

The BTDF data [61, 64] of the Laser cut panel (LCP) [125] was assigned to the polygon that accounts for the upper window in the office room. In order to determine the accuracy of RADIANCE simulations regarding the BTDF data resolution, the latter was carried-out fisrt using the full-size polygon that accounts for the upper window in the office room. Secondly, the polygon was subdivided into small sections of 10cm x 10cm, which correspond to the dimensions of the original LCP sample whose photometric properties [59, 132] were assessed with the bidirectional gonio-photometer [57, 124]. In total, the east upper window was subdivided into 150 elements of 10cm x 10cm as well as 6 elements of 6cm x 10cm for the remaining space which is next to the column located in the middle of the room; the west-upper window was subdivided into 72 elements of 10cm x 10cm plus 6 elements of 4cm next to the west wall.

Since the *bsdf* procedure reproduces the daylight propagation through the CFS directly using the BTDF data stored in the XML file, the use of window subdivisions will not induce any difference in the simulation results. Hence, when using the *bsdf* procedure the calculations were carried-out only with the full-size polygon. Three situations were then assessed: i) using mkillum with the full size window; ii) using mkillum with the subdivided window and iii) using the *bsdf* procedure. The final comparison was performed in two steps: a visual assessment was performed first by comparing renderings of the room interior from three different viewpoints, a second assessment was performed by comparing the simulated daylight distribution in the office room on the basis of IR values [43]. Illuminance was estimated for that purpose by placing points at desk height (0.75m), in the middle of the room at each 10 cm from the window up to 2.5m and each 20cm from there to the back of the room

3.3.2.1 Results

a) Visual Assessment

A straight view of the larger window in the office room is illustrated in Figure 3.12. It shows that when using the mkillum procedure with the full-size polygon, daylight is projected on the ceiling as if the entire window area was lit (left). However, when using mkillum with a sub-divided polygon, it shows that a more accurate calculation is performed (center); the light is redirected to the ceiling only for the lit area on the façade. In case of use of the *bsdf* procedure (right), the rendering shows that the calculation is performed taking only the lit area into account. However, when using the *bsdf* procedure, the CPU time is larger than when using the mkillum procedure for similar RADIANCE parameters. In order to obtain simulation results in a reasonable time using the *bsdf* procedure, the values of the parameters have to be reduced and likewise the quality of the pictures.

Figure 3.12 Visualization of the office room using mkillum with the full-size window (left; using mkillum with the subdivided window (centre) and the visualization obtained with the *bsdf* procedure (right).

A second rendering, illustrated on Figure 3.13, shows the office room viewed from the back. It allows a comparison of the modelling of the daylight distribution through the LCP for both windows. The picture shows a well-defined lighting redirection on the ceiling when the simulation is performed using mkillum with the subdivided window (center); a similar result is also achieved using the bsdf procedure (right). However, in the latter the redirected light flux shows a lower definition due to the low picture quality. This is due to the limited CPU time allowed for the *bsdf* procedure by the RADIANCE parameters. In this case, a rendering can take from 20min to one hour in low image quality with the corresponding simulation parameters (-ab 2, -aa 0.2, -ar 32, –ad 512); while when using mkillum it takes about 10 minutes in both cases (full-size window and subdivided window) in medium image quality with the corresponding simulation parameters (-ab 6, -aa 0.1, -ar 64 –ad 1024).

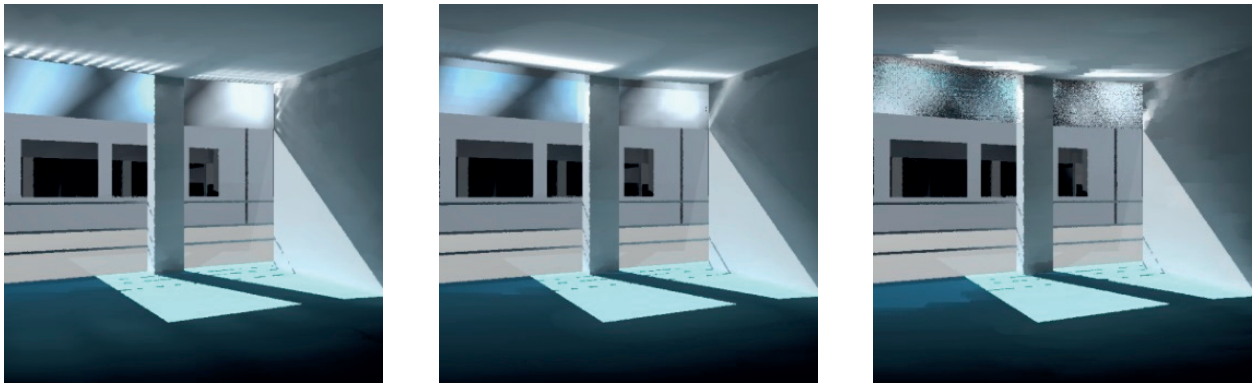

Figure 3.13 Visualizations of the interior of the office viewed from the back. Modelling of the daylight distribution through the LCP using mkillum with the full-size window (left), using mkillum with the subdivided window (centre) and using the *bsdf* procedure (right).

A third visualization was obtained, which shows a closer view of the window illustrated on Figure 3.14; it is possible to observe how daylight is redirected on the ceiling. When using mkillum with the subdivided polygon (center) the light pattern is regular and defined, while when using the full-size polygon it shows a discontinuous light projection (left). The simulation carried-out with the *bsdf* procedure shows an undefined light redirection due to the low quality of the picture (right).

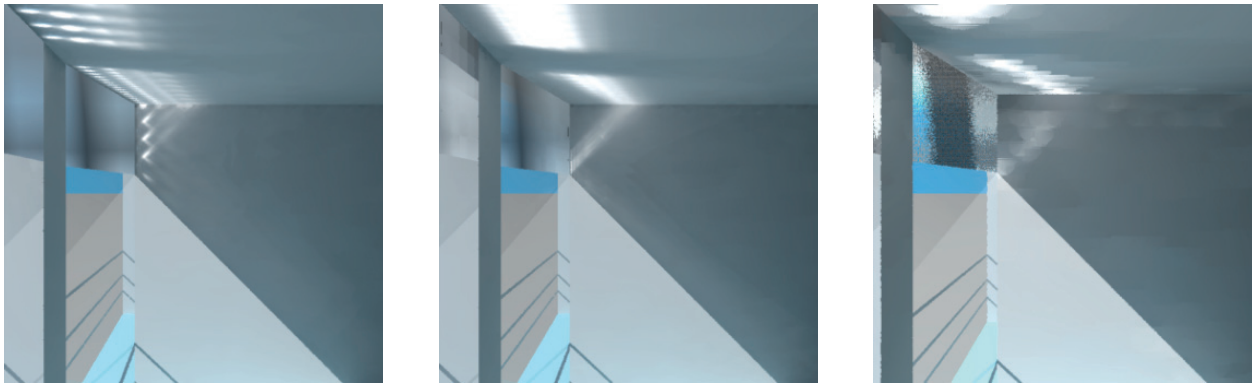

Figure 3.14 Transversal view of the window allowing detailed observation of the daylight propagation through the LCP using mkillum with the full-size window (left), with the subdivided window (center) and with the *bsdf* procedure (right).

b) Numerical assessment of daylight distribution through CFS in the office room

A second assessment was performed by analyzing the daylight distribution in the room by comparing the IR profiles obtained in the shadowed area of the room (at the centre of the larger window). Measurement points were placed for that purpose at 10cm distance from the window up to 2.5m and from there at 20cm to the back of the room. The results are illustrated on Figure 3.15; they show a very similar IR profile across the room with values ranging between 9-10% next to the window. However, the IR profile obtained using mkillum with the full-size window shows larger values at a distance of 1.0m to 1.8m from the window. When calculations are performed with the mkillum pre-process using the subdivided window and the *bsdf* procedures, IR values shows a continuous profile, meaning that no daylight is modelled in the shadowed area of the façade. All the IR profiles assessed using the three conditions are within a range of 10% accuracy. The larger values obtained using mkillum with the full-size window are not considered as significant in regards to the daylight distribution. The CPU time using mkillum was equal to 2 hours when using the full-size window and about 14 hours with a sudivided window. With the *bsdf* procedure, the CPU time is equal to 2 hours, the simulations being carried-out with the same RADIANCE simulation parameters in all cases (-ab 4, -aa 0.1, -ar 64, -ad 1024).

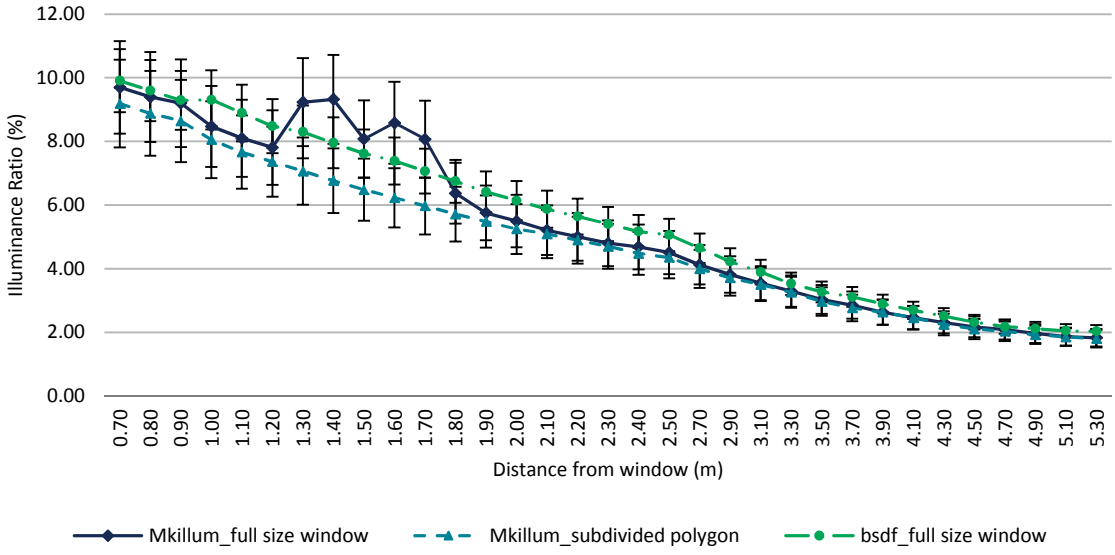

Figure 3.15 Illuminance Ratio profile through the room obtained using mkillum with the full-size window, the subdivided polygon and the *bsdf* procedure at 11h50 when shadows are projected on the façade.

3.3.3 Conclusions

The aim of this study was to investigate the impact of the BTDF data resolution assigned to a polygon representing a CFS on the simulation accuracy in presence of exterior obstructions. Simulations were carried-out using two RADIANCE routines: the mkillum pre-process and the *bsdf* procedure. A full-size polygon was used first and then a subdivided polygon associated to the BTDF data of LCP, in order to compare the renderings and the illuminance ratio profiles. The former showed that when simulations are carried-out with the full-size polygon, mkillum performs a calculation overlooking the shadow effect of the adjacent buildings, leading to inaccurate results. On the other hand, when the polygon is subdivided, the daylight distribution is calculated only taking in to account the areas that are not shadowed by the exterior obstructions; the same situation is observed when using the *bsdf* procedure. However, the assessment of the daylight distribution with the IR profiles showed no significant differences when using the two procedures.

To summarize, when using the mkillum procedure a polygon subdivision assigned to the BTDF data of the CFS is advisable. If the quality of the interior environment requires a quantifiable evaluation, such as illuminance ratio (IR) or daylight factor (DF) [75], the polygon subdivision associated to the BTDF data does not lead to a significant improvement. Another disadvantage of using such procedure is the CPU time required to perform the calculation given that it involves a pre-process to simulate the daylight propagation through the CFS (See Section 3.3.2). When using the RADIANCE procedure *bsdf* the calculation can be performed in a shorter time with an acceptable accuracy, its disadvantage being the quality of the picture which is compromised by the RADIANCE simulation parameters. In regards to this PhD thesis, this study allowed to assess the advantages and disadvantages of using either RADIANCE procedures in computer simulations that include the use of CFS in buildings. Therefore, considering the results, the *bsdf* procedure was selected to simulate the daylight propagation through CFS in the two office rooms. Such decision was made in view of the *bsdf* procedure advantages in terms of CPU time and accuracy rather than considering the disadvantages of using mkillum, given that the scenes created to simulate the two buildings considered in this thesis do not include external obstructions.

3.4 Assessment of the improved interior daylight distribution through CFS in the two office rooms

In order to assess the daylighting performance of the five selected CFS in the two office rooms (Building B1 and Building B2), computer simulations were carried-out using virtual models characterized and calibrated according to the features of the existing office rooms (see Section 2.4). The simulations were performed using the RADIANCE procedure *bsdf,* which was selected as a result of a comparison between the two other existing RADIANCE procedures that simulate the daylight propagation through CFS (Section 3.3.1). The BTDF data of the five CFS was applied to a polygon representing the upper part of the window. The dimensions of the polygon were defined according to a standard procedure used mainly in Europe, which takes into account an average height of the occupants' eyes as a reference to establish the position of the CFS (in order to avoid disturbances for the outside view). In Mexico, the average height of the population is 1.70 m, thus the position of the CFS was accordingly established. As a result, the height of the CFS of Building B1 was set to 1.5 m to reach the ceiling at 3.2m, while for Building B2 the height was 0.9 m to reach the ceiling at 2.6m.

The simulations were carried-out for the three days in which the room was monitored: spring equinox, winter and summer solstices at 9h00, 12h00, 15h00 and 17h00. Measurement points were similar to those used in the monitoring phase (see Section 2.4). The DF and the IR profiles obtained for the points located at the center of the room were compared with those obtained in the current situation. Image renderings were also obtained from different viewpoints in the room in order to perform a visual assessment. The RADIANCE simulation parameters were equal to those used for the calibration of the virtual model in order to achieve accurate results (see Table 2.7). However due to the long CPU time required to perform the simulation including the LCP, the parameters were adjusted in order to obtain results in a reasonable time frame (Table 3.6). Difficulties were also found in the picture rendering including the LCP therefore the simulation parameters were set to a lower value for this specific case (-ab 3, –ad 512, –as 128).

Simulation Parameter	Building B1		Building B2	
	Illuminance Calculation	Image Rendering	Illuminance Calculation	Image Rendering
Ambient Calculation				
-ab	6	6	6	6
-ad	4096	2084	4096	2048
-as	1024	512	1024	512
-ar	64	64	64	64
-aa	0.1	0.1	0.1	0.1
Direct Calculation				
-ds	0.01	0.01	0.01	0.01
-dj	0.9	0.9	0.9	0.9
-dt	0.05	0.05	0.05	0.05
-dc	0.17	0.17	0.17	0.17
-dr	3	3	3	3
-dp	4096	4096	4096	4096

Table 3.6 Simulation parameters for image rendering and illuminance calculation to assess the daylighting performance of the five selected CFS in Building B1 and B2.

3.4.1 Results

The results for 12 hourly time steps were obtained for each building (9h00, 12h00, 15h00 and 17h00) and for each of the three days considered (winter and summer solstices and spring equinox), they compare the simulations of the virtual model with standard double glazing with those using the five pre-selected CFS. However, due to space restrictions only one hour for each assesed day is shown in this document. The simulation results of Building B1 are shown first and then those of Building B2. A view inside the room equipped with conventional glazing is shown first in order to compare it with the renderings of the five pre-selected CFS, the latter renderings are shown as a human response view and in false color. The IR (in case of clear sky conditions) or DF profiles (in case of overcast sky conditions) using a glass visual transmittance of 80% and a CFS are shown in order to compare the daylight distribution in the room.

3.4.1.1 Building B1

a) Winter Solstice

12pm The results obtained for winter solstice (20th December at 12h00) comparing the IR profiles of the room simulated with glass τv 80% function and those obtained using the five pre-selected CFS show a subtle difference for the area close to the window. Through the room the difference is more perceptible: the IR profile of the double-glazing is larger than those of the CFS at distances of 0.6 to 1.2m from the window. The IR profile shows that the Film3M and CFS3 contribute to increase more the interior illuminance in the room, while CFS1 and LCP are the ones that contributed the least. A rendering using Glass τv 80% is shown on Figure 3.16, as human response and false color image. The IR profile is illustrated on Figure 3.18 and the renderings are shown on Figure 3.17. The relative erros MBE per room zone are shown also in Figure 3.18 for the five CFS, where it can be observed that almost all the CFS shown negative differences compared to the standard glass τv 80%, only the Film 3M shows positive differences in the center and back area of the room with a maximum of 15%. Which indicates an evident better performance of the Film 3M.

Figure 3.16 Rendering of the B1 room on Winter Solstice at 12h00 under intermediate sky conditions with the Glass τv80% function, showing the human-response view (left) and the false color image (right) whith the corresponding illuminance scale which is used also for the CFS images.

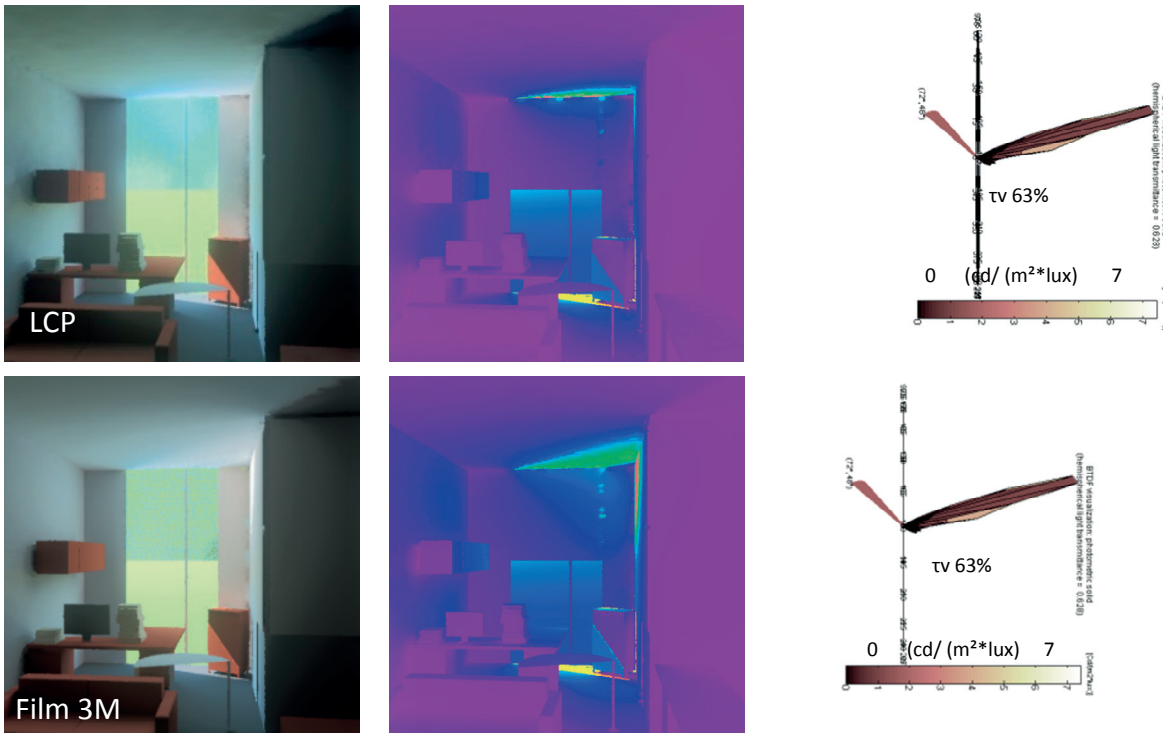

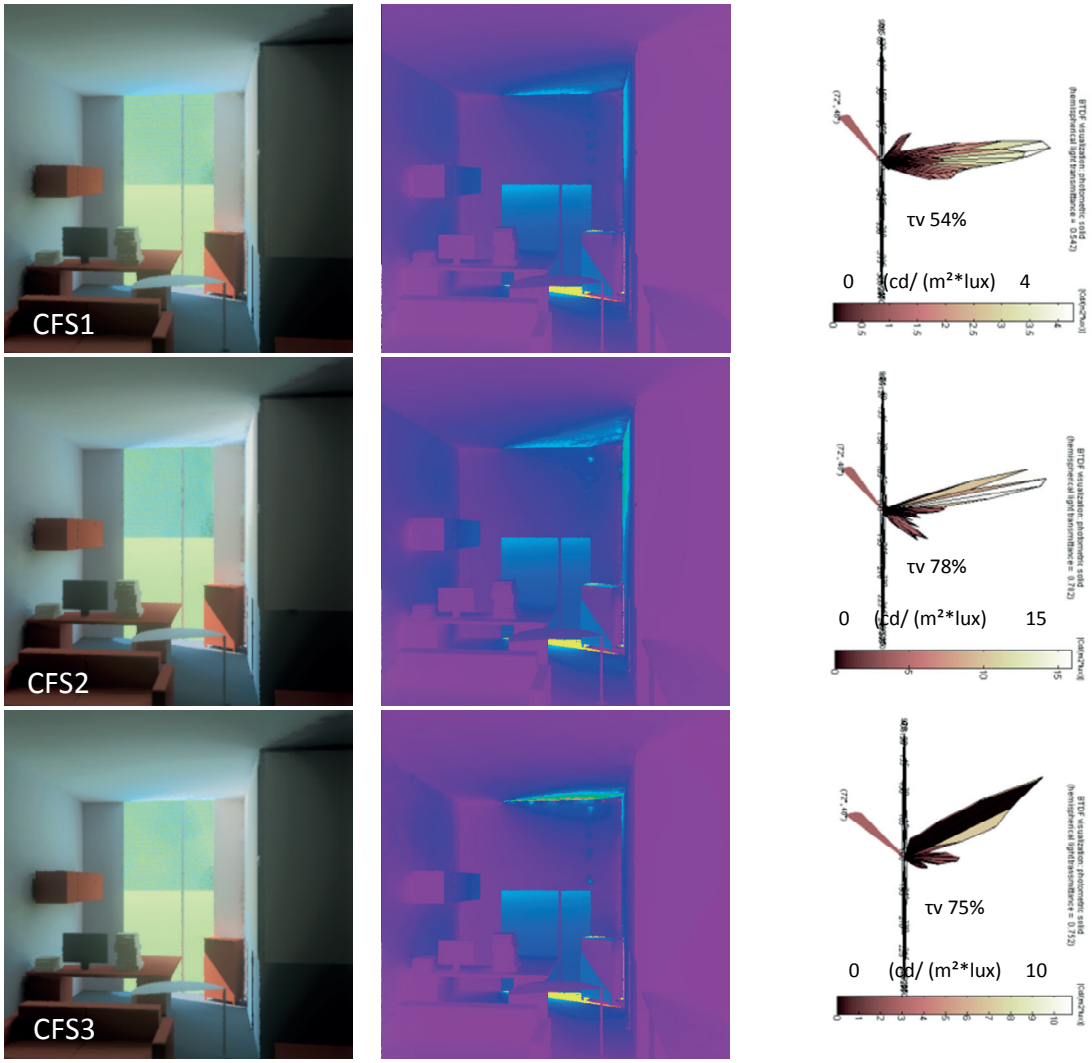

Figure 3.17 Renderings of the office from the back (left) and side of the room (centre) showing the extent of the daylight redirection through the five considered CFS. The BTDF diagram showing the lighting redirection is given for each CFS (right), while its corresponding scale range (cd/m ²*lux) is presented in text in the right column.

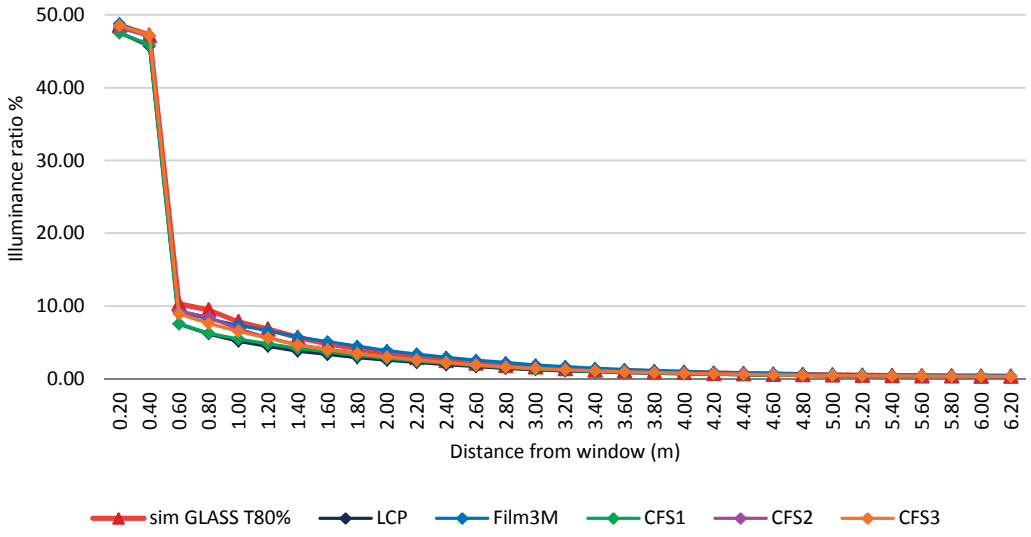

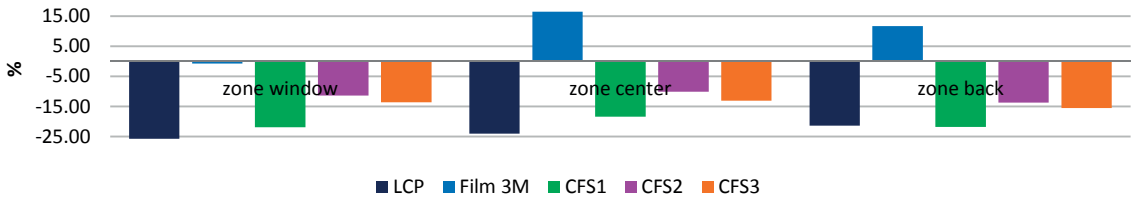

Figure 3.18 IR profiles illustrating the daylighting performance of the five CFS in the office room in B1 on Winter Solstice at 12h00 under intermediate sky conditions, the MBE per CFS per room zone (window, center and back of the room) is shown in the graph below.

b) Spring Equinox

15pm The simulations obtained for Building B1 at spring equinox (21th March at 15h00) show an increase of about 5% in the highest IR profile of the CFS (CFS3) compared to the Glass τv 80% at a distance of 0.2m from the window (Figure 3.21). It can be observed that CFS3 and Film3M allow larger daylight fluxes to enter the room, while CFS1 allow the lowest. It can be observed that the illuminance increase the most when using CFS2 and the Film3M and less when using CFS1. An additional assessment was performed in order to determine the performance of venetian blinds with a slats' angle of 0° and compare it with the other CFS. It can be observed that venetian blinds lead to lower daylighting illuminance in the room compared to the other CFS. The difference between the IR profile of the GLASS τv80% (which profile extends up to 2m distance from the window) and the five CFS is due to a fraction of light redirected to the ceiling and to the CFS which is acting as a shading device (as shown on Figure 3.19); the renderings using the double glazing show a larger sunlit area on the floor while the CFS (Figure 3.20) lead to a smaller one. This can be also seen in the fish eye view illustrated on Figure 3.22. The MBE show that the largest differences are found at the back of the room when using CFS2 with 190%, while next to the window the maximum difference is found when using LCP with -45%. The latter, reveals a better performance of CFS in the back of the room, being CFS2 with a noticeable better performance.

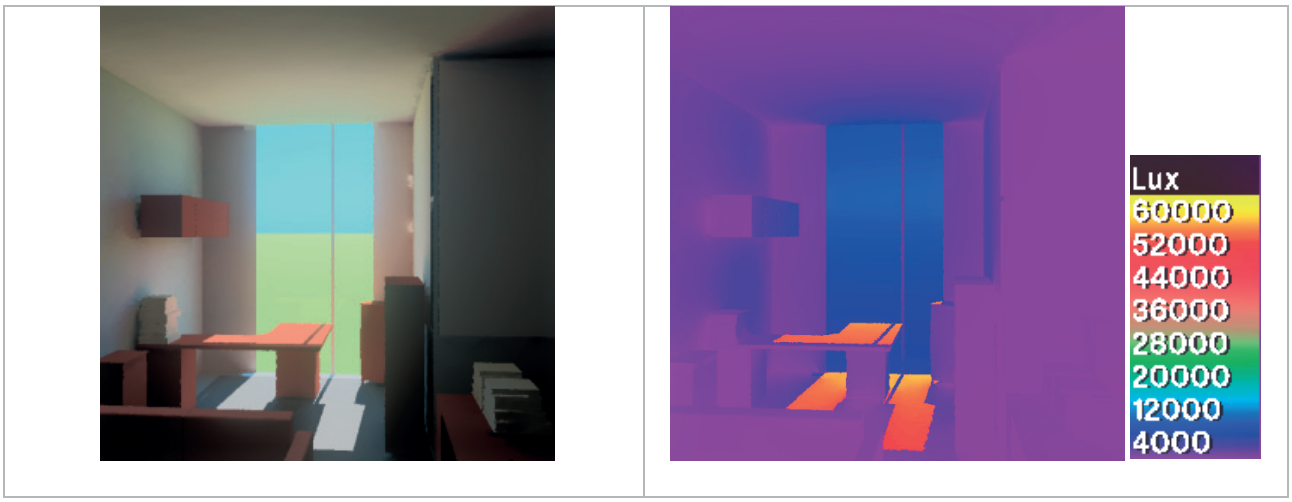

Figure 3.19 Rendering of the Building B1 room with GLASS τv 80% on March 21th at 15h00 under clear sky conditions, showing the human-response view (left) and the false color image (right).

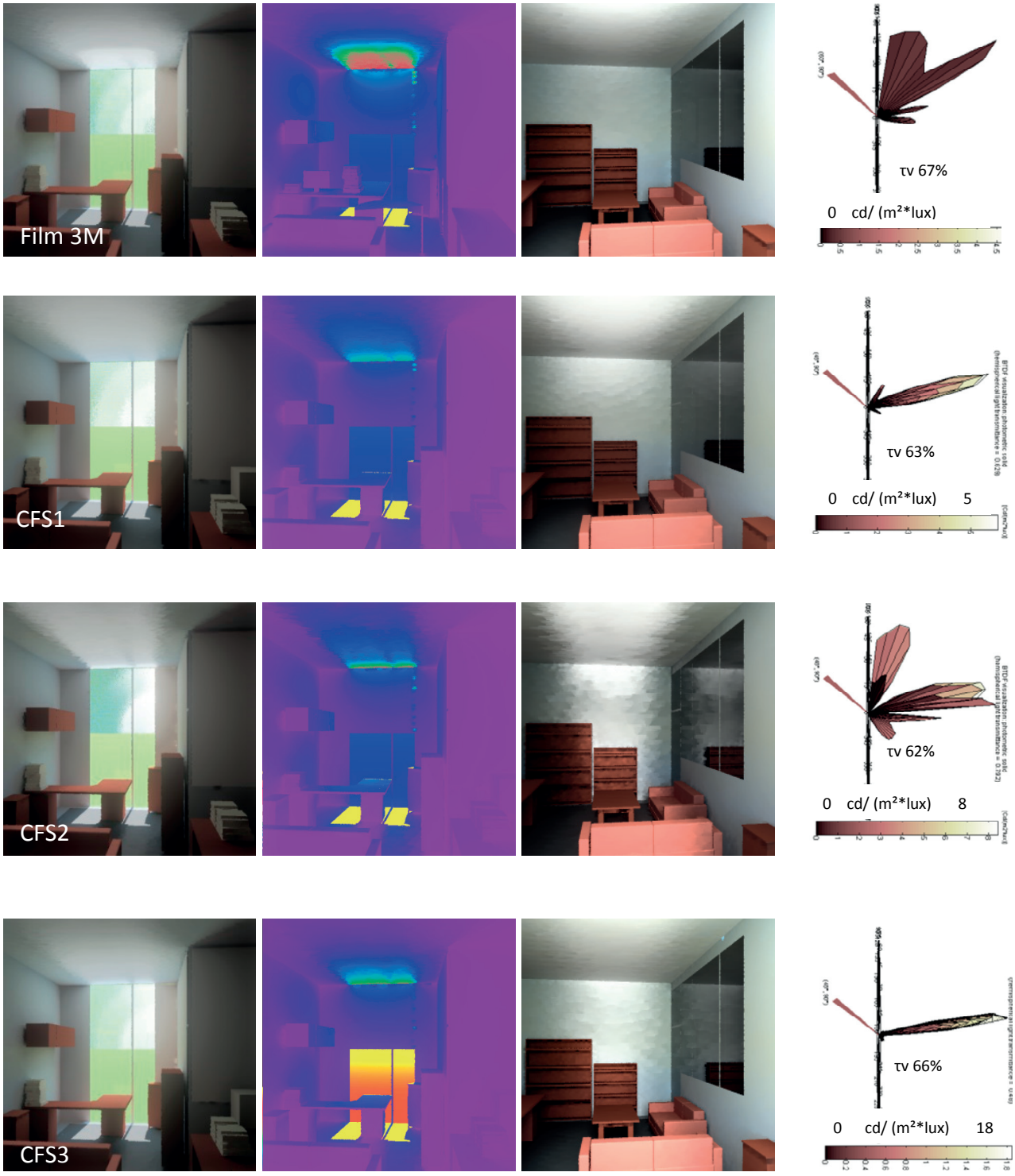

Figure 3.20 Renderings of the office viewed from the back of the room as human response view (left) and in false color (centre). A view from the SW window to the back of the room is shown (right) in order to visualize the extent of the daylight redirection through the room when using the tested CFS. The BTDF diagram on the right shows the lighting redirection and its transmitted flux expressed in percentage, while the scale range (cd/ (m ²*lux) is presented in text in the right column.

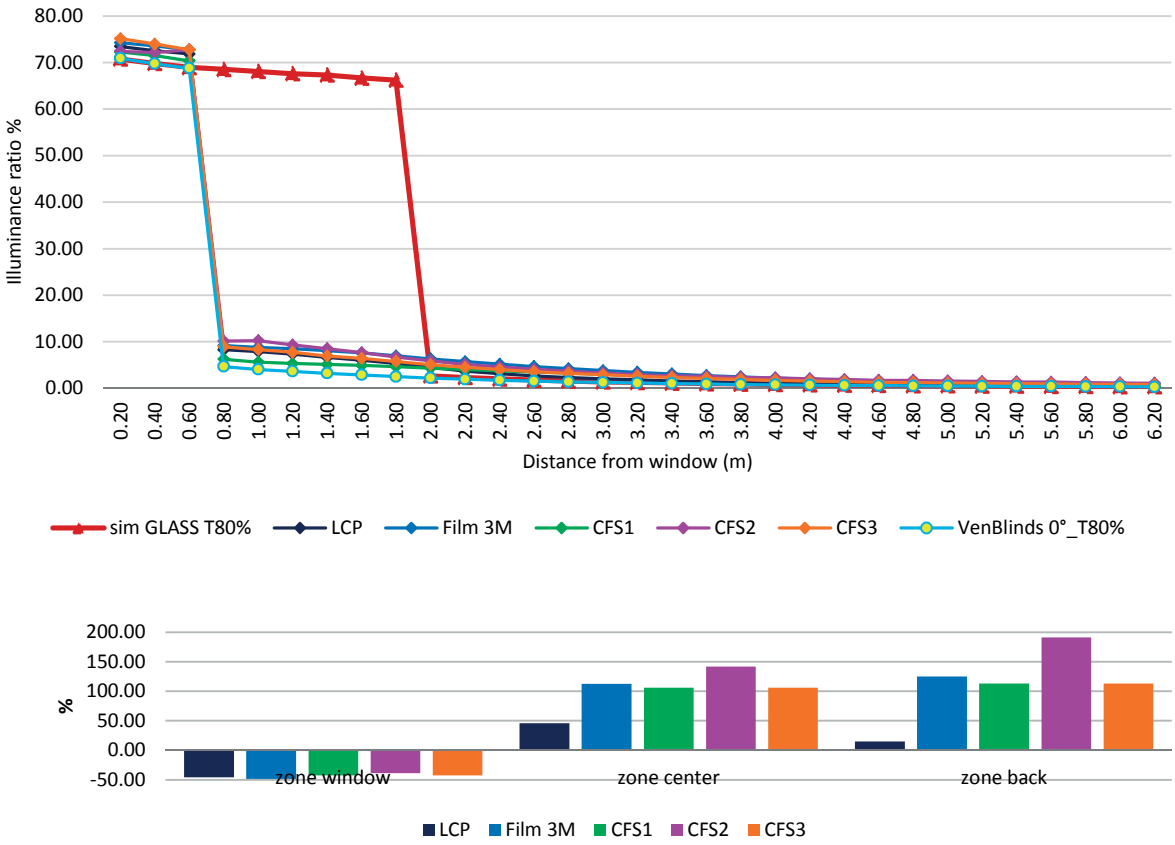

Figure 3.21 The IR profile that show the performance of the five CFS inside the office room in Building B1 in spring equinox at 15h00 under clear sky conditions, the MBE per CFS per room zone (window, center and back of the room) is shown in the graph below.

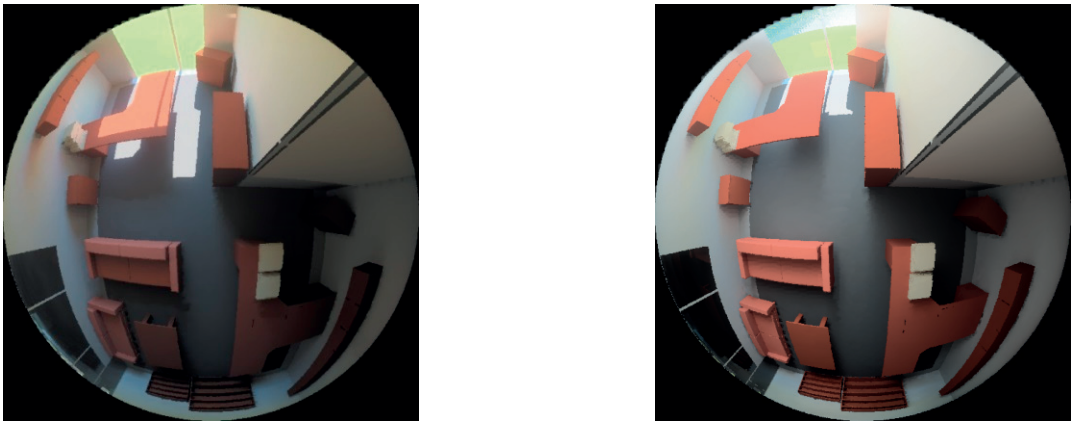

Figure 3.22 Fish eye view from the top of the office room showing the larger sun lit area when only glass is used in the window (left) and the shaded one by the CFS (right).

c) Summer Solstice

15pm The simulations obtained for Building B1 on summer solstice (21th June at 15h00) under intermediate sky conditions, show that the standard Glass τv80% presents a higher IR through the room compared with the ones achieved by the CFS. Of the five CFS compared is the Film 3M shows the higher IR especially at a distance from1.2 to 3.8m from the window, while CFS1 and LCP show the lower IR. At the back of the room the performance shows comparable results for the six fenestration systems compared. The simulation rendering of the existing situation is shown in Figure 3.23 including the false color image for the corresponding view, and the illumiance scale applied also for the CFS. The IR profiles are shown on Figure 3.25 and the renderings on Figure 3.24. The MBE shown also in Figure 3.25, shows mainly negative differences between the standard glass and the CFS, with a maximum of -40% when using CFS1 in the center and back zone of the room, the shortest difference is found when using the Film 3M with -16%. The latter shows, that in this case the use of standard glass represented higher illuminance levels in the room.

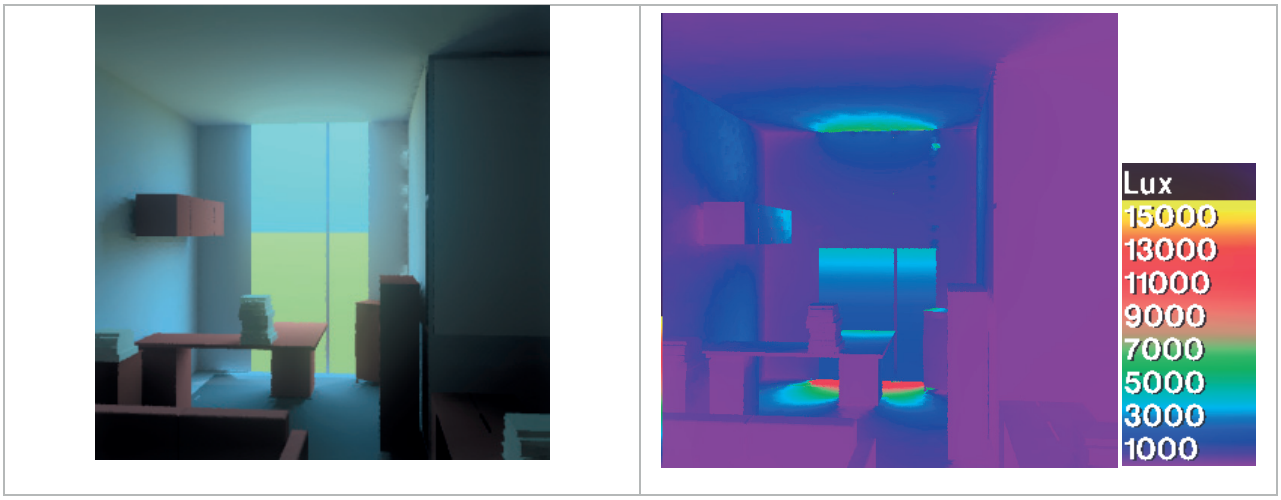

Figure 3.23 Rendering of the office room with GLASS τv80% on June 21th at 15h00 under intermediate sky conditions, showing the human-response view (left) and the false color image (right).

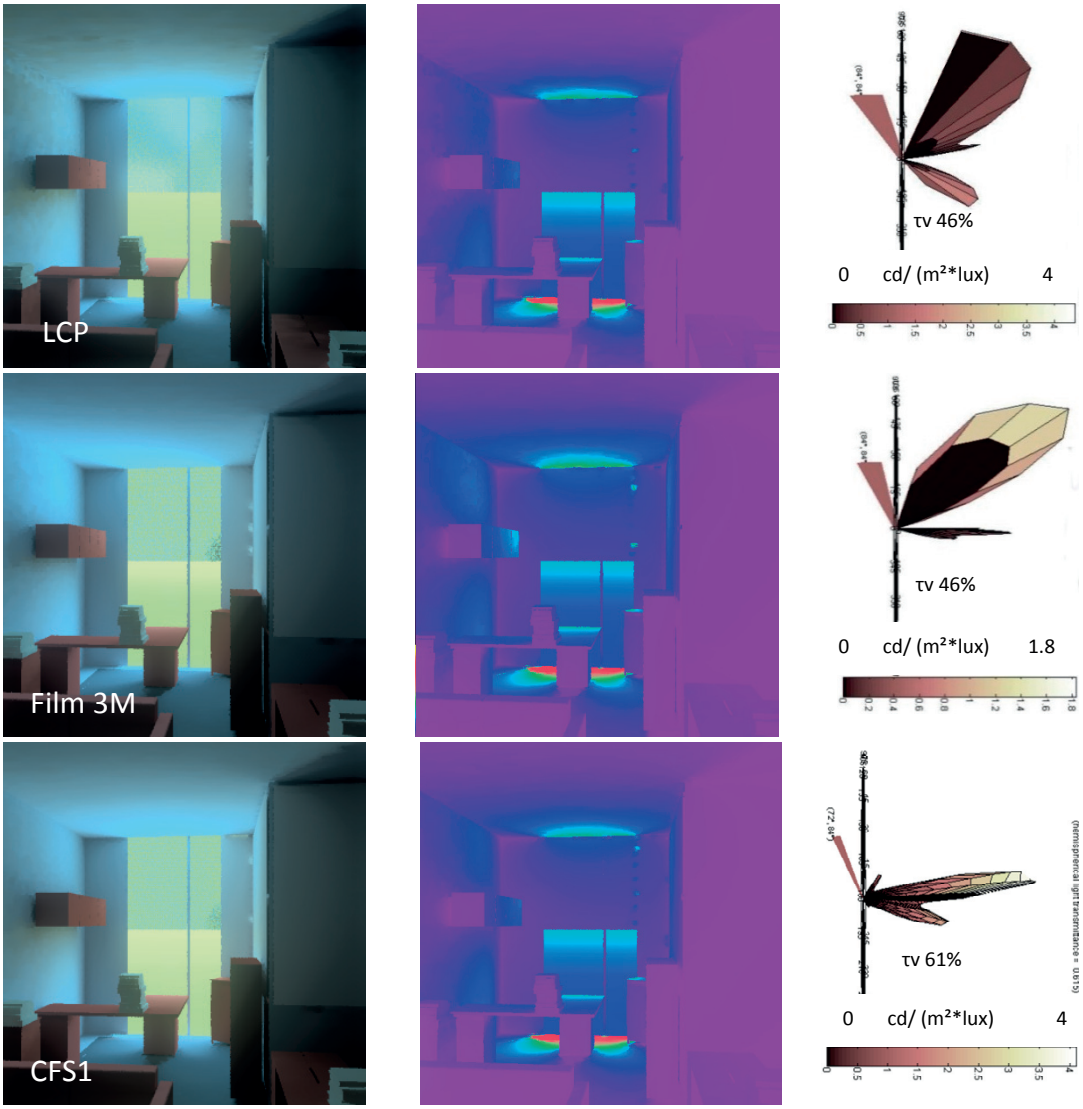

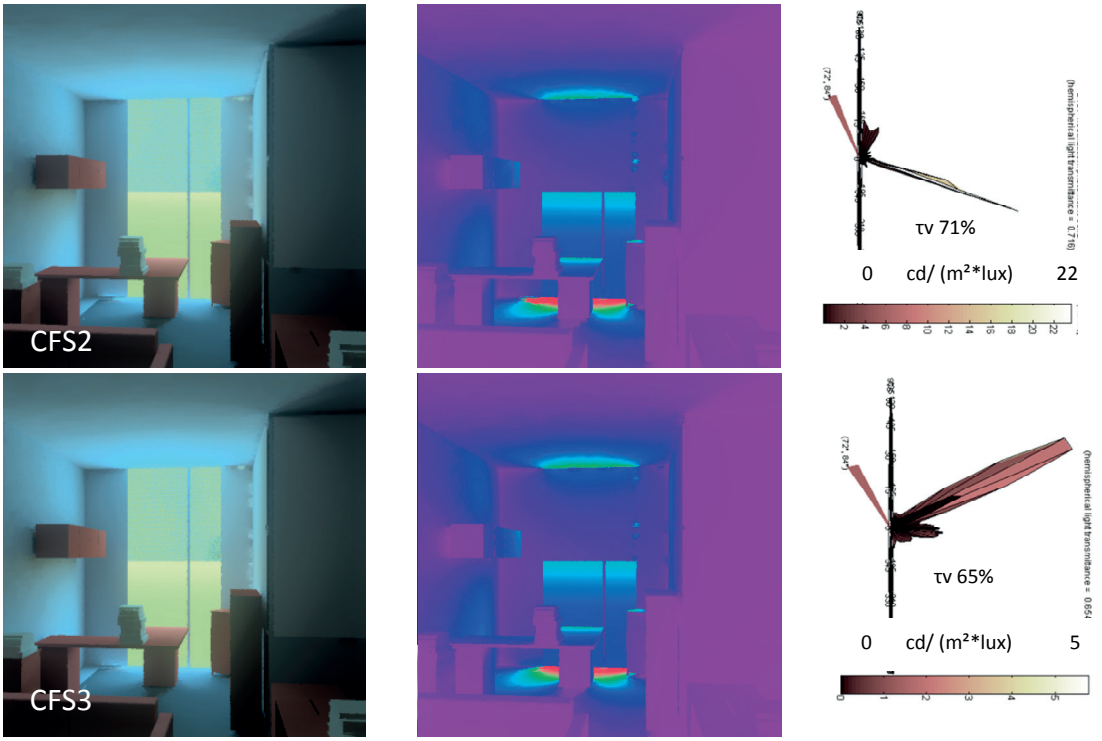

Figure 3.24 Renderings of the office viewed from the back of the room (left) from the side (centre) showing the extent of the daylight redirection through the room using the five considered CFS. The BTDF diagram shows the lighting redirection with its corresponding transmitted flux (right). Due to its small size, the scale-range referring to such diagram is shown in text.

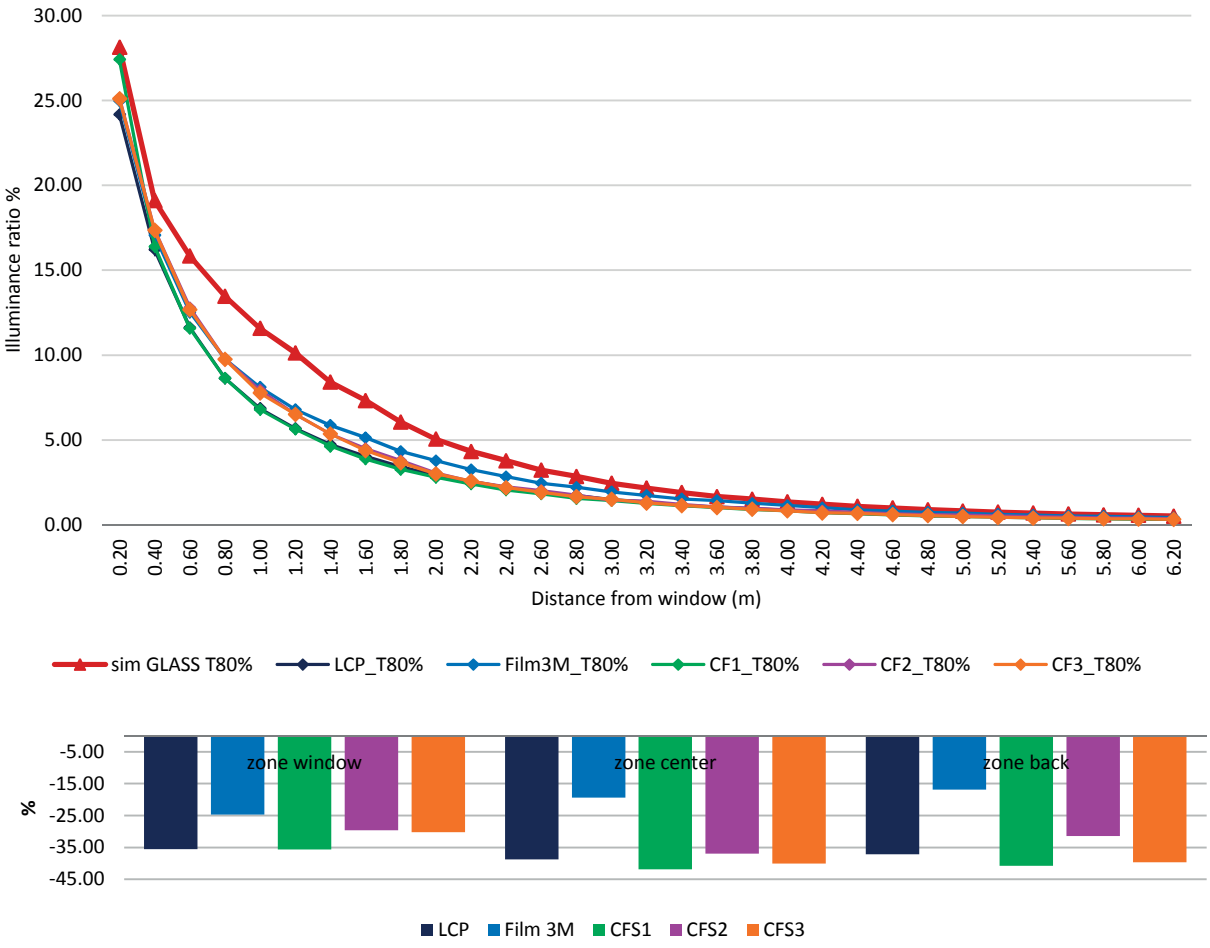

Figure 3.25 The IR profiles that show the performance of the five CFS inside the office room B1 in summer solstice at 15h00 under intermediate sky conditions, the MBE per CFS per room zone (window, center and back of the room) is shown in the graph below.

3.4.1.2 Building B2

a) Winter Solstice

9am The simulations obtained for Building B2 on winter solstice (17th December at 9h00) indicate that CFS1, CFS3 and Film 3M contribute more to increase the indoor daylighting illuminance for the area next to the window. At the centre of the room, Film 3M and CFS3 show the larger of IR values while CFS1 and CFS2 show lower figures. It can also be observed that the Film 3M brings more daylight at the back of the room. The IR profile of Venetian Blinds with a 0° tilt angle is illustrated with the five CFS, its IR profile showing the lowest illuminance compared with the other CFS except at the back of the room where it is only outpaced by Film 3M. The IR profiles show a marked decline at a distance of 2.2m, which is due to the shadow of the window frame. A rendering of GLASS τv70% is shown on Figure 3.26. The IR profiles are illustrated on Figure 3.29 and the renderings on Figure 3.27. A fish eye view from the top of the room is shown on Figure 3.28 in order to visualize the CFS impact as shading device. The MBE shown in Figure 3.29 shows a maximum positive difference when using Film 3M of 7% and negative when using CFS1 with 83% which is due to the effect of the CFS as shading device in the back of the room (see Figure 3.28). A slight improved daylight distribution is found in the window area when using CFS, as LCP and CFS3 achieved 5% and 7% differences compared with the use of standard glass.

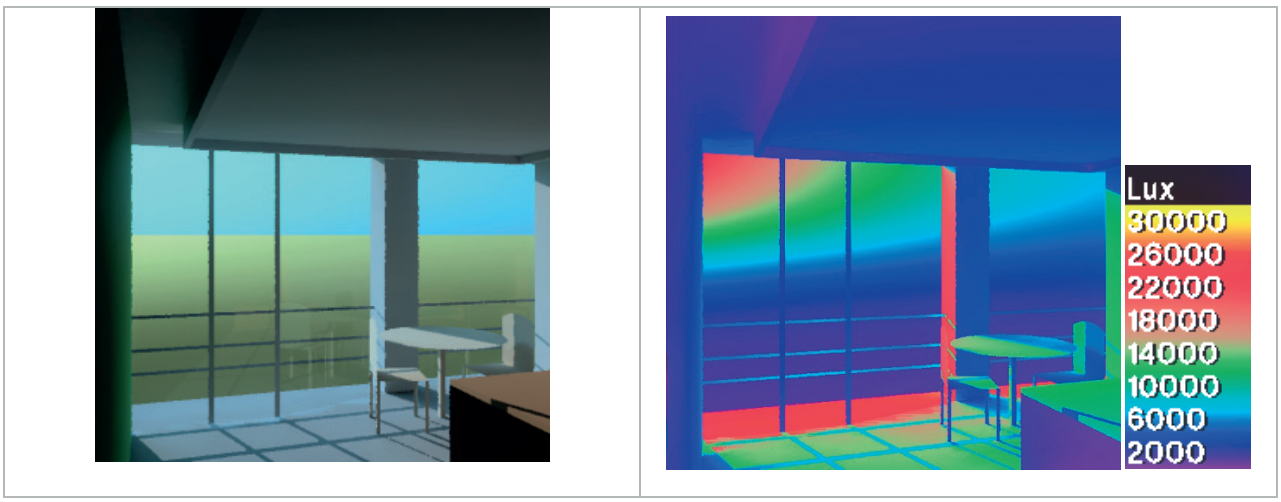

Figure 3.26 Rendering of the office room with GLASS τv70% on Winter Solstice at 9h00 under clear sky conditions, including the human-response view (left) and the false color image (right).

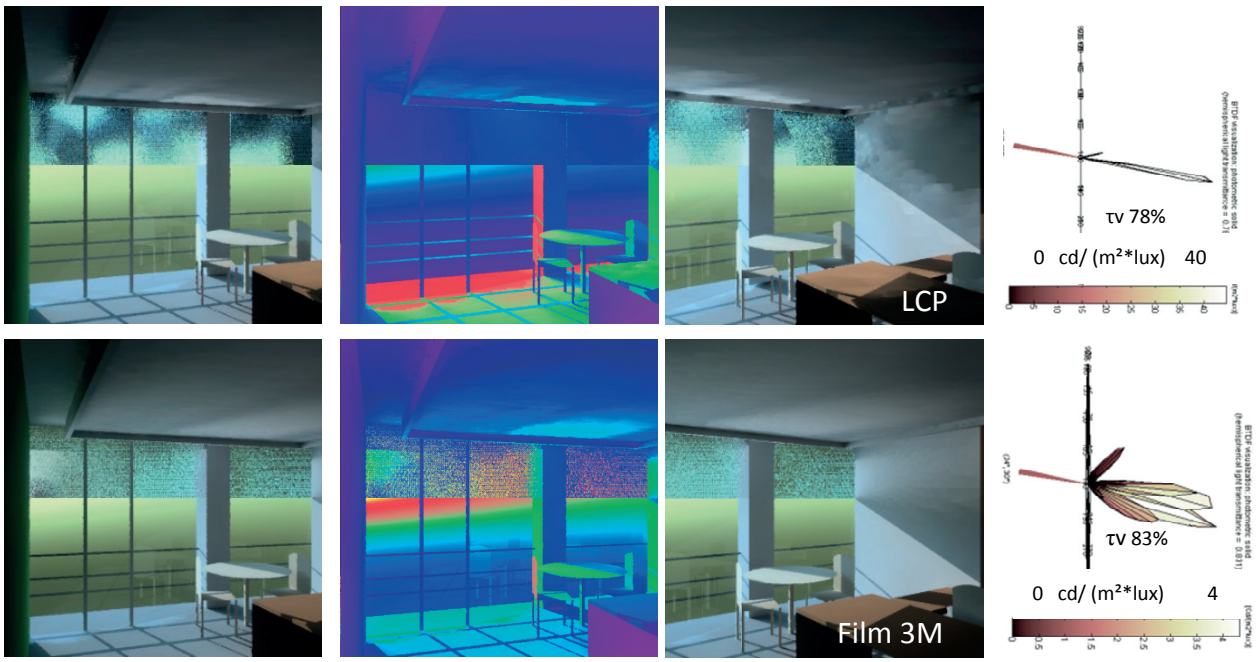

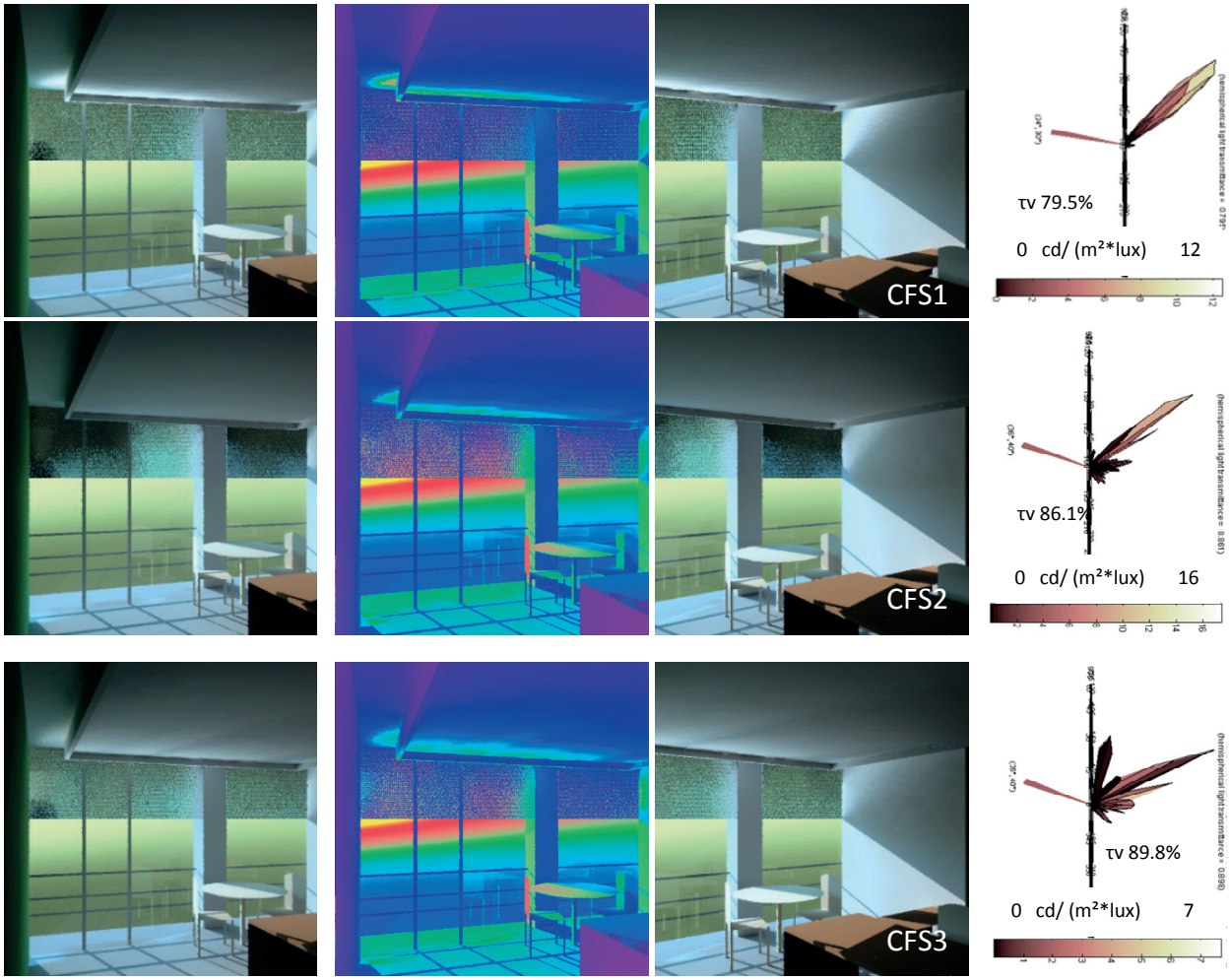

Figure 3.27 Renderings of the office room showing a human reponse view from the back (left), a corresponding false color view (center) and a view from the side (left) which shows in detail the daylight redirection consistent with the diagram of the transmitted flux shown in the left side. Due to its small size, the scale-range referring to such diagram is shown in text.

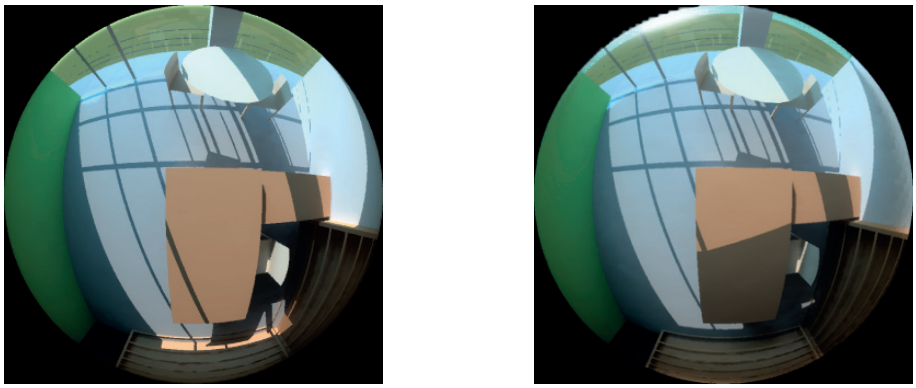

Figure 3.28 Fish-eye views from the top of the office room that show the effect as shading device of the CFS (compared) with the one using onyl Glass (left).

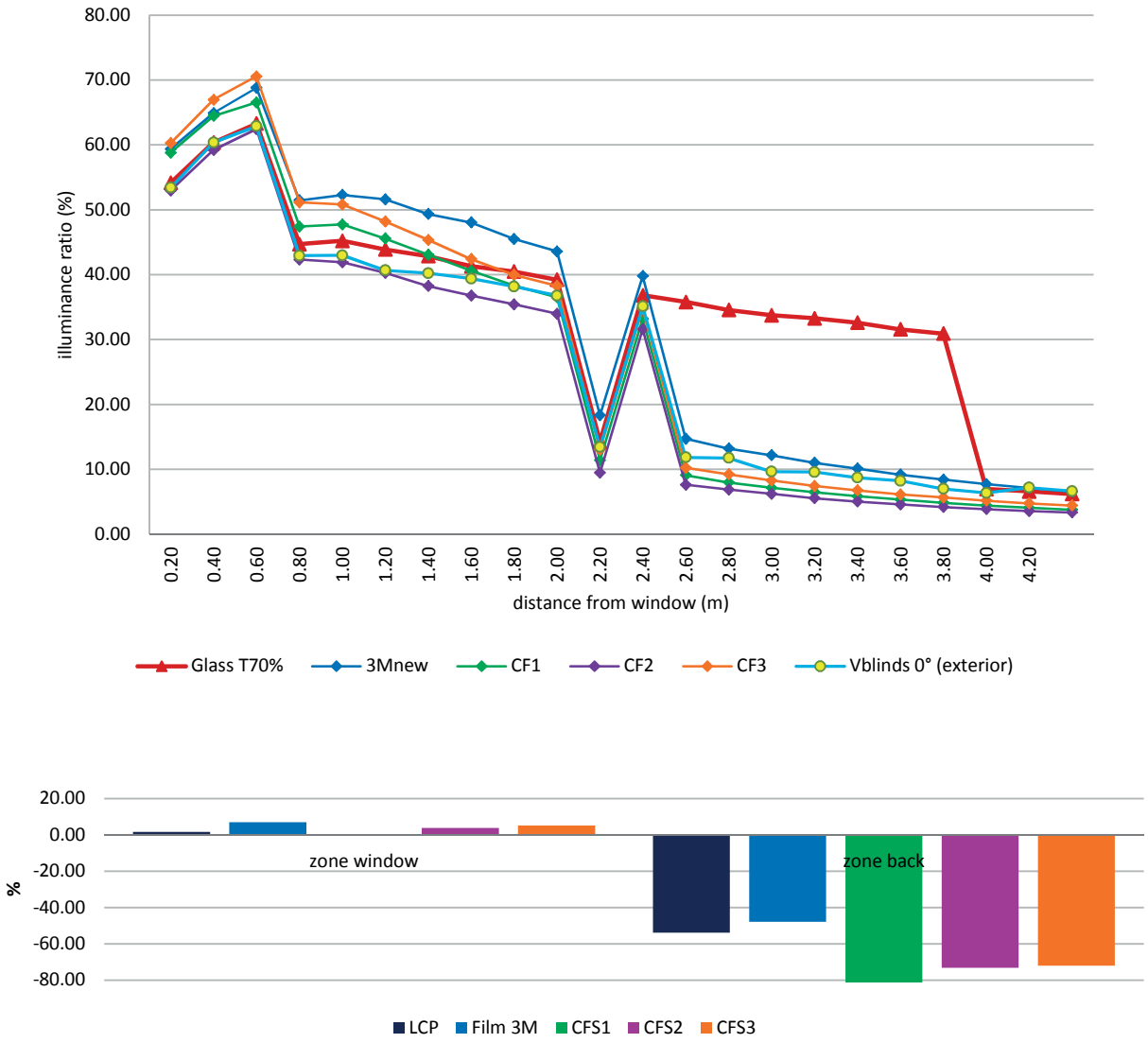

Figure 3.29 IR profiles showing the daylight performance of the five CFS in the office room B2 on the Winter Solstice at 9h00 under clear sky conditions, the MBE per CFS per room zone (window, center and back of the room) is shown in the graph below.

b) Spring Equinox

9am The simulations of Building B2 obtained for the spring equinox (20th March at 9h00) show a little difference on the IR profiles of the five CFS in the area next to the window (Figure 3.33). However, CFS3 and CFS2 contribute to a larger increase of the indoor illuminance in the room. At the centre of the room Film 3M and CFS3 show the largest IR values, while the LCP shows a sound performance at a distance of 1.2 to 1.6m. At the back of the room Film 3M achieves the largest IR values. A rendering using GLASS τv70% is illustrated on Figure 3.30 including the false color image and the corresponding illuminance scale applied also to the CFS. The renderings for the five CFS are shown in Figure 3.31, while the fish-eye views of the standard glass and Film 3M are shown in Figure 3.32. The MBE show that as a zone's averages, in the window zone the differences between the standard glass and the CFS are mainly within a negative range with LCP showing the largest value (-6%) while the Film 3M shows 6%. A similar situation is found in the back of the room with the largest negative range using LCP (-33%), while Film 3M shows 25%. The latter indicates that as an average the illumination provided by the most of the CFS would be reduced than that achieved with the use of a standard glass at this particular time-step. The latter shows, that the use of Film 3M would represent moderate improved interior daylight distribution next to the window 6%), and a clear improvement at the back of the room (24%).

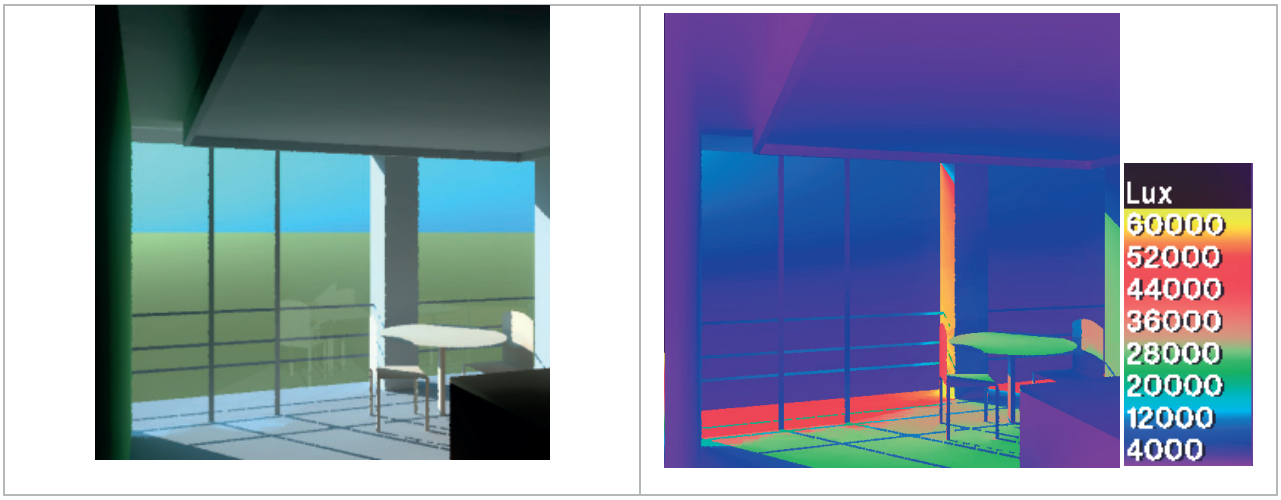

Figure 3.30 Rendering of the room with GLASS τv70% on Spring Equinox at 9h00 under clear sky conditions, the human-response view (left) and the false color image (right).

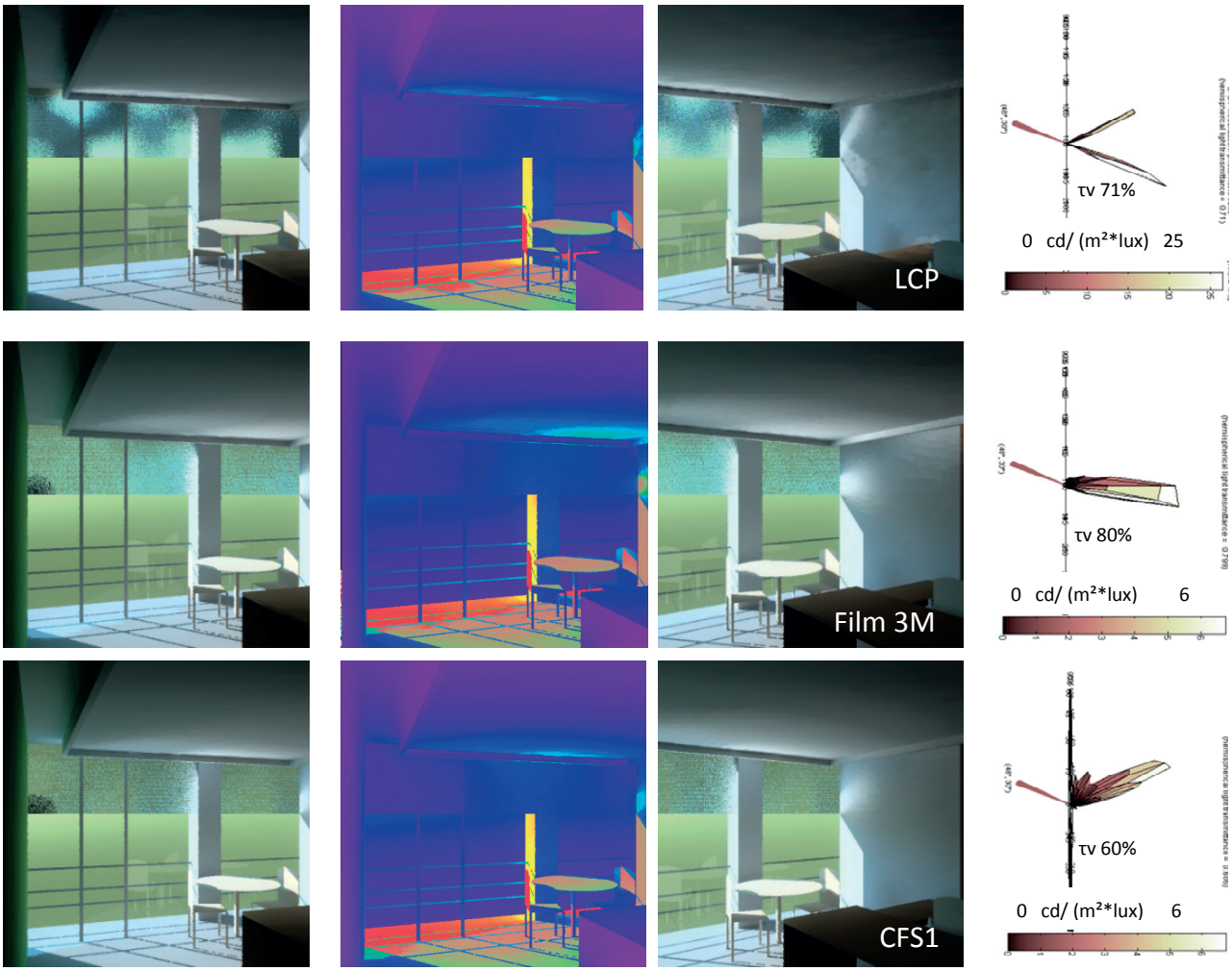

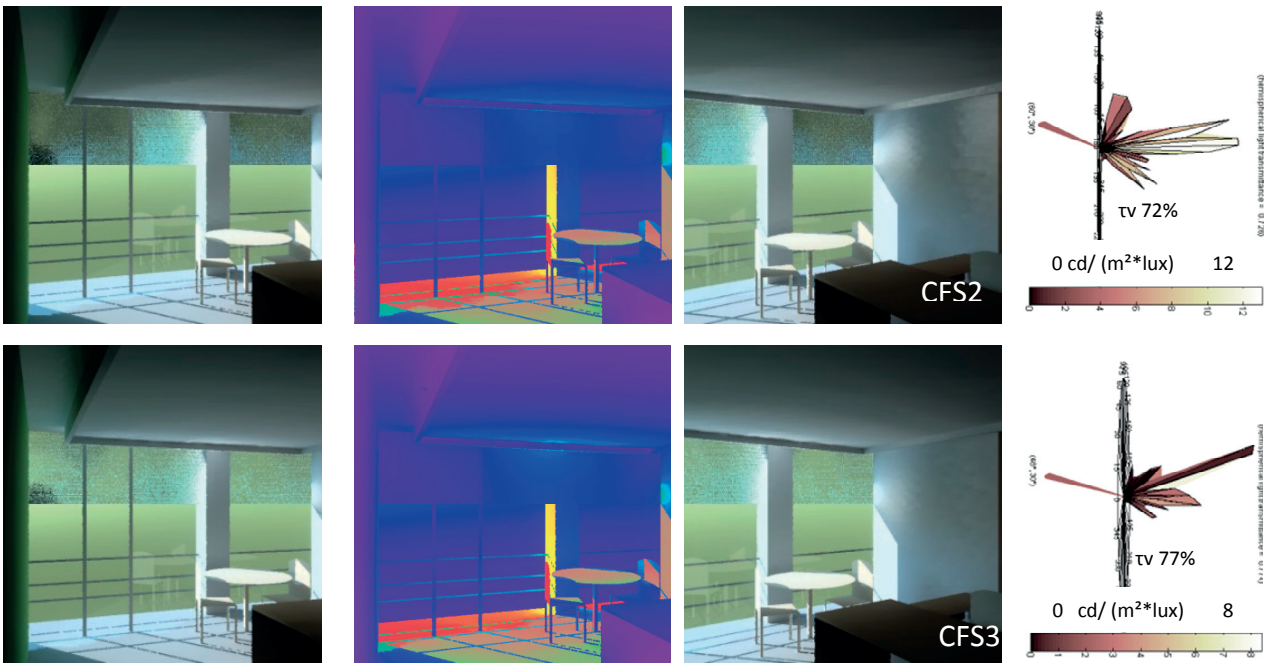

Figure 3.31 Renderings of the office room in a view from the back as human reponse (left) and false color image (centre). In the left a view from the side in order to visualize the daylight redirection consistent with the diagram of the lighting flux shown in the left column. Due to its small size, the scale-range referring to such diagram is shown in text.

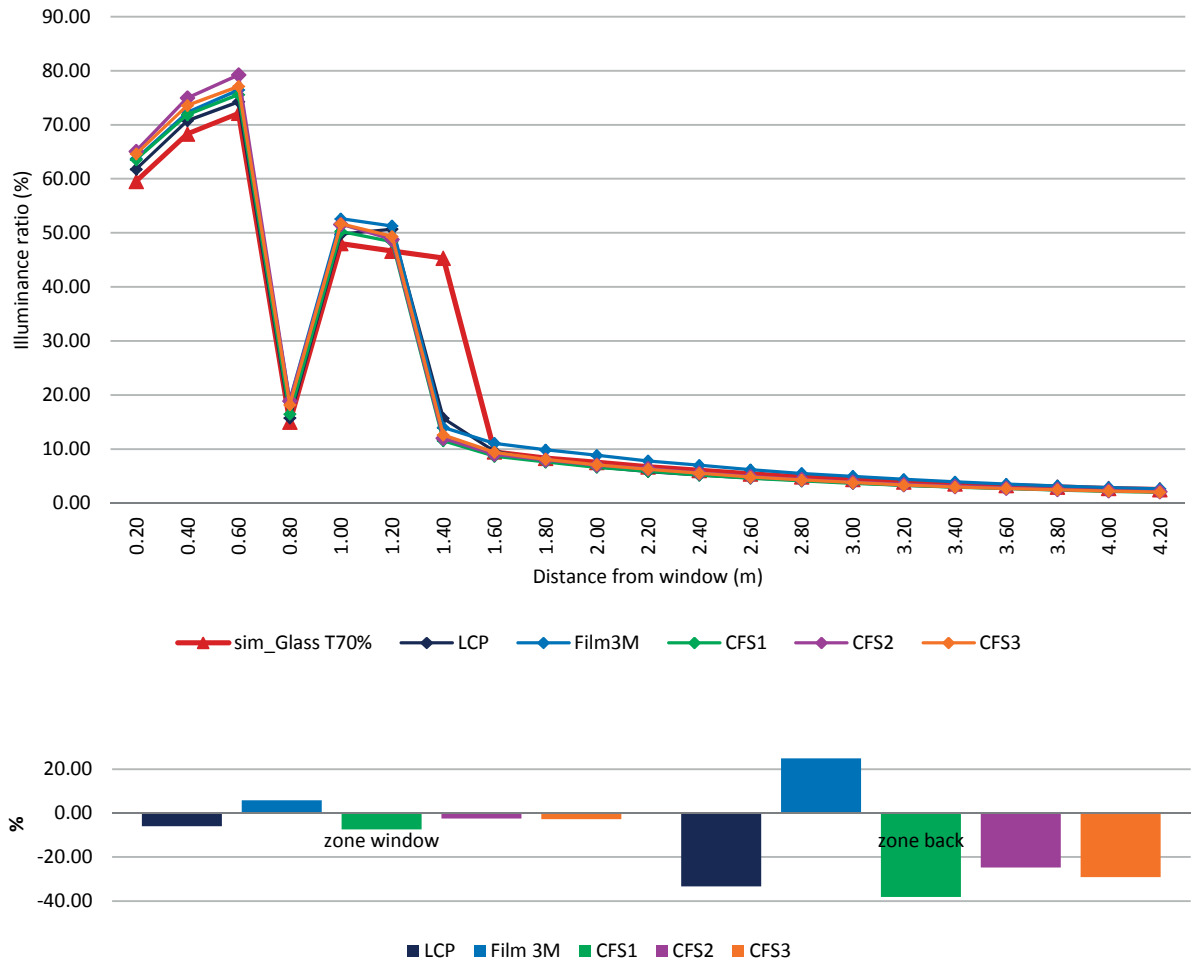

Figure 3.32 IR profiles showing the daylighting performance of the five CFS in the office room of Building B2 on Spring Equinox at 9h00 under clear sky conditions, the MBE per CFS per room zone (window, center and back of the room) is shown in the graph below.

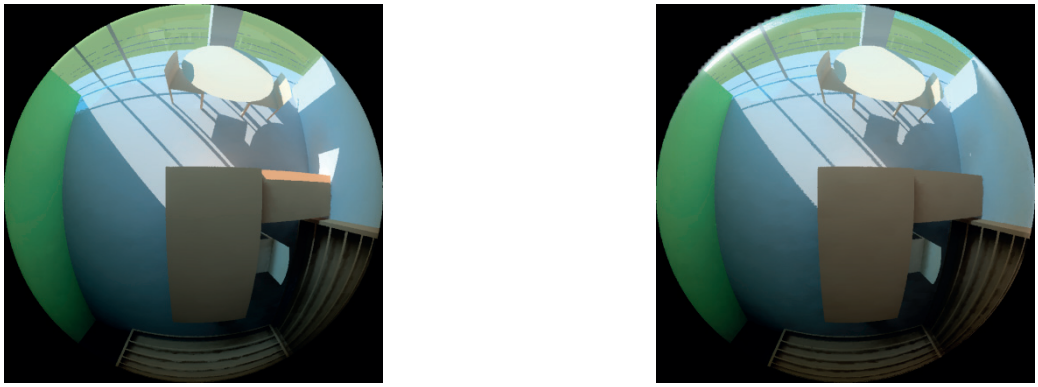

Figure 3.33 Fish-eye views from the top of the office room that show the effect as shading device of the CFS (compared) with the one using ony standard glass (left).

c) Summer solstice

12pm The simulations obtained for Building B2 on spring equinox (20th June at 12h00) show a better performance for the IR profiles of the Film 3M compared to the five CFS in the area next to the window (Figure 3.36). In this area, CFS3 shows also a good performance, while LCP, CFS1 and CFS2 lead to lower daylight illuminance inside the room. Through the room CFS2 shows the lowest IR profile while at the back of the room the Film3M performs in an equal way with the GLASS τv70%; however the latter shows values 1% lower than the IR profile of Film 3M next to the window. A rendering of the simulation using GLASS τv70% is given in Figure 3.34; it can be compared with the renderings of the other CFS illustrated on Figure 3.35. The relative errors shown in Figure 3.36 shown that as a zone average, the differences between the standard glass and the CFS are within a negative range for most of the CFS in the window area with the largest is shown by LCP (7.5%). In the area at the back of the room LCP shows -29% difference, while Film 3M shows 9% in the positive range. The latter shows that as an average, excepting Film 3M the most of the CFS would achive reduced illuminance levels than the use of standard glass in this particular time-step.

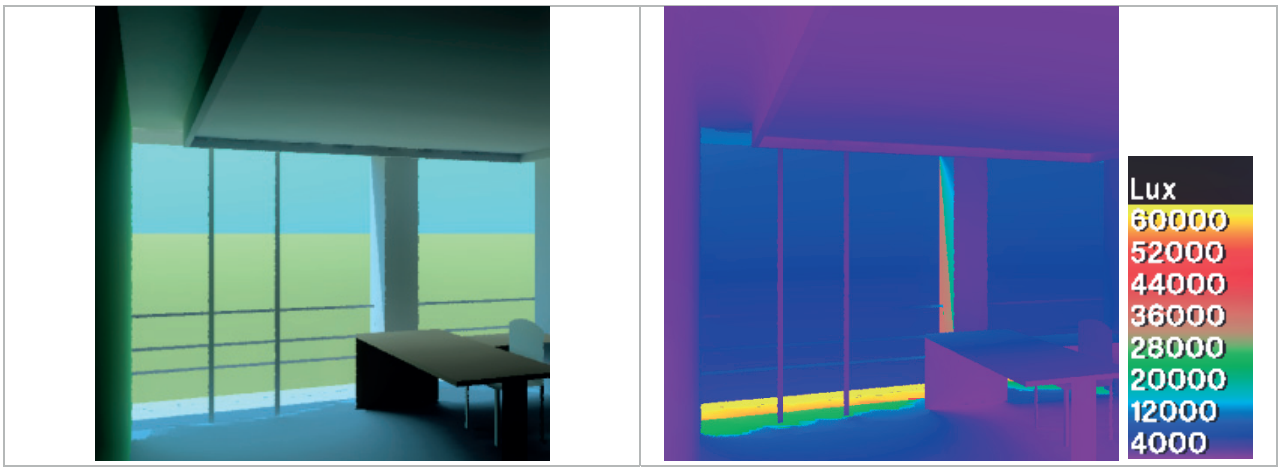

Figure 3.34 Rendering of the room with GLASS τv70% on Summer Solstice at 12h00 under intermediate sky conditions, the human-response view (left) and the false color image (right).

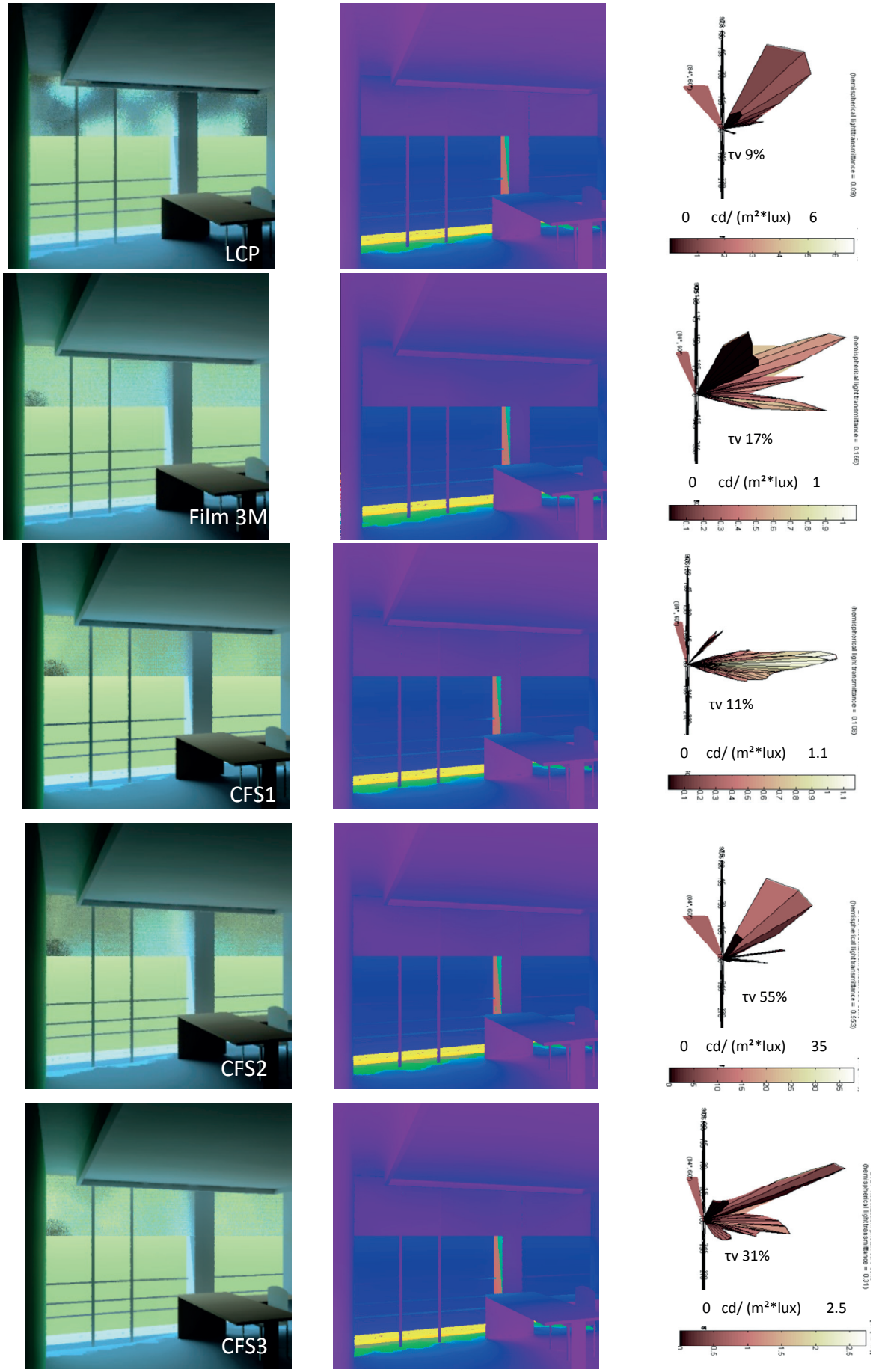

Figure 3.35 Renderings of the office room Building B2 with a view from the back (left) and from the side of the room (right). The diagram at the right shows the lighting redirection with its corresponding tranmitted flux expressed in percentage. Due to its small size, the scale-range referring to such diagram is shown in text.

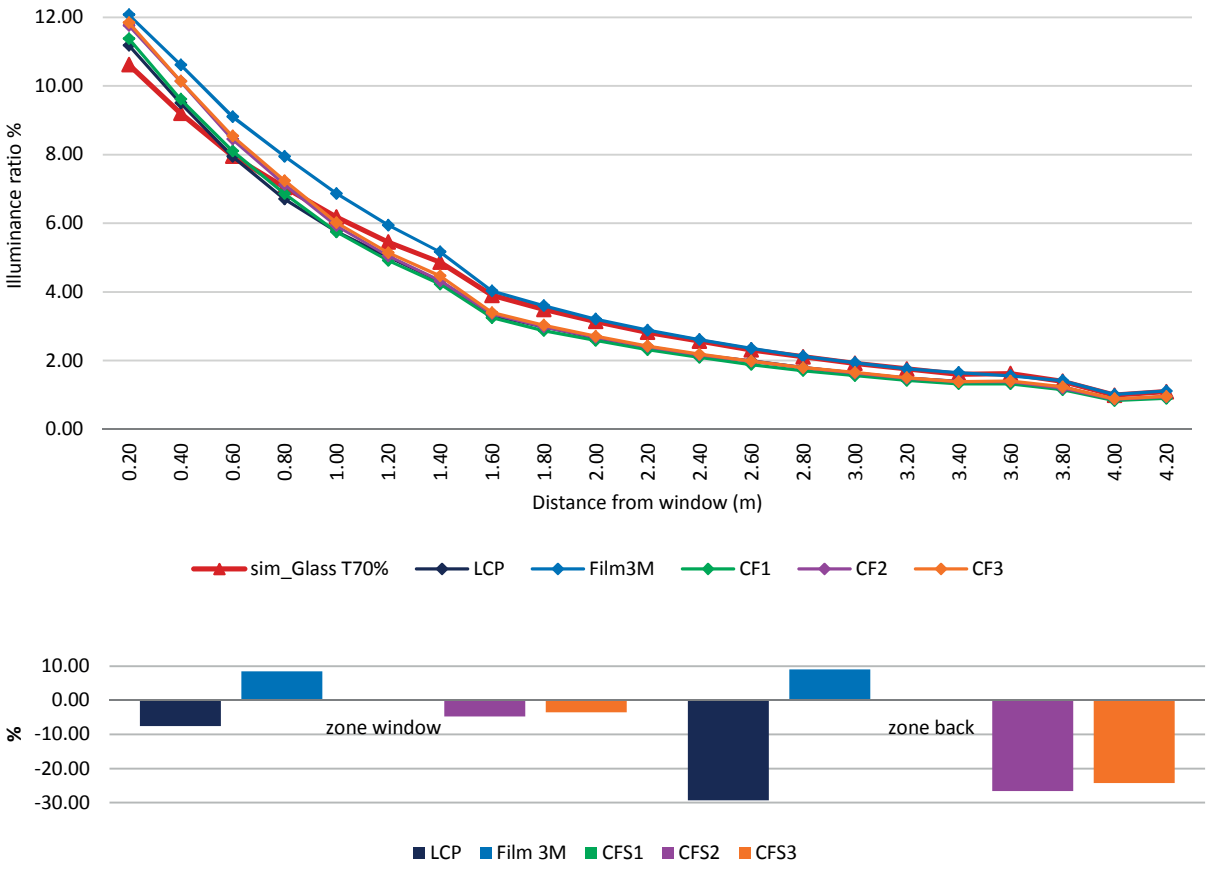

Figure 3.36 IR profiles showing the daylighting performance of the five CFS in the office room for Building B2 on Summer Solstice at 12h00 under intermediate sky conditions, the MBE per CFS per room zone (window, center and back of the room) is shown in the graph below.

3.4.2 Global assessment

Simulations of the daylight flux distribution through the five pre-selected CFS were carried-out for three typical periods: Winter and Summer Solstices as well as Spring Equinox at different hours (at 9h00, 12h00, 15h00 and 17h00). The evaluation of the daylighting performance was made first by categorizing the resultts according to a room zoning based on three areas: the area next to the window, the one in the centre of the room and the area at the back of the room (in the case of Building B1). Because of its smaller size the room of Building B2 was only subdivided in two zones (window zone and back of the room zone), each zone being charecterized by a depht of 2 m. The average Daylightig Factor (DF) and Illuminance Ratio (IR) were then compared between the variants. An additional assessment was made by determining the Illuminance Uniformity, in order to examine the spatial Illuminance distribution in the room, this was done by considering the zones corresponding to the visual field from each working space (as shown in Figure 2.18) then expressed for each zone by the minimum to maximum ratio (g2) and the minimum to average ratio (g1) [133]. Even if the latter is usually applied to artificial lighting, it was included in this study as a matter of analysis of the lighting quality. The recommendations suggest values larger than 0.7, values under this threshold leading to lower users acceptability [94].

The comparison of the average DF (see Figure 3.37) for each zone shows that the standard glass τv 80% lead to the highest value (above 12%) close to the window, while the highest DF for the CFS is equal to 10% for the same area,(the tinted glass hardly reaches 2%). A similar situation is observed at the centre and back of the room. The average IR occurring in winter time is presented in Figure 3.38; it shows that a higher average of IR is achieved in the three zones when using the standard double glazing; high values are also found for the Film 3M, while similar values prevail between CFS2 and CFS3. Lower averages are achieved by LCP and CFS1. The results of the current situation involving a tinted glazing (τv 12%) are also presented in order to outline the improvements achived by the CFS. For Spring Equinox (Figure 3.39), the results show that the standard double-glazing allows reaching about 20% average DF in the room, while the five CFS allow less than 15% at winter solstice.

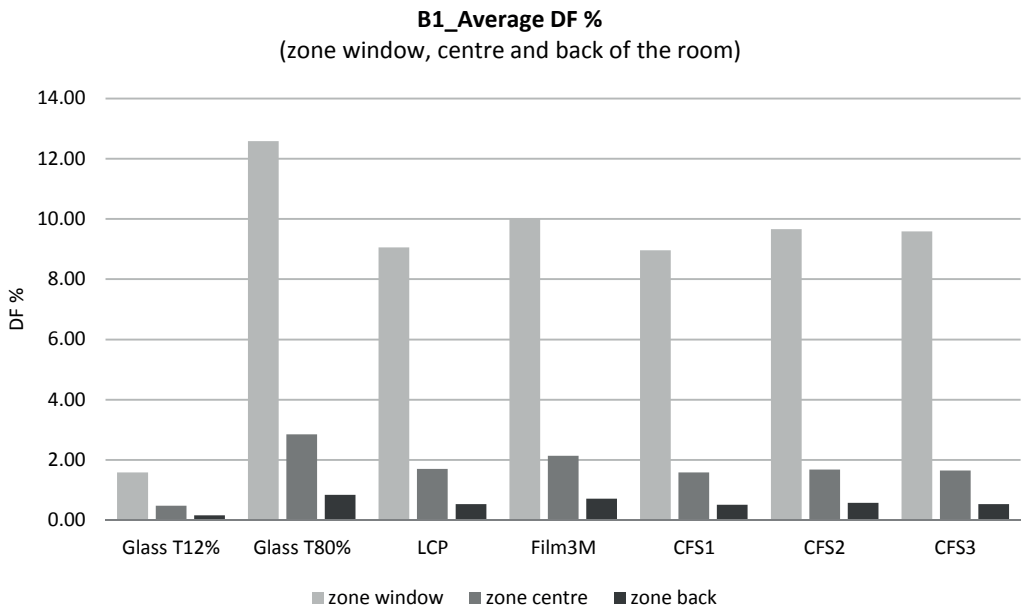

Figure 3.37 Comparison of average DF in Building B1 for the five CFS, the standard double glazing (τv 80%) and the tinted glass (τv 12%), which monitoring was carried-out in winter time.

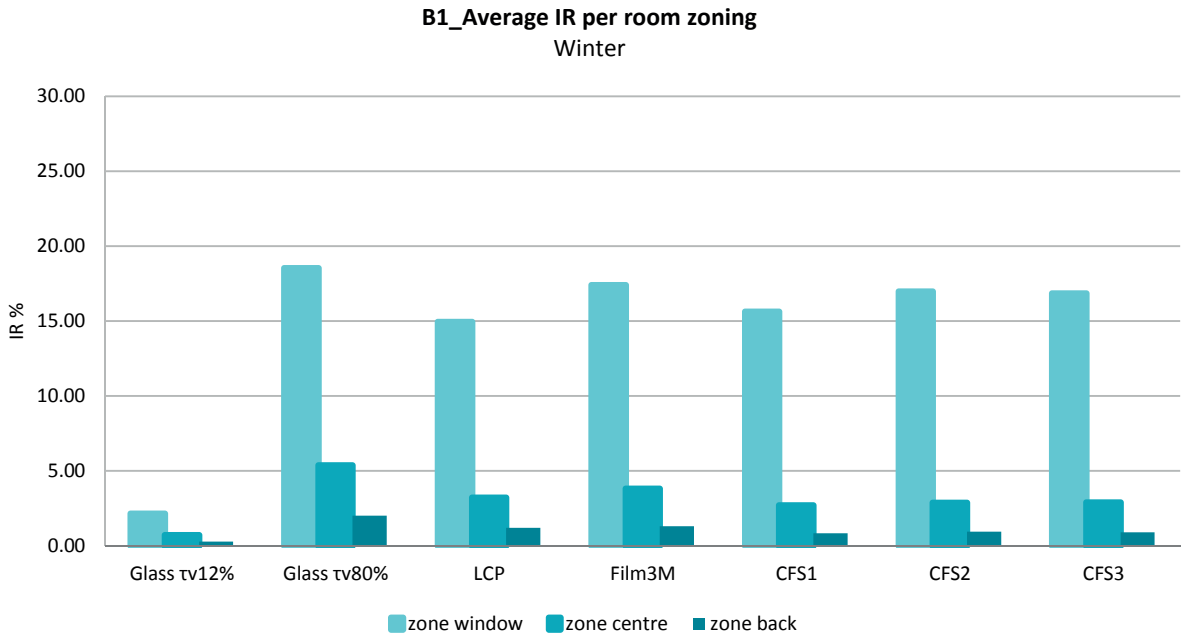

Figure 3.38 Comparison of the average IR in Building B1 for the five CFS, the standard double glazing (τv 80%) and the tinted glass (τv 12%), at Winter solstice.

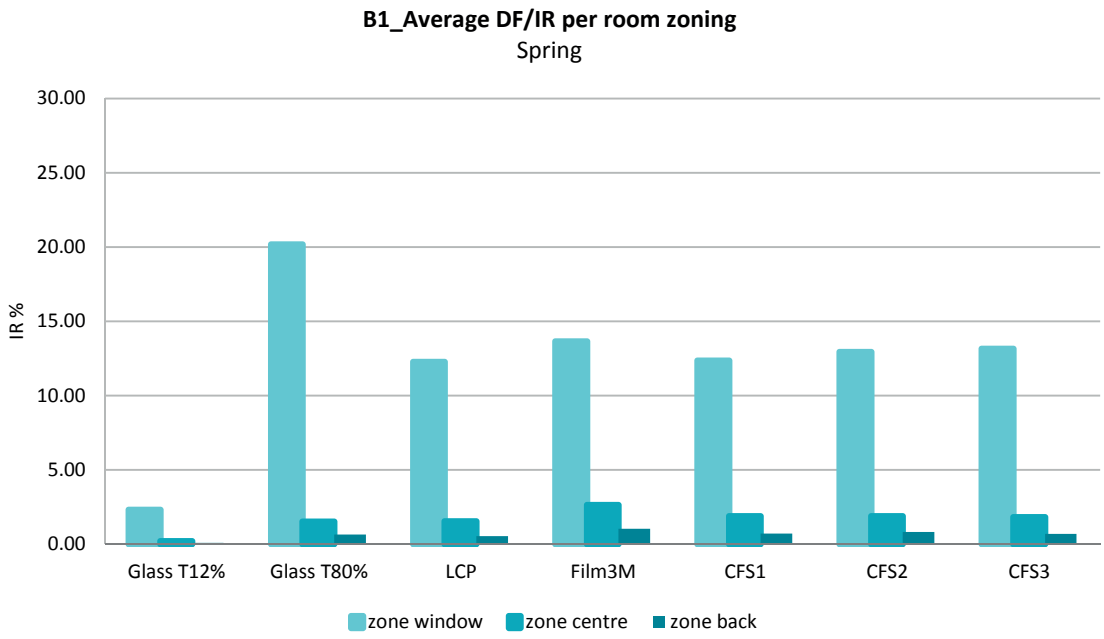

Figure 3.39 Comparison of the average IR in Building B1 for the five CFS, the standard double glazing (τv 80%) and the tinted glass (τv 12%), at Spring equinox.

The results of Summer Solstice are presented in Figure 3.40; similar performance to those obtained at Winter Solstice is observed, a higher average IR being achived by the standard double-glazing. Among the five CFS Film 3M presents larger average IR in the three zones; CFS2 and CFS3 maintain a similar trend while LCP and CFS1 showing the lower values are performing in a similar way. The Illuminance Uniformity (g1) is presented in Figure 3.41; it can be observed that next to the window the values are lower due to the high contrast that can be found between the sunlit and shadowed areas; besides the standard glass (0.47), the Film 3M show an improved uniformity in this area (0.43). Higher uniformities are also found deeper in the room; in the centre of the room CFS1 show the best illuminance uniformity, while for the back room values close to 0.7 are found for all the cases, the highest uniformities being achieved by Film3M and LCP.

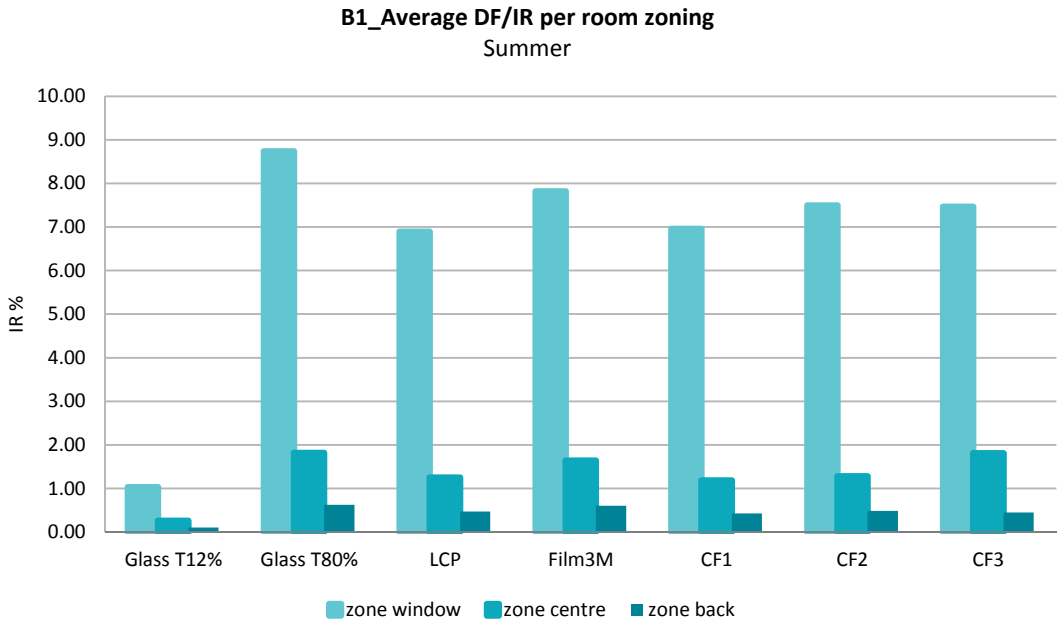

Figure 3.40 Comparison of the average IR in Building B1 between the CFS, the standard double glazing (τv 80%) and the tinted glass (τv 12%) at Summer solstice.

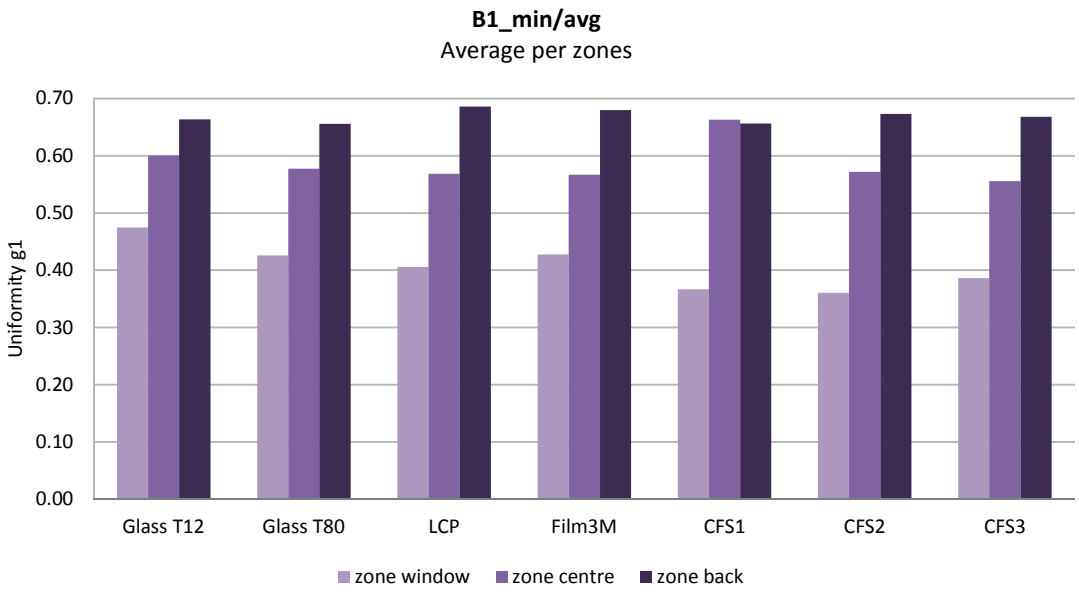

Figure 3.41 Comparison of the illluminance Uniformity g1 in Building B1 for the five CFS, the standard double glazing (τv 80%) and the tinted glass (τv 12%) at the Solstices and the Spring Equinox.

The average DF obtained for Building B2 are illustrated on Figure 3.42 In the window zone the larger average DF (9%) is achieved by the Film 3M followed closely by the standard glazing (τv 70%); the other CFS show an average DF larger than 8%. A similar situation is also observed at the back of the room with a minimum average DF of 2% for CFS1. When comparing the results of average IR at Winter Solstice (Figure 3.43) larger daylighting fluxes are obtained for the standard glazing in the two areas (window zone and back of the room), while Film 3M shows a sound performance, and is followed by CFS2 and CFS3. At Spring Equinox the predominance of the the standard glazing is obvious, especially in the area next to the window, presenting an average IR close to 30% while the five CFS show values slightly above 10%. Back in the room the values are similar for all cases, as shown by Figure 3.44. At Summer Solstice (Figure 3.45), the use of Film 3M allows larger daylighting fluxes to enter the room, reaching a relative fraction larger than 6% in the area close to the window; the standard glazing and CFS3 present also similar values. The same situation is observed back into the room.

In the case of Building B2, the Illuminance Uniformity is larger than 0.6 for the five CFS at the back of the room, for the standard glazing it is about 0.55 next to the window. Next to the window the Film 3M achieves the highest g1 (0.45), while all the others CFS achieve 0.43 as shown in Figure 3.46.

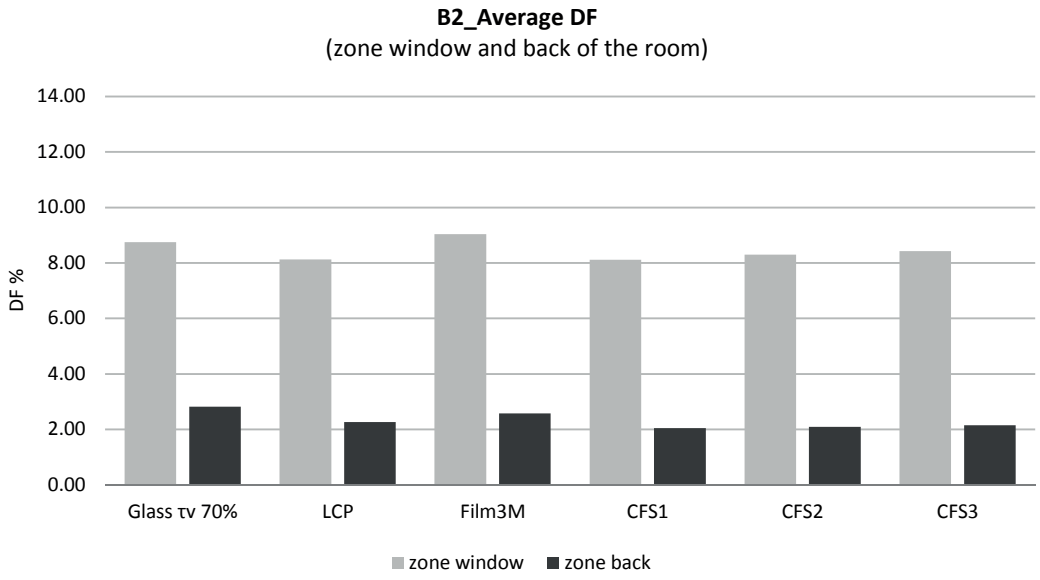

Figure 3.42 Comparison of average DF in Building B2 for the five CFS and the standard glazing (τv 70%), which monitoring was carried-out in winter time.

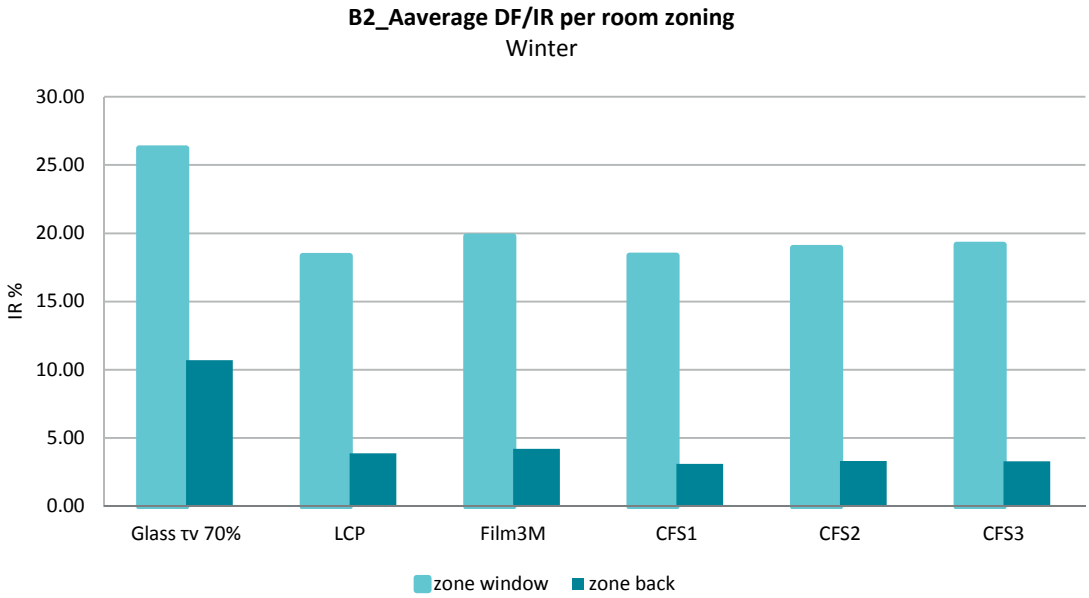

Figure 3.43 Comparison of average IR in Building B2 for the five CFS and the standard glazing (τv 70%) at Winter solstice.

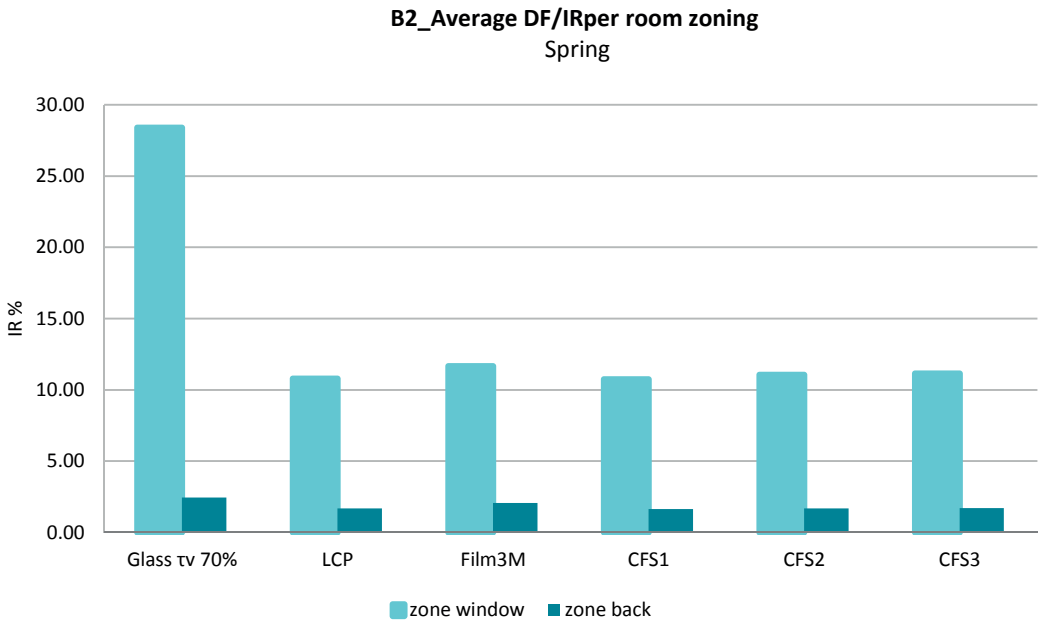

Figure 3.44 Comparison of average IR in Building B2 for the five CFS and the standard glazing (τv 70%) at Spring equinox.

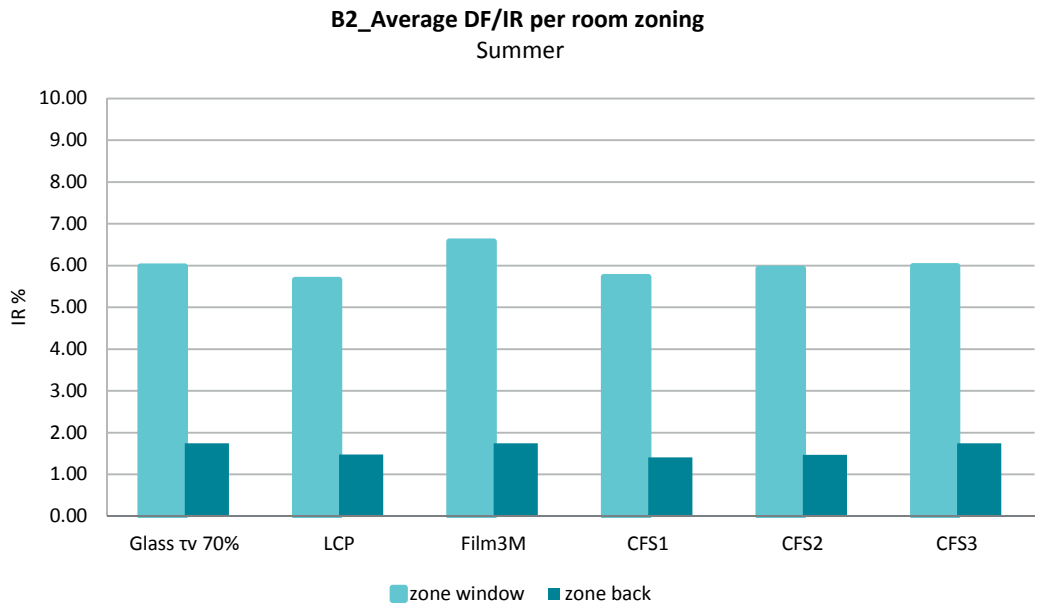

Figure 3.45 Comparison of average IR in Building B2 for the five CFS and the standard glazing (τv 70%) at Summer solstice per room zoning

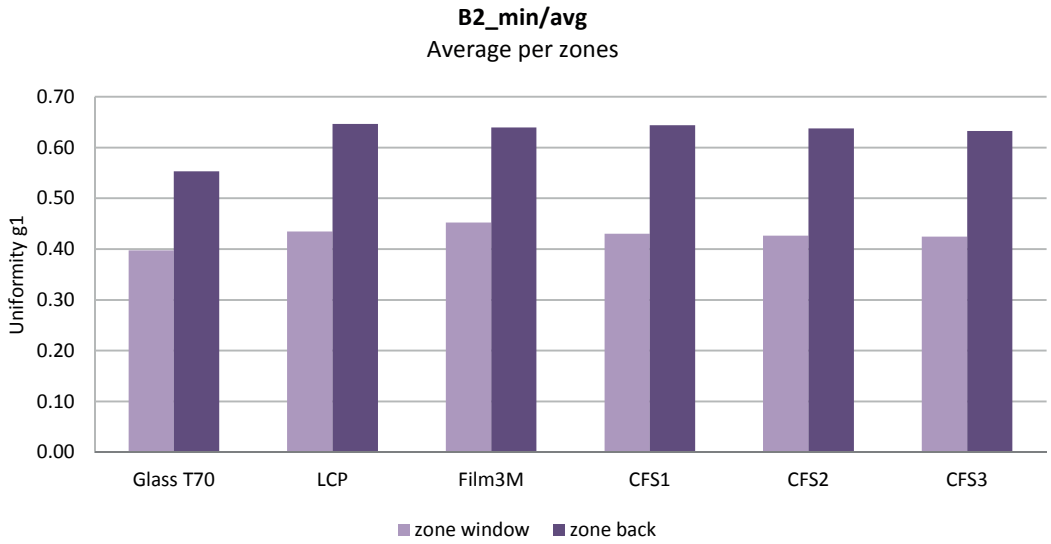

Figure 3.46 Average Illuminance Uniformity of the Solstices and Equinox from 9h to 17h, presented per zones. Comparison of Illuminance Uniformity g1 in Building B2 for the five CFS and the standard glazing (τv 70%) at the solstices and Spring equinox from 9h00 to 17h00.

3.4.3 Relative errors of the simulations using CFS

The mean bias error (MBE) of the simulations using the five pre-selected CFS were calculated using as a reference the results obtained of the corresponding standard glass in the two office rooms. The latter were calculated in order to estimate the differences obtained of the CFS illuminance values compared with the use of standard glass. Such are presented by comparing the relative erros calculated in Solstices and Equinox presented per room zones, as shown in Figure 3.47 for Building B1. The MBE shows a predominance of differences within the negative range with the highest values obtained by CFS1 (-48%). The difference between the standard glass and the CFS within a positive range was found when using Film 3M, CFS1, CFS2 and CFS3 with a maximum value of 45% when using Film 3M in the center area of the room. The latter indicates first that the CFS have more effect in the center and back side of the room. Secondly that as average of the three days when the simulations were carried-on the use of standard glass would allow higher extents of illuminance in the room, which might be due to the CFS function as a shading device.

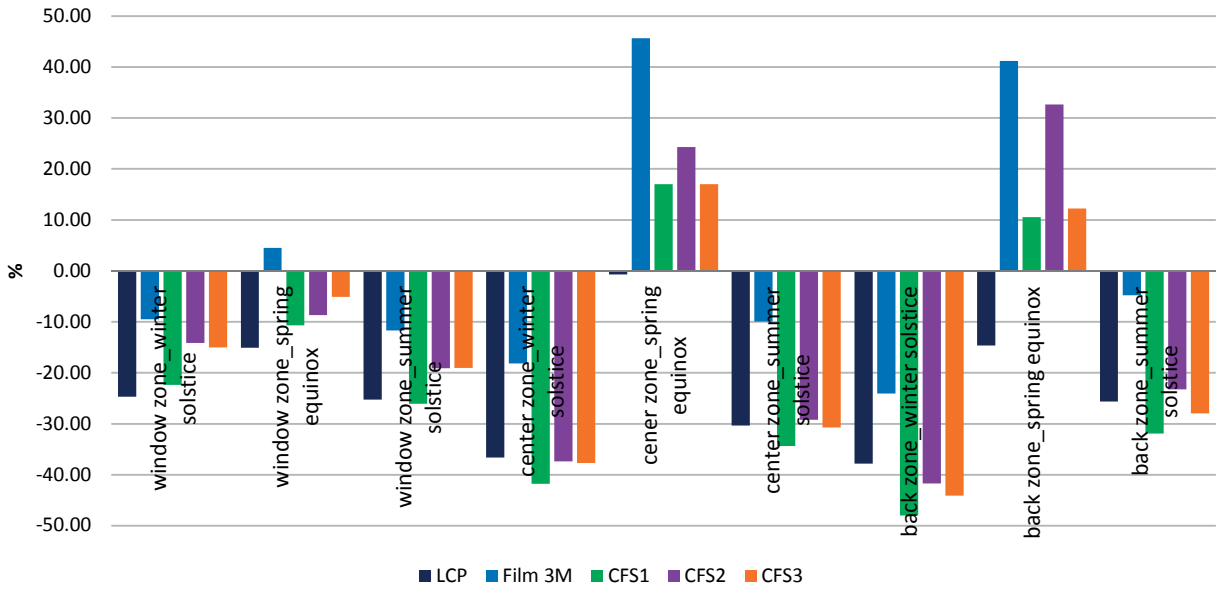

Figure 3.47 The MBE of the simulations between the standard glass and the CFS presented by room zones (window area, center area and back of the room area) as average of Solstices and Equinox in Building B1.

In the case of Building B2 the MBE are presented in Figure 3.48, the differences between the standard glass and the CFS within a negative range were found mainly at the back of the room, with a highest value of -33% when using CFS1. In this case, the differences within a positive range were found when using all the CFS alternatively with a highest value of 32% (LCP) and the lowest of 1% (Film 3M). The latter could be an indicator of a more solid effect of the CFS regarding daylight provision in the window area of this particular building.

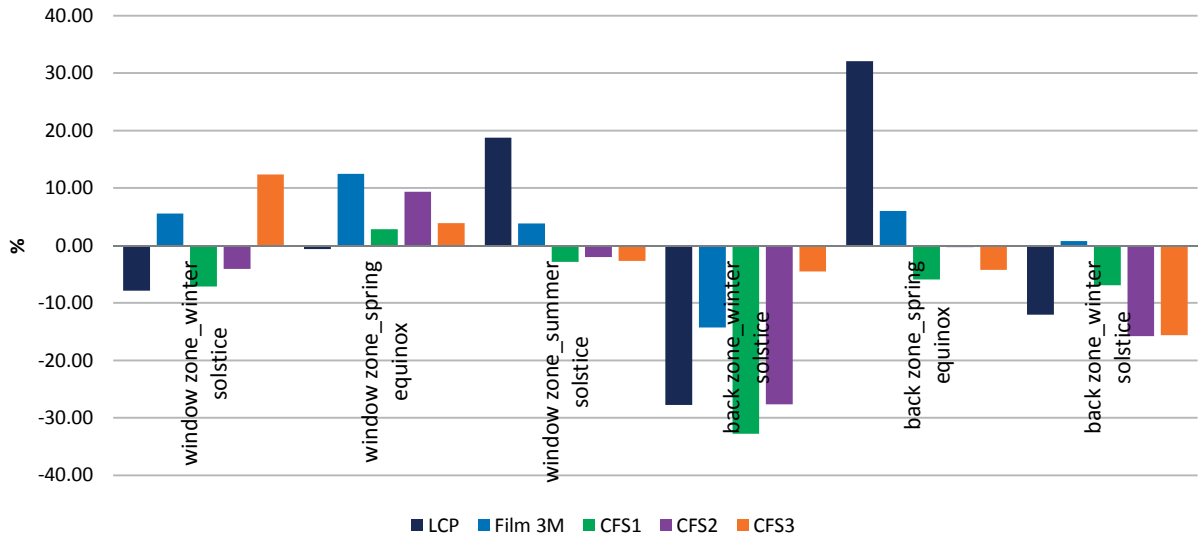

Figure 3.48 The MBE of the simulations between the standard glass and the CFS presented per room zones (window zone and back zone) as average of Solstices and Equinox in Building B2.

3.4.4 Conclusions

The assessment of the daylight distribution in the office rooms of the Building B1 and B2 was performed by comparing the average IR/DF obtained with the five CFS at three typical periods (Solstices and Equinox at 9h00, 12h00, 15h00 and 17h00). The Illuminance Uniformity **g1** was compared as well; the former was obtained by dividing the minimal DF/IR by the maximal value, while the latter was obtained by dividing the minimum by the average values. The results, show that in many cases the standard glazing lead to a higher daylighting flux into the room, especially at Spring Equinox where the IR is significantly larger than those of the CFS. When comparing the performance of CFS, Film 3M, CFS3 and CFS2 appears to be the ones that perform better regarding the admission of daylight into the room. In Building B1, the Standard -glazing (τv 70%) and Film 3M present a better Illuminance Uniformity next to the window and in the centre of the room, while at the back of the room the LCP, Film 3M and CFS2 show better values. In Building B2, Film 3M shows a higher Illuminance Uniformity next to the window, while at the back of the room the LCP is the one that show larger values. The calculation of the relative errors was useful to estimate the differences obtained when using CFS compared with the use of standard glass, especially in Building B1 the use of standard glass surpass the illuminance provision inside the room compared with the use of CFS, however is noteworthy that a higher extent of daylight provision is not an indicator of an appropiate interior daylight environment.

3.5 Visual Comfort assessment in the two office rooms

The evaluation of the visual comfort of the occupants in the two office rooms was assessed by computing the glare indexes using *Evalglare*. In order to do that, 180° fisheye renderings were generated from each working place in the two rooms, setting the view direction toward the workplane located in the view field of the occupants (see Figure 2.14). They were generated for Winter solstice and Spring equinox, which are the periods of the year that when the occupants are prone to experience higher glare risks due to the sun positions. For Building B1 a higher risk might occur at 15h and 17h when the sun directly enters the room, while for Building B2 a higher risk might occur at 9h and 12h. The corresponding images were generated and then assessed using the option –t to indicate the location of the workplane.

3.5.1 Results

Evalglare generated results for the following glare indexes DGP, DGI, UGR, VCP and CGI, the DGP index having been selected as reference for this work. This decision was based on the conclusions of a study carried-out in 2011, where different sky conditions were considered for glare predictions using the five mentioned glare indexes. The study concluded that DGP showed likely less inaccurate glare predictions [77]. The DGP index express the relative fraction of people disturbed by glare issued from daylight: if the value is larger or equal to 0.45 it is read as intolerable, while a value lower or equal to 0.3 is read as imperceptible. It has been established, that values lower than 0.2 are out of the range of the user acceptance tests on which the program is based; it would lead to a poor identification of the glare sources, therefore, a careful interpretation is recommended [83].

For Building B1, no values larger than 0.3 were found for the two periods assessed (Winter Solstice and Spring Equinox at 15h and 17h); however, values lower than 0.2 were observed for the Winter solstice at the Desk 1 position (see Table 3.7) for all cases, except for Film 3M and the standard glazing. This might be due to the dark environment at the back of the room located within the visual field of the assessed work place. However, according to the guidelines of the programme, an accurate interpretation of glare risks in these cases might be unfeasible. For the Winter Solstice at Desk 2 position (Table 3.8), larger values were obtained for the standard glazing, those were slightly lower for the five CFS, which might be due to a better distribution of daylight in the room.

For the assessment performed at Spring equinox at the Desk 1 position (Table 3.9) a very low value was observed for the standard glazing at 15h00 which might be explained by the very low illuminance observed in the visual field of the occupant. In this case, the DGP value increases when using the CFS, due to the daylight redirection to the ceiling; however they are still kept within the imperceptible range. In the case of the Desk 2 position (Table 3.10) very low DGP values are again found when using only the standard glazing at 15h00 and 17h00; it increases for the CFS reaching values above 0.2 only for the LCP and Film3M. The DGP for Spring equinox at the Desk 3 position (Table 3.11) shows lower values again for the standard glazing; it increases and overpasses 0.2 for all the five pre-selected CFS.

Winter Solstice	DGP Intolerable = > 0.45 Imperceptible =< 0.30 (lbs=low brightness scene)			
	15h00		17h00	
Desk 1	Human Response	Glare-fisheye HDR	Human Response	Glare-fisheye HDR
Glass τv80%	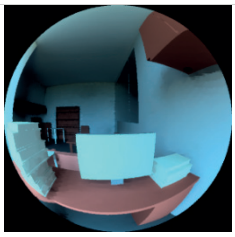	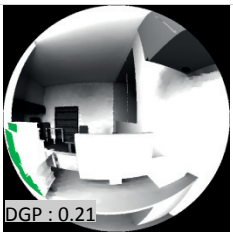 DGP : 0.21		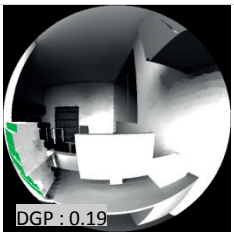 DGP : 0.19
LCP	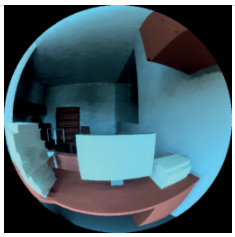	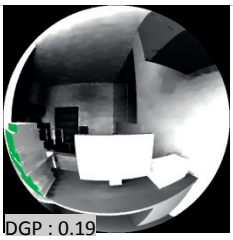 DGP : 0.19	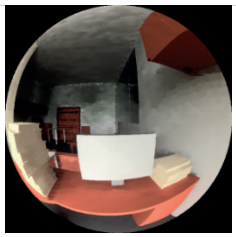	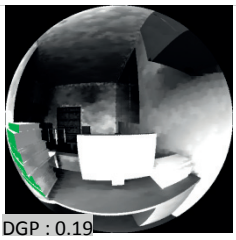 DGP : 0.19
Film 3M	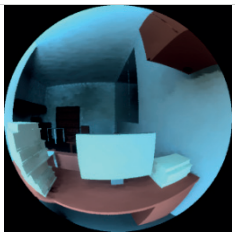	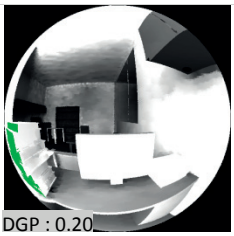 DGP : 0.20	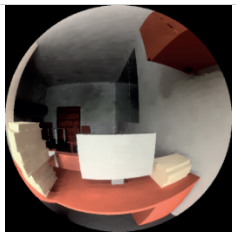	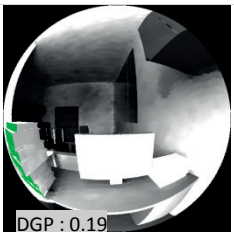 DGP : 0.19
CFS1	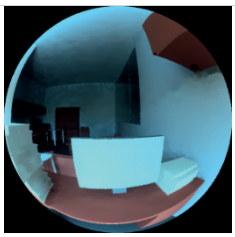	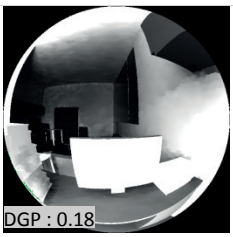 DGP : 0.18	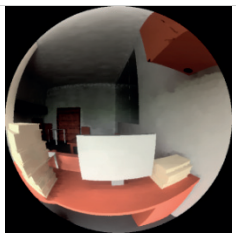	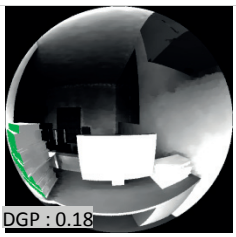 DGP : 0.18
CFS2	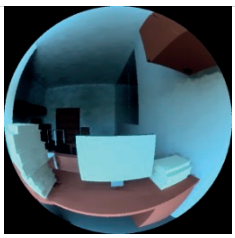	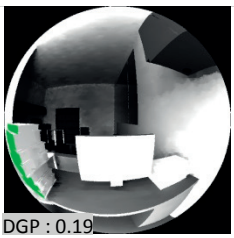 DGP : 0.19	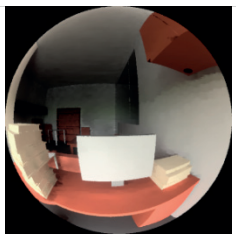	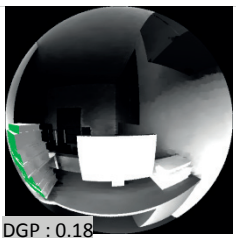 DGP : 0.18
CFS3	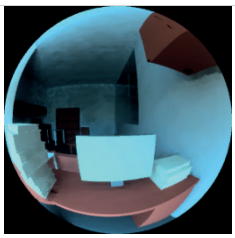	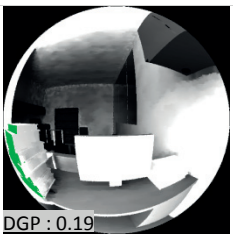 DGP : 0.19	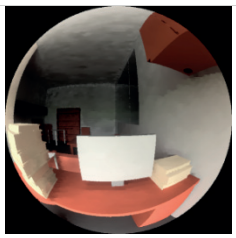	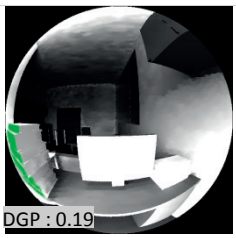 DGP : 0.19

Table 3.7 Daylight Glare Probability for Building B1 at Winter Solstice at 15h and 17h for the view position of Desk 1, at left the human response image and at right the DGP image result after applying evalglare to the HDR image.

B1/Winter Solstice	DGP Intolerable = > 0.45 Imperceptible=<0.30 (lbs=low brightness scene)			
	15h00		17h00	
Desk 2	Human Response	Glare-fisheye HDR	Human Response	Glare-fisheye HDR
Glass τv80%		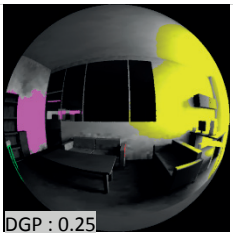 DGP : 0.25		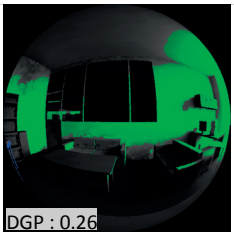 DGP : 0.26
LCP	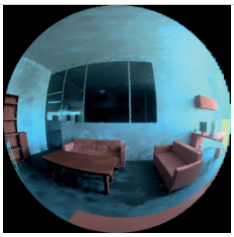	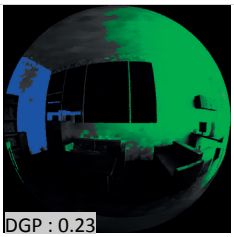 DGP : 0.23	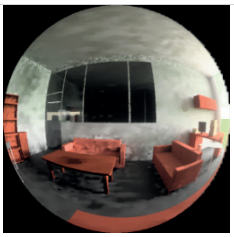	 DGP : 0.22
Film 3M	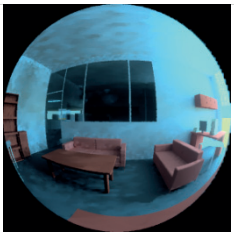	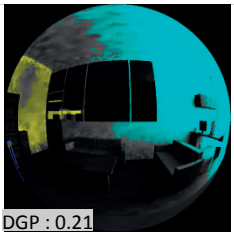 DGP : 0.21		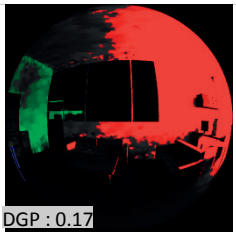 DGP : 0.17
CFS1	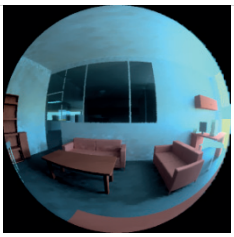	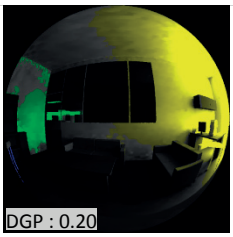 DGP : 0.20		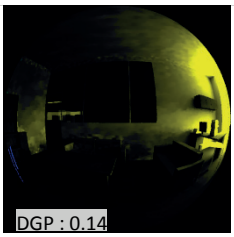 DGP : 0.14
CFS2	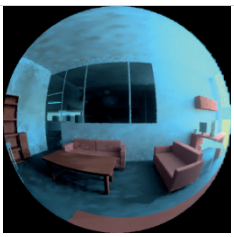	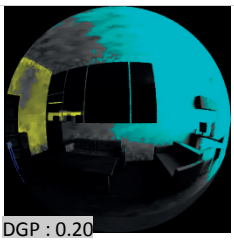 DGP : 0.20		 DGP : 0.10
CFS3	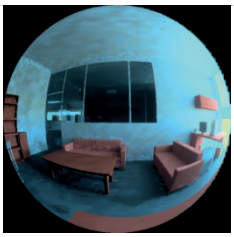	 DGP : 0.21		 DGP : 0.16

Table 3.8 Daylight Glare Probability for Building B1 at Winter Solstice at 15h00 and 17h00 for the view position of Desk 2

B1/Spring Equinox	DGP Intolerable = > 0.45 Imperceptible=<0.30 (lbs=low brightness scene)			
	15h00		17h00	
Desk 1	Human Response	Glare-fisheye HDR	Human Response	Glare-fisheye HDR
Glass τv80%	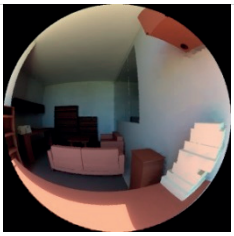	 DGP : 0.05	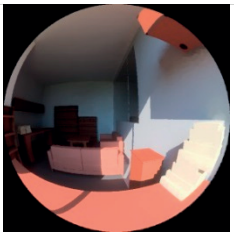	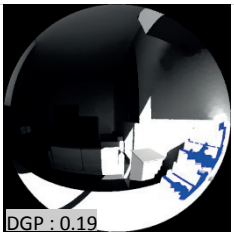 DGP : 0.19
LCP		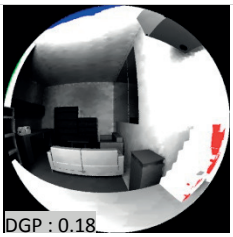 DGP : 0.18		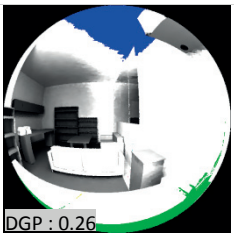 DGP : 0.26
Film 3M	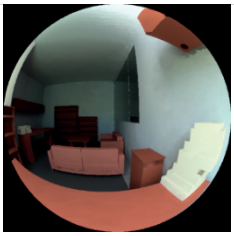	 DGP : 0.20		 DGP : 0.23
CFS1	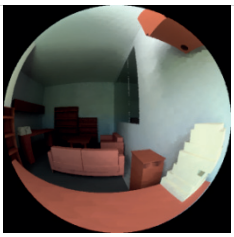	 DGP : 0.20		 DGP : 0.23
CFS2		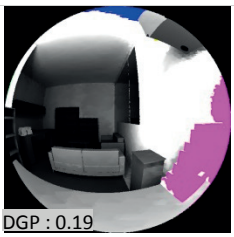 DGP : 0.19	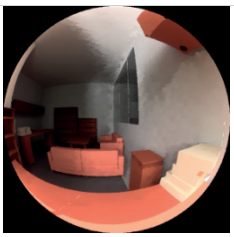	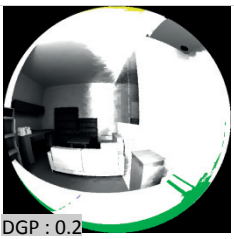 DGP : 0.2
CFS3	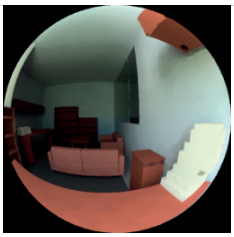	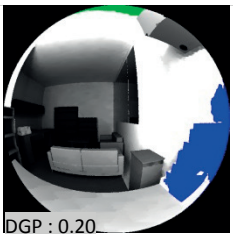 DGP : 0.20	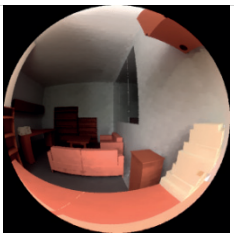	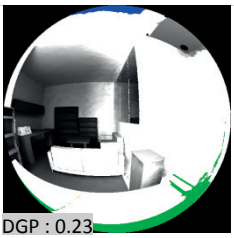 DGP : 0.23

Table 3.9 Daylight Glare Probability for Building B1 at Spring Equinox at 15h00 and 17h00 for the view position of Desk 1

B1/Spring Equinox	DGP Intolerable = > 0.45 Imperceptible=<0.30 (lbs=low brightness scene)			
	15h00		17h00	
Desk 2	Human Response	Glare-fisheye HDR	Human Response	Glare-fisheye HDR
Glass τv80%	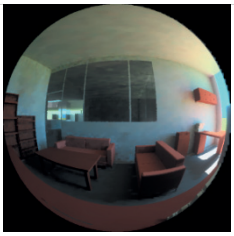	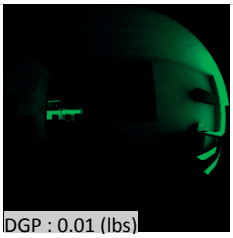 DGP : 0.01 (lbs)	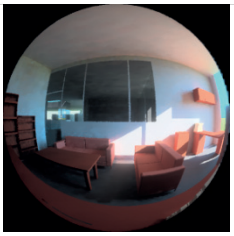	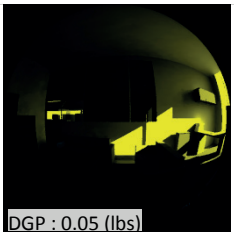 DGP : 0.05 (lbs)
LCP		 DGP : 0.21		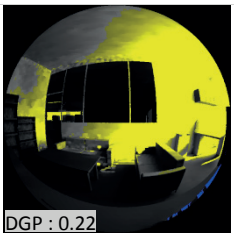 DGP : 0.22
Film 3M		 DGP : 0.20		 DGP : 0.24
CFS1		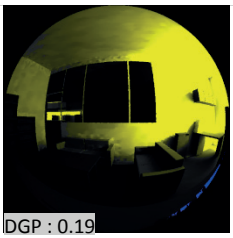 DGP : 0.19		 DGP : 0.22
CFS2		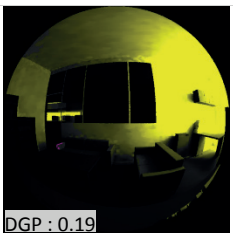 DGP : 0.19		 DGP : 0.21
CFS3		 DGP : 0.19		 DGP : 0.22

Table 3.10 Daylight Glare Probability for Building B1 at Spring Equinox at 15h00 and 17h00 for the view position of Desk 1

B1/Spring Equinox	DGP Intolerable = > 0.45 Imperceptible=<0.30 (lbs=low brightness scene)			
	15h00		17h00	
Desk 3	Human Response	Glare-fisheye HDR	Human Response	Glare-fisheye HDR
Glass τv80%		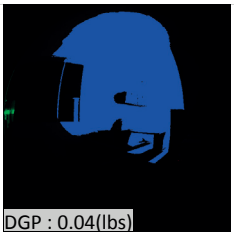 DGP : 0.04(lbs)	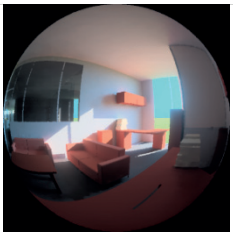	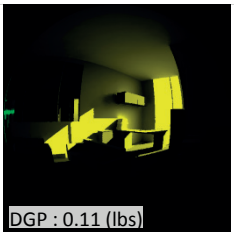 DGP : 0.11 (lbs)
LCP		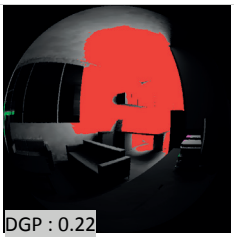 DGP : 0.22	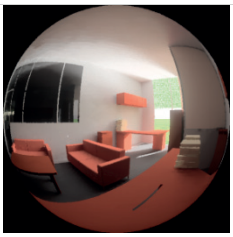	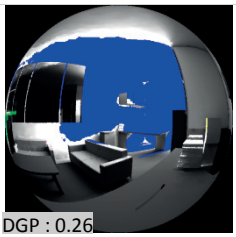 DGP : 0.26
Film 3M	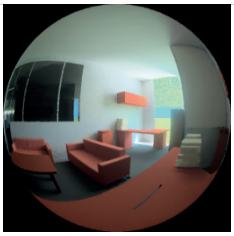	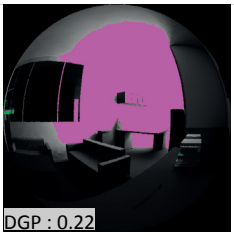 DGP : 0.22	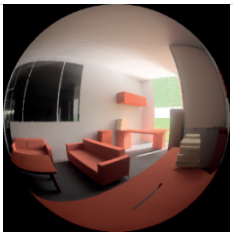	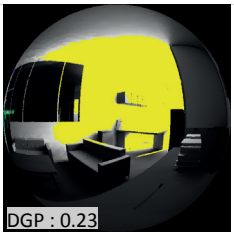 DGP : 0.23
CFS1	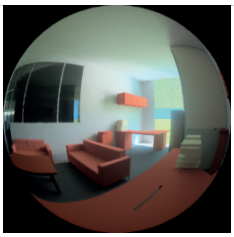	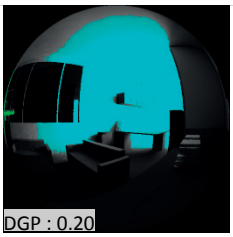 DGP : 0.20		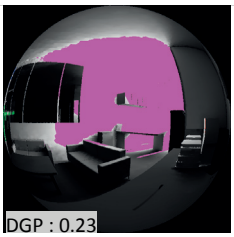 DGP : 0.23
CFS2		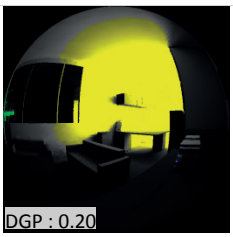 DGP : 0.20		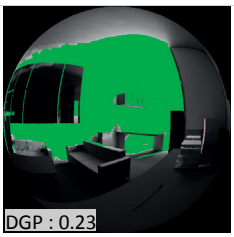 DGP : 0.23
CFS3	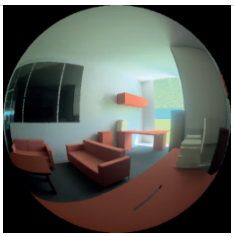	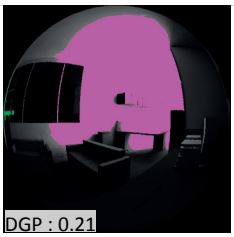 DGP : 0.21		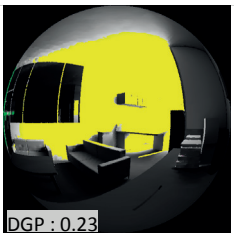 DGP : 0.23

Table 3.11 Daylight Glare Probability for Building B1 at Spring Equinox at 15h00 and 17h00 for the view position of Desk 3

For the office room located in Building B2, the glare assessment was performed only for one occupant's position. DGP values larger than than 0.45 were found for all cases (Winter Solstice and Spring Equinox at 9h00 and 12h00), except for Spring Equinox at 12h00 for CFS2 (Table 3.12). Such results indicate that due to its orientation and the large window-to-wall ratio (90%) the room presents serious glare problems, and that a large occupant's fraction might be disturbed by intolerable glare sensations. A larger risk was found for the standard glazing showing a DGP value of 1.0 at Winter Solstice at 9h00, due to the sun visible from the working space as shown on Table 3.13. For the other CFS the DGP decreases to about 0.55 confirming their shading function. However, a DGP value of 0.55 still implies an intolerable glare sensation for the occupants.

B2/Winter Solstice	DGP Intolerable = > 0.45 Imperceptible=<0.30 (lbs=low brightness scene)			
	9h00		12h00	
Desk 1	Human Response	Glare-fisheye HDR	Human Response	Glare-fisheye HDR
Glass τv70%	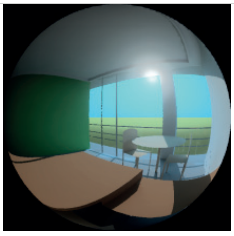	 DGP : 1.0	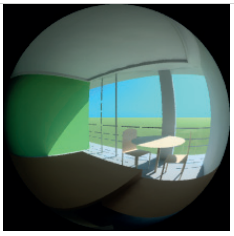	 DGP : 0.59
LCP	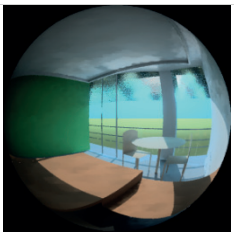	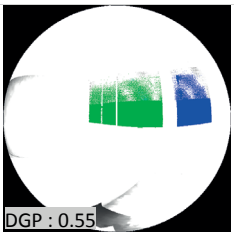 DGP : 0.55	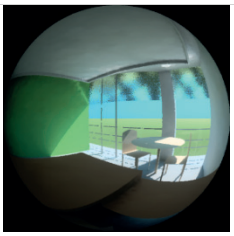	 DGP : 0.53
Film 3M	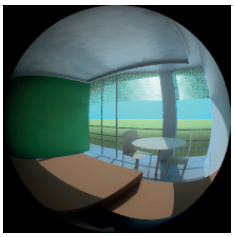	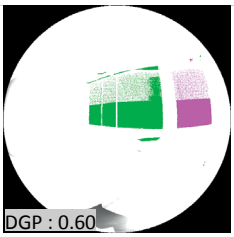 DGP : 0.60	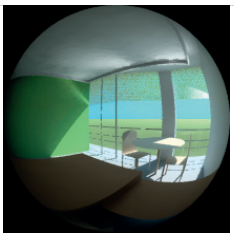	 DGP : 0.58
CFS1	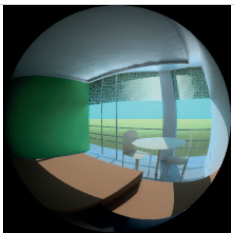	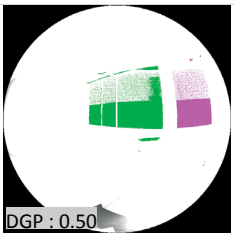 DGP : 0.50	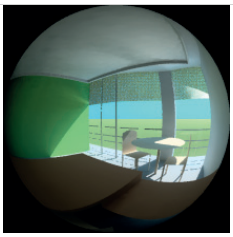	 DGP : 0.54
CFS2	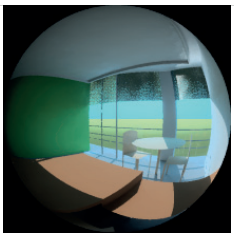	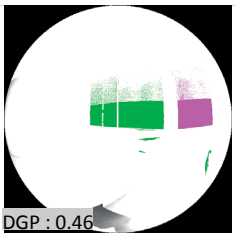 DGP : 0.46	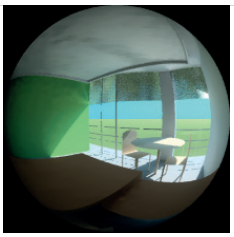	 DGP : 0.53
CFS3	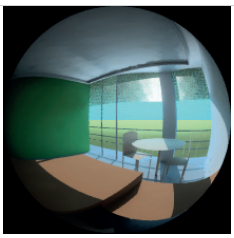	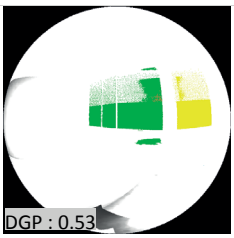 DGP : 0.53	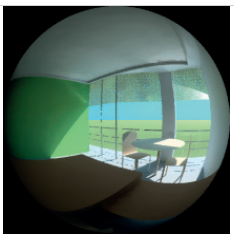	 DGP : 0.55

Table 3.12 Daylight Glare Probability for Building B2 at Winter Solstice at 9h00 and 12h00 for the view position of Desk 1

B2/Spring Equinox	DGP Intolerable = > 0.45 Imperceptible=<0.30 (lbs=low brightness scene)			
	9h00		12h00	
Desk 1	Human Response	Glare-fisheye HDR	Human Response	Glare-fisheye HDR
Glass τv70%	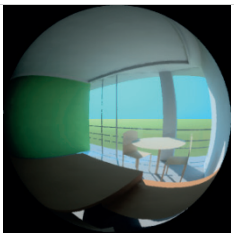	 DGP : 0.63	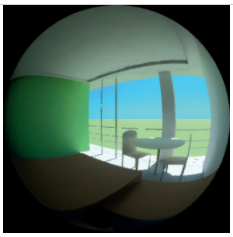	 DGP : 0.47
LCP	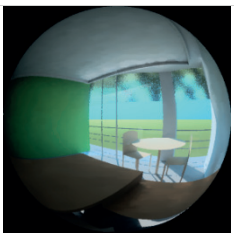	 DGP : 0.53	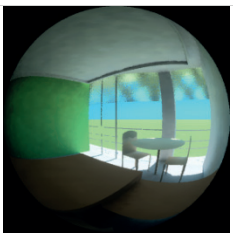	 DGP : 0.45
Film 3M	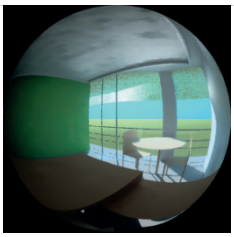	 DGP : 0.61	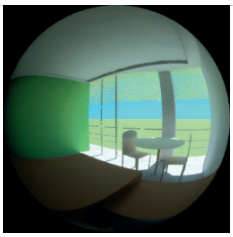	 DGP : 0.49
CFS1		 DGP : 0.52	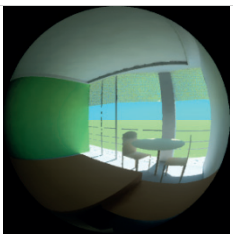	 DGP : 0.46
CFS2	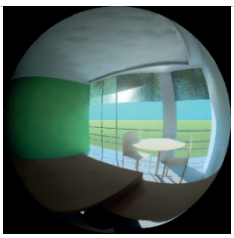	 DGP : 0.57	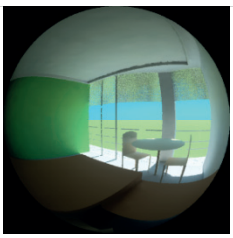	 DGP : 0.44
CFS3	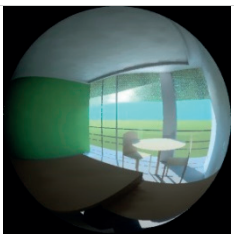	 DGP : 0.56	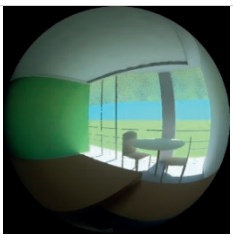	 DGP : 0.46

Table 3.13 Daylight Glare Probability for Building B2 at Spring Equinox at 9h00 and 12h00 for the view position of Desk 1.

3.5.2 Conclusions

The aim of this study is mainly to assess the performance of the five pre-selected CFS and compare it to the one of a standard double-glazing. The evaluation of glare risks associated to each system should also contribute to identify the CFS which reduce these risks and improve the visual comfort of users. From the study it can be conclude, in the case of Building B1, that the CFS does not increase the glare risks since the DGP values assessed with *evalglare* remain within the tolerance limit. All results are within the range corresponding to imperceptible glare sensations; this might be explained by the location of the three working spaces for without any direct view of the window in the view field. On the other hand, DGP values underneath 0.2 were observed at Spring Equinox for the three working places when using standard glazing; such value indicates a scene of very low brightness, a situation where the risks of glare might be underestimated. Daylighting is mainly concentrated in the area next to the window for the standard glazing, creating a dark environment in the rest of the office room, a situation where workplane illuminance are too low to perform visual tasks, implying the use of electric lighting. However, the daylight redirection towards the ceiling and the adjacent walls by the CFS contribute to create an even indoor daylight distribution, which is more adequate to perform working tasks. In the case of Building B2, the opposite situation was observed, DGP values larger than 0.45 were found in almost all the assessed situations, indicating that a large user's fraction would perceive intolerable glare sensations in the working environment. Such situation is observed unfortunately even when using CFS, meaning that the sunshadings is required to mitigate this effect.

3.6 Assessment of the CFS solar gains

The thermal comfort assessment in the two office rooms was carried out by determining the solar gains through the five CFS in two different ways. In a first approach (presented in this Chapter), the solar energy transmitted by the CFS during three typical periods at certain hours of the day was calculated when the sunrays hit the façade; a second approach refers to an annual assessment of the solar gains which is presented in Chapter 4.

For winter, summer solstices and spring equinox, as a first step, the vertical irradiance (W/m²) on the façade of the two office rooms was determined using RADIANCE simulations for the three assessed days at 9h00, 12h00, 15h00 and 17h00. As a second step, the values were multiplied by the visible transmittance of the CFS and the standard glazing. The latter, is depending from the incidence angle of sunlight for the CFS, was obtained from the BTDF data monitored using the bidirectional gonio-photometer and corresponding to each hourly time step. In the case of standard glazing it was obtained from calculations that take the number of glass panes into account as well as the type of coating used [3]. A strong hypothesis was however made, accordingly by supposing that the solar radiation (e.g. with wavelengths comprised between 0.2 and 2 um) is passing through the CFS in the same way that light is transmitted by the latter. Indeed, the BTDF data of the CFS are monitored using a bidirectional gonio-photometer, which only takes into account the visible fraction of the electromagnetic spectrum (e.g. 0.4 to 0.7 um), furthermore the absorbed heat transmitted inside is neglected.

3.6.1 Results

In the case of Building B1 the assessment was made at the Winter solstice and Spring equinox at 12h00, 15h00 and 17h00, and at Summer solstice at 12h00 and 15h00, which are the hours when sunrays are hitting the façade. The results of the solar energy transmitted into the room are presented in Figure 3.49. Those obtained with the tinted glass (τv12%), currently used in Building B1, are also presented as a matter of comparison. According to the daylighting approach applied in this study, a larger admission of solar gains is required in winter time while a lower tranmission of solar radiation is desired in summer time. The results show that a larger transmittance of solar energy is achieved by the Standard glazing for the three days assessed compared to the CFS; Film 3M and CFS2 seem however that allow a large amount of solar gains to enter the room. In the case of Building B2 (shown in Figure 3.50) sunrays are incident in the façade from 9h00 to 17h00 in winter time, from 9h00 to 15h00 in spring and only at 9h00 and 12h00 in summertime. The results show that Film 3M and CFS2 are the CFS allowing a large transmittance of solar radiation at winter solstice, while CFS1 and LCP allow less solar gains to enter the room at the same period. In a secondary axis, is indicated the corresponding percentage to those values using as a reference the current tinted glazing τv 12% and the standard glazing in both office rooms. The latter shows that in B1, there is an increased admission of Solar Energy of close to 650% when comparing the existing situation with the use of standard glass with a visible transmittance of 80%. A decreased percentage is observed between the reference component (standard glass τv 80%) and the CFS, due to the CFS effect as shading device. A similar situation can be observed in B2 with a transmitted solar energy decrease of minimum 20% compared with the use of CFS.

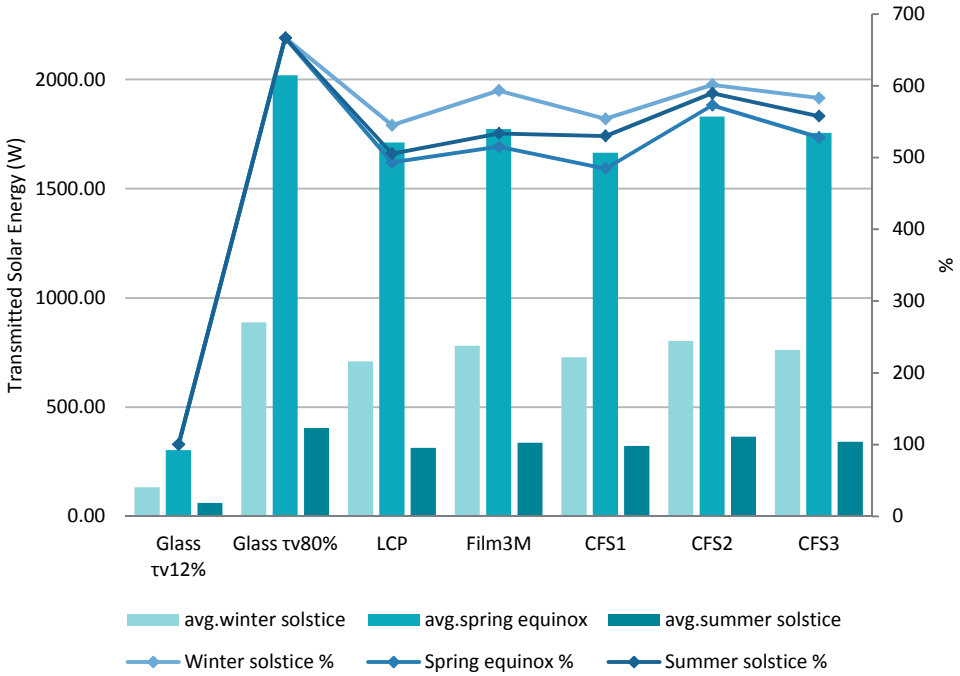

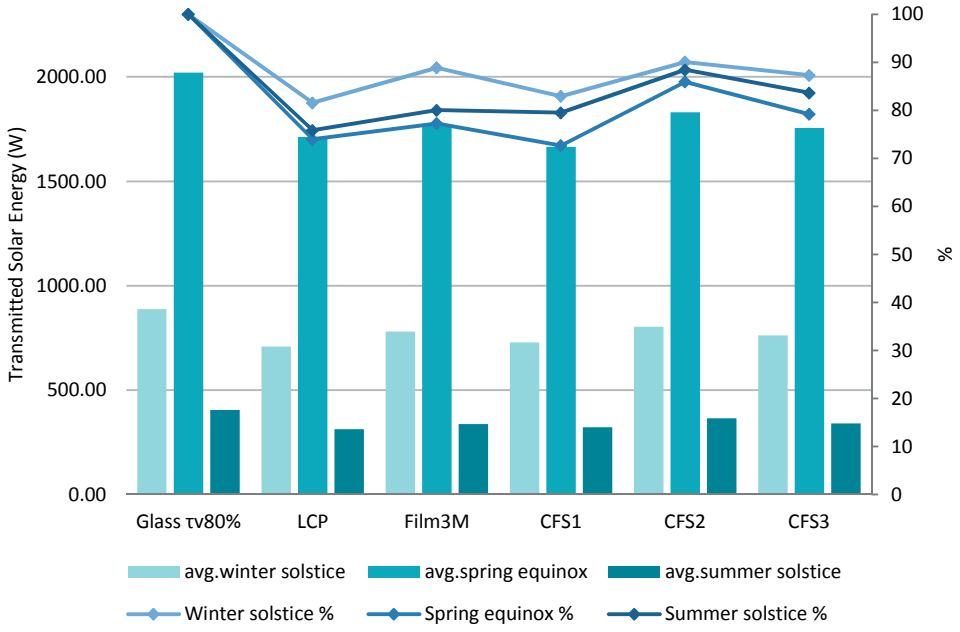

Figure 3.49 Solar energy transmitted into the office room in Building B1 at Winter and Summer Solstice and Spring equinox. The secondary axis indicates the corresponding percentage, above is shown the comparison using as a reference the tinted glazing τv 12%, while the graph below used as a reference the clear glass τv80%.

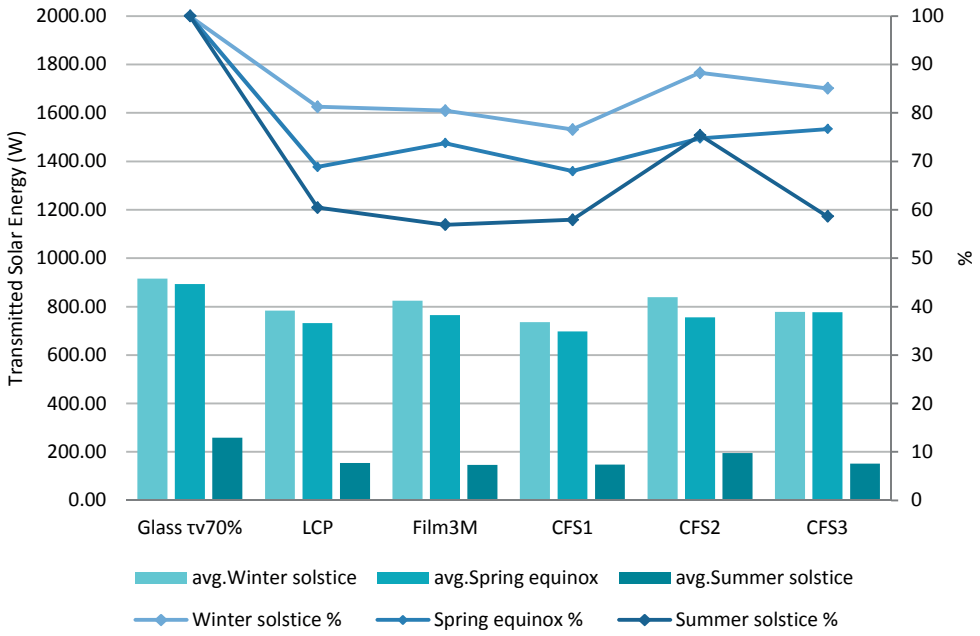

Figure 3.50 Solar energy transmitted into the office room in Building B2 at Winter and Summer Solstice and Spring equinox, showing in a second axis the corresponding percentace using as reference the standard glass τv70%.

3.6.2 Conclusions

The solar gains transmitted into the two office rooms during winter and summer solstices as well as spring equinox were assessed in order to perform a first estimation of the thermal comfort conditions for the occupants in the office rooms. The study shows that in the case of Building B1, Film 3M and CFS2 would be the best options for winter time, allowing larger solar gains to enter the room. In Summer time, LCP would be the best option as less solar energy is being transmitted into the room; the largest transmitted solar energy is observed for the standard glazing and CFS2. In the case of Building B2, the CFS that better performs at winter solstice is the CFS2, followed by Film 3M and CFS3; for Summer solstice the standard glazing transmits the largest fraction of solar radiation while Film 3M and CFS1 allow less of it to enter the room. These results allow us to conclude that regarding the thermal comfort assessment for winter and summer solstices, Film 3M could be considered as the most appropriate system since is the one performing well in the two buildings.

3.7 Multi-criterion analysis of the CFS daylighting performance

The overall assessment achieved for winter and summer Solstices as well as the Spring Equinox takes two main aspects into account: the daylight distribution in the room (which also includes the comparison of the frequency of illuminance and the Illuminance Uniformity) and the Visual and Thermal Comfort of the Occupants. The former was carried out using the DGP glare index as evaluation metric; the second one was achieved by comparing the Solar Gains (W/m^2) of the five CFS and the standard glazing. In order to perform an overall evaluation of all these devices and draw preliminary conclusions, a multi-criterion analysis of the CFS daylighting performance was implemented. The latter was done given the complexity of the evaluation procedure that includes comparison of different daylighting performance and comfort metrics which are then represented using different units.

Multiple-Criteria Analysis can be identified in several ways: Multiple-criteria desition making (MCDM), multiple-criteria desition analysis (MCDA) or multi-objective desition making (MODM). They are frequently used as a desition making tool in the energy efficient building environment due to the complexity that such evaluations represent as they involve the assessment of different disciplines (environment, technological, economical, comfort and so on), therefore the desition maker has to deal with multiple objectives. Few examples of their application in the built environment are: to determine life cycle models [134], in the application of building retrofit strategies [135], and daylighting strategies in buildings [136].

In order to apply the multicriteria analysis, two key factors are determined first: the Weighting Factor (WF), which is a value that represents the importance of each aspect considered in the evaluation process (shown in Table 3.14) and the Satisfaction Degree (SD), which is a value that indicates a level of satisfaction provided by each condition.

According to the proposed daylighting approach, the selection of an outstanding CFS will be the result of comparing their performance between one another. Thus, a distinct classification was proposed to perform this evaluation in the case of certain conditions considered in this chapter, such as: frequency of illuminances and the transmitted solar energy. Given that, for the latter conditions no reference value could assist in the classification of good or bad performance, as it would be the case of achieving a 5% of DF which indicates a good interior daylight distribution. Thus, in the case of Building B1, the satisfaction degree is classified based in seven grades that would be assigned to each variant (CFS or standard glass) to describe their performance according to each condition. The classification of the satisfaction degree criteria applied to Building B1 is show in Table 3.15, while the one applied to Building B2 is presented in Figure 3.16.

Importance of criteria	Weighting Factor (WF)
not important	1
unimportant	2
important	3
very important	4
extremely important	5

Table 3.14 Weighting Factors classifying the importance of each aspect of the evaluation criteria

Building B1		
Condition	Satisfaction Degree (SD)	
	→	↔
completely dissatisfied	0	6
dissatisfied	1	5
poorly satisfied	2	4
unsufficiently satisfied	3	3
sufficiently satisfied	4	2
well satisfied	5	1
perfectly satisfied	6	0

Table 3.15 Satisfaction Degree classifying the importance of each aspect of the evaluation criteria.

Building B2		
Condition	Satisfaction Degree (SD)	
	→	↔
dissatisfied	0	5
poorly satisfied	1	4
unsufficiently satisfied	2	3
sufficiently satisfied	3	2
well satisfied	4	1
perfectly satisfied	5	0

Table 3.16 Cassification of the Satisfaction Degree, which gives a rate to each condition according to its satisfaction degree.

Then, the definition of the satisfaction degree applied to each condition assessed is presented in Table 3.17 in the case of Building B1. For the assessment of the daylight distribution in the office rooms, the first considered aspect is the frequency of illuminances classified in different ranges, the CFS were classified according to their performance regarding each range of illuminance, assigning them a rate from 0 to 6 points in categories that correspond to the lowest (0), poor, moderate, good and best performance (6). On the other hand, for the assessment of DF, a value larger than 5% is rated with of 5 points, while for a value of 2% is given 2 points. For the assessment of Illuminance Uniformity, 5 points are granted when an IF value equal or larger than 0.7 is observed, while zero point is given when IF is equal or lower than 0.1.

B1		SATISFACTION DEGREE						
Condition		0	1	2	3	4	5	6
1. INTERIOR DAYLIGHT DISTRIBUTION	cbc	completely dissatisfied	dissatisfied	poorly satisfied	Unsufficiently satisfied	sufficiently satisfied	well satisfied	perfectly satisfied
1.1 Frequency of Illuminance (%) (S & E)								
not sufficient (<100 lx)	↔	highest	good	not bad	moderate	poor	bad	lowest
minimum (100-300 lx)	↔	highest	good	not bad	moderate	poor	bad	lowest
target (300-500 lx)		lowest	bad	poor	moderate	not bad	good	highest
sufficient (500-1800 lx)		lowest	bad	poor	moderate	not bad	good	highest
maximum (1800-2000 lx)		lowest	bad	poor	moderate	not bad	good	highest
risk (> 2000 lx)	↔	highest	good	not bad	moderate	poor	bad	lowest
1.2 Average DF %		< 1%	1%	2%	3%	4%	> 5%	-
1.3 Illuminance Uniformity								
Illuminance Uniformity g1 (min/avg)		0.1	0.3	0.4	0.5	0.6	> 0.7	-
Illuminance Uniformity g2 (min/max)		0.1	0.3	0.4	0.5	0.6	> 0.7	-
2. OCCUPANT'S COMFORT								
2.1 Visual Comfort (Solstices and Equinox)								
Glare (DGP)		Intolerable (> 0.45)	lbs (< 0.1)		lbs (< 0.1 - < 0.2)		Imperceptible (> 0.2 - < 0.3)	-
2.2 Thermal Comfort (Solstices and Equinox)								
Transmitted Solar Energy (W/m2)								
Winter		lowest	bad	poor	moderate	not bad	good	highest
Summer	↔	highest	good	not bad	moderate	poor	bad	lowest

Table 3.17 Scheme of the satisfaction degree criteria applied to Building B1 to evaluate the daylighting strategy at Solstices and Equinox.

In order to assess the visual comfort (risk of glare), three conditions are scored: Low brightness scene (below 0.2 DGP), Imperceptible Glare (below 0.3 DGP), and Intolerable glare corresponding to a DGP value larger than 0.45. Ann additional condition was included that would provide a score for the situation observed in Building B1 where very low brightness scenes are due to the standard glazing (Section 3.5.2). This was made to enhance the differences between the use of standard glazing and the CFS. The maximum value of 6 was not assigned in such assessments (DF, Illuminance Uniformity and Glare) in order to agree with the satisfaction degree applied for Building B2 shown in Figure 3.20.

The transmitted solar radiation was assessed in a similar way than the interior illuminance distribution, although a counter-balance criterion was applied in this case. Given that (as introduced in the daylighting improvement approach in Section 3.1), moderate solar gains are desired into the room during summertime; therefore a lower score is assigned when large solar gains enter the room. Such upturned-criterion is indicated with the symbol of the double arrow in the right column (cbc) of the assessed conditions.

The daylighting approach applied in this study endows higher priority to the admission of daylight into the rooms than to the protection of the interior space from the sun's incidence; therefore higher WF values are assigned to the conditions that agree with such conception. The WF assigned to the criteria assessed in this study are shown in Table 3.18, it can be seen that a value of 5 is assigned to the criterias that are considered as 'extremely important' for the overall evaluation such as achieving an illuminance within the 'target' and 'acceptable' illuminance ranges, and the admission of solar gains in winter time. On the other hand, criterias such as visual comfort (glare), the achievement of a range of illuminance within the 'risk' range and the admission of solar gains (during summer solstice in the case of the assessment performed during solstices and equinox) are considered as 'very important' by assigning them a WF of 4. The latter are considered as less important than the admission of daylight since, as mentioned before the use of a solar protection device would contribute to mitigate the effects described by such criterias. Achieving ranges of illuminance within the 'minimum' and 'maximum' ranges is considered as 'important' (WF equal to 3) since such ranges might signify the offset of electric light or might be still within the preferences of some users. Likewise, the Illuminance uniformity is considered as an 'important' criterion, as it represents an indicator of the distribution of daylight in the working area. The achievement of illuminance values within the range 'non sufficient' is considered as not important since such values are considered of short relevance for the human visual performance [137]. Regarding the DF, the WF was set to 4 since it represents a daylight situation in the presence of overcast sky conditions, which are less frequent in the regions subject of this study; however due to the results in both buildings, no difference was observed when setting the WF to the highest value representing extremely important criteria (5).

WEIGHTING FACTOR							
1. INTERIOR DAYLIGHT DISTRIBUTION	**1.1 Ranges of Illuminance (%)** (Solstices & Equinox and Annual Assessment)						
	not sufficient (<100 lx)	minimum (100-300 lx)	target (300-500 lx)	acceptable (500-1800 lx)	maximum (1800-2000 lx)	risk (> 2000 lx)	
	1 (f)	**3** (s)	**5** (f)	**5** (f)	**3** (s)	**4** (p)	
	1.2 Average DF % (Solstices & Equinox)						
	4 (f)						
	1.3 Illuminance Uniformity (Solstices & Equinox)						
	Illuminance Uniformity g1	Illuminance Uniformity g2					
	3 (s)	**3** (s)					
2. OCCUPANTS COMFORT	**2.1 Visual Comfort** (Solstices and Equinox)						
	Glare (DGP)						
	4 (s)						
	2.2 Thermal Comfort (Solstices and Equinox)						
	Transmitted Solar Energy (W/m2)						
	Winter solstice	Summer solstice					
	5 (f)	**4** (p)					
	2.3 Thermal Comfort (Annual Assessment)						
	Total Heat Gain Energy [MJ] (Hourly)						
	4 (p)						

Table 3.18 Weighting Factor values assigned to each of the criteria considered in the overall assessment. An insignia is indicated in parenthesis which identifies each sub-criteria account in the sensibility study: 'f' stands for fixed value, 'p' for primary interest while's' for secondary interest.

In order to assess the impact that the combination of the WF values assigned to each criteria has in the final result of the multicreteria assessment, a sensitivity study was carried-out by selecting two sets of criteria considered as of primary and secondary interst. The latter represent the criterias which WF is undefined, unlike criterias such as the 'target' range of illuminance which WF is clearly defined as 'extremely important'. Then, as a first step, the former were assigned different values and tested in combination with the latter criteria. For instance, the 'risk of illuminance' range was tested with a WF value from 1 to 4, and then its effect on the final result was assessed by changing the value of 'secondary interest' criterias such as the 'illuminance uniformity' and/or the 'minimum illuminance'. Then the same procedure was applied to the 'Glare' criteria (also considered as of primary interest), and tested in combination of different values of the 'secondary interest' criterias; in this way the effect of the 'secondary interest' criterias in the final result could be determined. As second step, the effect of the 'primary interest' criterias was tested against each other.

As result it could be observed that the modification of the WF had a main effect in the definition of the first and second position in the overall evaluation in B1, switching between LCP and Film 3M which might be due to the close results that they obtained. For instance, when testing the WF of the 'risk of illuminance' with the 'solar gains' criteria it was observed that a risk illuminance WF of 3 would favour Film 3M while a WF of 4 leans towards LCP. It was also observed that assigning a WF of 3 or 4 to the illuminance uniformity would return the same results, while for the 'minimum' illuminance a WF of 2, 3 or 4 would also represent the same

outcome. The effects of the WF-glare criteria have a higher effect when combined with the 'risk of illuminance' than with the 'thermal comfort' criterias. In B2, the effects of the 'primary interest' criterias lay mainly on the CFS, due to its proximity in the results. However it was observed a predominance of the first position between LCP and CFS1, while Film 3M, CFS2 and CFS3 keep a steady second or third position, while the standard glass preserves the last position. As result of the sensitivity analysis, the WF were set at the values shown in Table 3.18, is noteworthy that the combination of the WF would vary according to the objectives established for each particular case, thus preliminar results would also have an effect in its final definition.

The overall evaluation for the winter and summer solstices as well as the spring equinox for Building B1 is shown in Table 3.19. They point out that LCP obtains a higher score in the overall assessment with 395 points, followed closely by the standrad glazing (τv 80%) with 386 points; Film 3M is found in the third position, followed by CFS2, CFS3 and CFS1 in a consecutive order.It can be observed that the LCP is superior regarding the frequency of usefull illuminance available in the room, as can be seen the partial-results analysed by condition at the bottom of the table. In regards to the Illuminance Uniformity the tinted glass and the standard glass τv 80%) perform equally achieving the highest score, while LCP and Film 3M follow closely. In the comparison of the DF performance, the standard glass and the Film 3M perform equally, while a similar situation is found with the others CFS; in this case the tinted glazing achieved zero points. Regarding the visual comfort of the occupants, Film 3M offers a more confortable visual environment while LCP achieved a good performance, the use of standard glazing with a large tranmission coefficient (80%) and the tinted glazing might signify incomfortable visual situations. The thermal comfort was assessed only for winter and summer solstices in order to comply with the established daylighting objectives for this study (higher admission of solar gains in winter time, while reduced admission in summer time). In winter solstice, the standard glazing (τv 80%) CFS2 and the Film 3M allow larger solar gains in the room. A counterbalance criteria was applied in the case of summer solstice, thus the CFS allowing large solar gains in summer obtained a lower score, such as standard glazing τv 80%, and CFS2. On the other hand, those that allowed lower solar gains obtained higher scores: this is the case for CFS1 and LCP and also for the current tinted glass because of its very low transmission (τv 12%).

B1	WF	%	cbc	Glass τv12%		Glass τv 80%		LCP		Film3M		CFS1		CFS2		CFS3	
				SD	UV	SD	UV	SD	UV	SD	UV	SD	UV	SD	UV	SD	UV
1. INTERIOR DAYLIGHT DISTRIBUTION																	
1.1 Frequency of Illuminance (%) (Solstices & Equinox)																	
not sufficient (<100 lx)	1	2.27	↔	0	0.00	5	11.36	4	9.09	6	13.64	1	2.27	3	6.82	2	4.55
minimum (100-300 lx)	3	6.82	↔	0	0.00	6	40.91	3	20.45	5	34.09	1	6.82	4	27.27	2	13.64
target (300-500 lx)	5	11.36		1	11.36	5	56.82	6	68.18	3	34.09	2	22.73	4	45.45	3	34.09
acceptable (500-1800 lx)	5	11.36		0	0.00	6	68.18	4	45.45	5	56.82	3	34.09	1	11.36	2	22.73
maximum (1800-2000 lx)	3	6.82		3	20.45	4	27.27	5	34.09	5	34.09	4	27.27	6	40.91	6	40.91
risk (> 2000 lx)	4	9.09	↔	6	54.55	1	9.09	5	45.45	0	0.00	4	36.36	2	18.18	3	27.27
1.2 Average DF %	4	9.09		0	0.00	5	45.45	4	36.36	4	36.36	4	36.36	4	36.36	4	36.36
1.3 Illuminance Uniformity (Solstices & Equinox)																	
Illuminance Uniformity g1 (min/avg)	3	6.82		4	27.27	4	27.27	4	27.27	4	27.27	3	20.45	3	20.45	3	20.45
Illuminance Uniformity g2 (min/max)	3	6.82		2	13.64	2	13.64	1	6.82	1	6.82	1	6.82	1	6.82	1	6.82
2. OCCUPANT'S COMFORT																	
2.1 Visual Comfort (Solstices and Equinox)																	
Glare (DGP)	4	9.09		1	9.09	2	18.18	5	45.45	6	54.55	4	36.36	3	27.27	5	45.45
2.2 Thermal Comfort (Solstices and Equinox)																	
Transmitted Solar Energy (W/m2)																	
Winter solstice	5	11.36		0	0.00	6	68.18	1	11.36	4	45.45	2	22.73	5	56.82	3	34.09
Summer solstice	4	9.09	↔	6	54.55	0	0.00	5	45.45	3	27.27	4	36.36	1	9.09	2	18.18
		condition 1.1			86.36		213.64		222.73		172.73		129.55		150.00		143.18
		condition 1.2			0.00		36.23		28.99		36.23		28.99		28.99		28.99
		condition 1.3			40.91		40.91		34.09		34.09		27.27		27.27		27.27
		condition 2.1			7.25		14.49		36.23		43.48		28.99		21.74		28.99
		condition 2.2			54.55		68.18		56.82		72.73		59.09		65.91		52.27
	44	100.00			190.91		386.36		395.45		370.45		288.64		306.82		304.55

Table 3.19 The overall evaluation critera for the assessment of the performance of CFS in Winter and Summer Solstices and in Spring Equinox in Building B1.

The definition of the satisfaction degree criteria applied to Building B2 was based on six grades (described in Table 3.20), since in this case six variants are considered (standard glazing and five CFS). The results of the overall evaluation are presented in Table 3.21. They show that the six variants perform in a rather comparable way. However, a better performance is achieved by the CFS3 then the LCP, Film 3M and CFS1, CFS2 and CFS3 achieved a second position with quite similar results, while the standard glass τv 70% achieved the last. In the assessment of the DF performance, all the fenestration systems achieved the same score which might be due to the characteristics of this building which favors the conditons for good daylight in the room. Regarding the Illuminance Uniformity assessment, the LCP and Film3M performs better while the rest of the fenestration systems perform equally. Regarding Visual Comfort, all the cases were assigned a zero value, since all present DGP values higher than 0.45, which indicates a high glare risk which is synonimous of an intolerable glaring environment (see Section 3.5.1). In the assessment of the thermal comfort, the standard glass and CFS2 allow the largest solar gains into the room at winter solstice; while in summer, the Film 3M and CFS3 are the ones that allow the lowest solar gains and therefore obtained a higher score.

B2		SATISFACTION DEGREE					
Condition		0	1	2	3	4	5
1. INTERIOR DAYLIGHT DISTRIBUTION	cbc						
1.1 Frequency of Illuminance (%) (Annual Assessment)							
not sufficient (<100 lx)	↔	highest	good	not bad	moderate	poor	lowest
minimum (100-300 lx)	↔	highest	good	not bad	moderate	poor	lowest
target (300-500 lx)		lowest	poor	moderate	not bad	good	highest
sufficient (500-1800 lx)		lowest	poor	moderate	not bad	good	highest
maximum (1800-2000 lx)		lowest	poor	moderate	not bad	good	highest
risk (> 2000 lx)	↔	highest	good	not bad	moderate	poor	lowest
1.2 Average DF %		< 1%	1-2%	2-3%	3-4%	4-5%	>5%
1.3 Illuminance Uniformity							
Illuminance Uniformity g1 (min/avg)		0.1	0.3	0.4	0.5	0.6	> 0.7
Illuminance Uniformity g2 (min/max)		0.1	0.3	0.4	0.5	0.6	> 0.7
2. OCCUPANT'S COMFORT							
2.1 Visual Comfort (Solstices and Equinox)							
Glare (DGP)		Intolerable (Above 0.45)	Very Low Brightness Scene (Below 0.1)		Low Brightness Scene (Above 0.1 - Below 0.2)		Imperceptible (Above 0.2 - Below 0.3)
2.2 Thermal Comfort (Solstices and Equinox)							
Transmitted Solar Energy (W/m2)							
Winter		lowest	poor	moderate	not bad	good	highest
Summer	↔	highest	good	not bad	moderate	poor	lowest

Table 3.20 The scheme of the satisfaction degree criteria applied to Building B2 to evaluate the daylighting strategy in Equinox and Solstices.

B2	WF	%	cbc	Glass 70%		LCP		Film3M		CFS1		CFS2		CFS3	
				SD	UV	SD	UV	SD	UV	SD	UV	SD	UV	SD	UV
1. INTERIOR DAYLIGHT DISTRIBUTION															
1.1 Ranges of Illuminance (%) (Solstices & Equinox)															
not sufficient (<100 lx)	**1**	2.27	↔	5	11.36	5	11.36	5	11.36	5	11.36	5	11.36	5	11.36
minimum (100-300 lx)	**3**	6.82	↔	5	34.09	3	20.45	4	27.27	1	6.82	0	0.00	2	13.64
target (300-500 lx)	**5**	11.36		2	22.73	5	56.82	3	34.09	4	45.45	5	56.82	4	45.45
acceptable (500-1800 lx)	**5**	11.36		2	22.73	3	34.09	1	11.36	5	56.82	3	34.09	4	45.45
maximum (1800-2000 lx)	**3**	6.82		4	27.27	3	20.45	5	34.09	3	20.45	2	13.64	2	13.64
risk (> 2000 lx)	**4**	9.09	↔	1	9.09	2	18.18	0	0.00	4	36.36	3	27.27	2	18.18
1.2 Average DF %	**4**	9.09		5	45.45	5	45.45	5	45.45	5	45.45	5	45.45	5	45.45
1.3 Illuminance Uniformity (Solstices & Equinox)															
Illuminance Uniformity g1 (min/avg)	**3**	6.82		3	20.45	4	27.27	4	27.27	3	20.45	3	20.45	3	20.45
Illuminance Uniformity g2 (min/max)	**3**	6.82		1	6.82	2	13.64	2	13.64	1	6.82	1	6.82	1	6.82
		0.00													
2. OCCUPANT'S COMFORT															
2.1 Visual Comfort (Solstices and Equinox)															
Glare (DGP)	**4**	9.09		0	0.00	0	0.00	0	0.00	0	0.00	0	0.00	0	0.00
2.2 Thermal Comfort (Solstices and Equinox)															
Transmitted Solar Energy (W/m2)															
Winter solstice	**5**	11.36		5	56.82	1	11.36	3	34.09	0	0.00	4	45.45	3	34.09
Summer solstice	**4**	9.09	↔	0	0.00	2	18.18	4	36.36	3	27.27	1	9.09	5	45.45
		condition 1.1			127.27		161.36		118.18		177.27		143.18		147.73
		condition 1.2			36.23		36.23		36.23		36.23		36.23		36.23
		condition 1.3			27.27		40.91		40.91		27.27		27.27		27.27
		condition 2.1			0.00		0.00		0.00		0.00		0.00		0.00
		condition 2.2			56.82		29.55		70.45		27.27		54.55		79.55
	44	100.00			256.82		277.27		275.00		277.27		270.45		300.00

Table 3.21 The overall evaluation critera for the assessment of the performance of CFS in Winter and Summer Solstices and in Spring Equinox in Building B2.

3.7.1 Conclusions

As a preliminary conclusion, it can be observed that in Building B1 the LCP shows an advantage in the evaluation of the CFS performance in spring equinox and winter and summer solstices. While in Building B2, the CFS3 performs better than the other CFS. The homogeneous results observed in Building B2 between the CFS and the standard glass might be due to several factors, such as the convenient size of the room (4.17m x 5.25m), its squared shape which contributes to a better distribution of daylight, its favourable orientation (south east), its high Window to Wall ratio (90%) which allows large daylight flux to enter the room. However, the evaluation presented in this Chapter, represents only a partial assessment which for sake of simplicity takes into account only critical days regarding daylighting (winter and summer solstices and spring equinox). In order to perform an integral assessment outlining the advantages and drawbacks of the five pre-selected CFS for buildings located at low latitudes, an annual assessment of the considered criteria is required.

Chapter 4 Annual assessment of daylight improvement using CFS

In order to characterize the fluctuations of daylight occurring in a building during a whole year, daylighting optimization strategies must include an annual assessment of the interior daylight distribution, especially in locations with prevailing clear sky conditions. In the case of buildings located at low latitudes, showing rather a warm climate, the assessment of the solar heat gains associated to the daylight flux, must be part of the evaluation as well. For daylighting strategies that include the use of Complex Fenestration Systems (CFS), such assessments must naturally be also able to describe the physical impact of the CFS on the interior daylight distribution. The latter can be done using the RADIANCE 'Five Phase Method', which procedure is explained in Section 1.3.1, while the solar gains were evaluated using the energy simulation programme Energy Plus, which is explained in Section 1.3.3.

4.1 Optimization of the interior daylight distribution through CFS

The luminous contribution of each of the five pre-selected CFS in the two office buildings through a whole year was simulated using the RADIANCE Five Phase Method. In order to do that, weather data representative of the climatic local conditions was obtained using Meteonorm, a software that generates climatic data for any World location. [138]. As explained in Section 2.4, measurement points were placed at the centre of each room every 0.2m from the window side to the back of the room at the standard height of a workplane (0.75m). For each points a total of 8760 hourly illuminance values were obtained representing the entire year. However, the time steps values not belonging to the usual working time in México (9h to 14h and 16h to 20h) were removed from the annual results.

In order to validate the illuminance results obtained using the Five-Phase Method, a comparison was made between those and the results obtained of simulations using the *bsdf* procedure. In order to do that, the sky luminance distribution was simulated on March 21st 12h00 (Building B1) and March 20th 12h00 (Building B2) which correspond to the dates in Spring Equinox when each building was monitored. The sky was generated using gendaylit with the direct and diffuse Irradiance data (Ibn and Idh) contained in the weather data file obtained with Meteonorm. The illuminance results were compared with those obtained using the Five Phase Method for that particular time and date. For both cases, the existing situations were simulated and compared, thus in the case of Building B1, the simulation was carried-out using the tinted glass τv 12%, while in B2 was used the standard glass 70%. The validation of the Five-Phase Method vs the *bsdf* procedure of Building B1 is shown in Figure 4.1, it can be observed that a close correspondence is achieved when the illuminance profiles obtained with the two simulation methods are compared. Those results are useful to corroborate that virtual model, and the procedure applied in the Five-Phase Method correspond with those employed in the simulations using the *bsdf* procedure. The same situation is observed in Building B2, where a close correspondence is also obtained when comparing the illuminance results obtained with the two methods. Those results are shown in Figure 4.2.

Using the Five Phase Method, rendering images were also obtained for each hourly time steps; those are generated for each of the three terms of the Five-phase method and then combined at the end to obtain a final image representing the interior daylight distribution through the CFS. The assessment of the obtained numerical results was done using the Useful Daylight Illuminances (UDI), a metric first introduced in 2005 which takes into account daylight illuminances within a range and the frequency in which they are achieved in a year [137, 139]. Thus, the results obtained were classified in six categories that describe its profitableness, such classification was made first according to the illuminance recommendations for working environments (See Section 2.3), and secondly to the delineation of UDI's ranges based in previous relevant studies [137]. The categories applied for categorizing the annual results in this PhD Thesis are shown in Table 4.1.

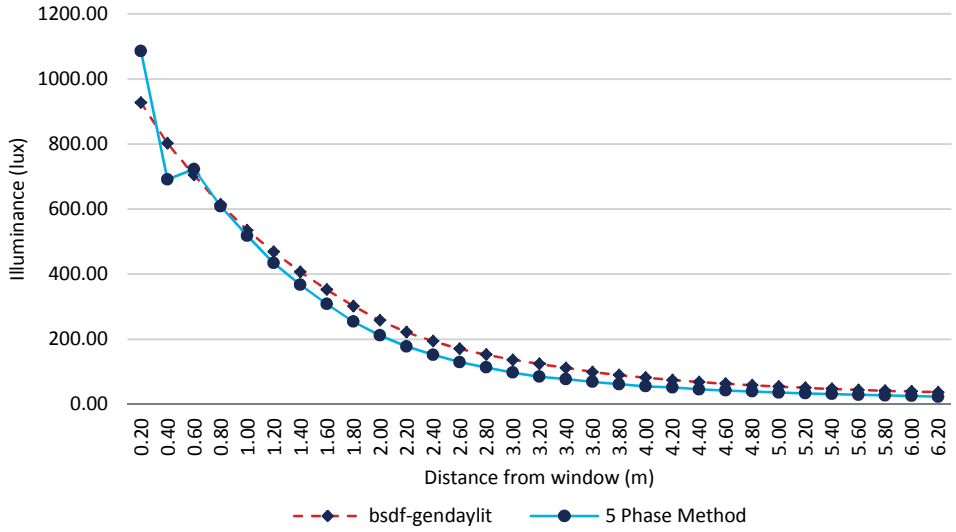

Figure 4.1 Comparison of the illuminance profiles obtained using the *bsdf* procedure and the 5 Phase Method in Building B1, on March 21st 12h00.

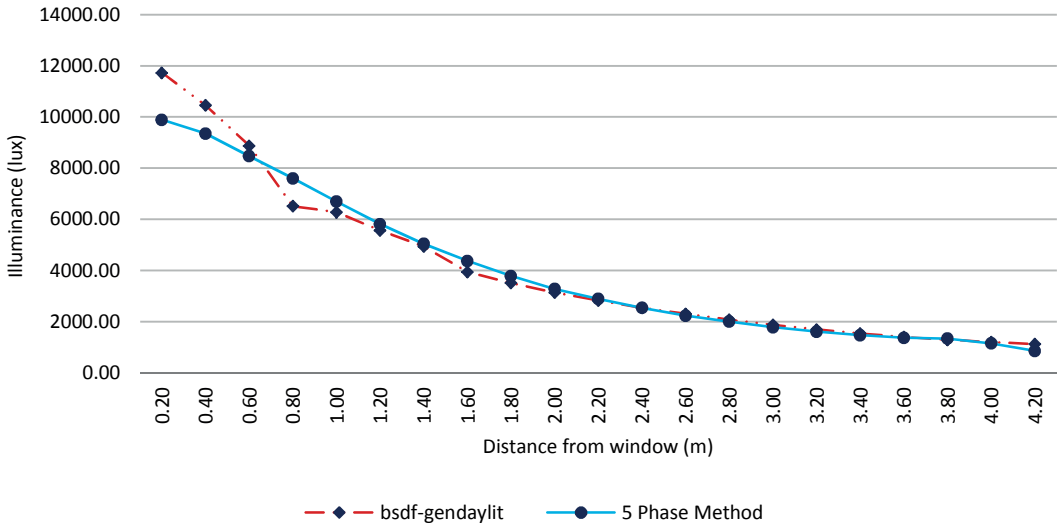

Figure 4.2 Comparison of the illuminance profiles obtained using the *bsdf* procedure and the 5 Phase Method in Building B2, on the 20th March 12h00.

Category	Range of Illuminance (lux)
Not sufficient	< 100
Minimum	100-300
Target	300-500
Acceptable	500-1800
Maximum	1800-2000
Glare or overheating risks	>2000

Table 4.1 UDI categories of applied to distinguish the illuminance results obtained in the two office rooms with the Five-phase method.

The resulting data was divided in six categories in order to evaluate the performance of each CFS according to different parameters and/or objectives. The 'Target category' corresponds to the illuminance values lying within the recommended range to reading/writing tasks; the 'Risk category' reports the illuminance range that would represent a risk of glare or overheating; the 'Minimum' or the 'Not sufficient' category corresponds to illuminance values below the recommendations, but that contribute to offset the use of electric lighting; finally the 'Acceptable' and the 'Maximum' categories are useful to identify the illuminance ranges that account for the compensation of electric light by daylight as well; they might be in the preference of some users or are in the adequate to perform other visual tasks and activities requiring higher work plane illuminance.

4.1.1 Results

As result, two main plots were generated, first the Annual Frequency of Illuminance, which is a count of the frequency in which certain ranges of illuminance occur during a certain period of time (See Table 4.1). This plot reflects the spatial distribution of daylight through the room when using the five CFS as well as the standard glazing; it is also useful to provide information regarding the placement of working place in the most illuminated area of the room. The second one is a Cumulative Curve Plot, which indicates the yearly relative fraction of time during the working hours in which a given illuminance range is available; the results were categorized in 50 lux bins and compared with the five assessed CFS, the existing tinted glass and the standard glazing (τv 80%) in the case of Building B1, and using standard glazing (τv 70%) for Building B2. In order to agree with the assessment presented in Chapter 3, where the performance of the five CFS was assessed during three days within critical daylighting conditions in a year (Winter and Summer Solstices and Spring Equinox), the results presented in this chapter include initially the assessment of the Winter, Spring and Summer as whole seasons. After that, specific cases showing the evaluation per periods in winter and summer time are presented as well.

4.1.1.1 Building B1

a) Illuminance Frequency

The results obtained for Building B1, are illustrated on Figure 4.3. They show the yearly frequency in which the illuminance lies within the range of 300-500 lux (target illuminance) occurs in a working hours. For this assessment, a period of time comprising winter, spring and summer time was taken into account. The results show that illuminance within the range of 300-500 lux is mainly distributed in the deepest half part of the room reaching a peak at a distance of 3.8m from the window. It is clear that LCP is the CFS that offers larger illuminance values in the room; just behind the standard glazing (τv 80%) which brings values within the target illuminance range during more than 40% of the year. Among the CFS the maximum of 30% of the year is achieved by CFS3, while the rest are slightly below this figure. The results of using the tinted glass (τv 12%) are also included in order to compare the existing situation with the improvements provided by the CFS. As it can be observed using the tinted glass, most of the target illuminance is achieved in the first area close to the window for about 27% of the yearly working hours, while at the back of the room the levels achieved using the tinted glass are nearly zero.

When assessing illuminance values within an acceptable range (500-1800 lux), shown in Figure 4.4, it can be observed that the larger illuminance is displaced towards the first half of the room. The peak is found at a distance of 2.20m from the window when using a standard glazing (τv 80%), representing 60% of the working time over the year when daylighting lies within the target range in the room. At the back of the room a maximum frequency of illuminance within the acceptable range is achieved by Film 3M at a distance of 5.0m during about 8% of the yearly working hours. For existing tinted glazing (τv 12%) the acceptable illuminance range is achieved during 20-30% of the yearly working hours at 1.0m distance from the window.

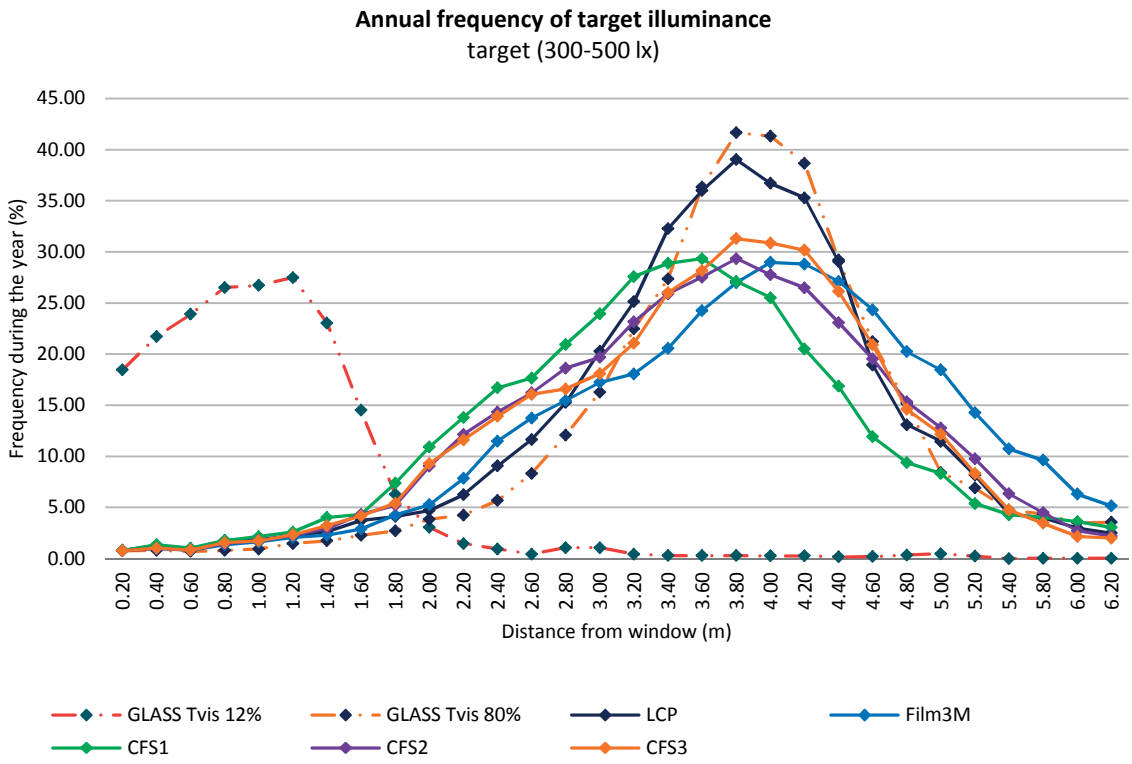

Figure 4.3 Annual frequency of daylight illuminance in the range of 300-500 lux occurring in the office room of Building B1.

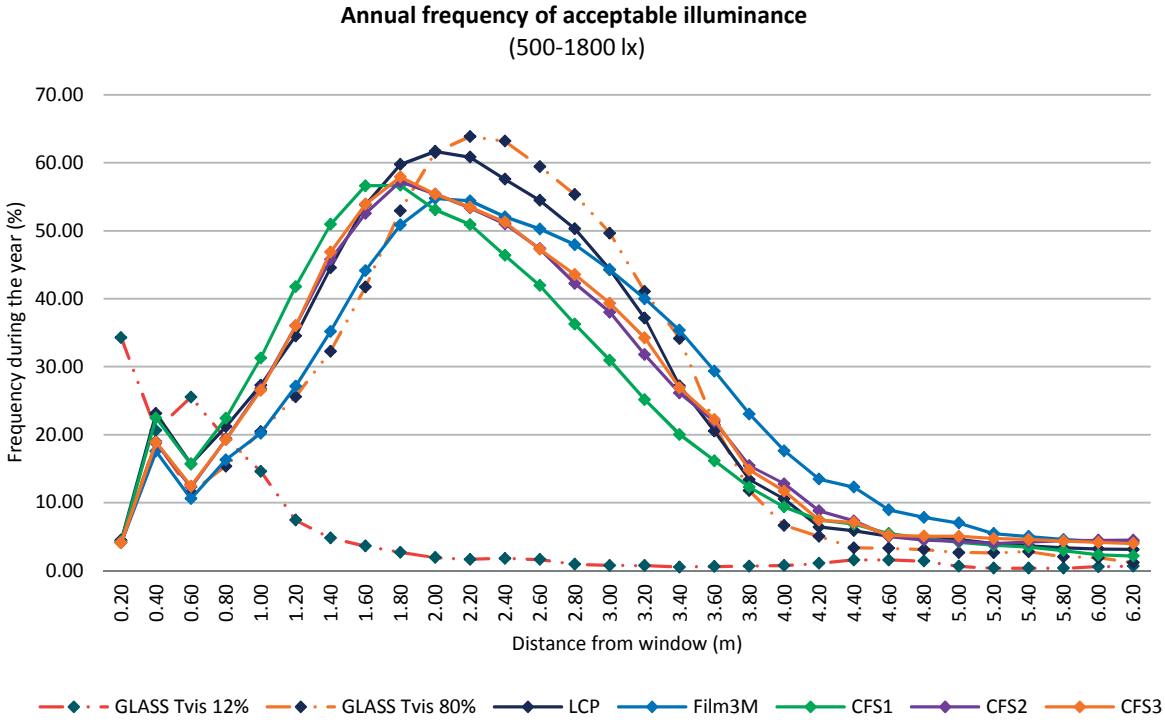

Figure 4.4 Annual frequency of illuminance in the range of 500-1800 lux occuring in the office room of Building B1.

When assessing the frequency of large and risky illuminance (>2000 lux) found in a year for the office room of Building B1 (Figure 4.5), one can observe that such range occurs about 65 to 75% of the yearly working hours at a distance of 0.2 - 0.6m from the window for all CFS as well as the standard glazing (τv 80%). In the case of the current tinted glass, such illuminace range is observed only during 8 to 15% of the yearly working hours at a distance of 0.2 - 0.4m from the window.

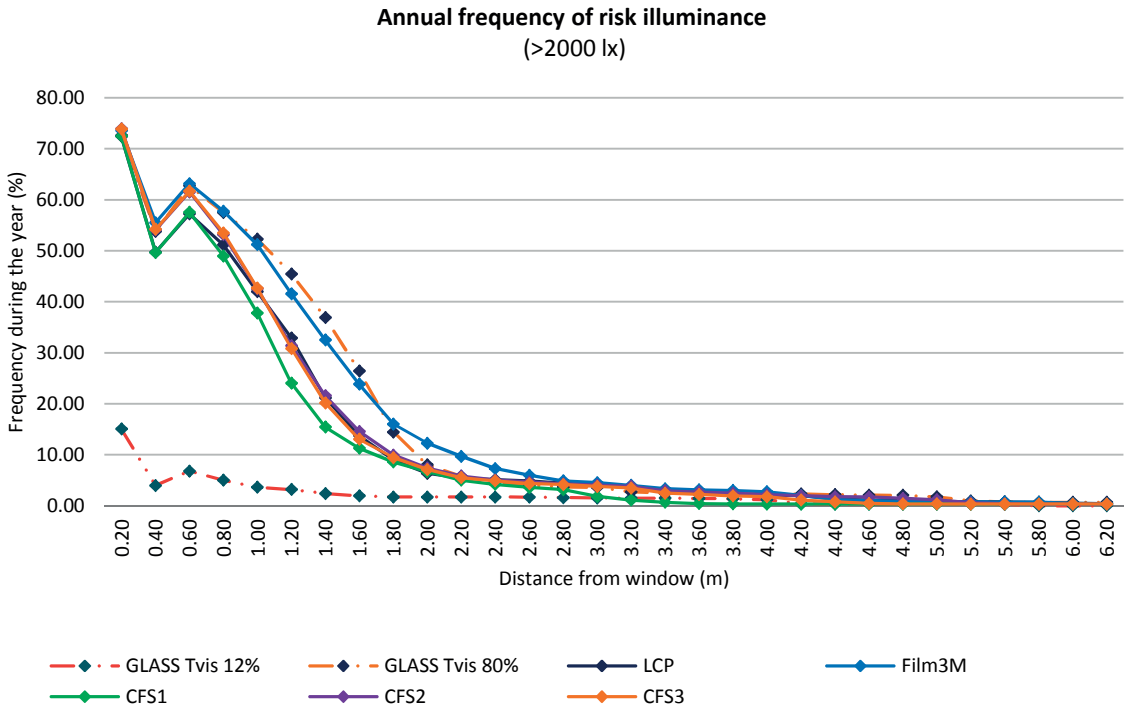

Figure 4.5 Annual frequency of illuminance in the range above 2000 lux occurring in the office room of Building B1.

The frequency of illuminance was then assessed focusing on specific situations in order to compare the improvement of the spatial distribution of the daylit zones in the office rooms that might be more representative of such illuminance range. Thus, the target illuminance (300-500 lux) was examined at the back of the room, while the risky illuminance range (> 2000 lux) was scrutinized next to the window during winter and summer time periods.

The frequency of the target illuminance at the back of the room for winter and summer time is presented in Figure 4.6 and 4.7 respectively. It can be observed that the use of a standard glazing (τv 80%) allows a higher frequency of the target illuminance in winter time reaching almost 25% of the working hours, while the CFS1 shows the lowest but steady performance through the room. In summer time the use of Film 3M shows higher frequency of the target illuminance through this area. LCP and the standard glass τv80% show a higher performance only in the centre of the room, while the CFS1 shows the lowest performance reaching only 17% of the working time at the centre of the room (at 4.2m distance from the window), and the lowest also at the back of the room.

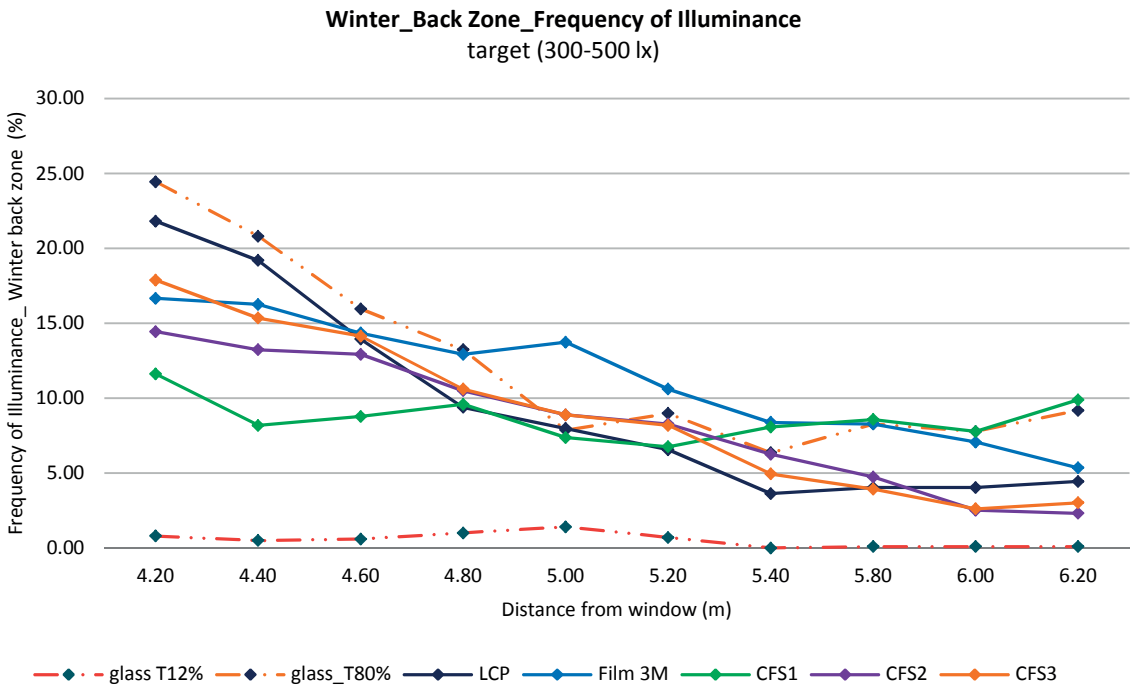

Figure 4.6 Frequency of the target illuminance (300-500 lux) occurring in Winter Time at the back of the room for Building B1.

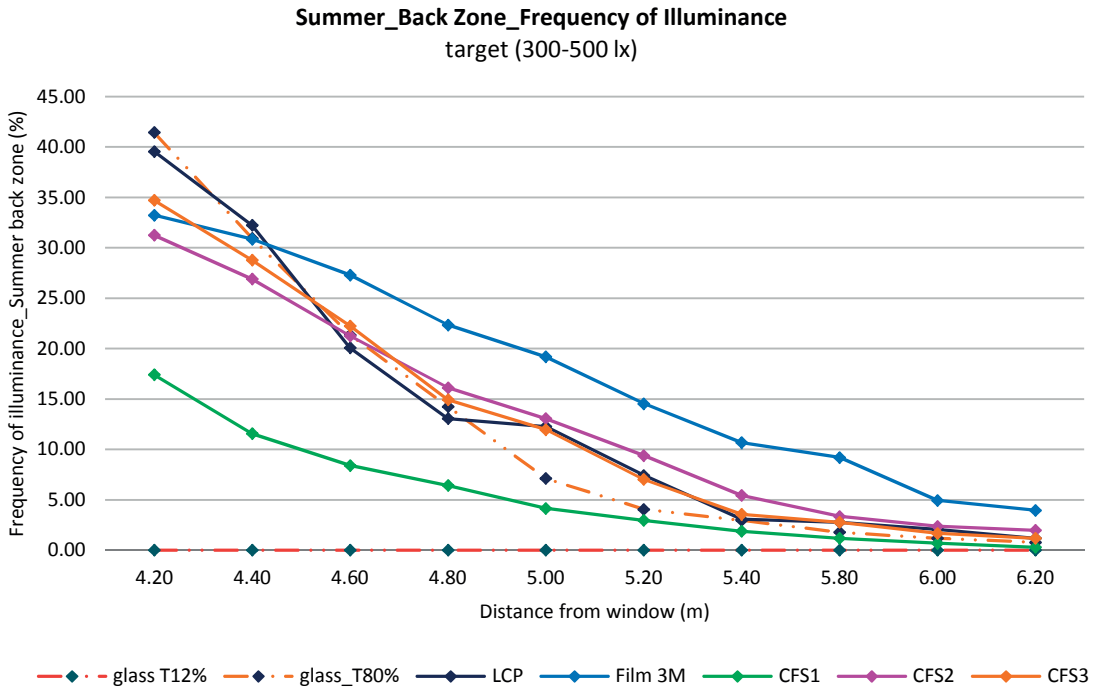

Figure 4.7 Frequency of the target illuminance (300-500 lux) occurring in Summer Time at the back of the room for Building B1.

The results of the risk Illuminance range (>2000 lux) for the area next to the window in winter and summer time are presented in Figure 4.8 and 4.9 respectively. In both graphs, a similar performance of the fenestration systems is found. The highest value for the yearly working hours (68-75%) of risky illuminance is achieved by four of the five CFS as well as the standard glazing at 0.2m from the window; across the room the standard glazing shows such levels of illuminance during a larger fraction of the year. However, when using CFS1 illuminances larger than 2000 lux are prevalent across the whole room during less time than the other CFS.

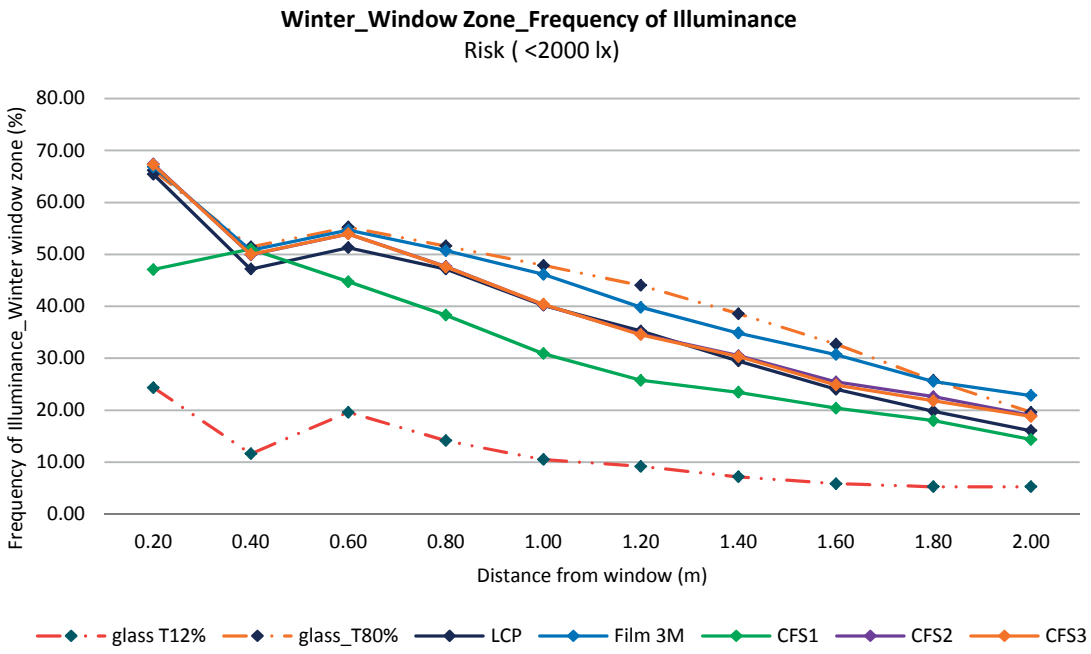

Figure 4.8 Frequency of the risky illuminance (> 2000 lux) occurring in Winter Time in the area next to the window for Building B1.

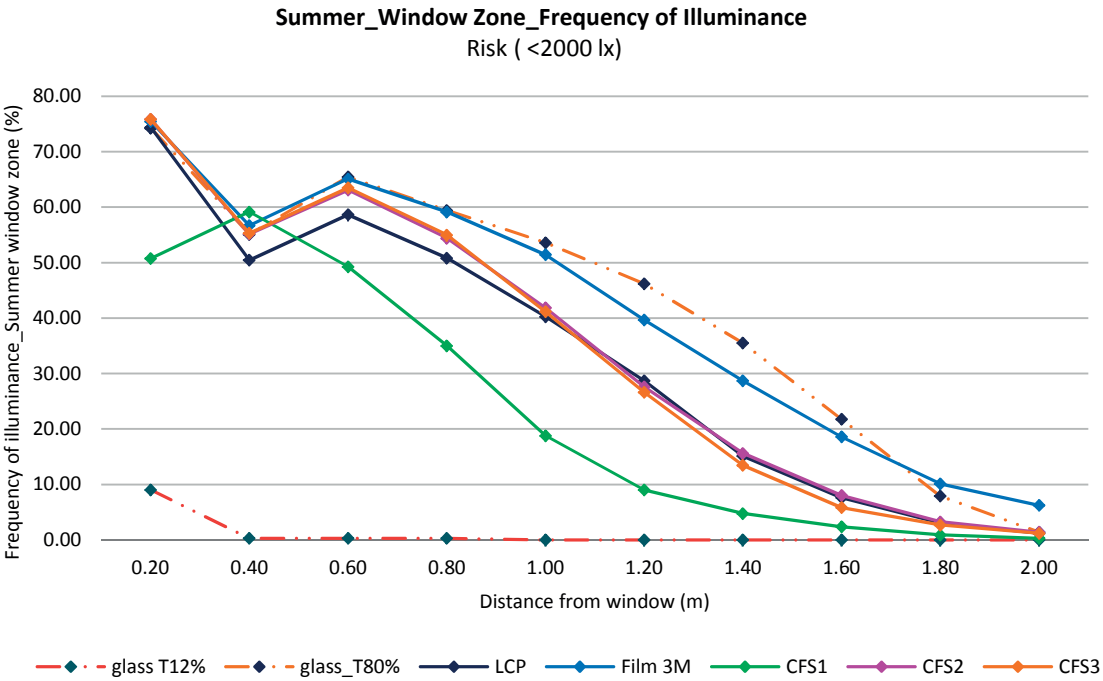

Figure 4.9 Frequency of the risky illuminance (> 2000 lux) occurring in Summer Time in the area next to the window for Building B1.

b) Illuminance Cumulative Plots

Cumulative plots were created in order to compare the daylight distribution performance of CFS in annual basis. Such plots indicate the proportion of the year that the cumulative illuminances are available inside the room, the results obtained for all the fenestration systems compared in each building in three diferent areas of the room (next to the window, center and back of the room) are presented in order to compare their performance. However, the results obtained in the calculation of the frequency of illuminances presented in this section (4.1.1 and 4.1.2) were those taken into account for the overall performance assessment of CFS presented in section 4.3.

The cumulative curve plots were assessed in three different locations in the office rooms: i) at 0.2m from the window, ii) in the centre of the room at a distance of 3.6m and iii) at the back of the room at 6.2m from the window. The assessment was performed, as previously, considering the three yearly periods of winter, spring and summer time. However, such results can be considered as being representative of an annual behaviour if one that the autumn solstice is comparable to spring regarding the sun course.

The results obtained for Building B1 at a distance of 0.2m from the window are illustrated on Figure 4.10, which results are shown for a maximum of 6000 lux. It shows that when using CFS2, CFS3 and Film 3M daylighting is available over the year for a larger fraction of the working hours compared to a standard glazing (τv 80%) and to LCP (which are slightly below CFS1). It is clear that next to the window, illuminance values above 2000 lux would be available during slightly longer periods using the Film 3M, CFS2 and CFS3. In order to compare the results with the current situation, the existing tinted glass (τv 12%) was considered showing that a recommended range of 300 to 500 lux would be available only during a maximum of 60% or the yearly working hours in this case, implying the use of electric light for more than 40% of the period. As a matter of comparison, at this part of the room the range of illuminance below to 50 lux would correspond to a 20% of the working time when using the tinted glazing, and to a 16% when using the standard glass τv 80%.

The results that show the daylight availability in the middle of the room (at 3.6m distance from the window) are shown in Figure 4.11. It can be observed that when using LCP and a standard glazing glass (τv 80%), the illuminance range from 300 to 500 lux would be available for a maximum of 60% of the yearly working hour; such range of illuminance would be achieved by CFS1 for a maximum of 54% of the time. Such percentage (53%) is reached by the tinted glazing (τv 12%) only up to 100 lux workplane illuminance. Values of about 500 to 1000 lux are available during a longer fraction of the year for the Film 3M (27% and 7% respectively); CFS1 showed to be the system that provides daylighting in the middle of the room for shorter periods. In order to compare, the range of illuminance below 50 lux would be available in this area of the room for about 47% of the working time when using the tinted glazing, and 22% when using the standard glass τv 80%.

Results at the back of the room are given in Figure 4.12, which results are presented for a maximum of 2000 lux. The Film 3M offers workplane illuminance in the range of 300-500 lux for about 16% to 5% of the yearly working hours respectively, while the other systems provide slightly lower yearly fractions (9 and 3% in the case of CFS1). The opposite performance is achieved by the standard glazing (τv 80%) which achieves lower illuminance leves for longer time and higher illuminance for shorter time. The tinted glass maintains a very dark luminous environment in this area, where it would only allow a maximum of 100 lux for about 5% of the yearly working hours and in the range from 300 to 500 lux only for about 0.7% of the working year. In this part of the room the range of illuminance below 50 lux would correspond to the 95% of the working year when using the tinted glazing and to a 25% when using the standard glass τv 80%. The latter value is exceeded for a maximum difference of 3% when compared with the performance of the CFS.

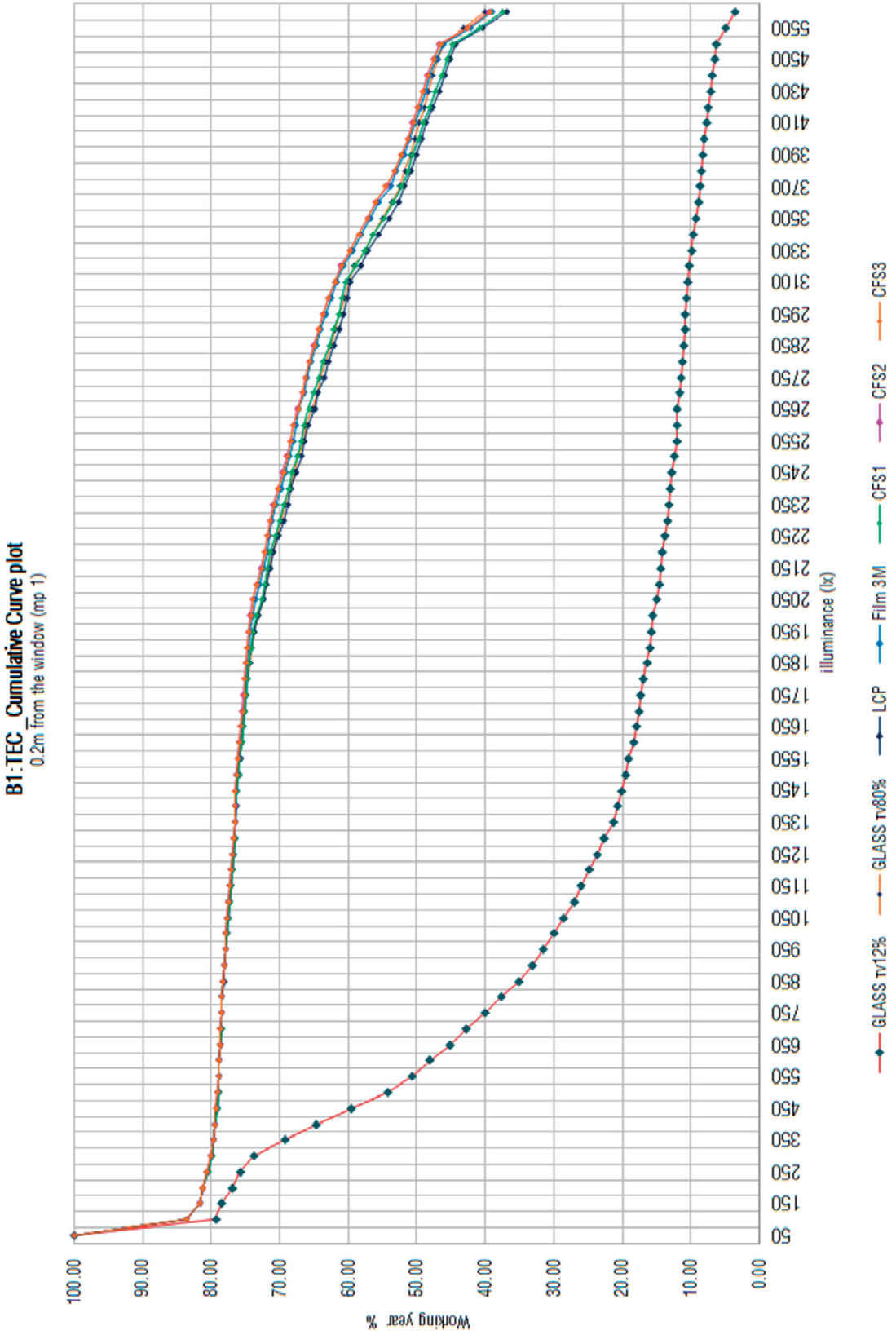

Figure 4.10 Cumulative daylight Illuminance of the office room located in Building B1 at a distance of 0.2m from the window.

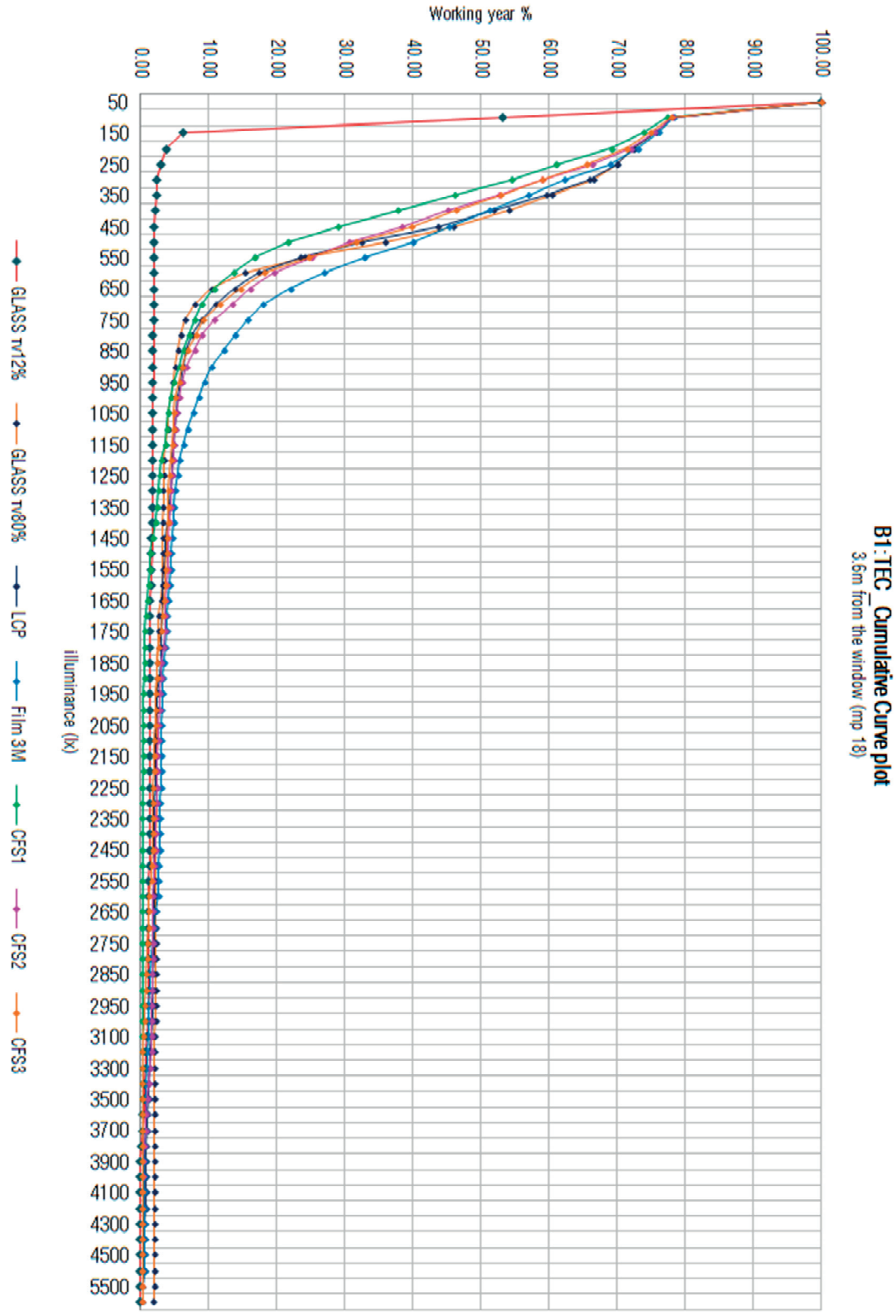

Figure 4.11 Cumulative Plot of the office room located in Building B1 at a distance of 3.6m from the window.

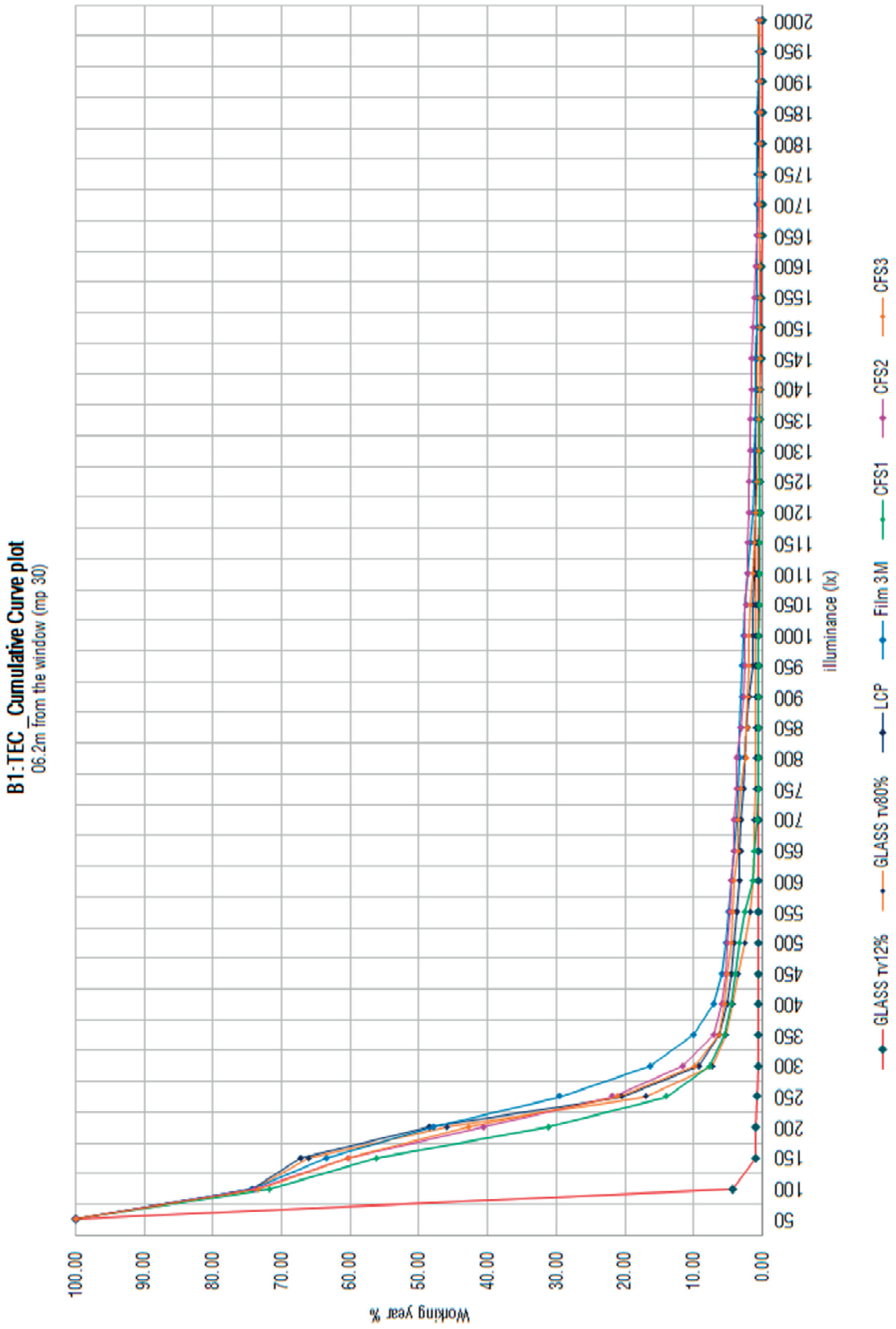

Figure 4.12 Cumulative Plot of the illuminance in the office room located in Building B1 at a distance of 6.2m from the window.

4.1.1.2 Building B2

a) Illuminance Frequency

The evaluation of the luminous performance of the CFS and the standard glazing in in the office room of Building B2 are presented first. As shown in Figure 4.13, the Annual Illuminance Frequency within the range of 300-500 lux is concentrated at the half back of the room. It can be observed that for this range a better performance is shown by CFS1, which provides with daylighting in the room during a larger annual portion of the working hours; the standard glazing (τv 70%) provides with a corresponding lower fraction of the working hours in the room.

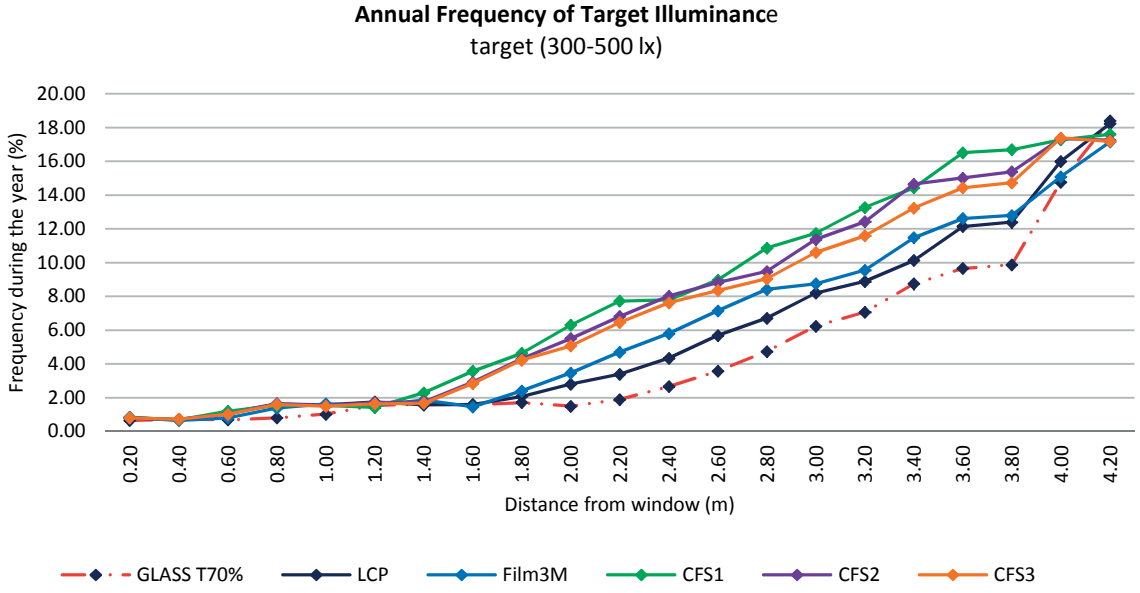

Figure 4.13 Annual frequency of illuminance within the range of 300-500 lux in the office room located in Building B2

The daylighting performance of CFS within the of acceptable illuminance range (500-1800 lux) are given in Figure 4.14. They show that CFS1 redirects daylight in such a range during a longer period of the working hours in the middle of the room (e.g. about 40% at a 2.0m distance from the window). However, it presents a slight mitigation at the back of the room, unlike the rest of the CFS and the standard glazing. At the back of the room, such illuminance is most frequently present with the standard glazing (τv 70%) and the LCP.

The range of illuminance that is larger than 2000 lux representing risks of glare or overheating for the office occupants is given on Figure 4.15. The latter shows that such a range would be present during a longer portion of the yearly working hours for the Film 3M (close to the window) and the standard glazing (in the centre of the room). The shorter period in which such illuminance range would be available across the room is achieved by the CFS1.

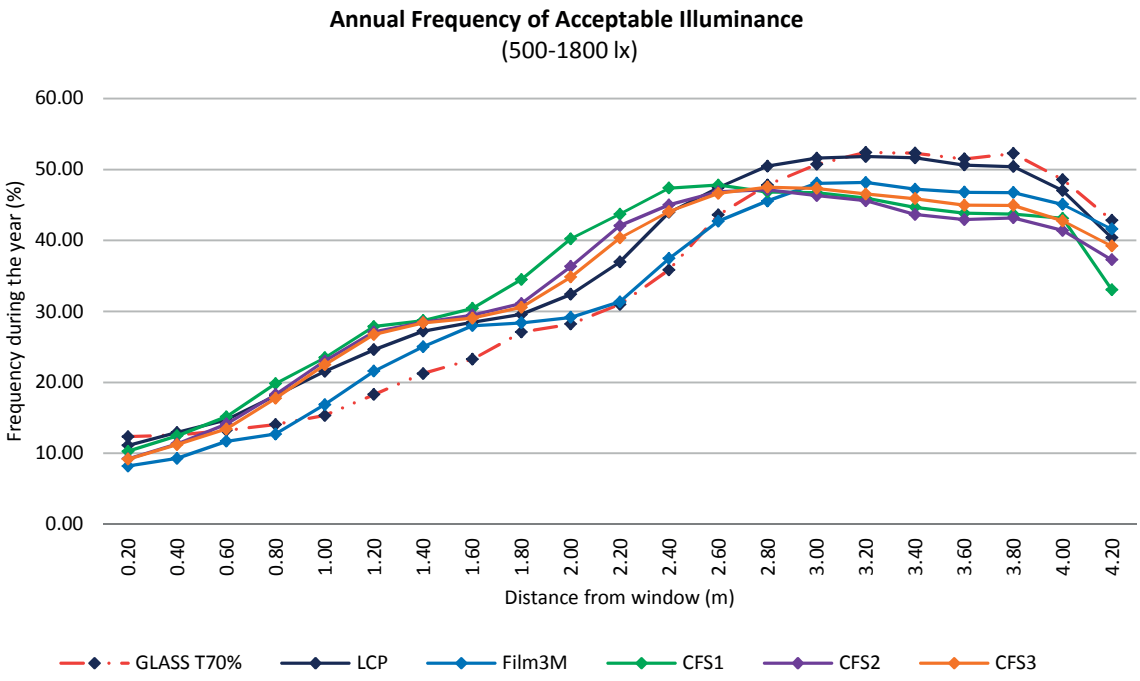

Figure 4.14 Annual frequency of illuminance within the range of 500-1800 lux in the office room located in Building B2.

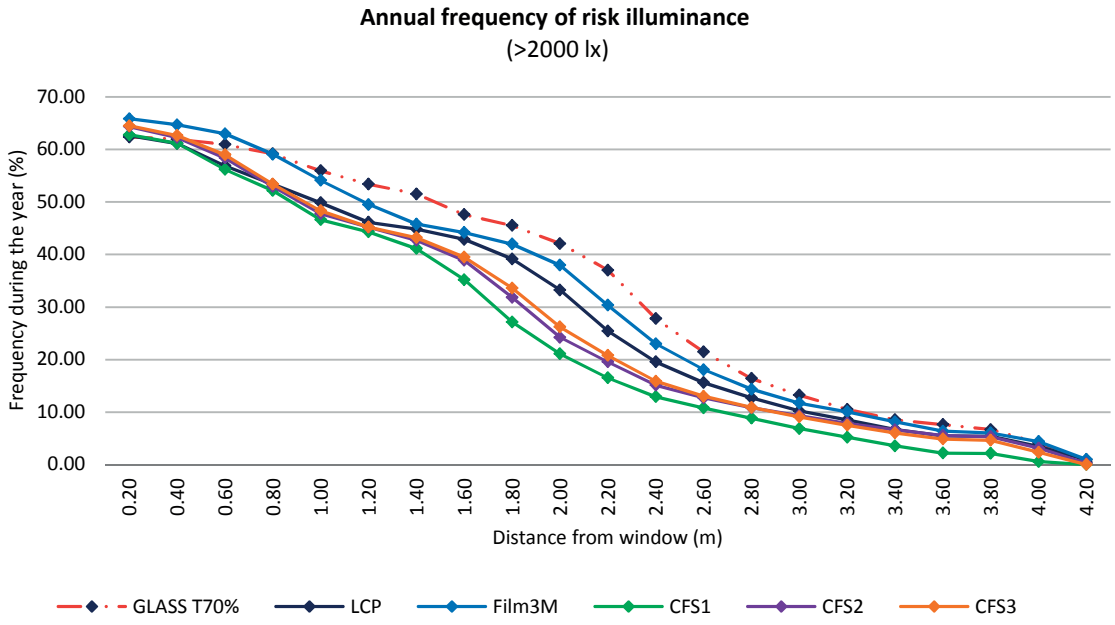

Figure 4.15 Annual Frequency of illuminance above 2000 lux in the entire office room located in Building B2.

Focusing on specific situations, the performance of CFS in providing illuminance within the range of illuminance from 300 to 500 lux at the back of the room are presented in Figure 4.16 for winter time and 4.17 for summer time. It can be observed that in winter a better performance is offered by CFS1, which allows the admission of daylight during a larger portion of the working time in the back of the room; the standard glazing (τv 70%) provides daylighting during less time over the year.

In Summer time which results are shown in Figure 4.17, a sound performance is achieved by CFS1 and CFS2, allowing the admission of daylight in the back of the room for longer periods comparing to the standard glazing. At the back of the room CFS1, CFS2 and CFS3 as well as LCP show a similar fraction close to 20% in which such range of illuminance would be available; Film 3M and the standard glass (τv 70%) are slightly below that value.

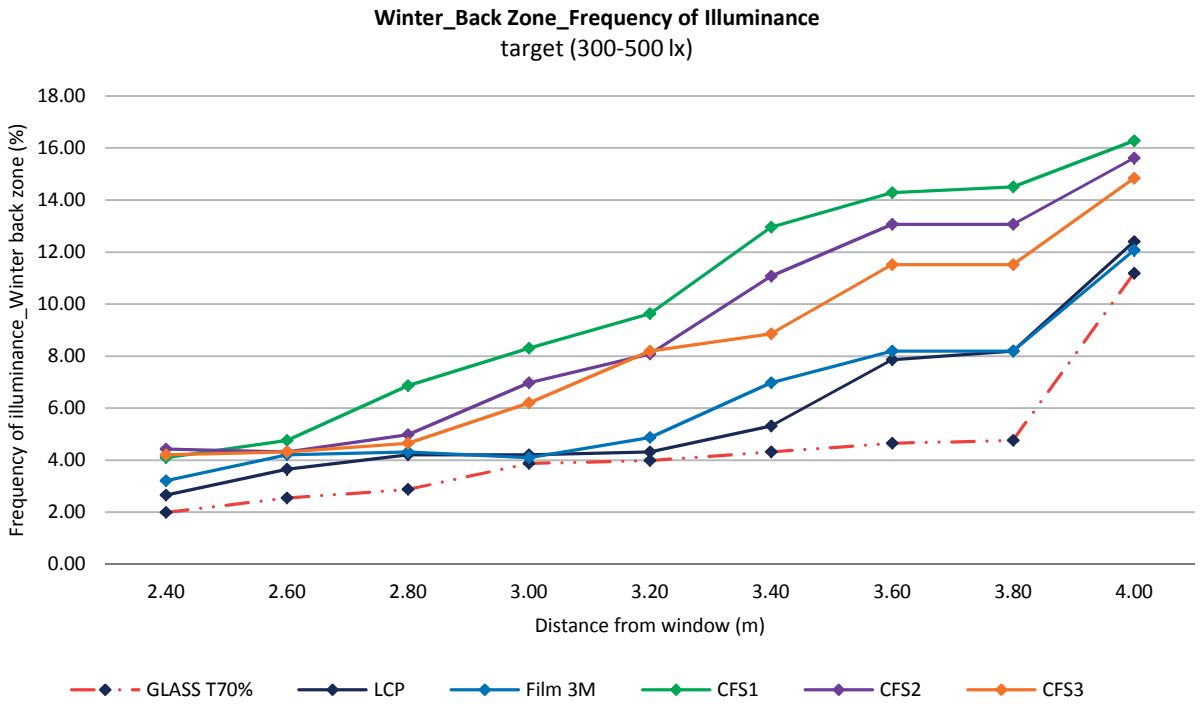

Figure 4.16 Frequency of daylight illuminance within the range of 300-500 lux in the back of the room of Building B2 during Winter time.

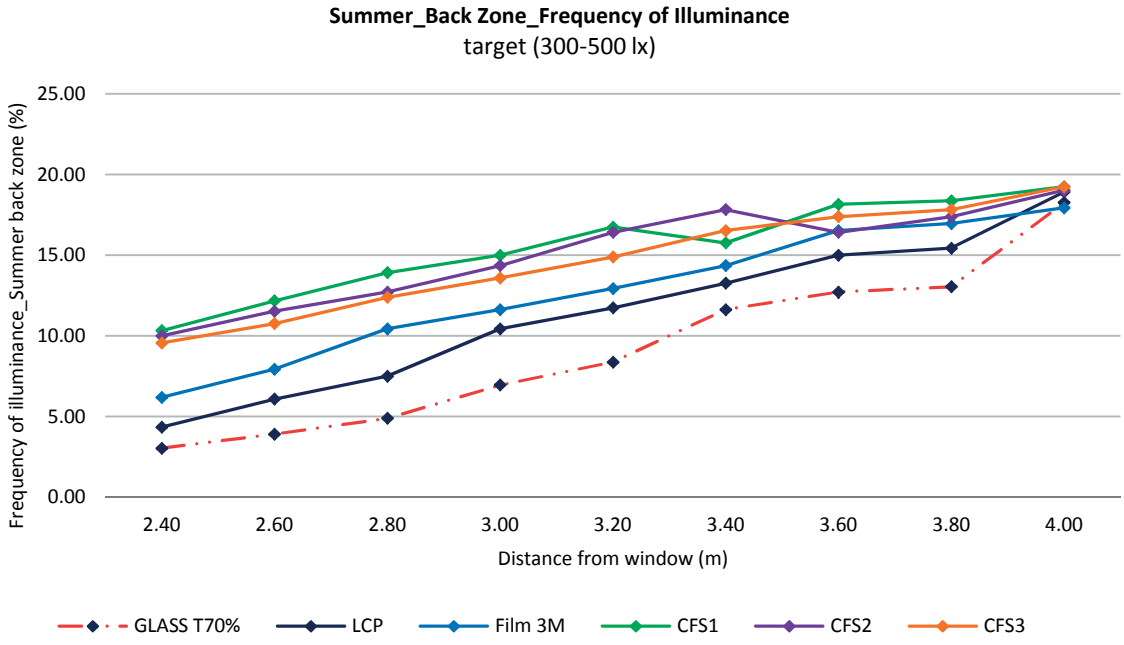

Figure 4.17 Frequency of daylight illuminance within the range of 300-500 lux in the back of the room of Building B2 during Summer time.

The results obtained when assessing illuminance larger than 2000 lux in the area close to the window are presented in Figure 4.18 for winter time. They show that the use of a standard glazing and the Film 3M would bring such range of illuminance during longer time in the year (above 65% at about 0.60m from the window). While CFS1, CFS2, CFS3 and LCP showed a comparable performance across the room.

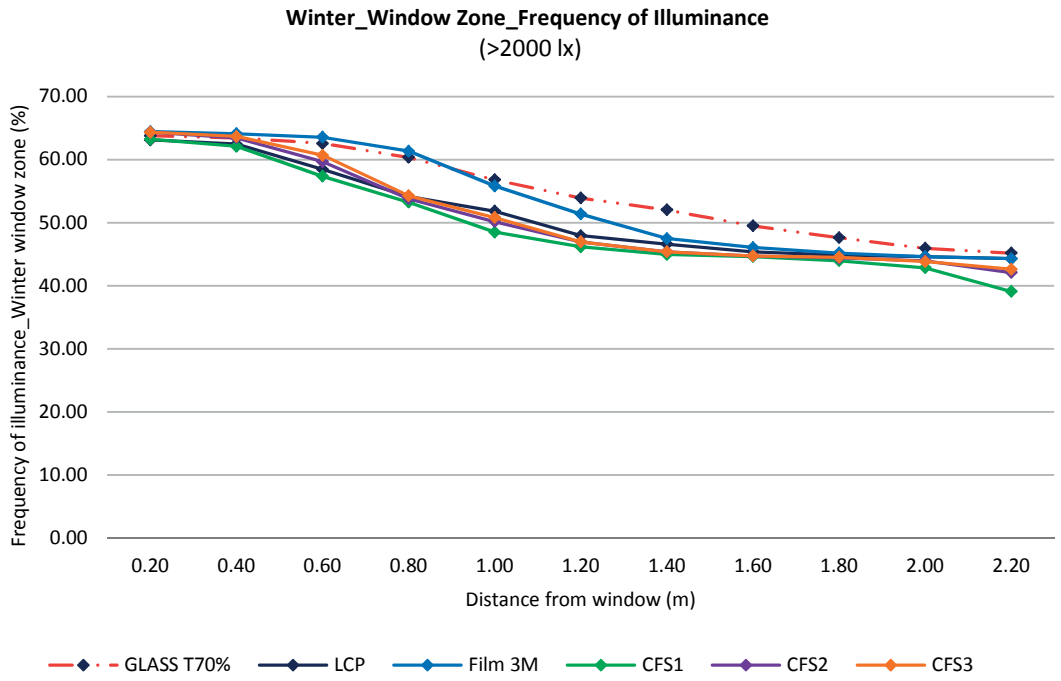

Figure 4.18 Frequency of daylight illuminances above 2000 lux in the area next to the window for Building B2 during winter time.

The frequency of daylight illuminance in Summer time next to the window was assessed considering the range illuminance above 2000 lux; the results are shown in Figure 4.19. This was done in order to identify the CFS that might contribute to increase the risk of glare or overheating in Building B2. The results show that at a distance of 0.2 from the window close to 70% of the annual working time would see illuminance larger than 2000 lux using Film 3M. Slightly lower values are achieved by CFS3 and CFS2, while using LCP and CFS1: the proportion is closer to 60%. The standard glazing (τv 70%) provides such illuminance values during longer periods across the room. While CFS1 shows an opposite behaviour, providing with illuminance in a range that represents glare risks for the occupants for the shortest period of the working time, compared with the other CFS.

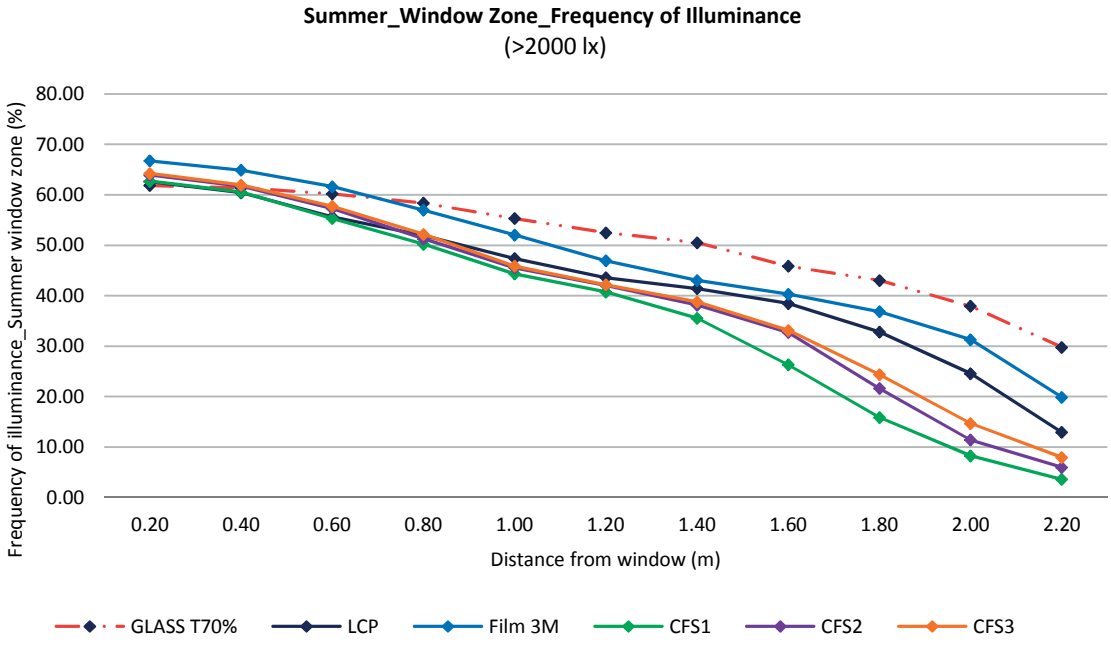

Figure 4.19 Frequency of daylight illuminance above 2000 lux in the area next to the window in the office room of Building B2 in Summer time.

b) Illuminance Cumulative Plots

For Building B2, illuminance cumulative plots were assessed for three different locations in the office room: at 0.2m from the window, in the centre of the room (at a distance of 2.2m) and at the back of the room (at distance of 4.2m from the window). Figure 4.20 shows the cumulative illuminance next to the window, showing that a range of illuminance between 300 and 500 lux is available for a fraction of about 78% of the annual working time with a little difference between the compared fenestration systems. For an illuminance range between 1000 to 2000 lux a higher percentage of the working year would be achieved by the Film 3M (from 65% to 72%), and the less when using the standard glass τv70% (between 62 to 73%). Such tendency is maintained for also for higher illuminance levels. In order to compare, illuminance levels below 50 lux are achieved by the 19% of the working time when using the existing situation (glass τv70%).

In the centre of the room (Figure 4.21), the standard glazing (τv 70%) would provide an illuminance range of 300-500 lux for about 73% of the yearly working time and during a lower fraction for CFS1 (67%). The difference in the performance between the standard glass and the CFS is more visible regarding higher Illuminance levels, for those between 500-1800 lux the stardard glass would achieve 73% and 40% respectively, LCP 69% and 26% while CFS1 64% and 17% being the one achieving the shortest period of time within such range. For illuminances above 2000 lux clearly the standard glass would achieve such range for longer time while CFS1 is the CFS which use would imply a reduced risk of glare and overheating in this room. In this area, illuminances below 50 lux are available for about 21% of the time when using the standard glass, with an increased difference of maximum 2% when using the CFS.

The results obtained at the back of the room at a distance of 4.2m from the window are presented in Figure 4.22. They show that a range of illuminance of 300 to 500 lux would be provided for about 66% and 45% respectively when using the stanrdard glass, the use of CFS would represent 64% and 42% of the time, with close results betwee LCP and Film 3M. Such tendency is prevailed for higher illuminance levels, for those between 500 and 1000 lux a difference of 10% to 5% is found betwee the stardard glass and the CFS1 which is the one allowing such range illuminane during shorter periods of time, thus contributing better to the glare and overheating prevention. Illuminance values below 50 lux are found for about 24% of the working year when using standard glass with a maximum difference of 1% when using CFS.

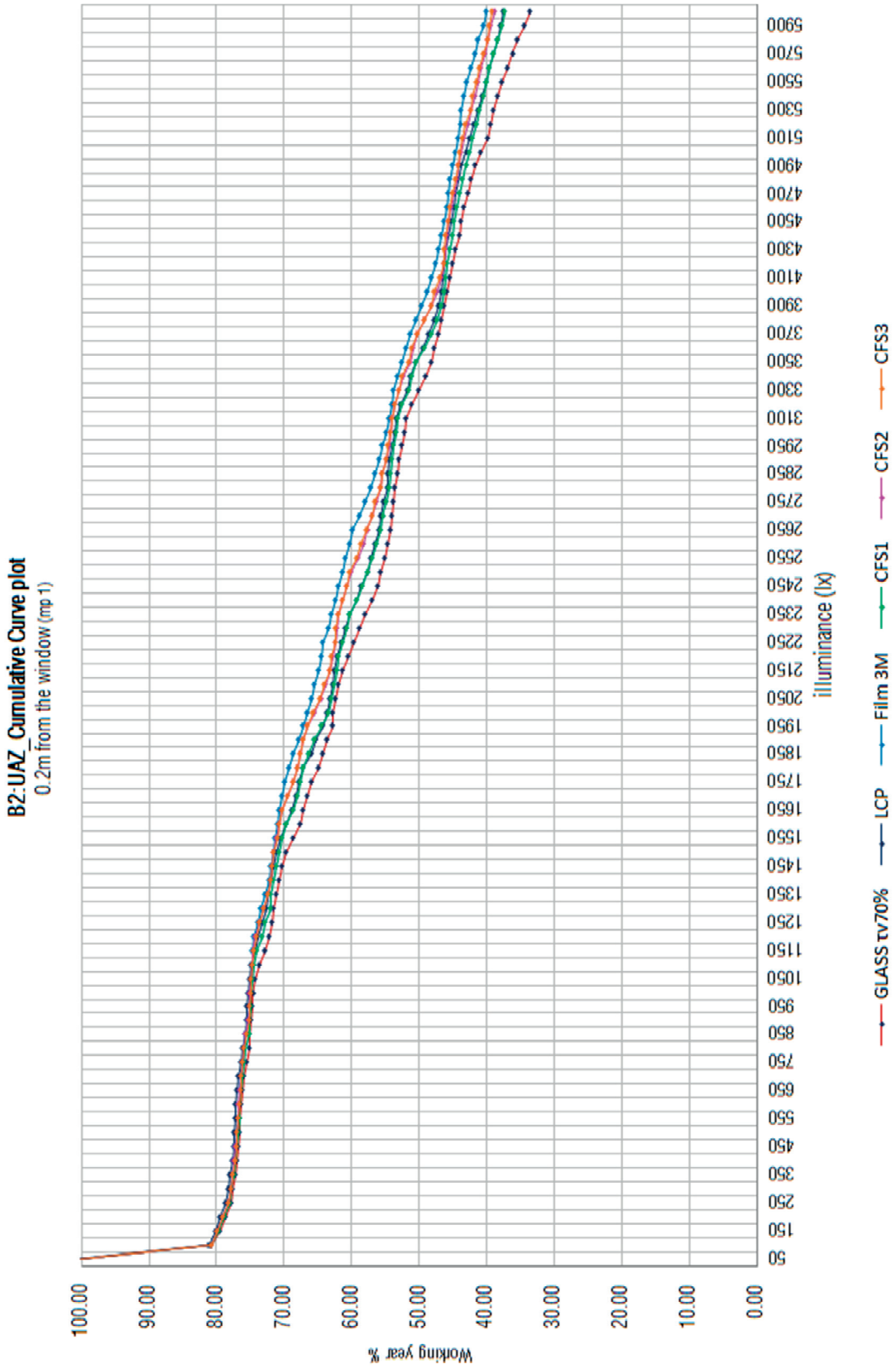

Figure 4.20 Cumulative Cumulative Plot of the daylighting illuminance in office room located in Building B2 at a distance of 0.2m from the window.

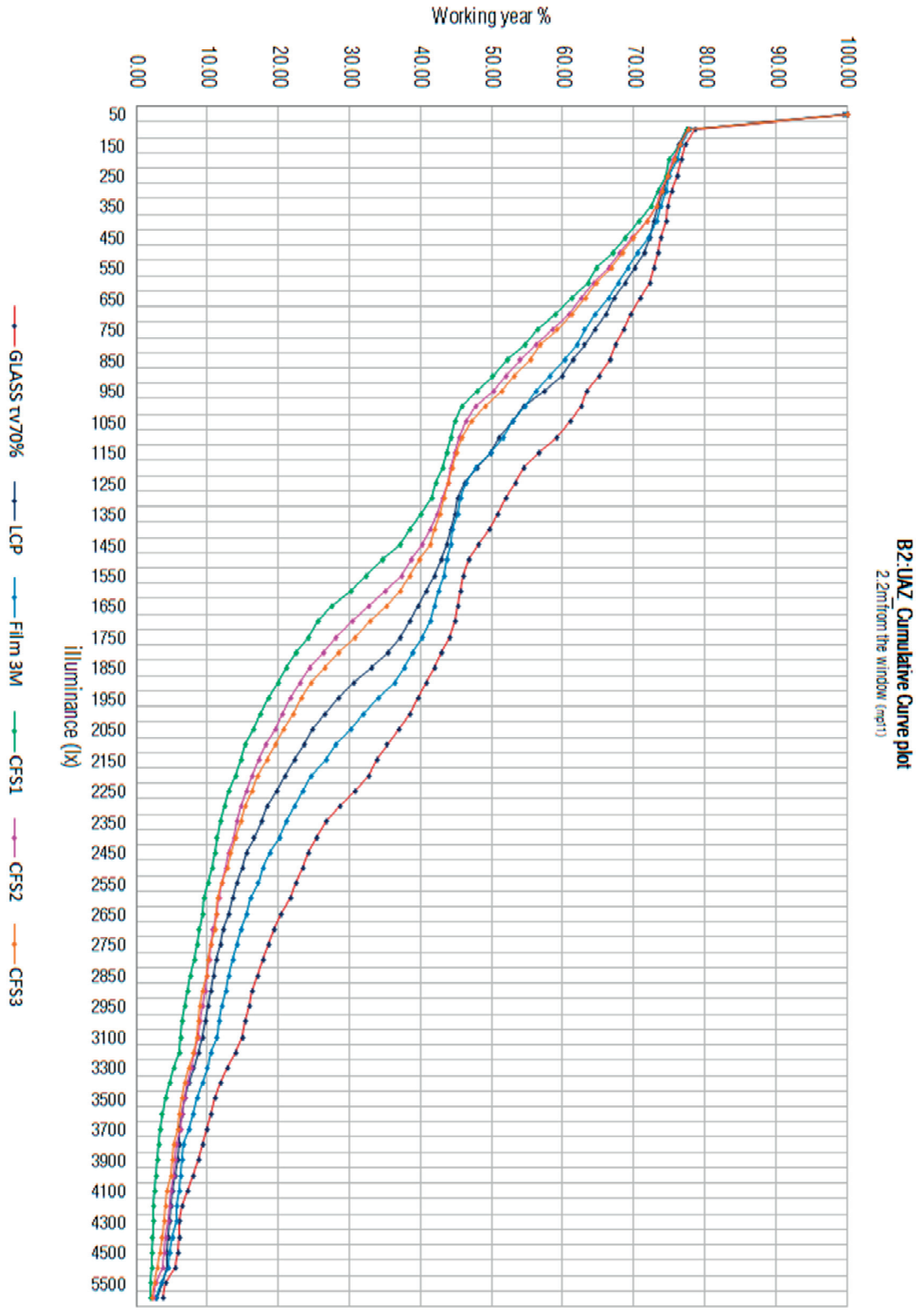

Figure 4.21 Cumulative Plot of the illuminance occurring during the working year in in Building B2 at a distance of 2.2m from the window.

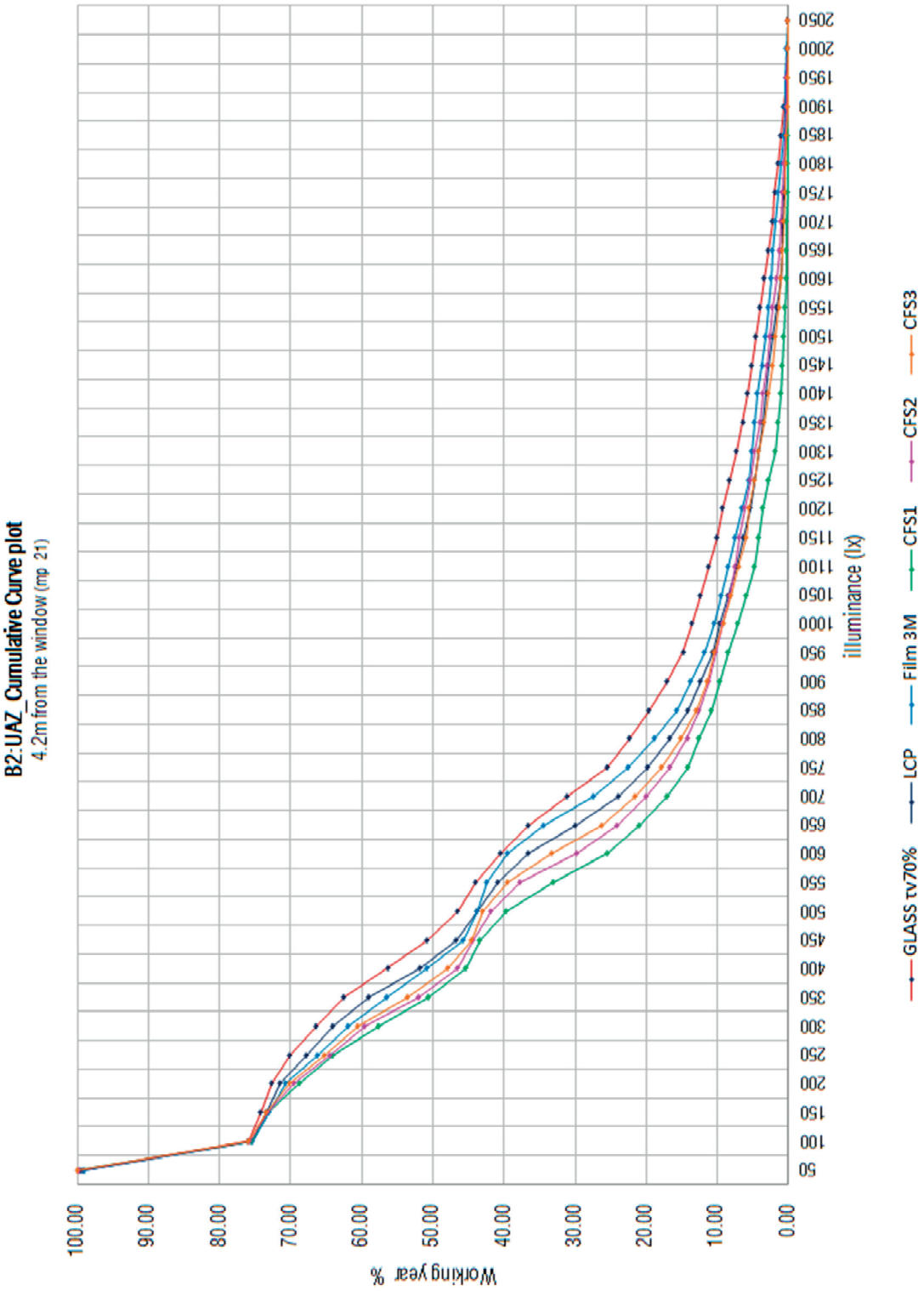

Figure 4.22 Cumulative Cumulative Plot of the illuminance occurring during the working year in in Building B2 at a distance of 4.2m from the window.

c) Five-phase method renderings

Renderings were generated using the Five-phase method for each of the three terms of the simulation process; they are combined at the end in order to create a visual rendering that represents the daylight propagation through CFS into the room. Thus a rendering is generated first to determine the indoor daylight distribution, and then a second term is generated after subtracting the direct sun contribution, a third rendering is generated subsequently to obtain a more accurate simulation of the direct sun component; the three terms are combined in a final image that reproduces a very accurate daylighting simulation. An example of these renderings obtained for Building B2 is shown in Figure 4.23; it illustrates the three-term-process that constitutes the five-phase method. The rendering obtained when calculating the interior daylight distribution in the first term of the five-phase method is shown first (left), secondly the rendering that represents the subtracted direct solar contribution in the second term (second left), subsequently the rendering representing a more accurate calculation of the direct solar contribution (second right), and finally the image combined representing the result of the whole process (right).

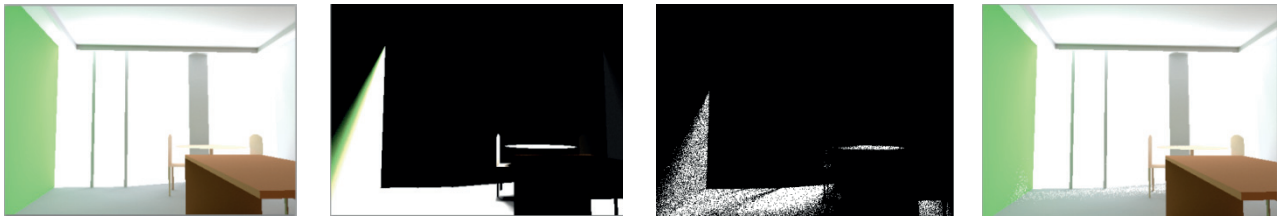

Figure 4.23 Renderings Renderings obtained during the three terms process of the five-phase method applied for Building B2.

Using this process, a total of 8760 images of each hourly time-step were generated for each term of the five-phase method. The final images were integrated in single ones to represent a full season in order to facilitate the interpretation of these data. Arranged in an array of 10 x 9 images the blend representing the daylighting situations occurring in Building B2 during winter and summer time are shown in Annex 4.1.

4.1.2 Overall assessment

In order to identify the CFS providing with larger illuminance in the two office rooms over the year, average daylight illuminances occurring in winter, spring and summer time were calculated for each room zone (window area, centre and back of the room). However, due to space restrictions and in order to carry-out the assessment according to the proposed strategy, only the winter and summer time results are shown in this chapter.

The average illuminance occurring in winter time in Building B1 is presented in Figure 4.24. They show that higher illuminance is found in the three zones for the standard glazing (τv 80%). The Film 3M follows showing a better performance than the other CFS in the area next to the window and in the centre of the room; at the back of the room, LCP and Film 3M show similar results, while the CFS1, CFS2 and CFS3 provides with the lower illuminance in this area. The results obtained when using the existing tinted glass are also shown for sake of comparisons. The average daylight illuminance occurring in summertime is presented in Figure 4.25. It shows a similar trend, larger daylighting illuminance are observed in the room with the standard glazing (τv 80%) next to the window. However in the centre of the room, higher illuminance are achieved with the Film 3M, while in the back of the room all CFS and the standard glazing (τv 80%) show similar performance. An overall assessment is presented in Figure 4.26, showing an average of the target illuminance range (300-500 lux) occurring in the entire room during winter time, as well as the average of the risky illuminance in summer time. Such results, show that a similar performance is achieved by almost all the CFS (except CFS2 and CFS3) and by the standard glazing (τv 80%) in winter time; in summer, the standard glazing and Film 3M allow a larger fraction of illuminance to lie above 2000 lux during the year.

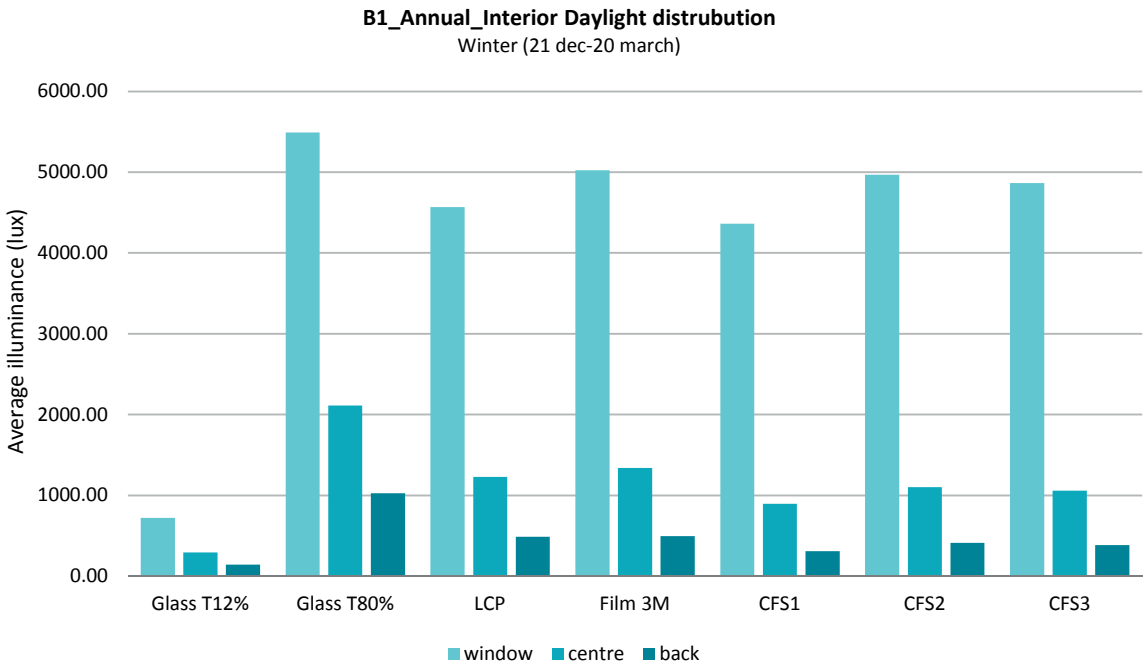

Figure 4.24 Average daylight illuminance achieved during Winter time by the CFS, the standard glazing (τv 80%) and the tinted glazing in Building B1.

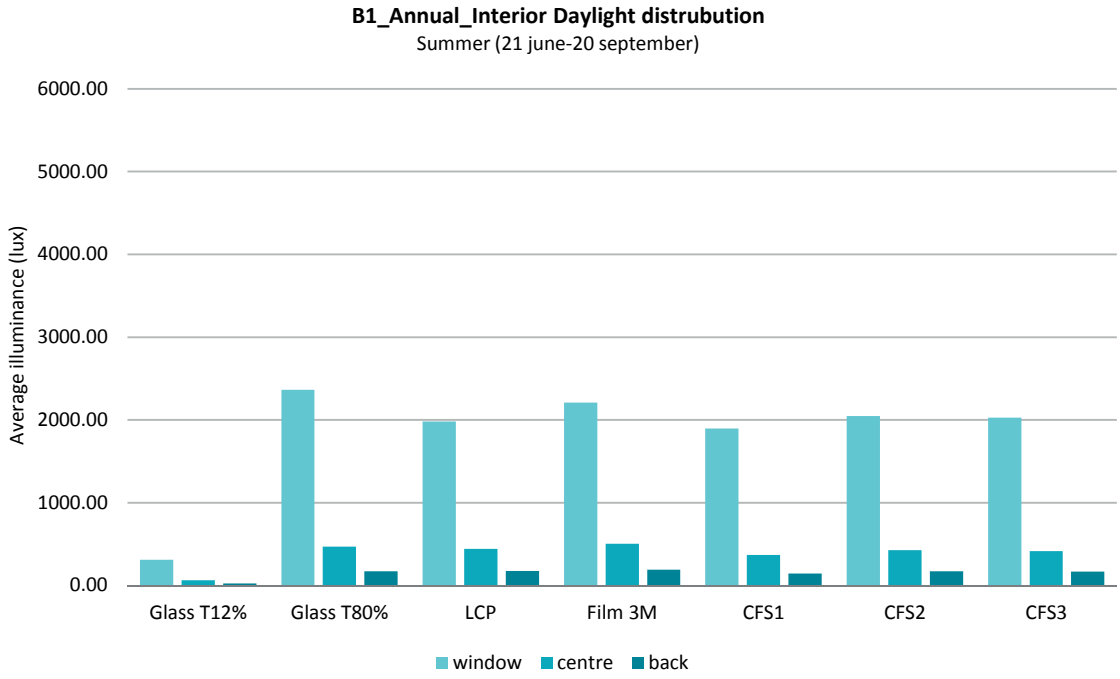

Figure 4.25 Average daylight illuminance achieved during Summer time by the CFS, the standard glazing (τv 80%) and the tinted glazing in Building B1.

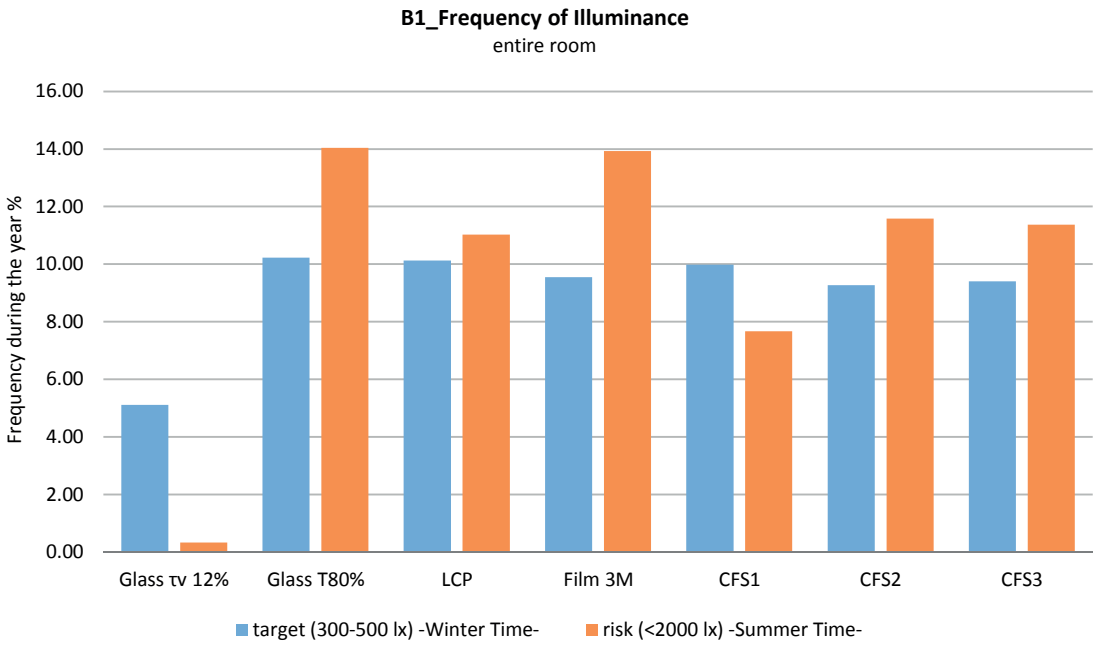

Figure 4.26 Average daylight illuminance achieved during Winter and Summer time by the CFS, the standard glazing (τv 80%) and the tinted glazing for the whole room of Building B1.

In the case of Building B2 and due to the size of the room, the area was divided in only two zones (window and back of the room). In winter time the larger average illuminance are achieved by LCP close to the window, and the lowest by CFS1. At the back of the room, the standard glazing which achieves the larger illuminance ranges, as shown in Figure 4.27. In summer time corresponding to Figure 4.28, similar ranges are achieved by the standard glazing (τv 70%) and by LCP, followed closely by the Film 3M. The lowest illuminances are achieved by CFS1, while CFS2 and CFS2 perform in a similar way. At the back of the room, a comparable situation is found, the highest ranges are achieved by the standard glazing, followed closely by LCP and Film 3M.

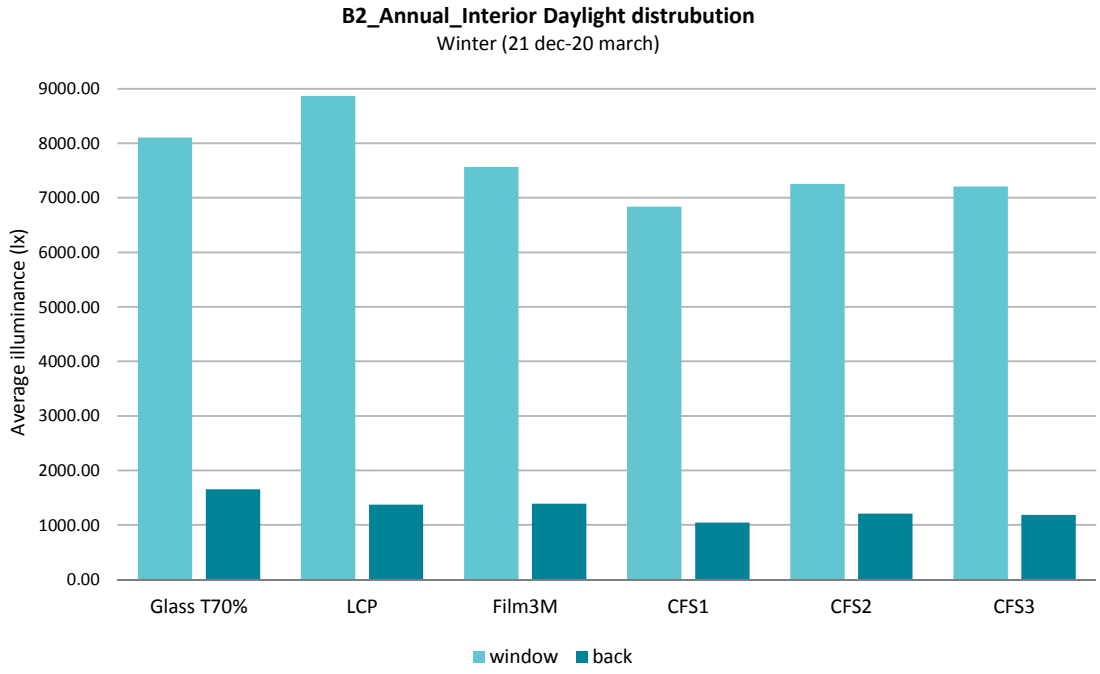

Figure 4.27 Average daylight illuminance achieved during Wintertime by the CFS, the standard glazing (τv 70%) in Building B2.

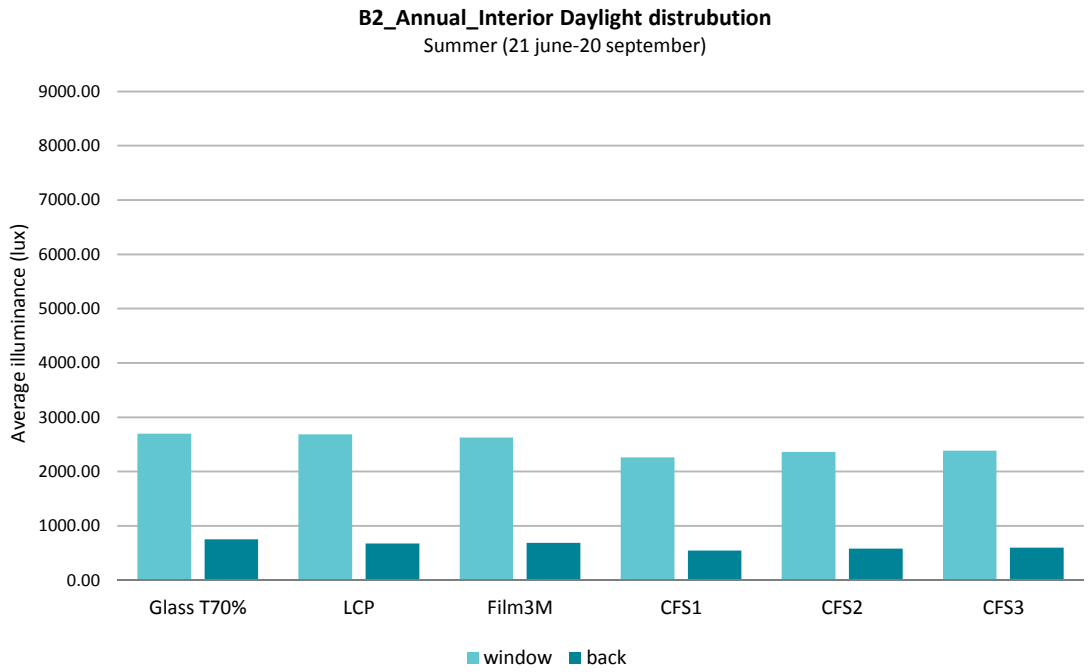

Figure 4.28 Average daylight illuminance achieved during Summer time by the CFS, the standard glass (τv 70%) in Building B2.

The overall assessment, which takes the target illuminance (300-500 lux) available during winter time for the entire room into account, as well as the risk illuminance range (> 2000 lux) available in summer time, is presented in Figure 4.29. It shows that in winter the target illuminance is more frequent in the room located in Building B2 for CFS1, CFS2 and CFS3, reaching around a fraction of 5% during the year. While for illuminance above 2000 lux, the standard glazing τv 70% and the Film 3M offer those levels into the room more frequently during the year.

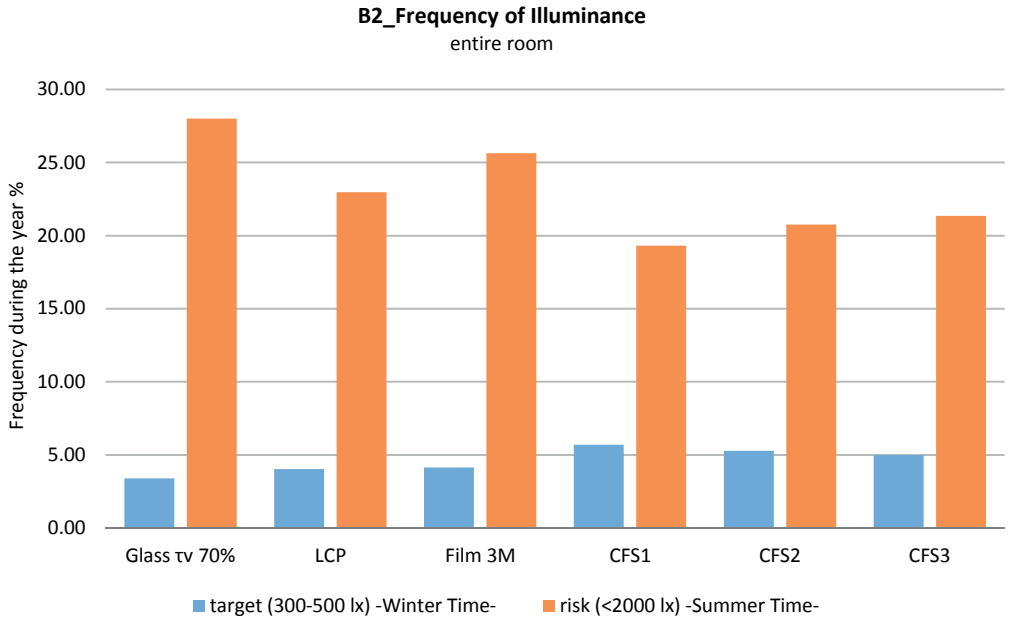

Figure 4.29 Average daylight illuminance achieved in Winter and Summer time through the entire office room of Building B2.

4.2 Annual assessment of thermal comfort using Energy Plus

As a result of the survey presented in Section 1.3.3, the Energy Plus software was selected to carry-out the thermal comfort assessment in the two office rooms: the latter allows using BSDF data to simulate the thermal impacts of CFS in buildings, a procedure that is not available for the other software considered in the survey. However, in the case of BTDF data of the CFS assessed in this PhD Thesis (monitored using a bidirectional gonio-photometer available at the LESO-PB/EPFL), an additional conversion was necessary; such procedure is explained as follows.

In order to assess the solar heat gains entering through the standard glazing and the five pre-selected CFS in the two office rooms and compare their performance, simpler virtual models were built as a first step using the computer programme Google Sketch-up. Then the definition of the thermal zones and the thermo-physical properties of the interior materials were assigned to the model and the desired output was set using the Open Studio plug-in for Google Sketch-up. Given that mainly the solar gains was of interest, and not the metabolic or electric appliances heat contribution, no luminaires or occupants were included in the computer model. The rooms were considered as single rooms setting the interior walls as 'adiabatic' in order to avoid the inclusion of additional loads from adjacent 'thermal zones' or from outdoor and to save time in the construction of the building model. The model was then converted to the Energy Plus input format (idf file), which was used to carry-out the simulations. The direct solar component was determined from measured direct normal irradiance issued from a weather file, while the sky diffuse component was determined using the Perez sky radiance distribution [140]. The weather file of the city of Zacatecas obtained with the software Meteonorm was used as an input to perform the thermal simulations in the two office rooms.

Energy Plus allows the use of BSDF data to simulate the performance of CFS regarding daylight distribution, thermal comfort assessment and the glare risks. Fenestration Systems are first created using Window 7 software and then converted to the Energy plus format (idf files). However, the Window 7 software bases its calculation of the CFS luminous transmission and reflection on the sky vault subdivision suggested by Klems [141] and does not support the Tregenza sky subdivision [58] corresponding to the format used in this PhD thesis (See Section 3.3.2). Therefore in order to be able to convert the BSDF data files that characterizing the five pre-selected CFS into the Energy Plus format, a preliminary conversion from the Tregenza angular system to the Klems system was necessary: this was carried-out using the *bsdf2klems* RADIANCE programme. An XML file was then created using the CFS-Klems converted files of LCP, CFS1, CFS2 and CFS3. An additional glass layer was added to the fenestration system to which the CFS was attached. The features of such glass layer were set according to those proposed in the daylighting strategies (See Section 3.1), thus for Building B1 the fenestration system had resulting transmittance of 80%, while for Building B2 the resulting transmittance was of 70%. In the case of the Film 3M, the sample available at LESO-PB/EPFL does not require a glass pane to be attached to. However, since the Window 7 software requires at least one glass layer to create a fenestration system, a glass layer with the largest possible visible transmittance was added to the Film3M-Klems file in order to create the idf Energy Plus input file. When creating the glazing system using Window 7, values of the temperature of the outer and inner surfaces of the glazing layers, the transmission and reflectance within the visible range, as well as the transmitted, reflected and absorbed solar energy are obtained as output. Thus, such are considered in the simulation of the transmitted solar energy inside the rooms, unlike the results obtained in Chapter 3 (Section 3.6) where the thermal comfort analysis made through the assessment of the transmitted solar energy into the room, was made using BTDF data that takes into account only the transmitted portion, neglecting the absorption in the calculation of the heat that is transmitted into the room.

The BSDF-idf converted files of the CFS were then imported into the Open Studio database and assigned to the upper part of the window of the office room in the virtual model. The computer simulations were carried-out taking into account only the upper part of the window assigned with the corresponding CFS or a standard glazing material; the lowest window was assigned a glass with zero transmittance in order to isolate the effects that the material (CFS or standard glass) assigned in the upper window might have in the room. The assessment was performed for an entire year.

4.2.1 Results

The results of the global solar heat gains (MJ/m²) obtained in Building B1 are illustrated on Figure 4.30. They show that larger solar gains are transmitted to the room with the standard glazing (τv 80%), the Film 3M is the CFS that would transmit the larger amount of solar energy into the room. For the other CFS, comparable results were obtained by CFS2 and CFS3; CFS1 is the one transmitting lower solar gains. As expected, the tinted glazing provides with lower solar gains into the room, comparable with those transmitted by CFS1. In the case of Building B2 (Figure 4.31), higher solar gains are transmitted into the room by the standard glazing (τv 70%), from the CFS the LCP and CFS3 are the ones that allow higher amounts of solar energy to get in, while CFS2 and CFS1 are the ones transmitting less solar energy into the room. A remarkable difference is observed when comparing the results obtained in the two buildings, since a maximum of 180 MJ/m² solar gains are transmitted in B1 when using the standard glass τv 80%, while in B2 the maximums of 57 MJ/m² is found when using standard glass with a relatively low transmittance (τv 70%). Due to different factors (building orientation and the higher proportion of WWR) higher solar gains transmittance would be expected in B2, however it has been found that the significant differences in the two buildings are due to the effect of the overhang. The results of a simulation carried-out in B2 when removing the overhang element in the virtual model are presented in Figure 4.32, where it can be observed an increment of the transmitted solar gains in B2 to above 200 MJ/m² with the use of the standard glass, which is higher than those obtained in B1 with a higher glazing transmittance.

In order to compare the ability of the analysed glazing systems in allowing the incident solar radiation into the room, their Solar Heat Gain Coefficient (SHGC) was obtained as an output of the software Energy Plus, which calculates the optical properties of the fenestrations systems using a spectral weighting data set derived from the ISO-9845 Global Norm [85]. SHCG is a property which refers to the glazing's ability to control solar heat gains. Such value indicates the fraction of incident solar radiation transmitted by the glazing, thus higher coefficient represents higher heat gains. Such comparison is presented in Table 4.2; it shows that in the case of Building B1 the lower fraction of solar radiation is transmitted by the tinted glass, while the higher is transmitted by the standard glass. In Building B2, the lower solar radiation is transmitted by the CFS1 and the higher by the glass τv 70%.

SHGC	Glass τv 12%	Glass τv 80% / 70%	LCP	Film 3M	CFS1	CFS2	CFS3
B1	0.34	0.72	0.52	0.69	0.38	0.48	0.47
B2	-	0.64	0.51	0.45	0.40	0.47	0.48

Table 4.2 Solar heat gain coefficient of each fenestration system in Building B1 and Building B2, obtained from Energy Plus.

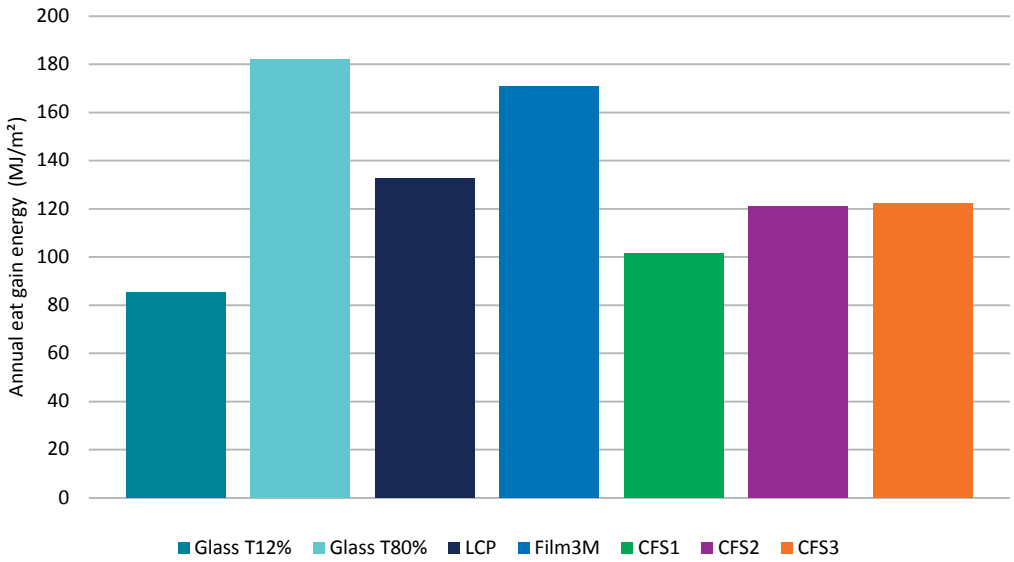

Figure 4.30 Annual total solar heat gain (MJ/m^2) transmitted during a whole year in the office room located in Building B1

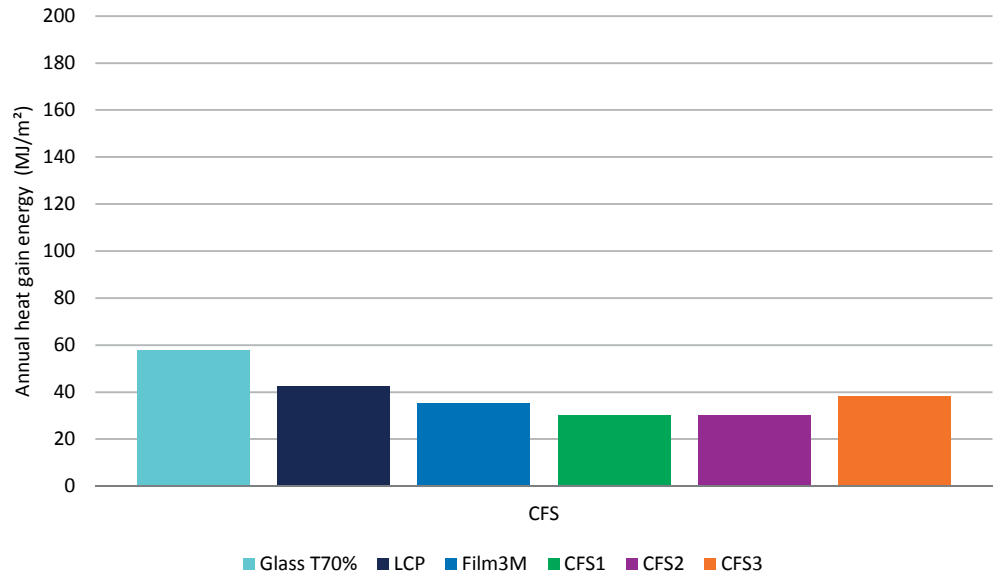

Figure 4.31 Annual total solar heat gain (MJ/m²) transmitted during a whole year in the office room located in Building B2, existing situation.

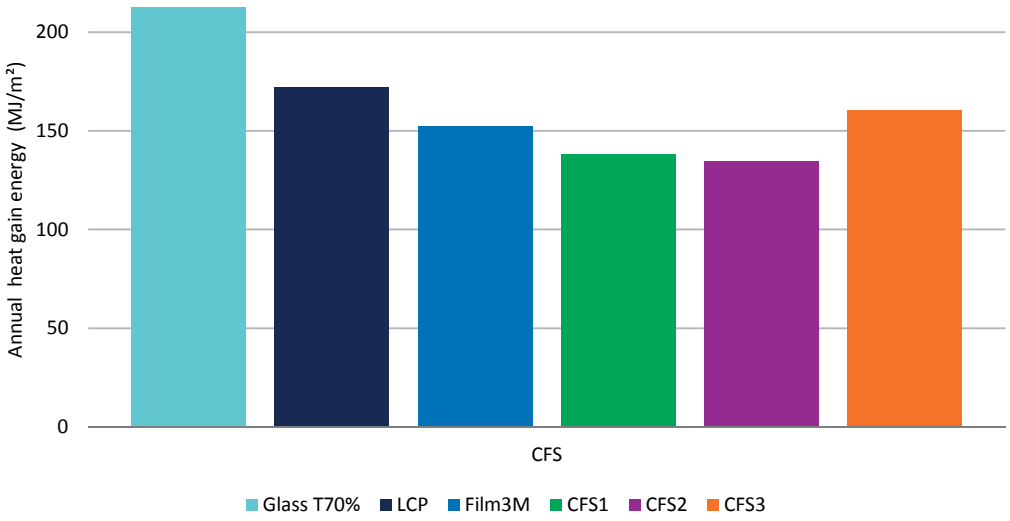

Figure 4.32 Annual total solar heat gain (MJ/m^2) transmitted in the office Building B2, when the exterior overhang was removed.

However, such results present certain inaccuracies, since the BTDF data representing the optical properties of the CFS used in this study to create the idf input-file of Energy Plus was generated taking into account only the front transmission data obtained with the use of the gonio-phometer. In order to be able to create the BSDF-idf file using Window 7, 'zero' data accounting for the back transmission, front and back reflectance was added at the end of the original file, which would signify an underestimation of the final results.

4.2.2 Conclusions

From the assessment of the annual heat gain energy in the two office rooms, we can conclude that the use of standard glass would allow higher extents of solar gains in the two office rooms. In the case of Building B1, a clear difference was found between the use of the tinted glazing and the standard glass τv 80% doubling the amount transmitted. From the CFS is Film 3M the one allowing higher extents of solar energy while CFS1 the one that allows less. In the case of Building B2, homogeneous results were obtained due to the effect of the overhang, however still the use of standard glass τv 70% would allow higher solar gains in the room, from the CFS the LCP would represent a risk of thermal comfort while the CFS2 would represent a better interior thermal environment.

4.3 Multi-criterion analysis

In the present chapter which evaluates the annual performance of the considered CFS, two main conditions are evaluated: first, the daylight distribution in the room and secondly the thermal comfort of the occupants. In the first case, the assessment was performed by calculating the frequency in which certain ranges of illuminance are present in the office rooms during the entire year. For the assessment of thermal comfort, the total solar gains allowed into the room (MJ/m²) were compared for the fenestration systems; such assessment was performed in annual basis. As it was explained in the previous chapter, a counter-balance criterion is applied when assessing certain conditions, where the lowest record is applied to the higher result obtained. The application of such reverse-criteria is shown by a double-arrow symbol in the classification of the satisfaction degree. For the assessment performed in Building B1, the satisfaction degree criterion is shown in Table 4.3.

While performing the present overall evaluation, a hierarchy was established to the objectives pursued by the daylighting approach proposed in this PhD thesis. Thus, a higher priority is given to the admission of daylight into the building over the control of solar rays, assuming that for the latter the use of a shading device can be invariably considered. According to that, in the evaluation criteria presented in Table 4.4, a higher WF value (See Section 3.7) is assigned to the frequency of the 'target' and 'acceptable' illuminances (assigned a WF of 5) while a lower value is given to the thermal comfort of the occupants (assigned 4). In the same way the 'minimum' illuminance was assigned with a value of 3, while the 'non-sufficient' illuminances was assigned with a WF value of 1, as they are less important for the overall evaluation.

B1		SATISFACTION DEGREE						
Condition		0	1	2	3	4	5	6
1. INTERIOR DAYLIGHT DISTRIBUTION	cbc							
1.4 Frequency of Illuminance (%) (Annual Assessment)								
not sufficient (<100 lx)	↔	highest	good	not bad	moderate	poor	bad	lowest
minimum (100-300 lx)	↔	highest	good	not bad	moderate	poor	bad	lowest
target (300-500 lx)		lowest	bad	poor	moderate	not bad	good	highest
sufficient (500-1800 lx)		lowest	bad	poor	moderate	not bad	good	highest
maximum (1800-2000 lx)		lowest	bad	poor	moderate	not bad	good	highest
risk (> 2000 lx)	↔	highest	good	not bad	moderate	poor	bad	lowest
2. OCCUPANT'S COMFORT								
2.3 Thermal Comfort (Annual Assessment)								
Annual Cumulative Heat Gain Energy [MJ/m²]	↔	highest	good	not bad	moderate	poor	bad	lowest

Table 4.3 Classification of the satisfaction degree assigned to each condition for the evaluation of the annual performance in Building B1.

The results of the annual assessment in Building B1 are shown in Table 4.4, in which partial results of the conditions 1.4 and 2.3 are shown at the bottom and added to obtain a final result highlighted in blue characters. When looking at the results by criteria, in the Frequency of Illuminance results, it's observed a better performance achieved by LCP followed by Film 3M. When considering the ranges of illuminance that count for risk of glare or overheating the standard glass obtained one of the lowest positions. In such condition, CFS1 and the existing situation (tinted glass τv 12%) were the ones obtaining lower results thus a better record. However, when comparing the existing situation with the CFS obtaining higher positions, the improvements obtained when using the latter vs. the tinted glass is evident. Since is possible to observe, the tinted glazing obtained the last position in allowing 'useful' illuminances inside the room.

Regarding the Thermal Comfort of the occupants, the lowest heat gains are admitted by the existing tinted glass achieving the highest rank. However, despite of its lower transmittance compared to the other glazing systems the tinted glass transmits levels of heat energy similar to CFS1. This might be due to its characteristics, because of its low transmittance and its exterior 'mirror-appearance' it would reflect an important portion of the incident solar radiation to the exterior, while another would be absorbed and transmitted later inside the room. Among the CFS the highest heat gains would be transmitted by the Film 3M and the standard glass τv 80%, therefore achieved a lower score. In summary, for the annual evaluation of the CFS performance in Building B1, it can be observed that better results were achieved by LCP followed closely by the Film 3M. CFS3 achieved also a good performance while CFS2 and the standard glass τv 80% obtained comparable results. CFS1 and the existing tinted glass τv 12% are found in the last positions.

B1	WF	%	cbc	Glass τv12%		Glass τv 80%		LCP		Film3M		CFS1		CFS2		CFS3	
				SD	UV	SD	UV	SD	UV	SD	UV	SD	UV	SD	UV	SD	UV
1. INTERIOR DAYLIGHT DISTRIBUTION																	
1.4 Frequency of Illuminance (%) (Annual Assessment)																	
not sufficient (<100 lx)	1	4.00	↔	0	0.00	6	24.00	5	20.00	4	16.00	1	4.00	3	12.00	2	8.00
minimum (100-300 lx)	3	12.00	↔	5	60.00	4	48.00	3	36.00	6	72.00	0	0.00	1	12.00	2	24.00
target (300-500 lx)	5	20.00		0	0.00	3	60.00	6	120.00	5	100.00	1	20.00	2	40.00	4	80.00
acceptable (500-1800 lx)	5	20.00		0	0.00	2	40.00	6	120.00	5	100.00	1	20.00	3	60.00	4	80.00
maximum (1800-2000 lx)	3	12.00		0	0.00	5	60.00	4	48.00	6	72.00	1	12.00	3	36.00	2	24.00
risk (> 2000 lx)	4	16.00	↔	6	96.00	1	16.00	4	64.00	0	0.00	5	80.00	2	32.00	3	48.00
2. OCCUPANT'S COMFORT																	
2.3 Thermal Comfort (Annual Assessment)																	
Annual Cumulative Heat Gain Energy [MJ/m²]	4	16.00	↔	6	96.00	0	0.00	2	32.00	1	16.00	5	80.00	3	48.00	4	64.00
		condition 1.4			156.00		248.00		408.00		360.00		136.00		192.00		264.00
		condition 2.3			34.78		0.00		11.59		5.80		28.99		17.39		23.19
	25	100.00			252.00		248.00		440.00		376.00		216.00		240.00		328.00

Table 4.4 Overall assessment of the annual performance of the considered variants in Building B1. In which SD stands for Satisfaction Degree, UV stands for Unit Value, WF stands for Weighting Factor and the 'cbc' column indicates the sense of evaluation criteria.

In the case of Building B2, the satisfaction degree criteria applied for the assessment of CFS is presented in Table 4.5, where 6 grades are taken into account in order to compare the six variants evaluated in this office room (CFS and the standard glazing *τv* 70%).

B2		SATISFACTION DEGREE					
Condition		0	1	2	3	4	5
1. INTERIOR DAYLIGHT DISTRIBUTION	cbc						
1.4 Frequency of Illuminance (%) (Annual Assessment)							
not sufficient (<100 lx)	↔	highest	good	not bad	moderate	poor	lowest
minimum (100-300 lx)	↔	highest	good	not bad	moderate	poor	lowest
target (300-500 lx)		lowest	poor	moderate	not bad	good	highest
sufficient (500-1800 lx)		lowest	poor	moderate	not bad	good	highest
maximum (1800-2000 lx)		lowest	poor	moderate	not bad	good	highest
risk (> 2000 lx)	↔	highest	good	not bad	moderate	poor	lowest
2. OCCUPANT'S COMFORT							
2.3 Thermal Comfort (Annual Assessment)							
Annual Cumulative Heat Gain Energy [MJ/m²]	↔	highest	good	not bad	moderate	poor	lowest

Table 4.5 Classification of the satisfaction degree assigned to each condition in order to evaluate the annual performance of CFS in B2.

In the results of the annual assessment obtained in Building B2 (Table 4.6), it was found that LCP and CFS1 show to allow useful ranges of illuminance during longer periods in the working year. Even if, in the evaluation of the frequency of illuminances within specific ranges (Section 4.2.1.2) CFS1 appeared to allow such levels during longer periods of time it also obtained low positions in the counter-balance criteria, allowing 'minimum' and 'non-sufficient' illuminance levels inside the room. However, such results are notorious since the performance of CFS1 in B1 show to be moderated. In the same way, a notorious difference in its performance was shown by Film 3M since unlike its results obtained in B1, in B2 is shows one of the lowest performances comparable with CFS3. The existing situation (standard glass τv 70%) show the worst performance by achieving higher points in the conditions that count with a lower WF, and lower positions in those that are more important for the overall assessment, thus it was poorly reflected in the final score. Regarding the annual assessment of the thermal comfort of the occupants, the use of the standard glass and LCP would be less recommended since are the ones allowing higher solar energy transmitted into the room (achieving the lowest rank). CFS1 and CFS2 are the CFS that better contribute to maintain a satisfactory thermal interior environment; however, the latter's good performance in this condition is reflected by its poor performance in allowing useful illuminance levels into the room, where achieved the lowest ranks.

In summary, in the annual evaluation of CFS for Building B2, the best performance was achieved by CFS1 followed by LCP which showed a good performance. The Film 3M and CFS3 achieved similar results, while the standard glass and CFS2 obtained the last positions.

B2	WF	%	cbc	Glass τv70%		LCP		Film3M		CFS1		CFS2		CFS3	
				SD	UV	SD	UV	SD	UV	SD	UV	SD	UV	SD	UV
1. INTERIOR DAYLIGHT DISTRIBUTION															
1.4 Frequency of Illuminance (%) (Annual Assessment)															
not sufficient (<100 lx)	1	4.00	↔	5	20.00	3	12.00	4	16.00	0	0.00	1	1.00	2	8.00
minimum (100-300 lx)	3	12.00	↔	5	60.00	4	48.00	3	36.00	0	0.00	1	3.00	2	24.00
target (300-500 lx)	5	20.00		0	0.00	1	20.00	2	40.00	5	100.00	4	20.00	3	60.00
acceptable (500-1800 lx)	5	20.00		1	20.00	5	100.00	0	0.00	4	80.00	2	10.00	3	60.00
maximum (1800-2000 lx)	3	12.00		4	48.00	5	60.00	3	36.00	2	24.00	1	3.00	0	0.00
risk (> 2000 lx)	4	16.00	↔	0	0.00	2	32.00	1	16.00	5	80.00	4	16.00	3	48.00
2. OCCUPANT'S COMFORT															
2.3 Thermal Comfort (Annual Assessment)															
Annual Cumulative Heat Gain Energy [MJ/m²]	4	16.00	↔	0	0.00	1	16.00	3	48.00	4	64.00	5	80.00	2	32.00
		condition 1.4			148.00		272.00		144.00		284.00		53.00		200.00
		condition 2.3			0.00		5.80		17.39		23.19		28.99		11.59
	25	100.00			148.00		288.00		192.00		348.00		133.00		232.00

Table 4.6 Overall assessment of the CFS's annual performance in Building B2. In which SD stands for Satisfaction Degree, UV stands for Unit Value, WF stands for Weighting Factor and the 'cbc' column indicates the sense of evaluation criteria.

4.4 Conclusions

The annual evaluation of the performance of CFS in two office rooms was carried-out by including the assessment of the Interior daylight distribution as well as thermal comfort. The former was determined using the RADIANCE Five-phase method, which results were classified based on the Useful Daylight Illuminance metric (UDI). Then, the evaluation was performed taking into account the Frequency in which certain ranges of Illuminance are present into the room (%). The thermal comfort of the occupants was calculated with the use of the software Energy Plus, from which, the output of the solar heat gains allowed into the room by each of the assessed fenestration systems were compared.

On the overall annual basis in Building B1, the optimal daylighting performance is achieved by the LCP and Film 3M while CFS3 achieved also a sound performance, comparable with the one of the standard glazing (τv 80%). It must be outlined, that the performance of the fenestration systems considered in Building B1 show a clear tendency, since LCP and the Film 3M maintain sound positions in the assessment performed during the Equinox and Solstices (Chapter 3), while the CFS1 and CFS2/CFS3 alternate their 'moderate/poor' performance. In Building B2, the CFS1 show the best performance, followed by LCP in the multi-criteria evaluation, while CFS3 was also found to perform well. In this case the performance shown by the CFS in the previous chapter differ, since for the equinox and solstices assessment Film 3M showed a remarkable performance. In the annual assessment presented in this chapter, as concluded for Building B1, in B2 the use of CFS has clearly shown advantages when compared to the performance of the current situation, since the standard glazing (τv 70%) achieved the lowest annual performance.

As a matter of fact, regarding to the differences observed for the performance of CFS1 in Building B1 and Building B2, this might be due to the light redirection properties of such systems depending from the sun altitude. As shown in Annex 3.1 (Figure A1.11), the larger transmittance of the micro-structured systems (CFS1, CFS2 and CFS3) lies in sun altitudes between 15° and 30°, while for higher altitudes their redirection performance decreases. In Building B1, due to the facade orientation (SW), the sun rays impinge the façade mainly in the afternoons; in Building B2 the facade orientation to the SE is favourable to the admission of daylight in the mornings, as it illustrated in Figure 4.33. Thus, for B1 the transmittance of CFS1 would be favourable only in winter and spring for a period of time between 15h and 17h, while B2 would benefit from a higher transmittance of the micro-structured systems during longer periods: mornings in winter, spring and equinox; during the afternoons in winter and in the evening in all seasons. A table showing the sun's elevation angles in spring equinox, and winter and summer solstices (from 9h to 17h) is shown in Table 4.7, the shadowed zones correspond to the times where the sun's face in the façade in both buildings. Additional graphs illustrating the sun's position regarding the building's orientation can be seen in Annex 2.3.

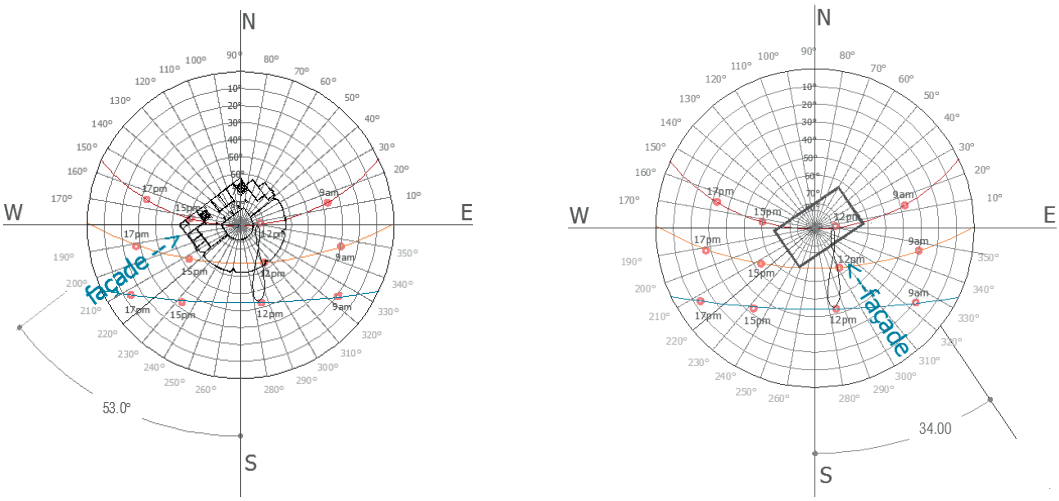

Figure 4.33 Illustration of the sun's trajectory regarding the buildings orientation, Building B1 (left) and Building B2 (right).

	B1 SW 53°			B2 SE 34°		
θ	winter solstice	spring equinox	summer solstice	winter solstice	spring equinox	summer solstice
9am	17	27	30 DLST	17	27	30 DLST
12pm	42	62	67 DLST	42	62	67 DLST
15pm	32	52	74 DLST	33	52	74 DLST
17pm	13	27	47 DLST	13	27	47 DLST

Table 4.7 Sun altitude in spring equinox, winter and summer solstices at 9h00, 12h00, 15h00 and 17h00. Shaded areas correspond to the times where the sun's is incident in the façade of the building.

As it can be observed, the results obtained for the Equinox and the Solstices differ often from those obtained in the annual assessment. In order to address conclusive results regarding the most suitable CFS for both office buildings, an integral evaluation including the results of both assessments is presented in the following Chapter.

Chapter 5 Analysis of the Results

5.1 Comprehensive results

The results obtained in the assessment carried-out in Solstices and Equinox (Chapter 3) and those obtained in the annual assessment (Chapter 4) are combined in Table 5.1. It can be seen first the summary of the results per condition assessed including the weighting factor (WF), the value assigned based in the satisfactory degree (SD), and the unit value (UD) which represent the score obtained for the corresponding condition. In Figure 5.2 an extract of such table including only the results obtained for each condition for sake of comparison, highlighted in green are the ones attaining the highest value per condition. The position of the five CFS the standard glass τv 80% and the existing situation (tinted glass τv 12%) respect to each other can be deduced from such results. The latter indicate that the LCP was the CFS which obtained the higher rank in the overall assessment, Film 3M and Glass τv 80% were ranked 2nd and 3rd, while CFS1 and the tinted glass τv 12% obtained the last position in the performance assessment in Building B1.

B1	WF	%	cbc	Glass τv12%		Glass τv 80%		LCP		Film3M		CFS1		CFS2		CFS3	
				SD	UV	SD	UV	SD	UV	SD	UV	SD	UV	SD	UV	SD	UV
1. INTERIOR DAYLIGHT DISTRIBUTION																	
1.1 Illuminance Ranges (%) (Solstices & Equinox)																	
not sufficient (<100 lx)	1	1.45	↔	0	0.00	5	7.25	4	5.80	6	8.70	1	1.45	3	4.35	2	2.90
minimum (100-300 lx)	3	4.35	↔	0	0.00	6	26.09	3	13.04	5	21.74	1	4.35	4	17.39	2	8.70
target (300-500 lx)	5	7.25		1	7.25	5	36.23	6	43.48	3	21.74	2	14.49	4	28.99	3	21.74
acceptable (500-1800 lx)	5	7.25		0	0.00	6	43.48	4	28.99	5	36.23	3	21.74	1	7.25	2	14.49
maximum (1800-2000 lx)	3	4.35		3	13.04	4	17.39	5	21.74	5	21.74	4	17.39	6	26.09	6	26.09
risk (> 2000 lx)	4	5.80	↔	6	34.78	1	5.80	5	28.99	0	0.00	4	23.19	2	11.59	3	17.39
1.2 Average DF %	4	5.80		0	0.00	5	28.99	4	23.19	4	23.19	4	23.19	4	23.19	4	23.19
1.3 Illuminance Uniformity (Solstices & Equinox)																	
Illuminance Uniformity g1 (min/avg)	3	4.35		4	17.39	4	17.39	4	17.39	4	17.39	3	13.04	3	13.04	3	13.04
Illuminance Uniformity g2 (min/max)	3	4.35		2	8.70	2	8.70	1	4.35	1	4.35	1	4.35	1	4.35	1	4.35
1.4 Frequency of Illuminance (%) (Annual Assessment)																	
not sufficient (<100 lx)	1	1.45	↔	0	0.00	6	8.70	5	7.25	4	5.80	1	1.45	3	4.35	2	2.90
minimum (100-300 lx)	3	4.35	↔	5	21.74	4	17.39	3	13.04	6	26.09	0	0.00	1	4.35	2	8.70
target (300-500 lx)	5	7.25		0	0.00	3	21.74	6	43.48	5	36.23	1	7.25	2	14.49	4	28.99
acceptable (500-1800 lx)	5	7.25		0	0.00	2	14.49	6	43.48	5	36.23	1	7.25	3	21.74	4	28.99
maximum (1800-2000 lx)	3	4.35		0	0.00	5	21.74	4	17.39	6	26.09	1	4.35	3	13.04	2	8.70
risk (> 2000 lx)	4	5.80	↔	6	34.78	1	5.80	4	23.19	0	0.00	5	28.99	2	11.59	3	17.39
2. OCCUPANT'S COMFORT																	
2.1 Visual Comfort (Solstices and Equinox)																	
Glare (DGP)	4	5.80		1	5.80	2	11.59	5	28.99	6	34.78	4	23.19	3	17.39	5	28.99
2.2 Thermal Comfort (Solstices and Equinox)																	
Transmitted Solar Energy (W/m2)																	
Winter solstice	5	7.25		0	0.00	6	43.48	1	7.25	4	28.99	2	14.49	5	36.23	3	21.74
Summer solstice	4	5.80	↔	6	34.78	0	0.00	5	28.99	3	17.39	4	23.19	1	5.80	2	11.59
2.3 Thermal Comfort (Annual Assessment)																	
Annual Cumulative Heat Gain Energy [MJ/m²]	4	5.80	↔	6	34.78	0	0.00	2	11.59	1	5.80	5	28.99	3	17.39	4	23.19
	69	100.00			213.04		336.23		411.59		372.46		262.32		282.61		313.04

Table 5.1 Summary of the results obtained in the CFS's assessment in solstices and equinox and in annual basis in Building B1.

Condition	Glass τv 12%	Glass τv 80%	LCP	Film3M	CFS1	CFS2	CFS3
1. INTERIOR DAYLIGHT DISTRIBUTION							
1.1 **Frequency of Illuminance (%)** (Solstices & Equinox)	55.07	136.23	142.03	110.14	82.61	95.65	91.30
1.2 **Average DF %** (Solstices & Equinox)	0.00	28.99	23.19	23.19	23.19	23.19	23.19
1.3 **Illuminance Uniformity** (Solstices & Equinox)	26.09	26.09	21.74	21.74	17.39	17.39	17.39
1.4 **Frequency of Illuminance (%)** (Annual Assessment)	56.52	89.86	147.83	130.43	49.28	69.57	95.65
2. OCCUPANT'S COMFORT							
2.1 **Visual Comfort** (Solstices and Equinox)	5.80	11.59	28.99	34.78	23.19	17.39	28.99
2.2 **Transmitted Solar Energy (W/m2)** (Solstices and Equinox)	34.78	43.48	36.23	46.38	37.68	42.03	33.33
2.3 **Annual Cumulative Heat Gain Energy [MJ/m²]** (Annual)	34.78	0.00	11.59	5.80	28.99	17.39	23.19
	213.04	336.23	411.59	372.46	262.32	282.61	313.04
	7	3	1	2	6	5	4

Table 5.2 Extract of the comprehensive results and the CFS's performance position in Building B1, deduced from the summary of results.

For Building B2, the summary of the results obtained in the solstices and equinox assessment and the one performed in annual basis is shown in Table 5.3. In the same way the extract of the results and the definition of the CFS's position relative to their performance respect to each other is shown in Figure 5.4. Which it shows that even if quite homogeneous values were obtained for the compared fenestration systems in this Building B2, still CFS1 attain the higher results while a second place is shared by the CFS2, CFS3 and the LCP, Film 3M achieved fourth and a revealing last position was achieved by the existing situation (standard glass τv 70%).

B2	WF	%	cbc	Glass 70%		LCP		Film3M		CFS1		CFS2		CFS3	
				SD	UV	SD	UV	SD	UV	SD	UV	SD	UV	SD	UV
1. INTERIOR DAYLIGHT DISTRIBUTION															
1.1 Ranges of Illuminance (%) (Solstices & Equinox)															
not sufficient (<100 lx)	1	1.45	↔	5	7.25	5	7.25	5	7.25	5	7.25	5	7.25	5	7.25
minimum (100-300 lx)	3	4.35	↔	5	21.74	3	13.04	4	17.39	1	4.35	0	0.00	2	8.70
target (300-500 lx)	5	7.25		2	14.49	5	36.23	3	21.74	4	28.99	5	36.23	4	28.99
acceptable (500-1800 lx)	5	7.25		2	14.49	3	21.74	1	7.25	5	36.23	3	21.74	4	28.99
maximum (1800-2000 lx)	3	4.35		4	17.39	3	13.04	5	21.74	3	13.04	2	8.70	2	8.70
risk (> 2000 lx)	4	5.80	↔	1	5.80	2	11.59	0	0.00	4	23.19	3	17.39	2	11.59
1.2 Average DF %	4	5.80		5	28.99	5	28.99	5	28.99	5	28.99	5	28.99	5	28.99
1.3 Illuminance Uniformity (Solstices & Equinox)															
Illuminance Uniformity g1 (min/avg)	3	4.35		3	13.04	4	17.39	4	17.39	3	13.04	3	13.04	3	13.04
Illuminance Uniformity g2 (min/max)	3	4.35		1	4.35	2	8.70	2	8.70	1	4.35	1	4.35	1	4.35
1.4 Frequency of Illuminance (%) (Annual Assessment)															
not sufficient (<100 lx)	1	1.45	↔	5	7.25	3	4.35	4	5.80	0	0.00	1	1.45	2	2.90
minimum (100-300 lx)	3	4.35	↔	5	21.74	4	17.39	3	13.04	0	0.00	1	4.35	2	8.70
target (300-500 lx)	5	7.25		0	0.00	1	7.25	2	14.49	5	36.23	4	28.99	3	21.74
acceptable (500-1800 lx)	5	7.25		1	7.25	5	36.23	0	0.00	4	28.99	2	14.49	3	21.74
maximum (1800-2000 lx)	3	4.35		4	17.39	5	21.74	3	13.04	2	8.70	1	4.35	0	0.00
risk (> 2000 lx)	4	5.80	↔	0	0.00	2	11.59	1	5.80	5	28.99	4	23.19	3	17.39
2. OCCUPANT'S COMFORT															
2.1 Visual Comfort (Solstices and Equinox)															
Glare (DGP)	4	5.80		0	0.00	0	0.00	0	0.00	0	0.00	0	0.00	0	0.00
2.2 Thermal Comfort (Solstices and Equinox)															
Transmitted Solar Energy (W/m2)															
Winter solstice	5	7.25		5	36.23	1	7.25	3	21.74	0	0.00	4	28.99	3	21.74
Summer solstice	4	5.80	↔	0	0.00	2	11.59	4	23.19	3	17.39	1	5.80	5	28.99
2.3 Thermal Comfort (Annual Assessment)															
Annual Cumulative Heat Gain Energy [MJ/m²] (Annua	4	5.80	↔	0	0.00	1	5.80	3	17.39	4	23.19	5	28.99	2	11.59
	69	100.00			217.39		281.16		244.93		302.90		278.26		275.36

Table 5.3 Summary of the results obtained in the CFS's assessment in solstices and equinox and in annual basis in Building B2.

Condition	Glass τv 70%	LCP	Film3M	CFS1	CFS2	CFS3
1. INTERIOR DAYLIGHT DISTRIBUTION						
1.1 **Frequency of Illuminance (%)** (Solstices & Equinox)	81.16	102.90	75.36	113.04	91.30	94.20
1.2 **Average DF %** (Solstices & Equinox)	28.99	28.99	28.99	28.99	28.99	28.99
1.3 **Illuminance Uniformity** (Solstices & Equinox)	17.39	26.09	26.09	17.39	17.39	17.39
1.4 **Frequency of Illuminance (%)** (Annual Assessment)	53.62	98.55	52.17	102.90	76.81	72.46
2. OCCUPANT'S COMFORT						
2.1 **Visual Comfort** (Solstices and Equinox)	0.00	0.00	0.00	0.00	0.00	0.00
2.2 **Transmitted Solar Energy (W/m2)** (Solstices and Equinox)	36.23	18.84	44.93	17.39	34.78	50.72
2.3 **Annual Cumulative Heat Gain Energy [MJ/m²]** (Annual)	0.00	5.80	17.39	23.19	28.99	11.59
	217.39	281.16	244.93	302.90	278.26	275.36
	4	2	3	1	2	2

Table 5.4 Extract of the comprehensive results and the CFS's performance position in Building B2, deduced from the summary of results.

5.2 Strengthess and Weakness Analysis

The present analysis is also useful to estimate the intrinsic qualities of each CFS regarding the assessed conditions. In order to review the overall performance of each CFS in the conditions assessed, a comparative diagram was created which shows their strengths and deficiencies by classifying them in a scale in order to grade the considered fenestration systems in each building. In the case of Building B1, the scale ranges from 0 to 6 considering the existing situation (glass τv 12%), the standard glass τv 80% and the five pre-selected CFS; in Building B2 the scale ranges from 0 to 5 taking into account six fenestration systems: the existing situation τv 70% and the five CFS. In such comparison, zero represents the last position obtained when compared the performance of the assessed fenestration systems, while 6/5 represents the best performance found among them. The analysis took into account the procedures presented in Chapter 3 and Chapter 4, thus two main conditions are evaluated, first the assessment of the interior daylight distribution and secondly those that comprehend the visual and thermal comfort of the occupants. Each sub-condition is identified in the graph by a number referring to its associated condition indicating in parenthesis the period of time considered in the assessment: the Solstices and Equinox or in Annual basis. Such categorization is shown in Table 5.5.

Assessed Conditions	**Legend in the graph**
1. INTERIOR DAYLIGHT DISTRIBUTION	
1.1 Frequency of useful Illuminances (%) (Solstices & Equinox)	1.1 Frequency of UDI (Solstice and Equinox)
1.2 Average DF % (Solstices & Equinox)	1.2 Average DF (Solstice and Equinox)
1.3 Illuminance Uniformity (Solstices & Equinox)	1.3 Illuminance Uniformity (Solstice and Equinox)
1.4 Frequency of useful Illuminances (%) (Annual Assessment)	1.4 Frequency of UDI (Annual Assessment)
2. OCCUPANT'S COMFORT	
2.1 Visual Comfort (Solstices and Equinox)	2.1 Visual Comfort (Solstice and Equinox)
2.2 Transmitted Solar Energy (W/m²) (Solstices and Equinox)	2.2 Transmitted Solar Energy (Solstice and Equinox)
2.3 Total Heat Gain Energy [MJ/m²] (Annual Assessment)	2.3 Heat Gain Energy (Annual Assessment)

Table 5.5 Conditions assessed in a CFS's individual evaluation showing the legend that identifies them in the assessment graph.

Regarding the present review, two important remarks are worth mentioning:

1. The Frequency of useful illuminances (for Solstices and Equinox as well as the annual assessment) takes into account only the ranges of illuminances that are considered advantageous for the human visual performance in an interior space. Thus, for the present review only the front-criteria conditions that assess the interior daylight distribution were considered. The conditions where the counterbalance criterion was applied were dismissed (e.g. the range of illuminances that are above 2000 lux or below 100 lux).

2. The Solar Gains assessed for the Solstices and Equinox takes only summer time results into account. The balance obtained between winter and summer time would represent the performance of the fenestration system relative to its performance for both situations: allowing solar gain in the room in winter and/or preventing it in summer. However in this review we are mainly interested in having a real view of the thermal comfort impact of the CFS in the office rooms.

5.2.1 Building B1

In the case of the current situation in Building B1, illustrated on Figure 5.1, the tinted glazing τv 12% obtained the weakest position almost for all the assessed conditions related to the interior daylight distribution. Except for the rank obtained in the assessment of the illuminance uniformity (1.3), which is probably due to its ability to filter the sun rays leading to lower workplane illuminance next to the window and thus creating a more uniform indoor daylighting environment. Its strength lies accordingly in its capability to prevent the solar heat gains to enter the office room compared to the other CFS. As it can be seen in the annual thermal comfort assessment (2.2 and 2.3) the tinted glazing is the fenestration system that reduces the cooling loads in the office room.

A significant improvement can be observed for the overall performance of the standard glazing (e.g. clear glass τv 80%) shown in Figure 5.2. Unlike the tinted glass, its main features lie in allowing a larger 'useful' illuminance provision into the room. The performance of the standard glazing regarding thermal comfort was less favourable; it allows larger solar heat gains into the room therefore its poor '0' mark for this criterion. Regarding the visual comfort assessment, the poor record obtained by the standard glazing can be explained by the low DGP values obtained at spring equinox compared to those obtained by the CFS (Section 3.5.1). The standard glazing 'concentrate' daylight in the area close to the window, creating a darker interior environment in the rest of the room. As a consequence the use of clear glass created an unbalanced indoor lighting environment impacting the visual performance in a negative way, unlike the CFS, which redirecting features contribute to a more uniform daylight distribution.

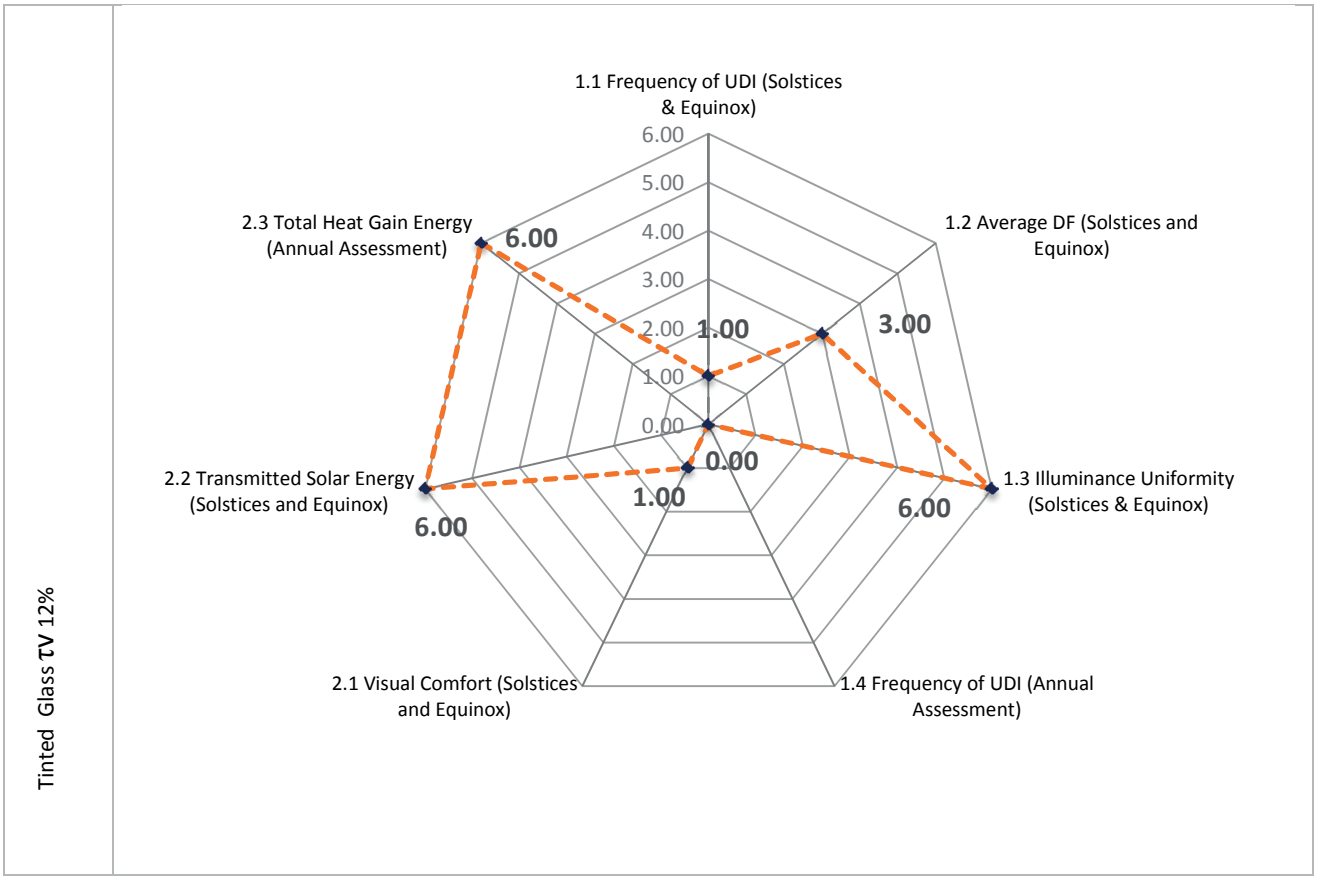

Figure 5.1 Performance review of tinted glass (τv 12%) in Building B1 comparing its achievements for seven performance criteria.

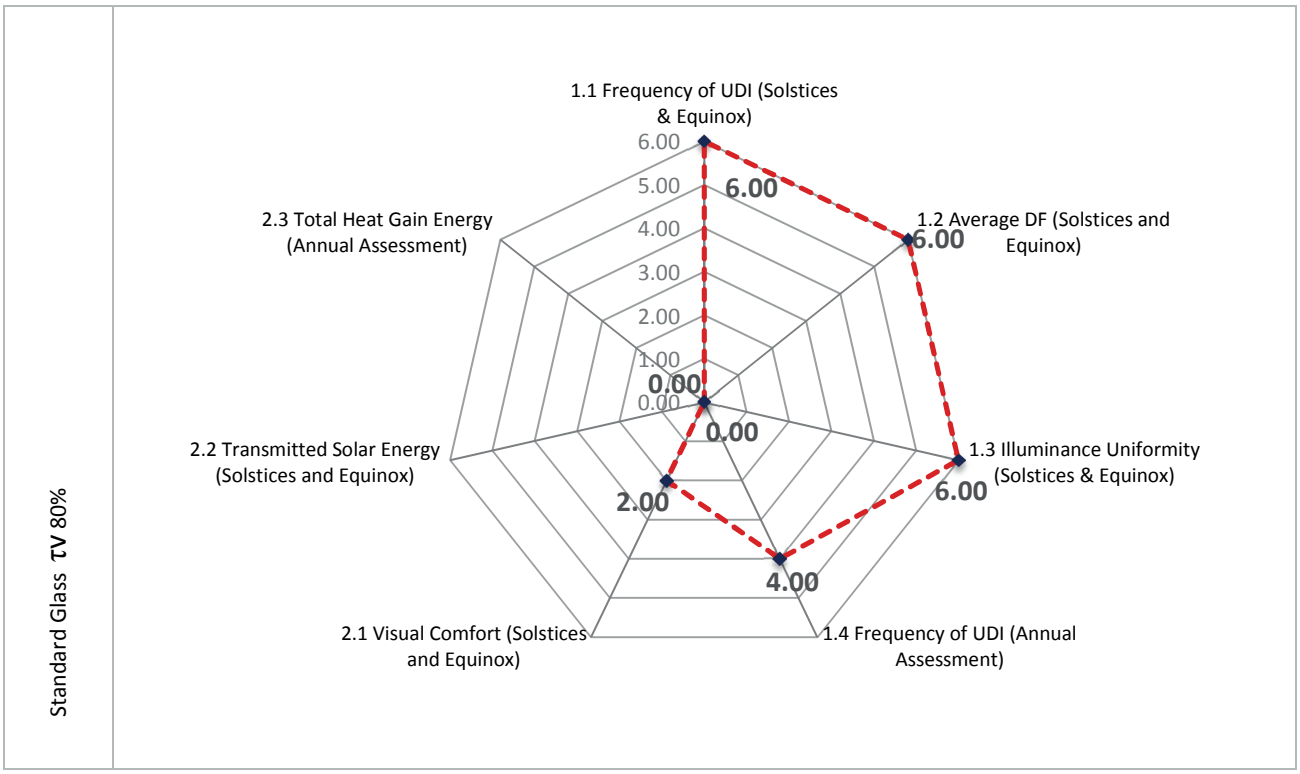

Figure 5.2 Performance review of clear glass (τv 80%) in Building B1 comparing its achievements for seven performance criteria.

The advantages of using LCP is an improved daylight distribution as illustrated on Figure 5.3; it shows that the strongest aspects of LCP lie in the frequency in which useful ranges of illuminance are found for this system; in this condition the LCP obtained the best marks for both assessments: solstices and equinox as well as on an annual basis. Its performance regarding the uniformity of illuminance is also sound; it also obtains a good mark only when assessed under overcast sky conditions where it ranked '5'. However, for visual comfort, the LCP showed a good performance, while for thermal comfort in the annual assessment it showed to be one of the fenestration systems that allow the largest solar heat gains entering the room (Section 4.3).

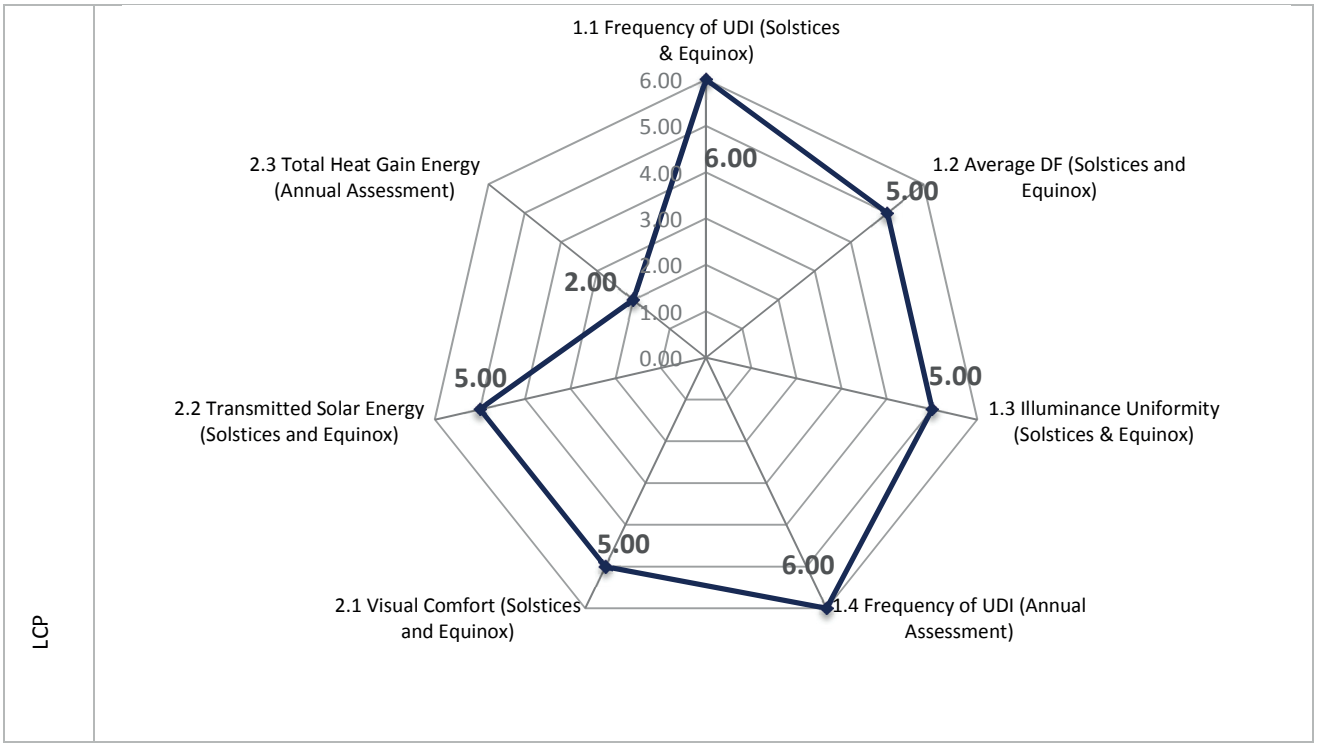

Figure 5.3 Performance review of LCP in Building B1 comparing its achievements for seven performance criteria.

The performance review of the Film 3M is illustrated on Figure 5.4; it shows that this system has less capabilities to reduce the heat gains transmitted to the interior while is better in maintaining a good interior daylight distribution and visual comfort achieving from good to excellent to marks for all of them. Its performance regarding thermal comfort assessed in equinox and solstices show moderated results, while in the assessment that takes into account a whole year the Film 3M reports to have a poor performance, meaning that large solar gains are allowed in the office room: movable sun shadings would be accordingly commended for this system.

The CFS1's performance review is presented in Figure 5.5; in this case its deficiencies are relative to the interior daylight distribution. Where, for the frequency of illuminances in solstices and equinox (1.1,) it obtained a low rank, showing that it fails to bring the 'useful' ranges of workplane illuminance into the room, compared to the other CFS. The same assessment performed on an annual basis show also poor results (1.4). Consinstently, for the assessment of the thermal comfort CFS1 obtained a good mark, which is probably due to the low illuminance it allows into the room next to the window. Regarding visual, CFS1 does not perform well as it shows few of the DGP values below 0.2, which indicates a scene of low brightness; yet, in such situation other fenestration systems achieved a better performance (Section 3.5.1).

The review of the performance of CFS2 in Building B1 is shown in Figure 5.6, which capabilities present a 'moderate' performance in all the conditions assessed. Thus for the criterion that take the daylight distribution inside the room into account, CFS2 presents a 'not bad' performance in most of them, only for the condition 1.4 where achieved '2'. For visual comfort, its performance shows deficiencies respect to the other fenestration systems, being one of the last in providing a sound environment for the human visual performance. As in the case of CFS1 this is due to the low DGP values obtained during the glare risks assessment. For thermal comfort (2.2 and 2.3), the performance of CFS2 shows to be better in the annual assessment with moderate performance, while in what constitutes solstices and equinox it shows a rather poor performance.

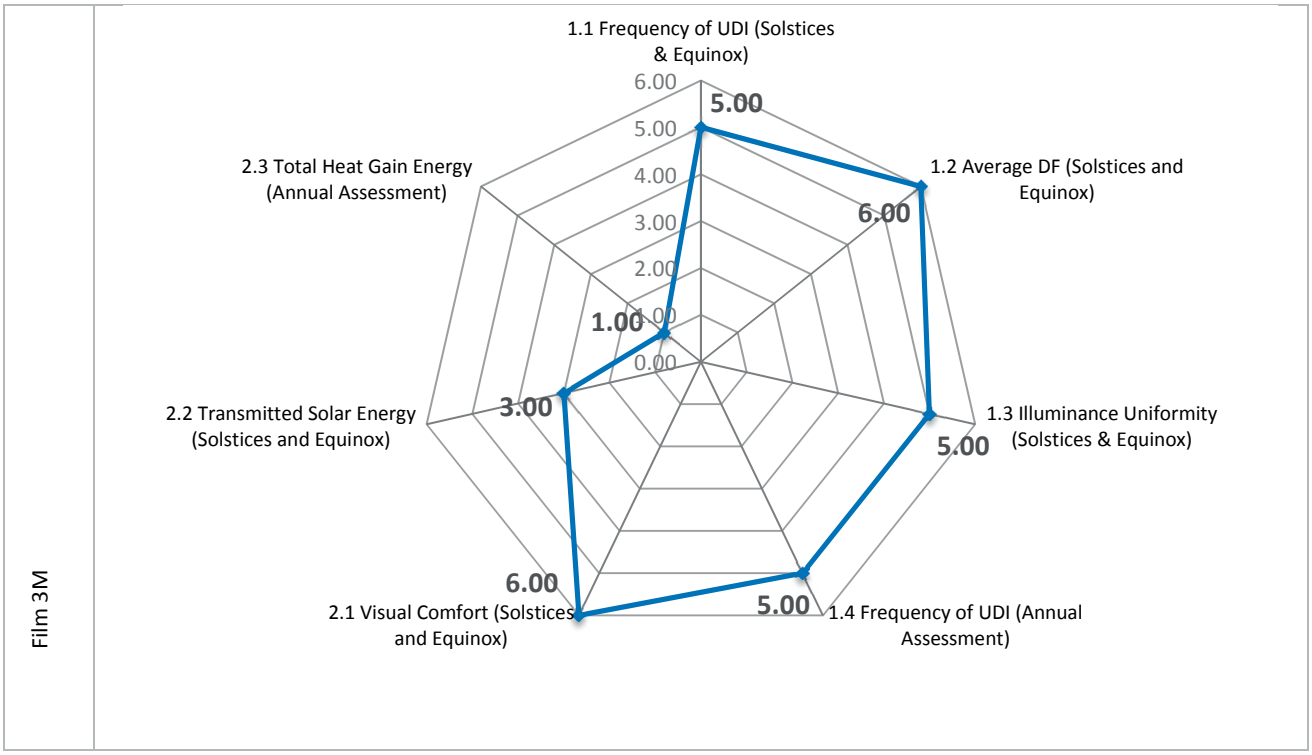

Figure 5.4 Performance review of The Film 3M in Building B1 comparing its achievements for seven performance criteria

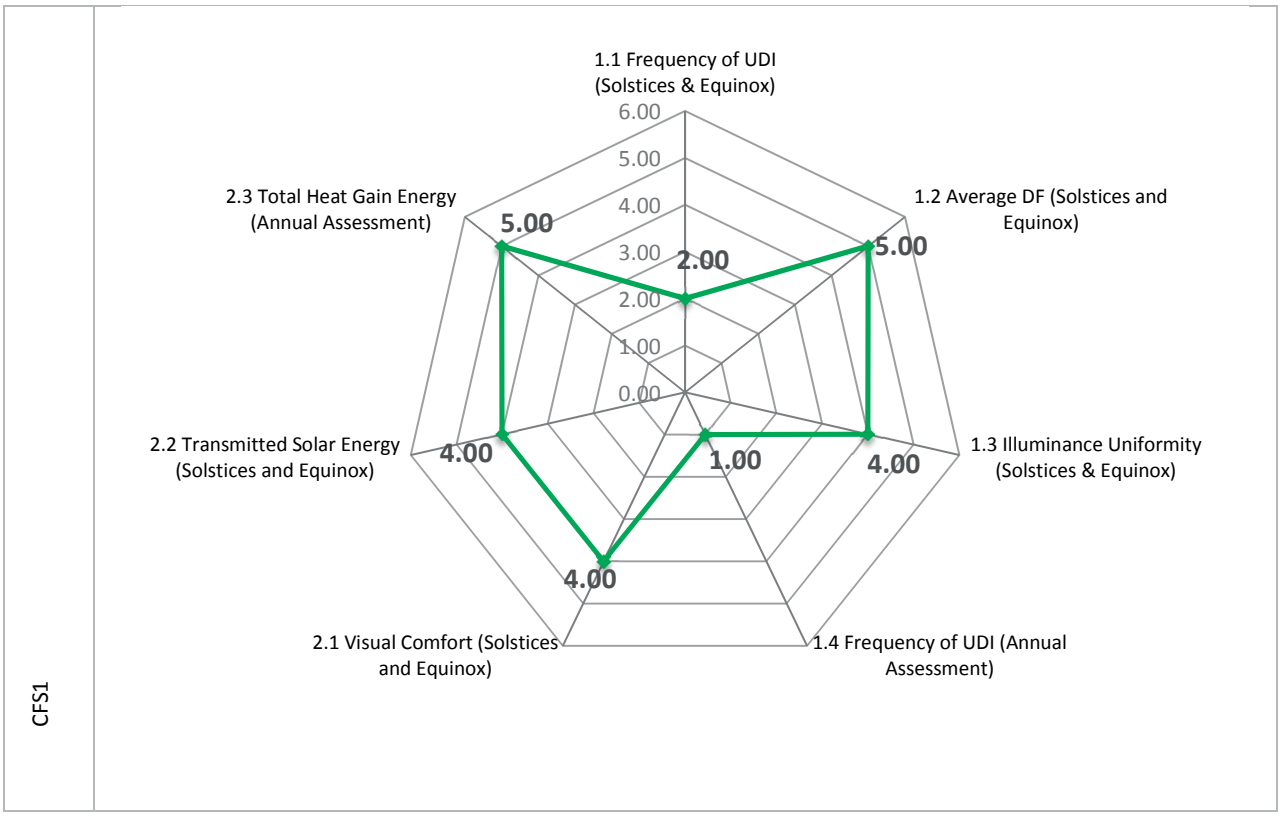

Figure 5.5 Performance review of CFS1 in Building B1 comparing its achievements for seven performance criteria.

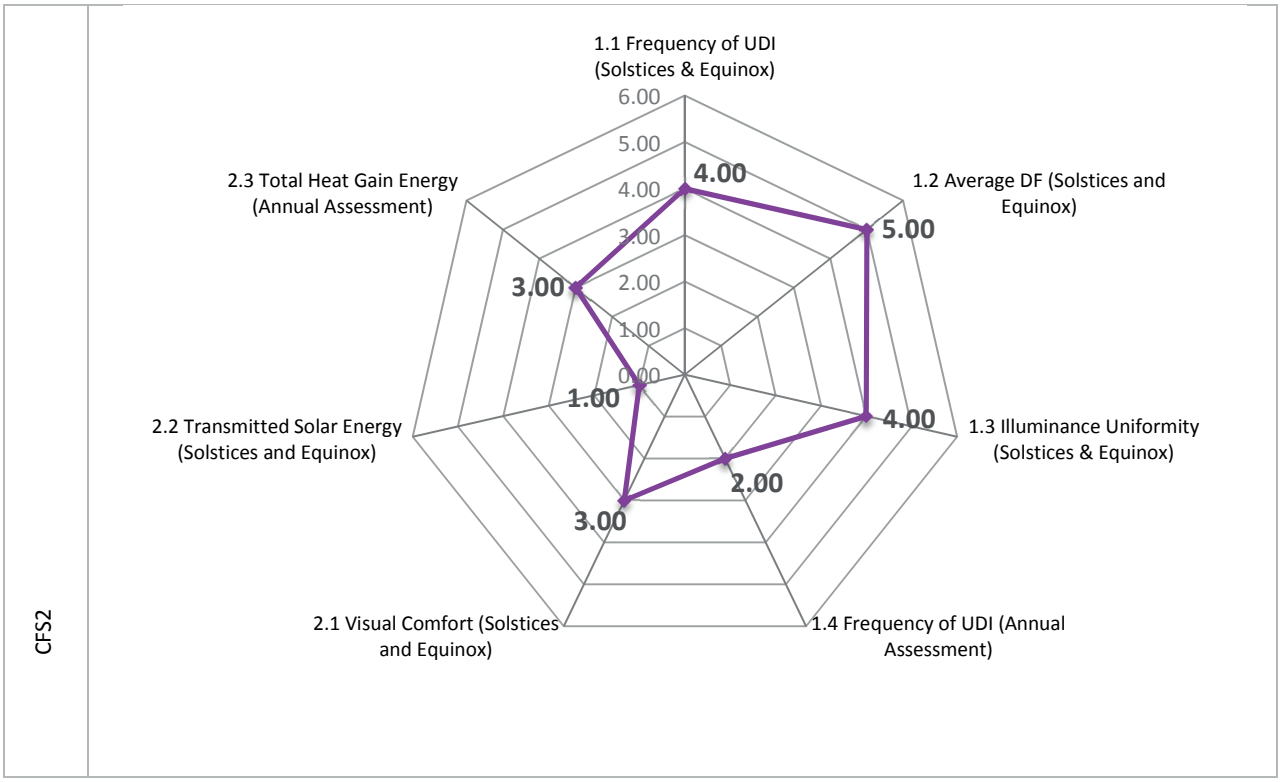

Figure 5.6 Performance review of CFS2 in Building B1 comparing its achievements for seven performance criteria.

The review of the performance of CFS3 in Building B1 is presented in Figure 5.7, which shows that it performs in a moderate way in almost all the conditions evaluated, compared to the other CFS. A 'good' performance was obtained in the assessment of its performance under overcast sky conditions (1.2) and 'not bad' in the uniformity of illuminances. In the assessment of 'frequency of useful illuminances' the CFS3 achieves equal results on annual basis to those obtained at winter and summer solstices. A good performance is reached for the visual comfort assessment, while a 'not bad' to 'poor' perofmance is achieved in the thermal comfort assessments, showing that CFS3 would represent a good option as it balances 'not bad' performances for all the assessed conditions.

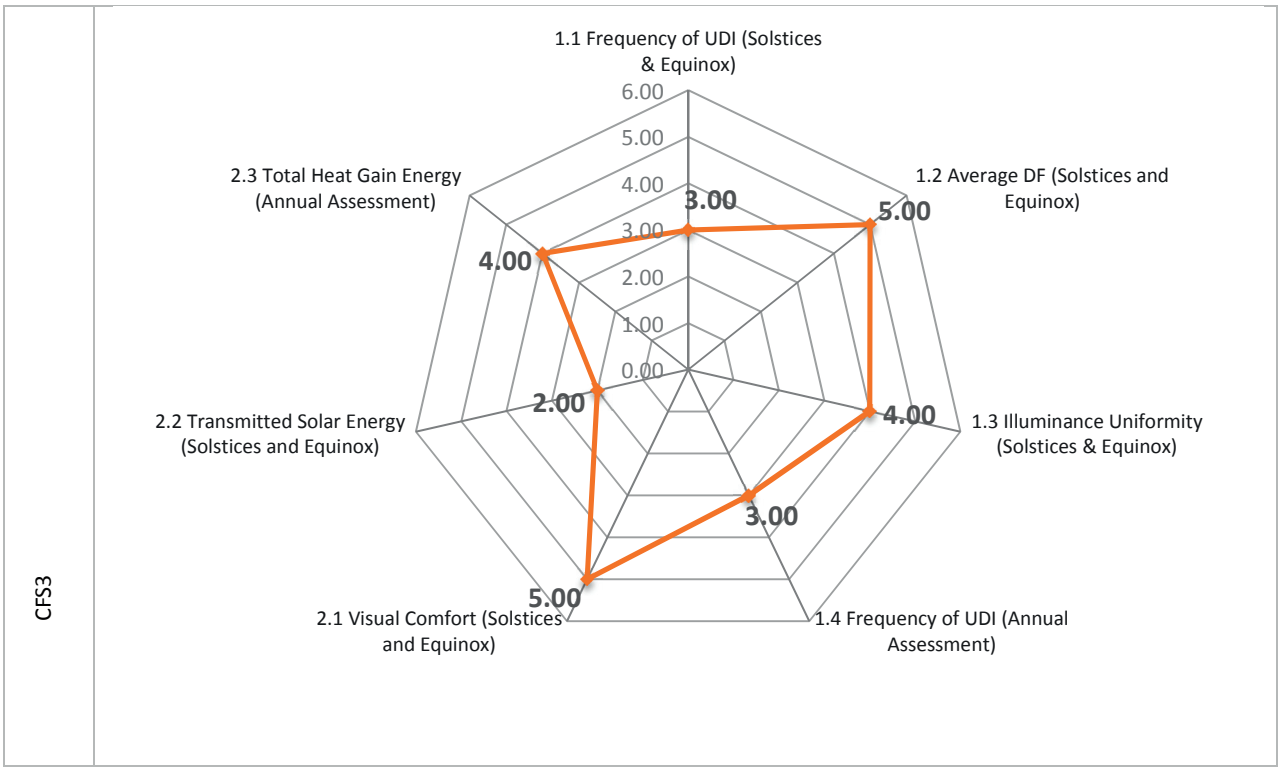

Figure 5.7 Performance review of CFS3 in Building B1 comparing its achievements for seven performance criteria.

5.2.2 Building B2

In the review of the fenestration systems performance in Building B2, which comprises five CFS and the standard glazing (e.g. clear glass τv70%) it was observed that the CFS performance were contrasting in some cases with those observed in Building B1. This might be due to the angle-dependence of the CFS's light redirection properties in relation to the building façade orientation: SW in the case of B1 and SE in the case of B2 (See Annex 2.3). In this case, the review is based on a '0' to '5', in order to classify the five CFS and the standard glass τv70% according to their performance.

The performance review of the standard glazing (τv70%) is shown in Figure 5.8, in which a bad performance can be observed for the thermal and visual comfort of the occupants. Regarding the indoor daylight distribution, it shows an excellent performance under overcast sky conditions. However, it is worth mentioning that the building design might contribute to an optimal interior daylight distribution in such conditions due to the size of the room (4.17m by 5.2m) and its square shape; thus all the fenestration systems assessed show a DF larger than 5%, obtaining the same ranking value (Section 3.4.2). When it comes to the illuminance uniformity, the standard glazing shows a 'not-bad' performance compared to the other CFS. Since, one of its disadvantages is allowing higher illuminance in the area next to the window, however in this case due to the room size such higher luminous contrasts are not observed. An example of this is the nil values below 100 lux that were obtained in the frequency of illuminance assessment for solstices and equinox in this building.

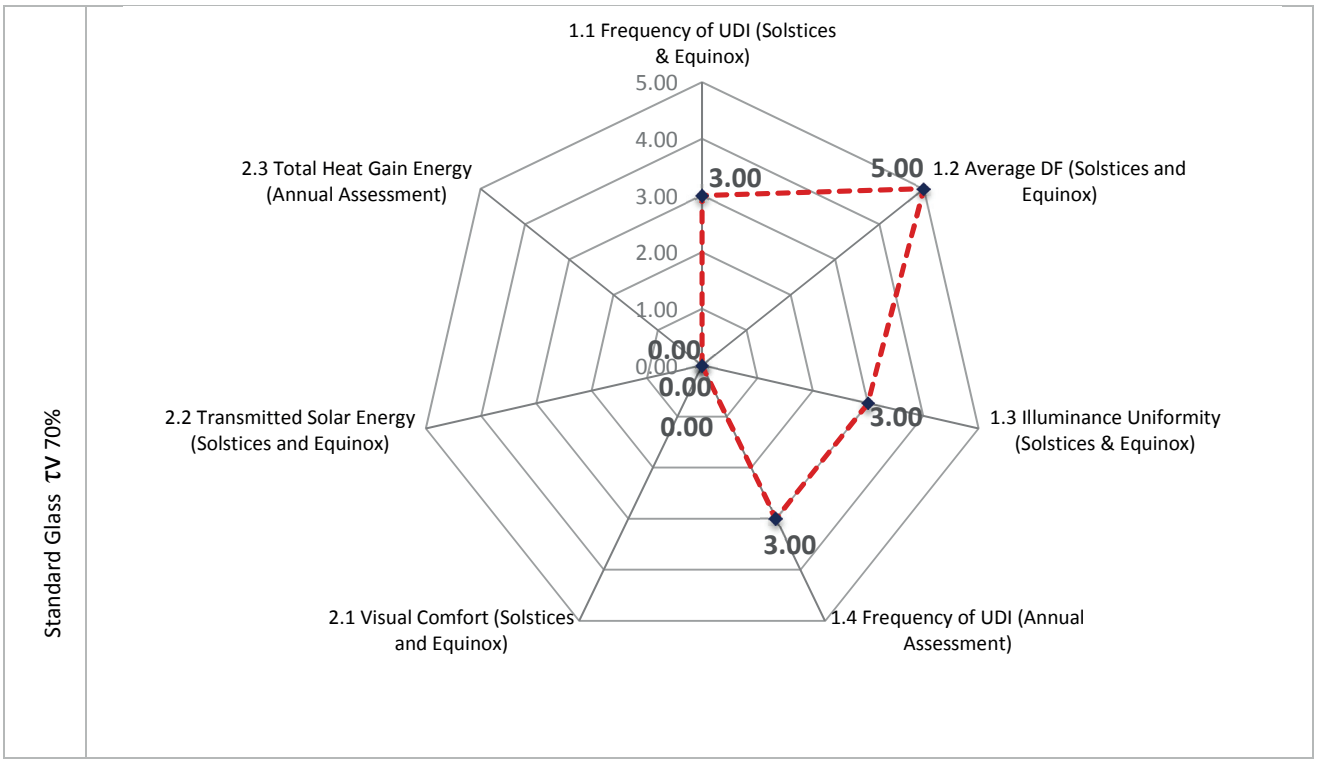

Figure 5.8 Performance review of standard glazing (τv70%) in Building B2 comparing its achievements for seven performance criteria.

The performance's review of LCP in Building B2 is presented in Figure 5.9, which shows that the capabilities of LCP are better in the conditions related to creating an optimal interior daylight distribution. For the latter, 'good' and 'best' performance are obtained in the four corresponding conditions. Thus, for the assessment of the 'useful' illuminance ranges present in the room when using LCP, it obtained a very good mark, while good illuminance uniformity was also shown for this system. Its weakness lies in the visual comfort assessment where it obtains the last position. However, this seems to be an inherent problem of the building design, since all CFS fail to maintain a sound visual comfort for the occupants in this case (Section 3.5.1). In the same way, for the assessments of thermal comfort (solstices and equinox and in annual basis), the LCP shows a bad performance. In brief, even LCP present excellent qualities regarding the interior daylight distribution, its performance in regards to the occupant's comfort is discouraging. The use of a mobile sun shading device remains a possible solution in this case, however its combined performance should be evaluated, and other CFS might however perform better in this building.

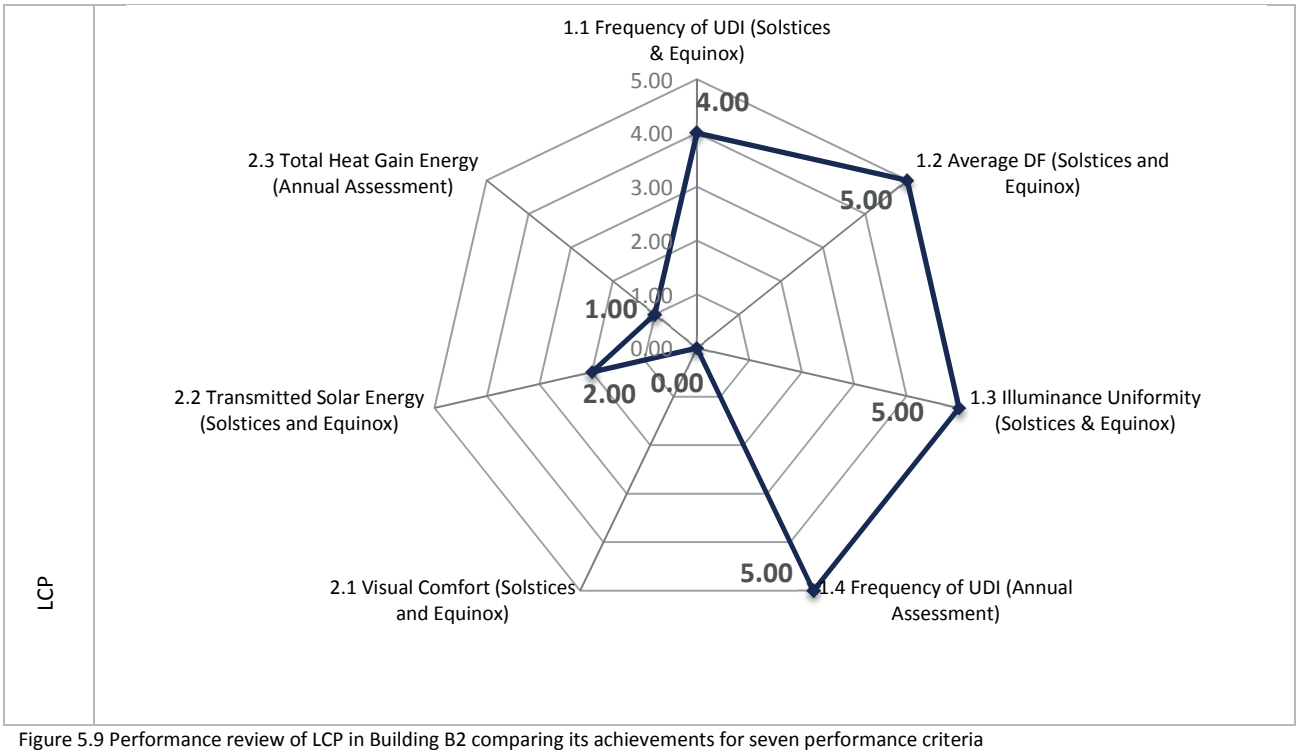

Figure 5.9 Performance review of LCP in Building B2 comparing its achievements for seven performance criteria

The review of the performance of Film 3M is illustrated on Figure 5.10, showing that the advantage of this system in Building 2 lies in its capability to maintain a uniform illuminance in the office room. On the other hand, it shows a poor performance in maintaining illuminance within the useful ranges (See Section 4.2.1.2), as it obtained a moderate ranking for such assessments (1.1 and 1.4). Regarding the thermal comfort of the occupants, Film 3M offers of a sound thermal comfort for the winter and summer solstices, while on an annual basis it shows also a mixed result.

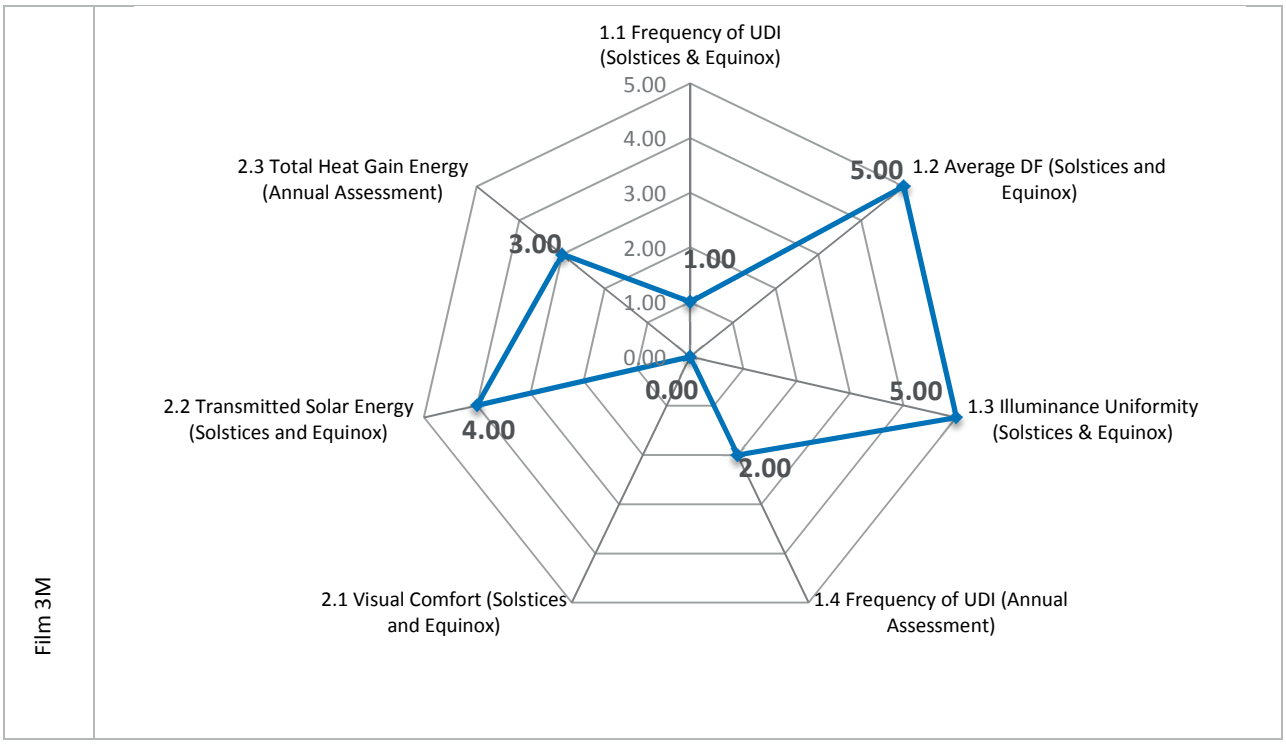

Figure 5.10 Performance review of Film 3M in Building B2 comparing its achievements for seven performance criteria.

The overall performance of CFS1 relative to the conditions assessed is shown in Figure 5.11. It can be observed that CFS1 shows a sound performance in the prevalence of illuminances within the 'useful' range in the room, obtaining a good mark for both annual and the solstices and equinox assessment (1.1 and 1.4). One of its weak points lies in the illuminance uniformity as it shows a moderate performance compared to the other five CFS. Regarding thermal comfort CFS1 shows better performance on an annual basis (2.3) than in the solstices and equinox assessment (2.2).

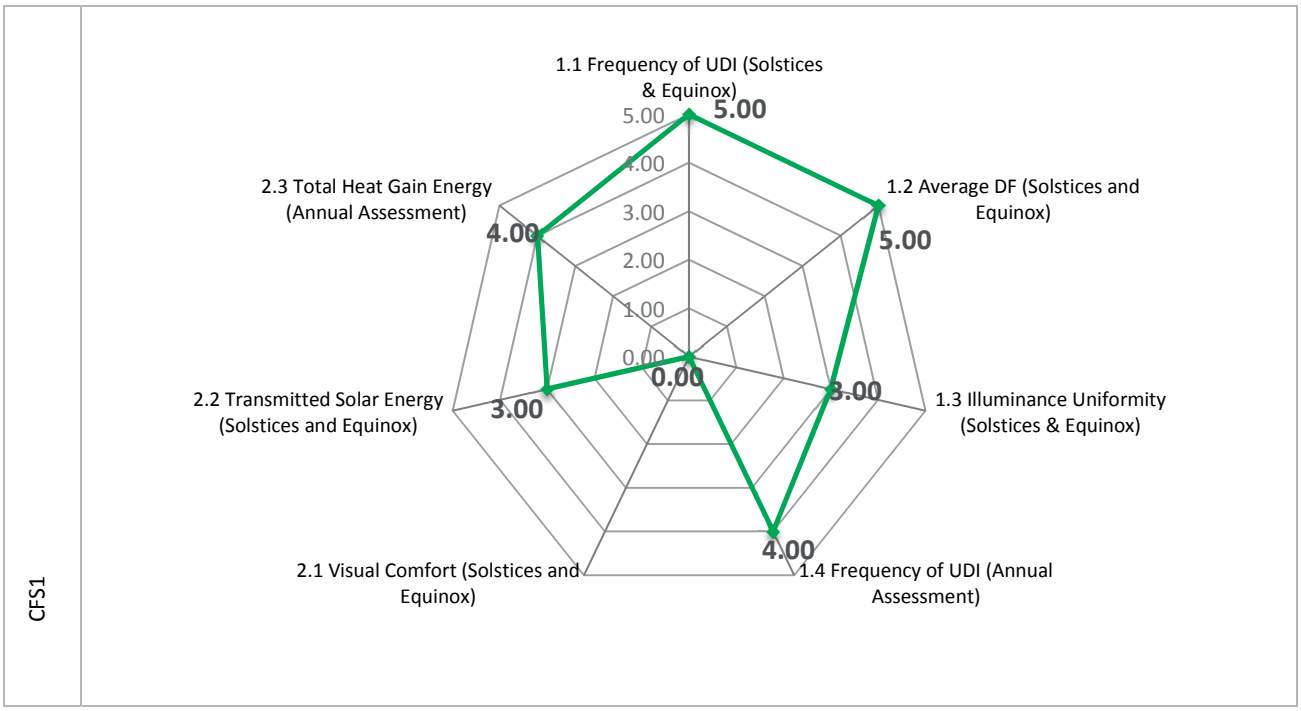

Figure 5.11 Performance review of CFS1 in Building B2 comparing its achievements for seven performance criteria.

The performance review of CFS2 is illustrated on Figure 5.12, which shows moderate to bad performance for the prevalence of illuminance within useful ranges for this system as it obtained one of the lowest marks for this criterion. As shown in Section 4.2.1.2, CFS2, is one of the bests in allowing the target range (300-500 lux) of illuminance in the room and is still questinable in maintaining a prevalence of the acceptable range (500 – 1800 lux). One advantage of CFS2 in this building lies in its capacity to offer a sound thermal comfort environment on an annual basis compared to the other CFS; however in the assessments for equinox and solstices it shows a rather poor performance. Visual comfort, as explained previously, is however rather poor showed for all the assessed fenestration systems.

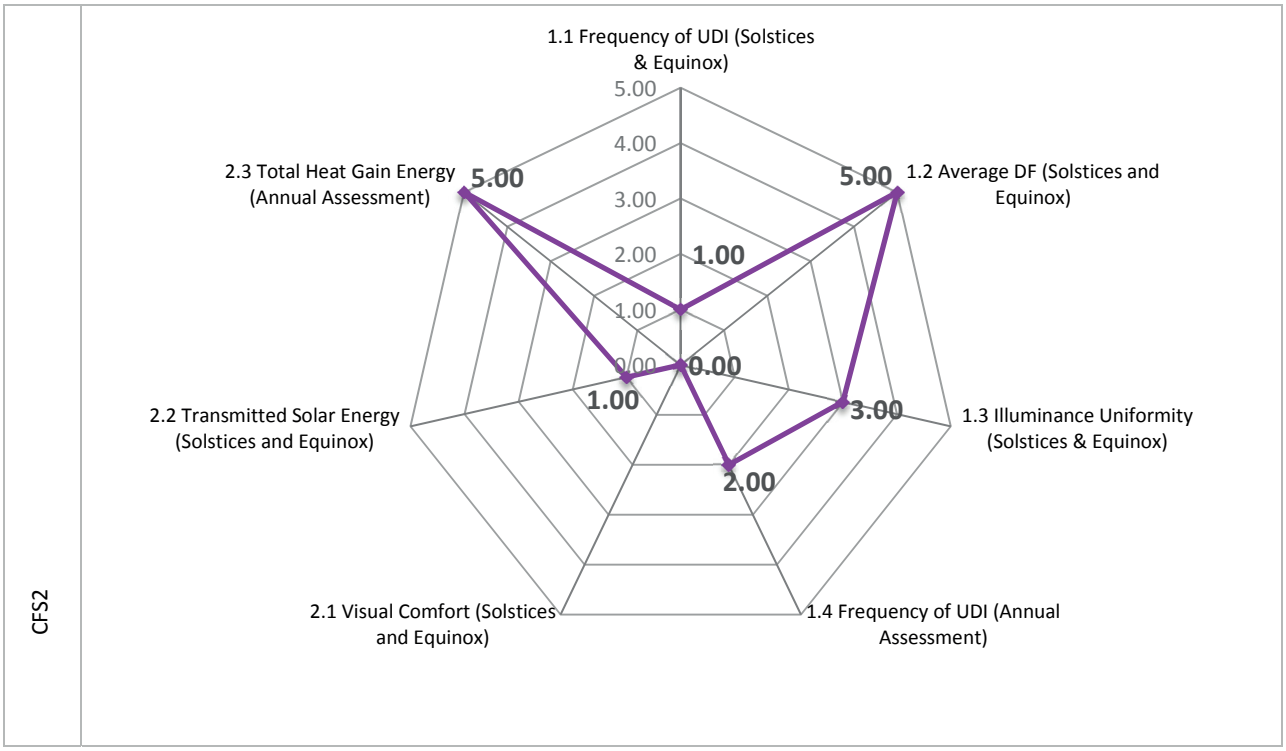

Figure 5.12 Performance review of CFS2 in Building B2 comparing its achievements for seven performance criteria.

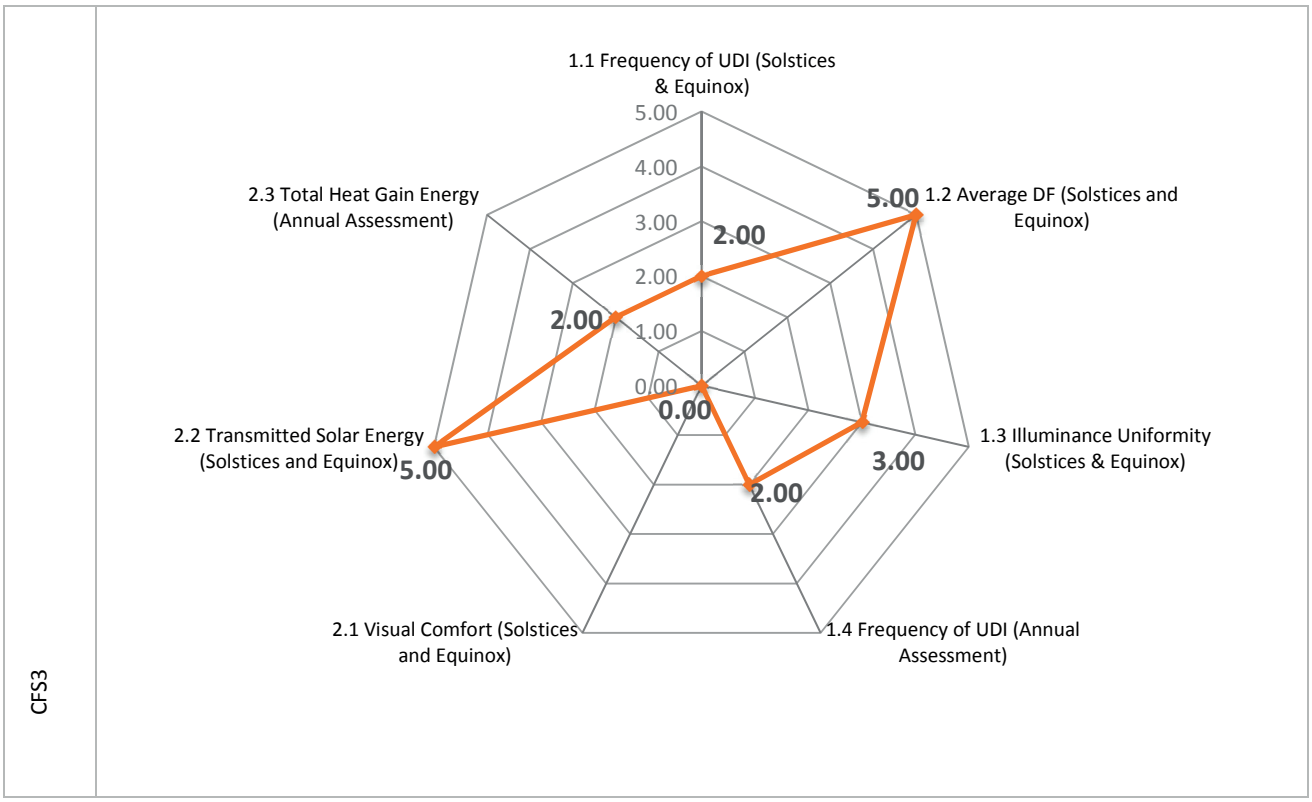

Figure 5.13 Performance review of CFS3 in Building B2 comparing its achievements for seven performance criteria.

As it can be seen in Figure 5.13, CFS3 shows a good performance under overcast sky conditions (1.2), a result rather similar for all the considered fenestration systems; it must be emphasised again that the characteristics of the office room in Building B2 contribute to maintain a sound illuminance distribution for diffuse daylighting. CFS3 shows advantage regarding thermal comfort for the assessment at the solstices and equinox, unlike the annual results basis, which are probably more reliable for this kind of assessment. In the annual assessment its performance was moderate being one of the three fenestration systems allowing the larger solar heat gains into the room (e.g. it is only overcome by the LCP and the standard glazing τv70%.) For indoor daylight distribution, mixed performance was achieved in the condition that assesses the uniformity of illuminance and in the ability of keeping a prevalence of illuminance within useful ranges in equinox and solstices; on an annual basis it obtained a poor mark compared with the other CFS.

5.3 Analysis of costs

Given the different characteristics of the considered CFS, the cost of the material and installation plays an important role in the convenience of their use. In order to take that in to account, a brief analysis of the commercial prize of the systems is included in this section. For most of the systems it was provided an approximate price that would include the material and installation, since its abosolute price varies accordingly to particular situations (sidelight or skylight installation, new building or retrofitting and so on). However, it was found that the systems CFS1, CFS2 and CFS2 are still in the phase of testing technologies; therefore no information can currently be provided regarding its cost. In the case of the Film 3M, the price provided it's a rough estimation that includes the window sash which is recommended for its use with the system. However it has been emphasized by the manufacturer that the height of a window has a large effect on the cost due to the sizes in which the system is produced. In the case of LCP, the price varies mainly on the kind of installation to be performed. In the case of vertical windows an exterior installation would be more expensive than an interior one, for skylights a retrofitting installation would be more expensive than the one performed at the time of the building construction. The price estimation is presented in Table 5.6.

Fenestration System			**Approximate price / m²**	**Installation required**
Standard clear glass	**simple**	4mm	65€-80CHF	standard
		6mm	80€-98CHF	standard
	double	4mm + 16mm air	150€-180CHF	standard
		4mm + 16mm argon	280€-340CHF	standard
CFS	**LCP**	-	$300USD-285CHF	attached to glass panes
	Film3M	retrofit	$380-480USD-360-460CHF	laminated to/between glass panes
		new construction	$270-370USD-260-370CHF	
	CF1	-	N/A	joint to a glass pane or laminated to a continuous glass pane
	CF2	-	N/A	
	CF3	-	N/A	

Table 5.6 Approximate price estimation including clear standard glass and CFS as provided by their manufacturers [142, 143].

Chapter 6 Conclusions

6.1 Main results

The objective of this Thesis was to investigate the potentiality of incorporating Complex Fenestration Systems (CFS) in a daylighting procedure applied to buildings located at low latitudes. Such purpose represents a challenge due to the unfavourable effects that the inclusion of daylight in buildings may imply in those regions, such as the increment in the risk of glare and overheating. In order to explore such potentiality five CFS were selected to be virtually tested using computer simulations in two office rooms located in the centre-north of México (Zacatecas 22° 783' N., 102° 583' W, Altitude: 2543m). Their performance was assessed according to three main criteria: the interior daylight distribution, the visual and the thermal comfort of the occupants. The assessment was performed in two ways, first their performance was assessed during the three most critical yearly periods in terms of daylight conditions: winter and summer solstices, and spring equinox; a second assessment was perform on an annual basis. The first way might provide more accurate results regarding the daylighting performance given that the simulations were carried-out using real-time weather data obtained from the closest local meteorological station; additionally the simulation procedures applied in the first case might even provide more accurate results (See Section 3.2). Nonetheless, the weather data file employed for the annual simulation of the second way represents a several years' average of the local climate. In the case of thermal comfort assessments, annual year-round evaluation can provide more reliable results than a single day assessment at winter or summer solstices. The simulation results using the five pre-selected CFS were compared with those obtained for the current existing conditions in the two office rooms; in order to evaluate the improvements achieved using CFS over the actual daylighting practice at low latitudes.

The results obtained in this study allow concluding that the use of CFS represents an opportunity for improving the indoor daylighting situations in buildings located at low latitudes. The latter comprises not only an improved daylight distribution, but also a more comfortable visual and thermal environment for the occupants. However, it can mustbe outlined that in order to carry-out an appropriate CFS selection, a comprehensive assessment of its features and daylighting performance relative to the proper sky conditions of the building site is imperative. Such statement is made according to the results of this study, which show that the detailed assessment of the daylighting performance of five CFS was favourable enough to evidence their advantages and drawbacks regarding their application for buildings with predominant clear sky conditions.

For such weather conditions, the aforesaid relative merits are more relevant in regards to the thermal and visual comfort of occupants: an adequate CFS has the potential of contributing significantly to maintain a satisfactory indoor environment for the occupants, as demonstrated by the investigations carried-out on the five selected CFS. However, as mentioned in Chapter 4, the improvement of the interior daylight distribution was predominant for the leading CFS over the one of thermal comfort. Given that the use of external movable sun shadings is invariably commended to mitigate unfavourable cooling loads in these regions.

It can also be asserted that CFS performance assessments, especially for sites with severe climatic conditions (such as those of low latitudes), require an annual assessment to be fully convincing. Given that, it was observed that the partial assessment that took only the Solstices and the Equinox into account shows results differing from those obtained with the annual assessment. However by comparing the monitored daylighting performance of the current fenestration systems of the two office rooms with the computer simulations of the five different CFS, their suitability for the location was established; a selection of a stand-out CFS was even made.

6.2 Summary

This thesis explored the application of an integrated daylighting approach for buildings located in sunny climate conditions; such approach included the assessment of three different criteria that are relevant to the inclusion of daylight in such areas: assessment of the interior daylight distribution, the thermal and the visual comfort of the occupants. The latter were carried-out using advanced computer simulations with recent capabilities for the CFS performance assessement on annual basis, which represent an innovation. Such integral assessment led to determine the CFS potential to improve the interior daylight environment in the two office rooms. A review of such assessment results is presented in this section.

6.2.1 Building B1

This study outlined the potential of the five considered CFS to improve the interior daylight distribution in Building B1. It was observed that the use of standard glass leads to a higher daylight flux inside the room, however as mentioned in the conclusions presented in Section 3.4.4, a higher extent of daylight provision is not a sufficient indicator of an appropriate interior daylight environment. Regarding the CFS potential to improve the visual comfort, DGP values below 0.2 were found when assessing the risk of glare in Building B1 which indicates a very low brightness scene which leads to an imprecise prediction of glare sources. The latter reveals a downside of the use of standard glass in this room. In regards to the thermal effects of the fenestration systems in this room, larger solar energy was allowed by the standard glass, a situation that might be found convenient in winter time but that provides unfavourable effects in summer time for buildings located in sunny climates. Considering the existing situation (tinted glass τv 12%), the use of standard glass with a lighting transmittance of 80% signified a 700% increase in terms of solar gains into the room. However it was found that the use of Film 3M and CFS2 also signify larger amounts while the use of CFS1 signified less, thus it can be recommended for this building regarding the creation of a satisfactory thermal interior environment. In the overall assessment, LCP attained the highest score compared with the other fenestration systems, a second position was achieved by Film 3M with a difference of around 40 points: such difference is considered to be sufficient to determine the most convenient CFS to use. However, when it comes to a final decision an important aspect to consider is the price of the system. Even if such aspect is hardous to be precisely estimate, it can be observed that the Film 3M might be slightly more expensive since its application for retroffiting would represent an increment of about 120-160% compared with the use of LCP: thus in this case it confirms the advantage of the LCP.

6.2.2 Building B2

The assessment of the potential of CFS to improve the interior daylight distribution in Building B2 showed that larger daylight fluxes are admitted into the room when using the standard glass, while the use of CFS reduced the admission of daylight in the room. Regarding the CFS potential to create an adequate interior visual environment for the occupants, the assessment of the glare risk showed that the use of standard glass and CFS would lead to risks of intolerable glare sensation. In this case, the use of CFS did not contribute to an improved visual comfort situation in this building, therefore its potential regarding the reduction of the risk of glare was found as limited. In such cases the use of a solar protection would be necessary. Nonetheless, when considering other opportunities to mitigate such effects, a possible solution would be the reduction of the size of the window. However, besides of the uncertain financial convenience, such action would alter the exterior appearance of the building, requiring the agreement of the landowner and the consent of the architect, who in many cases would consider the exterior appearance of the building as first priority. In such cases, when building design leads and therefore the architectural modification is not an option, the use of CFS might represent an opportunity for using CFS combined with a solar protection device in order to improve the interior daylight environment in retroffiting building or new construction. In regards of the convenience of using CFS for creating a satisfactory interior thermal environment, the results in Building B2 were quite similar for the six fenestration systems considered. The standard glass admits slightly larger solar gains into the room, among the CFS, the LCP allowed higher levels while CFS3 allowed less, thus it could be recommended when the only objective is to attain a comfortable thermal interior environment. In the overall assessment, CFS1 attain the highest score while three CFS shared a second position with a slight difference of about 20 points. Due to the small difference, the comparison of their costs represents an important aspect to consider. The latter, would lead in this case on using either CFS1 or LCP: unfortunately due to the lack of information regarding the microstructured daylighting systems costs (CFS1, CFS2, and CFS3) it is impossible to include such aspect in the final decision.

6.3 A computer based daylighting integrated approach for buildings located in sunny climates

The selection of an outstanding CFS that contributes to improve the interior daylight environment in a building located in predominant sunny sky conditions represents a challenge not only due to different aspects that are taken into account, but mainly due to the counteractions that each of those aspects have in an overall result. The implementation of an integrated assessment is fundamental to effectively determine the occasions in which the inclusion of daylight would signify favourable or unfavourable effects in a room. Such deduction would be the result of a detailed evaluation of the 'all-possible' occurring daylight situations, thus by the performance of an annual based assessment.

The CFS performance is strongly related to the sunlight incidence angles on the building's façade as it was also shown by the results obtained in this study, thus the building location and orientation are key aspects influencing the performance of CFS in a building. Additionally, this study has also shown that the design of the building influences the CFS performance as well. It was observed in Building B2 that the integrated overhang was determinant in the reduction of the solar gains in the room. In the same way, the large WWR is determinant to create an interior environment with an elevated risk of discomfort glare sensation, for which the CFS induces insignificant to none improving effects. In brief, one can conclude that the selection of an adequate CFS cannot be easily standardized, yet it would be the result of a comprehensive assessment that takes into account all the aspects involved in the building's architecture. Therefore, the results of this study, in which the comprehensive assessment of the performance of five CFS lead to affirm that LCP and CFS1 are those that improve more the interior daylighting situation, a conclusion for the two particular buildings presented in this study. However, the procedure employed in this study can be useful to be applied in other studies in order to assess the performance of CFS for selecting the most appropriate one to be used in any particular case.

Additionally to the results of this study, a relevant aspect to take into account regarding the convenience of using CFS to improve the interior daylight situation in buidings is their cost, which might be determinant in many cases due to the larger cost of the CFS compared to standard glass (See Section 5.3). As shown in the assessment of the interior daylight distribution presented in this study, the use of standard glass signifies large indoor illuminance levels, although unfavourable in some cases (especially in low latitude locations), such effects can be mitigated with the use of a sun shading, in some cases at a lower extent than the use of a CFS. However such extent and thus the convenience of using either a standard glass or a CFS can only be determined following a comprehensive assessment, such as the one presented in this study. Regarding this, it should be noted that this study focused its objective in assessing the CFS potential to improve the interior daylight environment in buildings located in prevailing sunny sky conditions, which represents an advanced daylighting approach. However, in order to achieve an improved interior daylight situation the use of basic steps should be considered beforehand, as briefly explained in Annex 6.1.

6.4 Future outlook

In buildings located at low latitudes, the intensive use of daylighting represents a major risk for the visual and thermal comfort of the occupants. It has been however shown in this study that the use of an appropriate-selected CFS can improve the interior daylight distribution in buildings located in such regions (mostly dominated sunny climates); moreover their additional functioning as a shading device might also contribute to improve the visual and thermal comfort. However, it has also been evident that in regards to the mitigation of glare risks in some cases the effect of CFS is overcome by the overall building environment. In such cases, the use of additional sun shading becomes imperative in order to offer a satisfactory indoor environment quality to the occupants by reducing glare and overheating risks. Thus, the performance assessment of CFS combined with a simultaneous use of different configurations of shading devices (overhangs, exterior blinds, venetian blinds, fins, etc.) would be a relevant step in the direction of achieving an optimal interior daylighting in buildings located at low latitudes. In this case, the inclusion of thermal and visual comfort assessments and year round evaluations (similar to the ones carried-out in this study) would provide reliable results.

This work can be improved by the use of other leading-edge existing evaluation thechniques, such as the use of HDR images for assessing the on-site luminance of the interior surfaces in the office rooms, thus its implications regarding visual comfort. Such data could be later used to compare the results obtained of simulations using CFS. An additional improvement could be the possibility of performing glare annual assessments; however such evaluation is currently unavailable with the use of BSDF data of CFS.

A further aspect to investigate would be to determine the implications that the use of CFS would have in the energy reduction for electric lighting then accordingly quantifying the financial return of using CFS. The latter would be done by assessing the performance of CFS in combination with the use of lighting controls, in order to determine the impact that the use of CFS due to its lighting redirection effect, might have in the reduction of electric lighting especially at the back of the room.

References

1. Gruzinski, S., *The Aztecs, Rise and Fall of an Empire*. 2003 ed. New Horizons. 1992, London, UK: Thames & Hudson.
2. CONACULTA. *Instituto Nacional de Antropología e Historia*. 2010; Available from: http://www.inah.gob.mx/.
3. Aveni, A., *Skywatchers of Ancient México*. Texas PanAmerican Series. 1980: University of Texas Press.
4. Mazria, E., *The Passive Solar Energy Book*. 1979, USA: Rodale Press, Emaus, Pa.
5. Richter, C., D. Lincot, and C.A. Gueymard, *Solar Energy*. 2012, New York: Springer.
6. Suri, M. and T. Cebecauer. *GeoModel Solar, High Resolution Solar Data*. 2008; Available from: www.solargis.info.com.
7. Gasca, C.A.E., et al., *Vision a Largo Plazo Sobre la Utilizacion de las Energias Renovables en México*, in *Energia Solar*. 2005, Centro de Investigacion en Energia, UNAM: México D.F, MEX.
8. C.V, S.S.A.d., *Irradiaciones Global, Directa y Difusa en Superficies Horizontales e Inclinadas, así como Irradiación Directa Normal para la República Mexicana*. 2003, Solartronic: Cuernavaca, Morelos, MX.
9. Lacomba, R., et al., *Arquitectura Solar y Sustentabilidad*. 2012, Mexico D.F: Editorial Trillas.
10. Anselmo, F. and J. Mardaljevic, *Daylight Mapping, Planet Earth*, in *Daylight and Architecture VELUX*. 2013, VELUX. p. 13-21.
11. Federal Office of Meteorology and Climatology, M. *Satellite-based information for planning solar energy applications*. 2005 05.02.2013; Available from: www.meteoswiss.admin.ch.
12. Roldan, F.T. and E.G. Morales, *Renewable Energies for Sustainable Development in México*. 2006: Mexico D.F. MEX.
13. IEA. *International Energy Agency*. 2014; Available from: www.iea.org.
14. Torgal, F.P., et al., *Nearly Zero Energy Building Refurbishment, A Multidisciplinary Approach*. 2013, London UK: Springer.
15. Torcellini, P., S. Pless, and M. Deru, *Zero Energy in Buildings: A critical Look at the Definition*, in *ACEEE Summer Study on Energy Efficiency of Buildings* 2006: Pacific Grove, California.
16. Carmody, J., et al., *Window Systems for High-Performance Buildings*. 2004, New York, USA: Norton & Company, Inc.
17. Kurnitski, J., et al., *How to define nearly net zero energy buildings nZEB.* REHVA Federation of European Heating Ventilation and Air-conditioning Associations, 2011.
18. Galvez, D.M., *Efificacion Sustentable en México: Retos y Oportunidades*. 2011, Academia de Ingenieria, México: México City.
19. Molina, C.M., *Estrategias Institucionales para Fomentar la Edificacion Sustentable en América del Norte: Caso México*. 2007: Cocoyoc Morelos, México.
20. Gobierno de la Republica, M., *Plan Nacional de Desarrollo 2013-2018*. 2013: México City.
21. Darula, S. and R. Kittler, *Lighting Energy Savings due to Daylight: Time Efectiveness based on Bratislava Data.* Building Research Journal, 2008. **56**(4): p. 241-253.
22. Altomonte, S., *Daylight for Energy Savings and Psycho-Psysiological Well-Being in Sustainable Built Environments.* Journal of Sustainable Development, 2008. **1**(3).
23. Boyce, P., C. Hunter, and O. Howlett, *The Benefits of Daylight through Windows*. 2003, Lighting Research Center, Rensselaer Polytechnic Institute: Troy, New York.
24. Brainard, G.C., et al., *Human Melatonin Regulation is not Mediated by the Three Cone Photopic Visual System.* Journal of Clinical Endocrinology and Metabolism, 2001. **86**(1): p. 433-436.
25. Cajochen, C., *Alerting effects of light.* Sleep Medicine Reviews, Elsevier, 2007. **11**: p. 453-464.
26. Scartezzini, J.-L. and G. Courret, *Anidolic Daylight Systems.* Solar Energy, 2002. **73**(2): p. 123-135.
27. Wittkopf, S.K., *Daylight performance of anidolic ceiling under different sky conditions.* Solar Energy, 2006. **81**(2): p. 151-161.
28. Wittkopf, S.K., E. Yuniarti, and L.K. Soon, *Prediction of energy savings with anidolic integrated ceiling across different daylight climates.* Energy and Buildings, 2006. **38**(9): p. 1120-1129.
29. Linhart, F., S. Wittkopf, and J.-L. Scartezzini, *Performance of Anidolic Daylighting Systems in Tropical climates-Parametric studies for identification of main influencing factors.* Solar Energy, Elsevier, 2010. **84**: p. 1085-1094.
30. Ochoa, C.E. and I.G. Capeluto, *Evaluating visual comfort and performance of three natural lighting systems for deep office buildings in hightly luminous climates.* Building and Environment, 2006. **41**(8): p. 1128-1135.

31. Tsikaloudaki, K., S. Anagnoustou, and K. Nichoritis, *Investigating the performance of anidolic vertical openings under real conditions in Greece*, in *Conference on Passive and Low Energy Architecture, PLEA*. 2008: Dublin, Ireland.
32. Soler, A. and P. Oteiza, *Light Shelf performance in Madrid, Spain.* Building and Environment, 1997. **32**(2): p. 87-93.
33. SABRY, H.M.K., *The impact of daylighting-guiding systems on indoor natural light penetration, simulation analysis for light-shelves*, in *PLEA 2006 - The 23rd Conference on Passive and Low Energy Architecture,*. 2006: Geneva, Switzerland.
34. Freewan, A.A., L. Shao, and S. Riffat, *Optimizing performance of the lightshelf by modifying ceiling geometry in highly luminous climates.* Solar Energy, 2007. **82**: p. 343-353.
35. Edmonds, I.R. and P.J. Greenup, *Daylighting in the tropics.* Solar Energy, 2002. **73**(2): p. 111-121.
36. G.Ward and R. Shakespeare, *Rendering with Radiance, The Art and Science of Lighting Visualization*. 1997: Morgan Kaufmann.
37. Sibilio, S., P. Falconetti, and L. Maffei, *Daylighting design for low energy buildings in South Italy*, in *25th Conference on Passive and Low Energy Architecture, PLEA*. 2008: Dublin, Ireland.
38. Luther, M.B., *Studies on a Daylight-guiding System for an Office.* Anzses, 2006: p. 1-8.
39. Carli, M.D. and V.D. Giuli, *Optimization of daylight in buildings to save energy and to improve visual comfort: analysis in different latitudes*, in *11th International IBPSA Conference*: Glasgow, Scotland.
40. Lenoir, A., et al., *Optimisation Methodology for the Design of Solar Shading for Thermal and Visual Comfort in Tropical Climates*, in *13 Conference of International Building Performance Simulation Association*. 2013: Chambéry, France.
41. Bodart, M. and A.D. Herde, *Global energy savings in offices buildings by the use of daylighting.* Energy and Buildings, Elsevier, 2001. **34**: p. 421-429.
42. Scartezzini, J.-L., et al., *Laboratoire de Lumiere Naturelle, Programme Interdisciplinaire LUMEN, Projet OFEN*. 1994, Université de Genève, Ecole Polytechnique Fédérale de Lausanne: Lausanne.
43. Thanachareonkit, A., *Comparing physical and virtual methods for daylight performance modelling including complex fenestration systems*, in *LESO-PB*. 2008, École Polytechnique Fédérale de Lausanne: Lausanne.
44. Reinhart, C. and A. Fitz, *Findings from a survey on the current use of daylight simulations in building design.* Energy and Buildings, 2006. **38**(7): p. 824-835.
45. Ochoa, C.E., M.B.C. Aries, and J.L.M. Hensen, *State of the art in lighting simulation for building science: a literature review* Building Performance Simulation, 2011.
46. Moeck, M. and S.E. Selkowitz, *A computer-based daylight systems design tool.* Elsevier, 1996. **5**: p. 193-209.
47. Reinhart, C. and P.-F. Breton, *Experimental validation of 3Ds Max design 2009 and Daysim 3.0*, in *Building Simulation, Eleventh International IBPSA Conference* 2009: Glasgow, Scotland.
48. Reinhart, C. and J. Wienold. *DAYSIM*. 1998; Software for Daylight prediction]. Available from: http://www.daysim.com/.
49. Perez, R., R. Seals, and J. Michalsky, *All-Weather Model for Sky Luminance Distribution, preliminary configuration and validation.* Solar Energy, 1993. **50**(3): p. 235-245.
50. Andersen, M., et al., *An intuitive daylighting performance analysis and optimization approach.* Building Research & Information, 2008. **36**(6).
51. Paule, B., F. Flourentzou, and M. Bauer. *Estia. Mise en oeuvre du développement durable dans l'environnement construit*. Available from: www.estia.ch.
52. Lagios, K. *DIVA for Rhino*. 2014; Available from: www.diva4rhino.com.
53. Kämpf, J., C. Basurto, and J.L. Scartezzini. *Geronimo, visualization of the impact of complex fenestration systems based on Radiance*. 2011; Available from: http://leso.epfl.ch/page-75134-fr.html.
54. Kämpf, J. and J.-L. Scartezzini, *GERONIMO: the CFS Daylighting Wizard*, in *4th VELUX Daylight Symposium*. 2011: Lausanne, Switzerland.
55. Relux Informatik, A., *Raytracing Manual*. 2011.
56. Andersen, M. and J.d. Boer, *Goniophotometry and assessment of bidirectional photometric properties of complex fenestration systems.* Energy and Buildings, 2006. **38**: p. 836-848.
57. Scartezzini, J.-L., et al., *Bi-directional photogoniometer for the assessment of the luminous properties of fenestration systems*, in *CTI Project-Scientific Report*. 2000, EPFL: Lausanne.
58. Tregenza, P.R., *Subdivision of the sky Hemisphere for Luminance Measurements.* Lighting Res. Technology, 1987. **19**(13): p. 13-14.
59. Andersen, M., *Innovative bidirectional video-goniophotometer for advanced fenestration systems*, in *Architecture; Faculté Environnement Naturel, Architectural et Construit*. 2004, Ecole Polytechnique Fédérale de Lausanne: Lausanne, Switzerland.
60. Aydinli, S. and H. Kaase, *Measurement of Luminous Characteristics of Daylighting Materials, IEA SHCP TASK 21 / ECBCS ANNEX29*. 1999, Technischen Universität Berlin: Berlin.

61. Kämpf, J. and J.-L. Scartezzini, *Integration of BT(R)DF data into Radiance Lighting Simulation Programme, Technical Report* 2004, EPFL: Lausanne.
62. Greenup, P.J., I.R. Edmonds, and R. Compagnon, *Radiance algorithm to simulate laser-cut panel light-redirecting elements.* Lighting Research and Technology, 1999. **32**(2): p. 49-54.
63. LBNL. *LBNL Window 6 & Daylighting Software*. 2006; Available from: http://windows.lbl.gov/software/window/6/.
64. Kämpf, J.H. and J.-L. Scartezzini. *Ray-Tracing simulation of Complex Fenestration Systems Based on Digitally Processed BTDF data.* in *CISBAT 2011*. 2011. Lausanne, Switzerland.
65. G. Ward, R.M., E. S. Lee, A. McNeil, J. Jonsson, *Simulating the Daylight Performance of Complex Fenestration Systems Using Bidirectional Scattering Distribution Functions with Radiance.* Journal of the Illuminating Engineering Society of North America, 2011.
66. Tregenza, P.R., *Daylight Coefficients*, in *CIBS National Lighting Conference*. 1982: Warwick, UK. p. 65-71.
67. Littlefair, P.J., *Daylight coefficients for practical computation of internal illuminances.* Lighting Research and Technology, 1992. **24**(3): p. 127-135.
68. Mardaljevic, J., *Simulation of annual daylighting profiles for internal illuminance.* Lighting Research and Technology, 2000. **32**(3): p. 111-118.
69. Bourgeois, D., C.F. Reinhart, and G. Ward, *Standard daylight coefficient model for dynamic daylighting simulations*. 2013, Ecole d'architecture, Université Laval: Québec, Canada.
70. Klems, J.H., *A new method for predicting the solar heat gain of complex fenestration systems II. Detailed description of the matrix layer calculation*, in *ASHRAE Transactions*. 1993, Lawrence Berkeley Laboratory, University of California: Berkeley, CA.
71. McNeil, A. and E. Lee, *A validation of the Radiance three-phase simulation method for modeling annual daylight performance of optically complex fenestration systems.* Journal of Building Performance simulation 2012. **1**(14): p. 1-20.
72. Klems, J.H., *A new Method for Predicting the Solar Heat Gain of Complex Fenestration Systems*. 1994, Lawrence Berkeley Laboratory: Berkeley, CA.
73. McNeil, A., *The Three-Phase Method for Simulating Complex Fenestration with Radiance*. 2010, Lawrence Berkeley National Laboratory: Berkeley, CA p. 1-35.
74. McNeil, A., *The Five-Phase Method for Simulating Complex Fenestration with Radiance*. 2013, Lawrence Berkeley National Laboratory: Berkeley, CA.
75. IESNA, *IES Lighting Handbook, Reference Volume*. 1984: Illuminating Engineering Society of North America (IESNA).
76. Bellia, L., et al., *Daylight glare: A review of discomfort indexes*, Università degli Studi di Napoli Federico II: Naples, Italy. p. 1-6.
77. Jakubiec, J.A. and C.F. Reinhart, *The 'adaptive zone' - A concept for assessing discompfort glare throught daylight spaces.* Lighting Research and Technology, 2011. **44**(149): p. 1-23.
78. Wienold, J. and J. Christoffersen, *Evaluation methods and development of a new glare prediction model for daylight environments with the use of CCD cameras.* Energy and Buildings, 2006. **38**: p. 743-757.
79. Chauvel, P., *Glare for windows: current views of the problem.* Lighting Res. Technology, 1982. **14**(1): p. 31-46.
80. Wienold, J., *Dynamic Daylight Glare Evaluation*, in *11th International IBPSA Conference*. 2009: Glasgow, Scotland.
81. Becchi, E., et al., *Daylighting in Architecture, an european reference book*, ed. N. Baker, A. Fanchiotti, and K. Steemers. 1993: James & James for the Comission of the European Communities, Directorate-General XII for Science, Research and Development.
82. Nazzal, A.A., *A new daylight glare evaluation method: Introduction of the monitoring protocol and calculation method.* Energy and Buildings, 2001. **33**(13): p. 257-265.
83. Wienold, J., *Evalglare documentation v. 1.0*. 2012, Fraunhofer Insitute for Solar Systems: Freiburg, Germany.
84. Crawley, D.B., et al., *Energy Plus: creating a new generation building energy simulation programme.* Energy and Buildings, 2001. **33**: p. 319-331.
85. Energy, U.S.D.o. *Energy Plus*. 1996 2003; Available from: http://apps1.eere.energy.gov/buildings/energyplus/.
86. Servicio Meteorologico Nacional, M. *CONAGUA Comision Nacional del Agua*. 2010; Available from: www.smn.cna.gob.mx.
87. Tyson, P.J. *Sunshine Guides*. 2002 2010; Available from: www.climates.com.
88. Geo-Mexico. *Geo-Mexico, the geography and dynamics of modern Mexico*. 2010-2014; Available from: www.geo-mexico.com.
89. Boyce, P.R., *Evaluating Lighting Quality*, in *3rd European conference on Energy-Efficient Lighting*. 1995: Newcastle Upon Tyne, England. p. 189-196.

90. Boyce, P.R., et al., *Lighting quality and office work: two field simulation experiments.* Lighting Research and Technology, 2006. **38**(3): p. 191-223.
91. Boyce, P.R., et al., *Lighting Quality and Office Work: a Field simulation Study*. 2003, U.S. Department of Energy: Washington.
92. Commission Internationale de l'Eclairage, C.T.-. *A Unified Framework of Methods for Evaluating Visual Performance Aspects of Lighting.* 1972. **19**.
93. Weston, H.C., *The relation between illumination and visual efficiency-the effect of brightness contrast.* Medical Research Council, 1945. **87**: p. 35.
94. IESNA, *IESNA Lighting Handbook: Reference and Application*. 2000, New York: Illuminating Engineering Society of North America.
95. CIBSE, *Lighting Handbook* 1994, London, UK: The Chartered Institution of Building Services Engineers.
96. Scartezzini, J.-L. and B. Paule, *Eclairage des Bureau, Programme d'action RAVEL*, ed. RAVEL. 1994: Societé Suisse des Ingenieurs et des Architectes.
97. Fontoynont, M., et al., *Diagnostic en Eclairage, College des Pales Lutry s/ Lausanne*. 1989: Lausanne, Switzerland.
98. Michel, L., *Méthode Expérimentale d'Evaluation des performances lumineuses de Bâtiments*, in *Architecture*. 1999, Ecole Polytechnique Fédérale de Lausanne: Lausanne, Suisse. p. 209.
99. Licht, F.G. (2000) *Lighting with Artificial Light*. Licht wissen.
100. Fontoynont, M., *Daylight Performance of Buildings*. 1999, Lyon, France: James & James.
101. Moon, P. and P. Spencer, *Illumination from a non-uniform sky.* Illumination Engineering, 1942. **37**(10): p. 707-726.
102. CIE, C.I.d.L.E., *Natural Daylight, Official Recommendation*. 1955. p. 2-4.
103. Kittler, R. *Standardization of outdoor conditions for the calculation of daylight factor with clear skies*. in *The CIE International Conference on Sunlight in Buildings*. 1967. Rotterdam, Netherlands.
104. Igawa, N., H. Nakamura, and K. Matsuura, *Sky Luminance distribution model for simulation of daylit environment.* Building and Environment, 2001.
105. CIE, C.I.d.L.E., *Standardisation of luminance distribution on clear skies*. 1973: Paris, France.
106. Kittler, R. *Luminance models of homogeneous skies for design and energy performance prediction*. in *2nd International Daylighting Conference*. 1986. Atlanta, GA.
107. Nakamura, H., M. Oki, and Y. Hayashi, *Luminance distribution of intermediate sky.* Light and Visible Environment, 1985. **9**(1): p. 6-13.
108. Littlefair, P.J., *The Luminance distribution of an Average Sky.* Lighting Research and Technology, 1981. **13**(4): p. 192-198.
109. Kittler, R., *Luminance distribution characteristics of homogeneous skies: a measurement and prediction strategy.* Lighting Research and Technology, 1985. **17**(4): p. 183-188.
110. Perraudeau, M., *Luminance models*, in *National Lighting Conference 1988*. 1988: Cambridge, UK. p. 291-292.
111. Comission International de L'Eclairage, C., *Spatial distribution of daylight, CIE standard general sky*. 2002, CIE: Vienna, Austria.
112. Kittler, R., S. Darula, and R. Perez, *A set of standard skies, characterizing daylight conditions for computer and energy conscious design*. 1998, American-Slovak grant project US-SK 92052.
113. Kittler, R., R. Perez, and S. Darula. *A new generation of sky standards*. in *Conference Lux Europa*. 1997. Amsterdam, Netherlands.
114. Igawa, N., et al., *Models of sky radiance distribution and sky luminance distribution.* Solar Energy, 2004. **77**: p. 137-157.
115. Littlefair, P.J., *Measurements of the luminous efficacy of daylight.* Lighting Research and Technology, 1998. **20**: p. 177-188.
116. Robledo, L. and A. Soler, *Luminous efficacy of global solar radiation for clear skies.* Energy Conversion and Management, 2000. **41**: p. 1769-1779.
117. Perez, R., et al., *Modeling daylight availability and irradiance components from direct and global irradiance.* Solar Energy, 1990. **44**: p. 271-289.
118. Perez, R.R., et al., *Dynamic Global-to-Direct Irradiance Conversion Models.* ASHRAE, 1992. **98**(1).
119. Slater, T.F. (1999) *Constructing a Portable Sundial*. Astro Notes **37**.
120. LESO-PB, *CitySim* Lausanne. p. Urban energy planners support software.
121. Hosting, G.P., *su2rad Radiance exporter script for Sketchup*. 2008.
122. Arnoux, G.C., *Lightmeters C.A 811, C.A 813*. 2004, Chauvin Arnoux: Paris, France.
123. Ruck, N., et al., *Daylight in Buildings*. 2000: International Energy Agency (IEA).
124. Andersen, M., *Light distribution through advanced fenestration systems.* Builiding Research & Information, 2010. **30**(4): p. 264-281.

125. Edmonds, I.R., *Performance of laser cut light deflecting panels in daylighting applications.* Solar Energy Materials and Solar Cells, 1993. **29**: p. 1-26.
126. 3M, *3M Optical Lighting Film*, in *Technical Specification* 3M, Editor. 2000, Specified Construction Products Department: Minessota, US.
127. Saint-Gobain, *Lumitop, Daylighting glazing which redirects light*, Saint-Gobain, Editor: Yorkshire, UK.
128. Klammt, S., A. Neyer, and H.F.O. Müller, *Microoptics for Efficient Redirection of Sunlight.* Applied Optics, 2012. **51**(12): p. 2051-2056.
129. Padiyath, R., *Daylight Redirecting Window Films*. 2013, 3M Company. p. 217.
130. Thanachareonkit, A., E. Lee, and A. McNeil, *Empirical assessment of a prismatic daylight redirecting window film in a full-scale office testbed*, in *IESNA 2013*. 2013: Huntington Beach, CA.
131. Darula, S. and R. Kittler. *CIE General Sky Standard Defining Luminance Distributions*. in *eSim, La Conférence canadienne sur la simulation énergétique des bâtiments*. 2002. Montréal Canadà.
132. Tharin, J., *Remise en état du Photogoniomètre*. 2012, Ecole Polytechnique Fédérale de Lausanne, LESO-PB: Lausanne.
133. Normung, D.D.I.f., *Guide to DIN EN 12464-1 Lighting of work places*, N. Lichttechnick, Editor. 2003.
134. Kaklauskas, A., et al., *Multiple-Criteria Analysis of Life Cycle of Energy-Efficient Built Environment*, in *Nearly zero energy building refurbishment*, F.P. Torgal, Editor. 2013. p. 299-324.
135. Asadi, E., et al., *Selection Using Multi-objective Optimization and Genetic Algorithms*, in *Nearly zero energy building refurbishment*, F.P. Torgal, Editor. 2013. p. 279-297.
136. Scartezzini, J.-L. and B. Paule, *Eclairage dans l'Industrie*. 1994: Ravel, Office Fédéral des questions conjoncturelles.
137. Nabil, A. and J. Mardaljevic, *Useful daylight illuminances: a replacement for daylight factors.* Energy and Buildings, 2006. **38**(7): p. 905-913.
138. Meteotest, *Meteonorm*: Bern, Switzerland.
139. Nabil, A. and J. Mardaljevic, *Useful daylight illuminance: a new paradigm for assessing daylight in buildings.* Lighting Research and Technology, 2005. **37**(1): p. 41-59.
140. Winkelmann, F.C. *Modeling Windows in Energy Plus*. in *IBPSA Building Simulation* 2001. Rio de Janeiro, Brazil.
141. Klems, J.H., J.L. Warner, and G.O. Kelley. *A Comparison Between Calculated and Measured SHGC for Complex Fenestration Systems* in *ASHRAE Winter Meeting* 1995. Atlanta, GA.
142. Center, M., *Optical Lighting Film, Technical Specification*, 3M, Editor. 2000: St. Paul, MN.
143. Edmonds, I. *Solartran Pty Ltd*. Available from: www.solartran.com.au.
144. Saxe, S.G., *Progress in the development of prism light guides*, in *Materials and Optics for Solar Energy Conversion and Advanced Lighting Technology*. 1986, 3M Optics Technology Center: St. Paul, MN.
145. Padiyath, R., C.A. Marttila, and M.K. Nestegard, *Light Redirecting Constructions*. 2013: MN, US.
146. Thanachareonkit, A., E.S. Lee, and A. McNeil, *Empirical assessment of a prismatic daylight redirecting window film in a full-scale office testbed*, in *IESNA 2013 Annual Conference*. 2013, Leukos, IESNA: Huntington Beach, CA.
147. Rubbert, F., *Sundirecting Glazing - A new development in daylighting for deep plan offices*, Institute for Light and Building Technology ILB, Cologne: Aachen, Germany.
148. Klammt, S., A. Neyer, and H.F.O. Müller, *Redirection of Sunlight by Microstructured Components - Simulation, Fabrication and Experimental Results*, TUD Dortmund University: Dortmund, Germany.
149. Klammt, S., H.F.O. Müller, and A. Nayer, *Building Integration of Non-Tracking Systems for Sunlight Redirection*, in *World Renewable Energy Congress* 2013: Australia.

Annex 2.1 Building's Geographical location

The geographical location of Building B1 and B2 México (Zacatecas 22° 783' N., 102° 583' W, Altitude: 2543m) in the image above, and the indication of the office room's window subject of this study in the images below.

Annex 2.2 Offices room's floor plan

The floor plan views including dimensions and interior distribution of the office rooms located in Building B1 and Building B2.

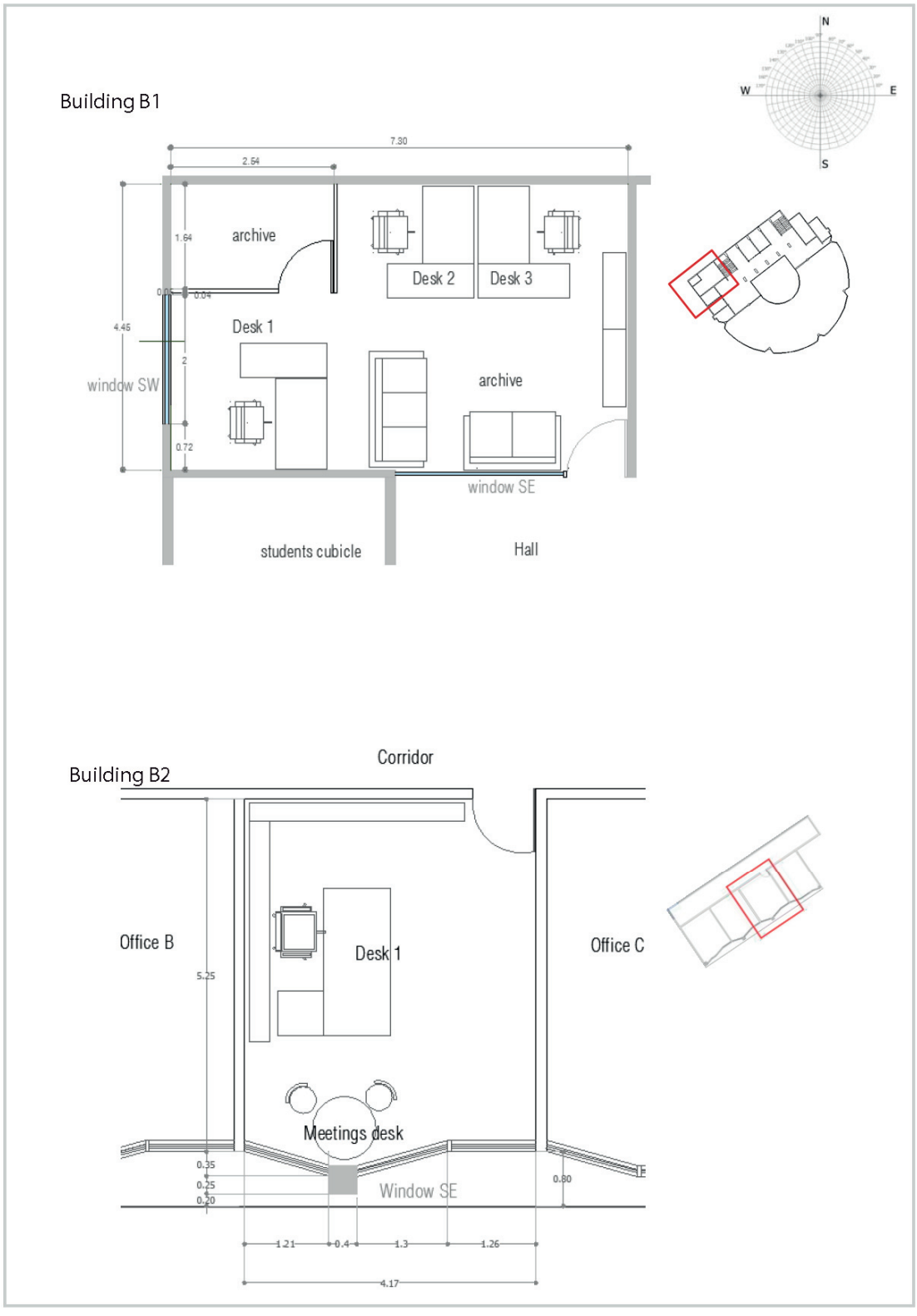

Annex 2.3 Sun path with respect to the offices room's façade

Floor plan views and elevation of the sun's trajectory (elevation) in Winter and Summer Solstices and Spring Equinox at 9h00, 12h00, 15h00 and 17h00 respect to the orientation of the building's considered façade: in Building B1 (a) and in Building B2 (b).

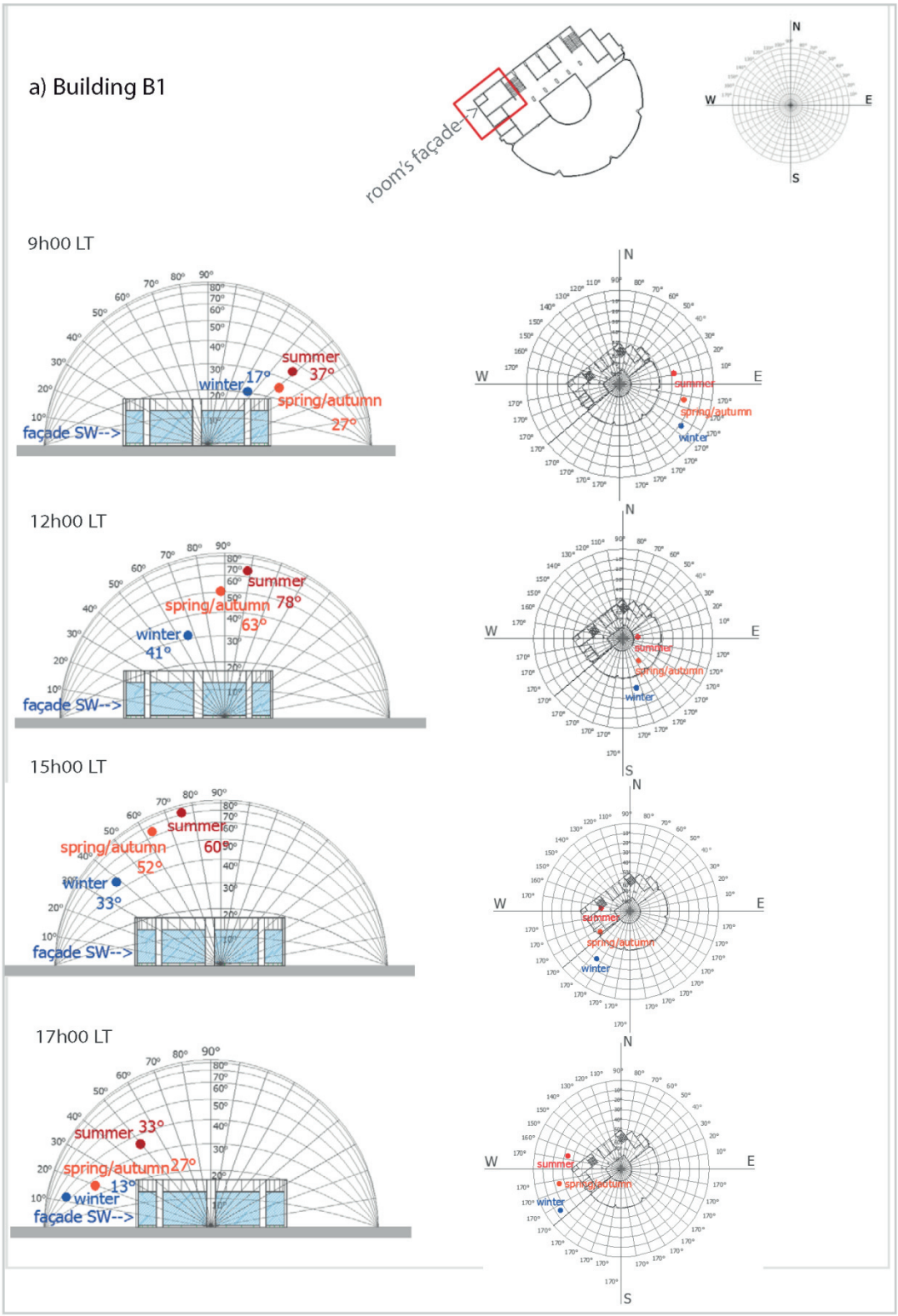

b) Building B2

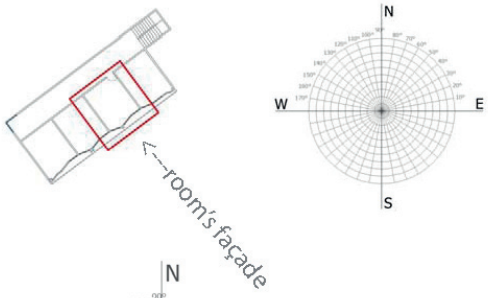

9h00 LT

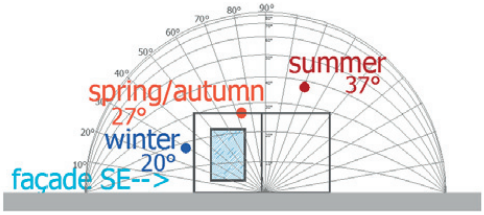

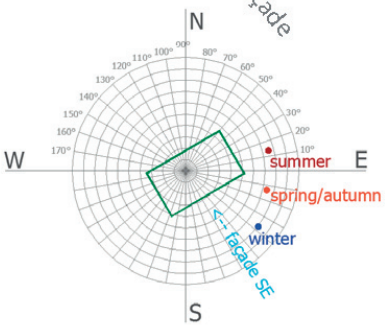

12h00 LT

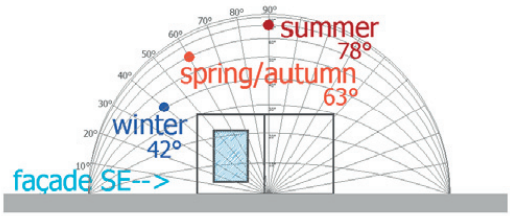

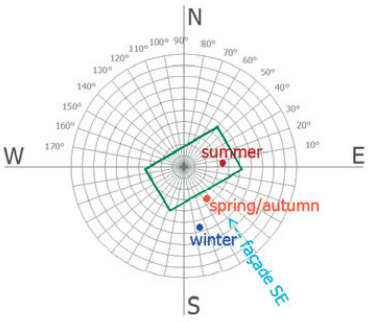

15h00 LT

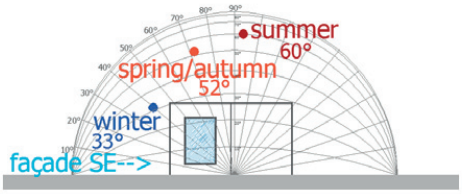

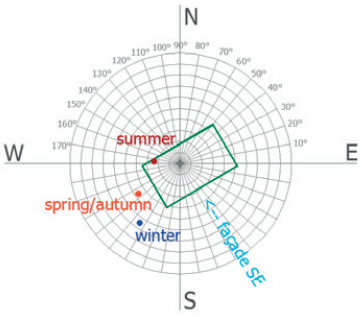

17h00 LT

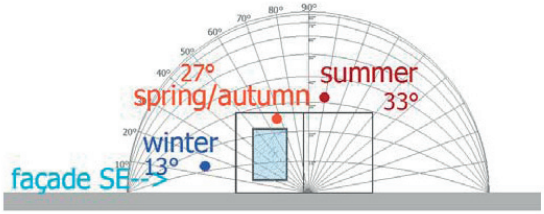

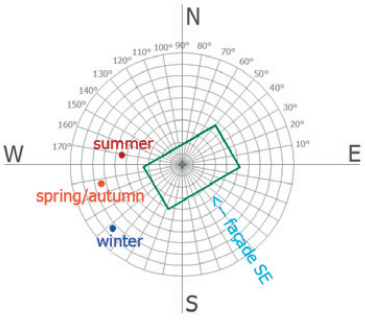

Annex 3.1 Description of the pre-selected CFS

3.1.1 Lasercut Panel (LCP)

The LCP system was created as a solution to simplify the transportation and redirection of daylight through systems such as solar tracking mirrors and light pipes, simplest solutions are the use of prismatic glass which has as a main inconvenience that the view to the exterior might be compromise by its geometry. The search for a system that was similar to glass in appearance, viewing transparency, method of installation and maintenance originated the creation of LCP. It is based on the principles of light deflection and internal reflection when passing through a parallelepiped [143] as it is shown in Figure 1.1, when direct sunlight passes through LCP, the larger portion of light is deflected upwards while a portion of the light is reflected to the exterior, however the proportion and redirection of the light depends on the incident angle. LCP is defined by four parameters: the distance between the cuts, the distance the cuts extend the through the sheet, the angle of the cuts relative to the normal and the refractive index of the material. A

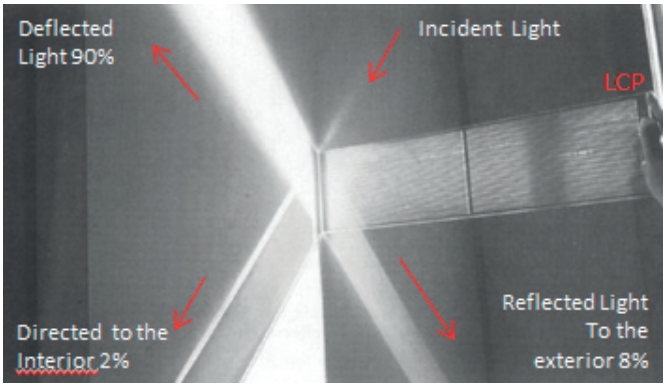

Figure A 1.1 A view that shows the deflected, reflected and redirected incident light when passing through the LCP [125].

LCP is produced from a plastic or acrylic sheet divided into arrays of laser cuts that produce internal reflecting interfaces in the material. Its installation would require the use of one or two sheets of glass for protection. The Figure A 1.2 shows a cross-section of two LCP laminated between two glass sheets of 1.5mm, the upper panel is 6mm thick while the lower panel is a panel of 5.5mm between two glass sheets [125]. The application of LCP can be in sidelight windows, skylights or incorporated in tilt able slats in which the tilted angle should be adjusted according to the angle of the sun's incidence on the panel [125]. One of the main advantages of LCP is its transparency that contributes to the view to the outside as shown in Figure 1.3.

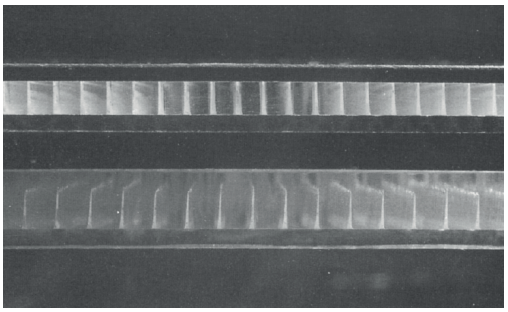

Figure A 1.2 Cross-section through LCP showing a panel of 6mm thick (up) and a panel of 7mm thick (down) [125].

Figure A 1.3 A close view of LCP that shows the transparency of the panel to contribute to a better view of the exterior environment [143].

3.1.2 Daylight Redirecting Film 3M

Prismatic light guides were first employed in artificial light applications (lamps and luminaires), they take advantage of the prismatic shape given its ability to redirect light while minimizing absorption and backscatter [144]. The Optical Lighting Film (OLF) is a lighting system that can be used as a daylight redirecting system and for artificial light applications as well, such as light boxes or pole lights. They are flexible films with micro-replicated prism forms on one side and smooth finish in the other, for daylighting applications they are used to transport and distribute light when placing them in the upper parts of the window [126].

However, an evolution of a 3M light redirecting film has been designed as a daylight redirection system is the 3M daylight redirecting film (DRF), which uses microstructure prisms to direct sunlight towards the ceiling, an example of its performance can be seen in Figure 1.5. Such microstructures are formed in an arrangement of asymmetrical multi-sided refractive prisms, which are carried by an optical film that serves also as a sun shading device, its thickness is about 300 microns [129, 145] a cross-section is shown in Figure 1.4. The 3M Film depends on the availability of sunlight; under overcast sky conditions the Film has reported to reduce its efficiency, the same situation is presented when applied to northern façades, or obstructed windows [129], It is better suitable for buildings that might experience problems of glare or that are exposed to overheating. One of its disadvantages is that it reduces the view to the exterior environment as can be seen in Figure 1.5, therefore is advisable its installation in the upper part of the window.

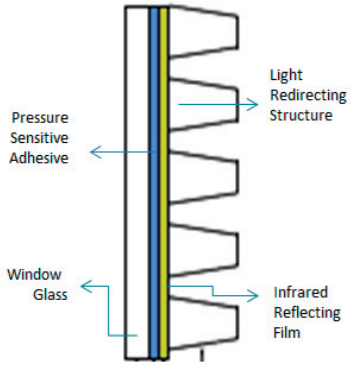

Figure A 1.4 Cross-section of the micro-structured Film3M [129].

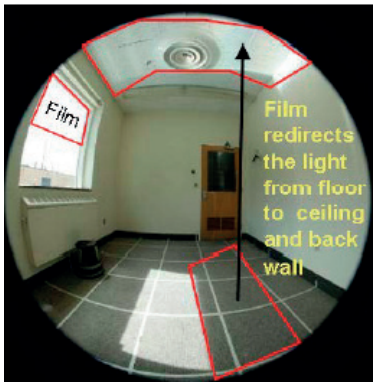

Figure A1.5 The interior view of a room that shows the performance of Film 3M installed in the upper part of the window [129]

Figure A1.6 A view of a window using Film 3M in the upper-left panes [129].

Studies have been carried-out to test the performance of Film 3M, they had shown that when using the system the illuminance levels at the back of the analysed room were substantially increased, however perceptible levels of discomfort glare where also found when tested under sun light conditions. A second version of the systems that uses a diffusing material was found to control glare to imperceptible levels [146].

3.1.3 TU Dortmund University, Germany (CFS1, CFS2, CFS3)

The Micro-structured daylight systems CFS1, CFS2 and CFS3, were created and produced by the University of Dortmund in Germany, as an evolution of the non-tracked light directing glasses named Lumitop [127], which are extruded PMMA (acrylic glass) profiles of a width of 12mm used as light conductors to redirect light for angles of incidence between 15° to 65° [147, 148]. The Lumitop system was designed to avoid light emissions below the horizontal in order to avoid the risk of glare, a cross-section of the system is illustrated in Figure 1.7 [147]. The evolution of the new Lumitop had as objective to broaden the range of solar altitude angles that the systems can efficiently redirect and to simplify the element while reducing its cost. This was done by substituting the complex light conductors to a continuous microstructured PMMA pane, reducing the thickness of the system (from 12mm to 4mm), and employing a cost-reduced manufacturing process. An additional benefit is that the use of a continuous pane would improve the thermal qualities of the glazing. A comparison of the two systems can be seen in Figure 1.8.

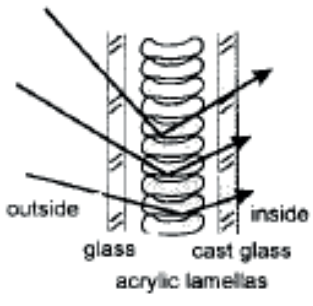

Figure A1.7 A cross-section of the original Lumitop daylighting system, indicating its main characteristics [147].

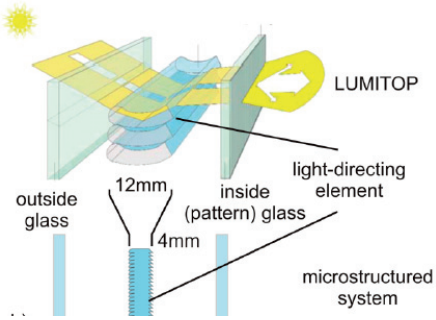

Figure A 1.8 An illustration that compares the characteristics of the Lumitop daylighting system with the improved new system [128].

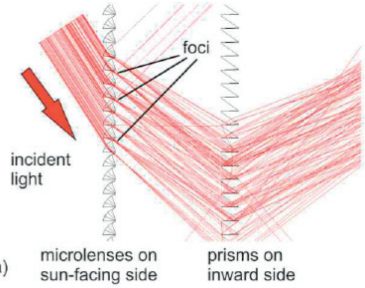

Figure A1.9 Detailed cross-section of the new system, showing the micro lenses at the sun side panel [149].

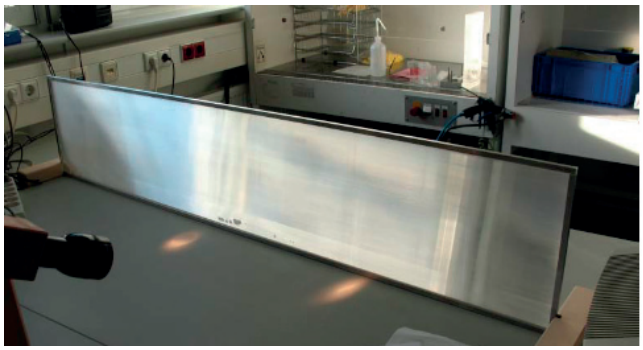

Figure A 1.10 A large-scale sample of the TUD lighting system prototype to be tested in windows [148].

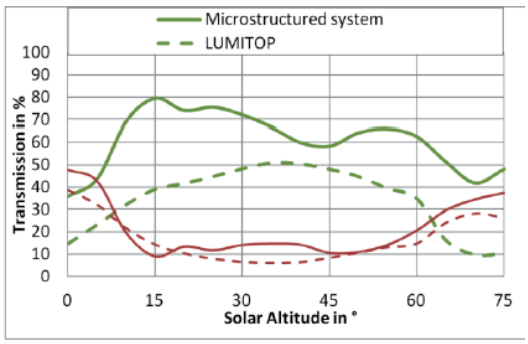

Figure A1.11 Diagram of the redirection performance of the micro-structured daylighting system [128].

The efficiency of the improved system was tested and showed that the range of altitude angles of incident light that the system efficiently redirects was broaden to 15° to more than 65°. By modifying the prismatic structures by lens-like structures on the side of the incident light an homogeneous angular redirection efficiency was achieved and the quality of the daylight distribution was also improved with the new system, which also reduces the risk of glare, as can be seen in Figure 1.9 [128]. An improvement on the lighting transmittance was also found between the Lumitop and the new system, the latter achieved a transmittance of 79% (at perpendicular incident light), while the previous Lumitop was 43% [128].

Annex 4.1 Renderings using the Five-phase method

The Renderings of the interior in the office room located in Building B2 obtained with the use of the Five-phase method are presented as follows. Those presented first were generated using standard glass, in this page the group corresponding to winter time at 12h00 (a) while in the next page is presented the group corresponding to summertime (b).

a)

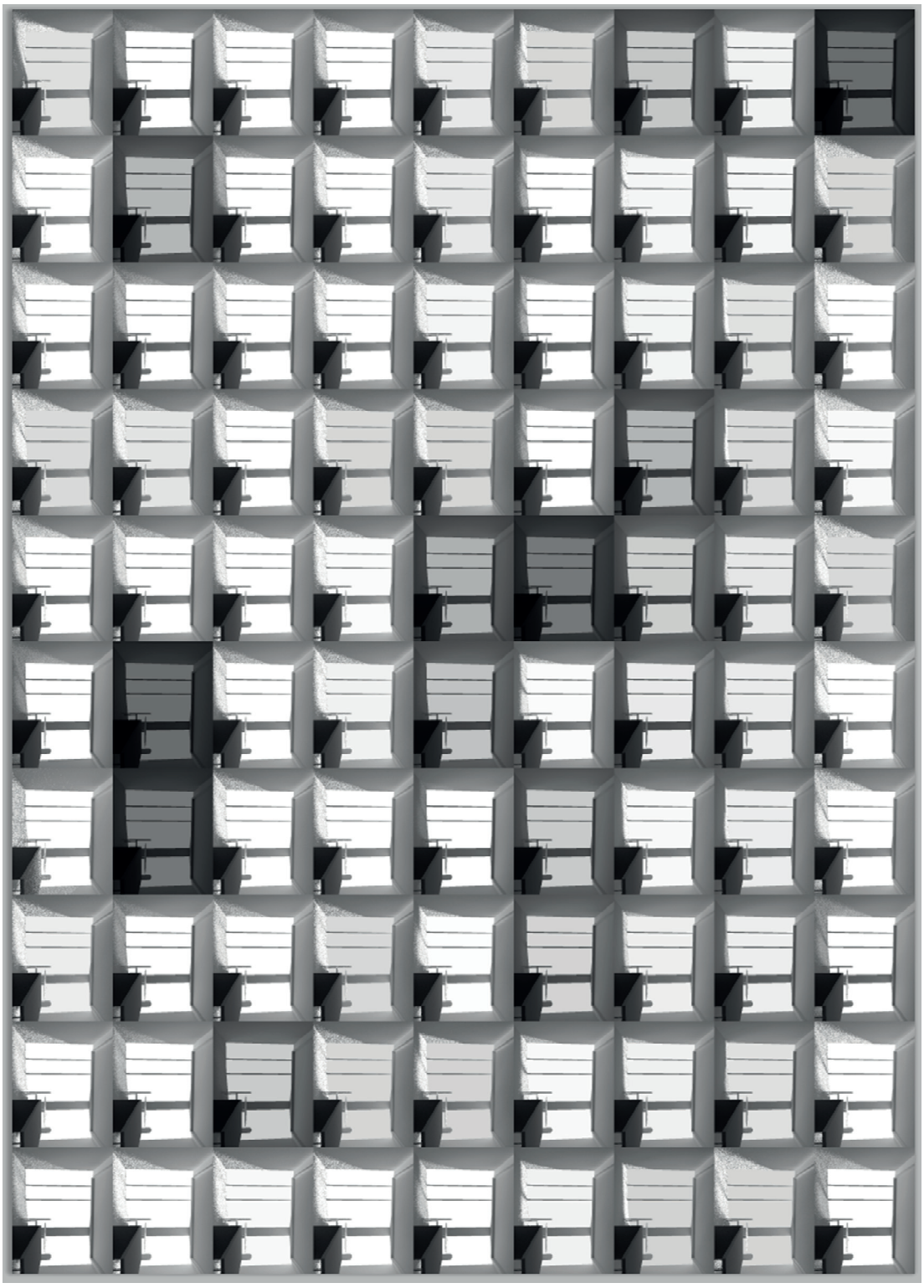

b)

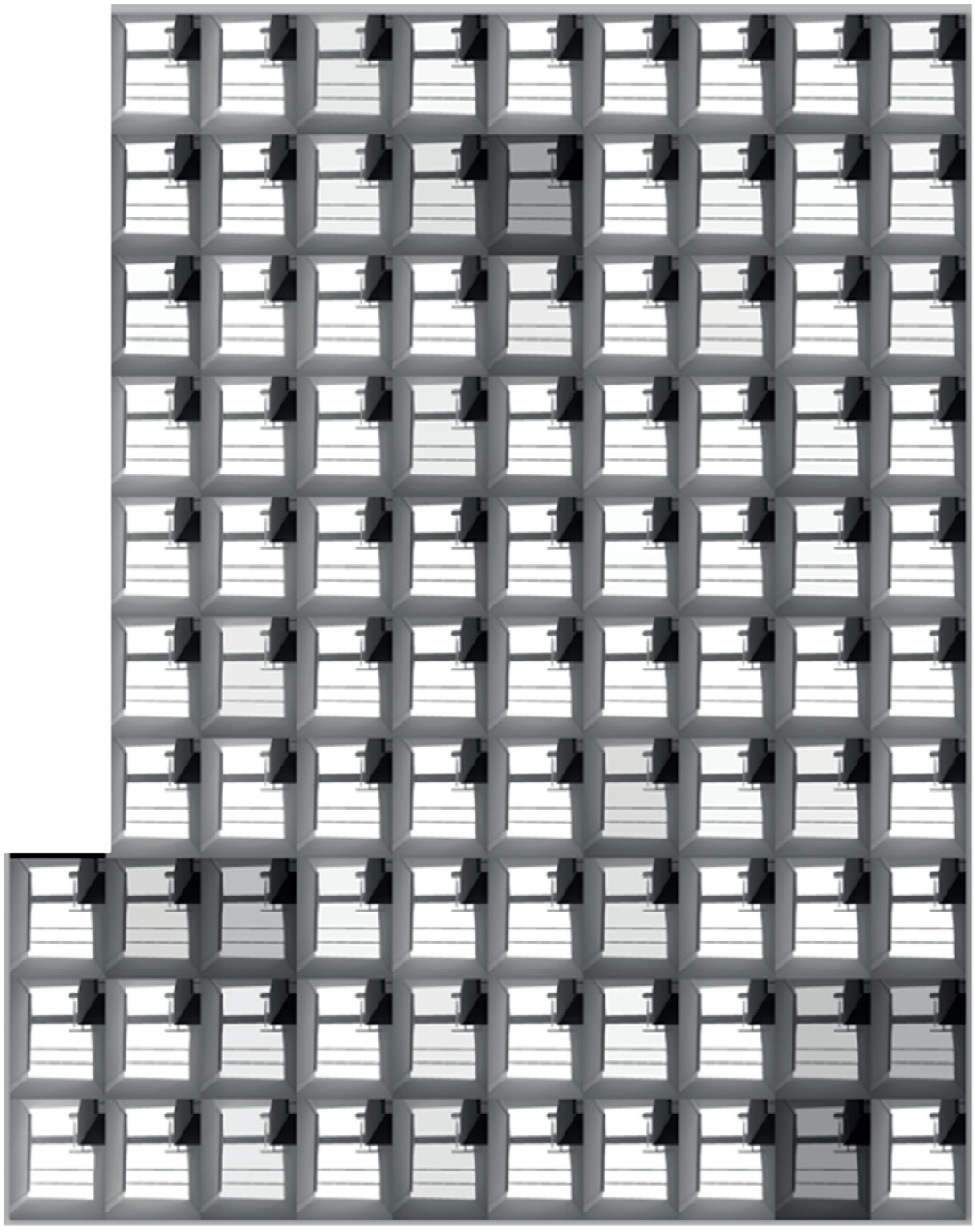

The renderings presented as follows were generated using LCP. In this page the group that corresponds to wintertime at 12h00 (c) while in the next page is presented the one corresponding to summertime (d). It should be noted that the renderings obtained when using standard glass (a, b) and those using LCP (c, d) were generated on a different stage of this work, thus the arrangement of the images do not correspond to each other. However, they are shown in order to visualize and compare the daylight distribution inside the room when using the starndard glass and CFS.

c) 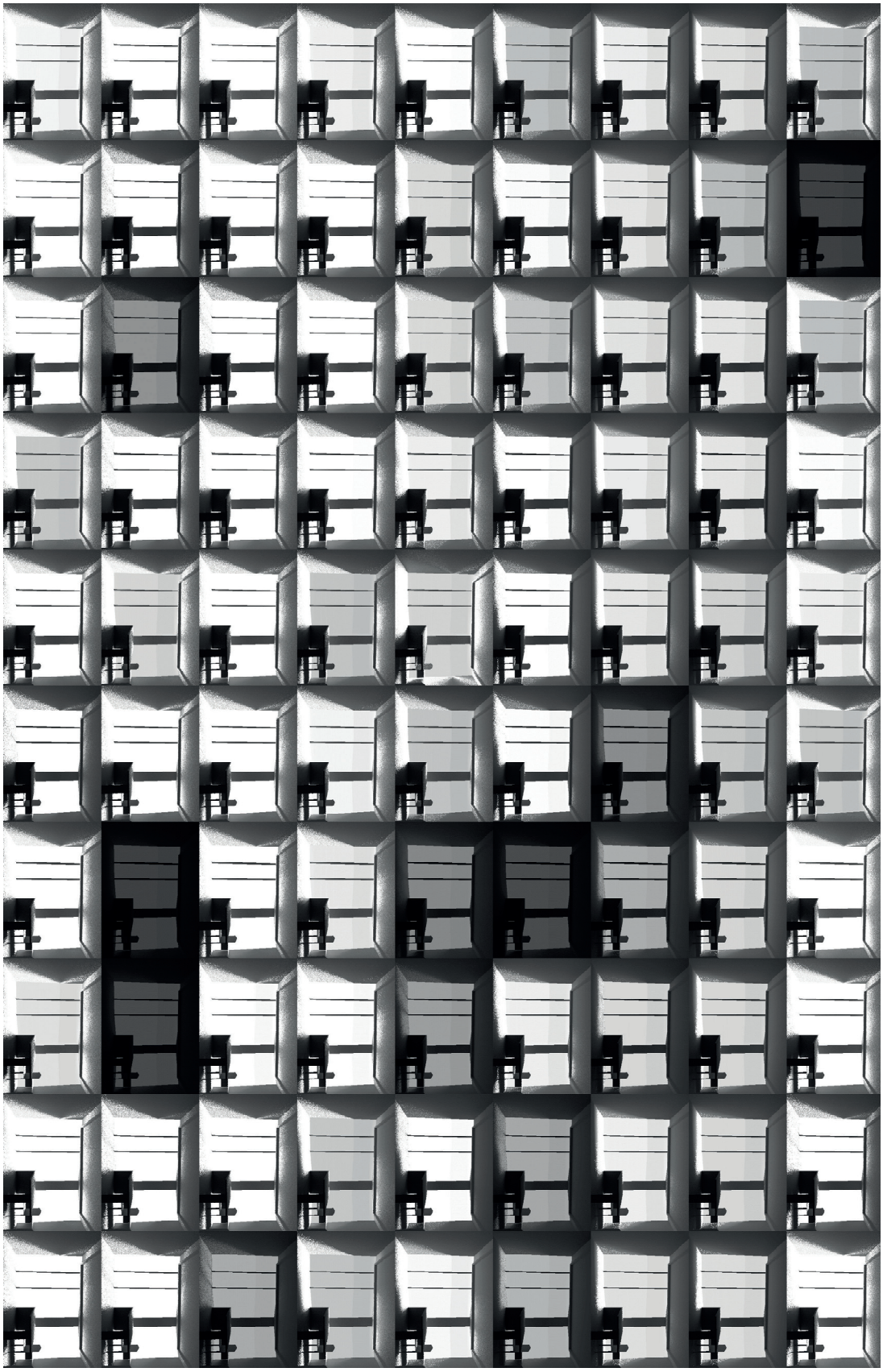

d)

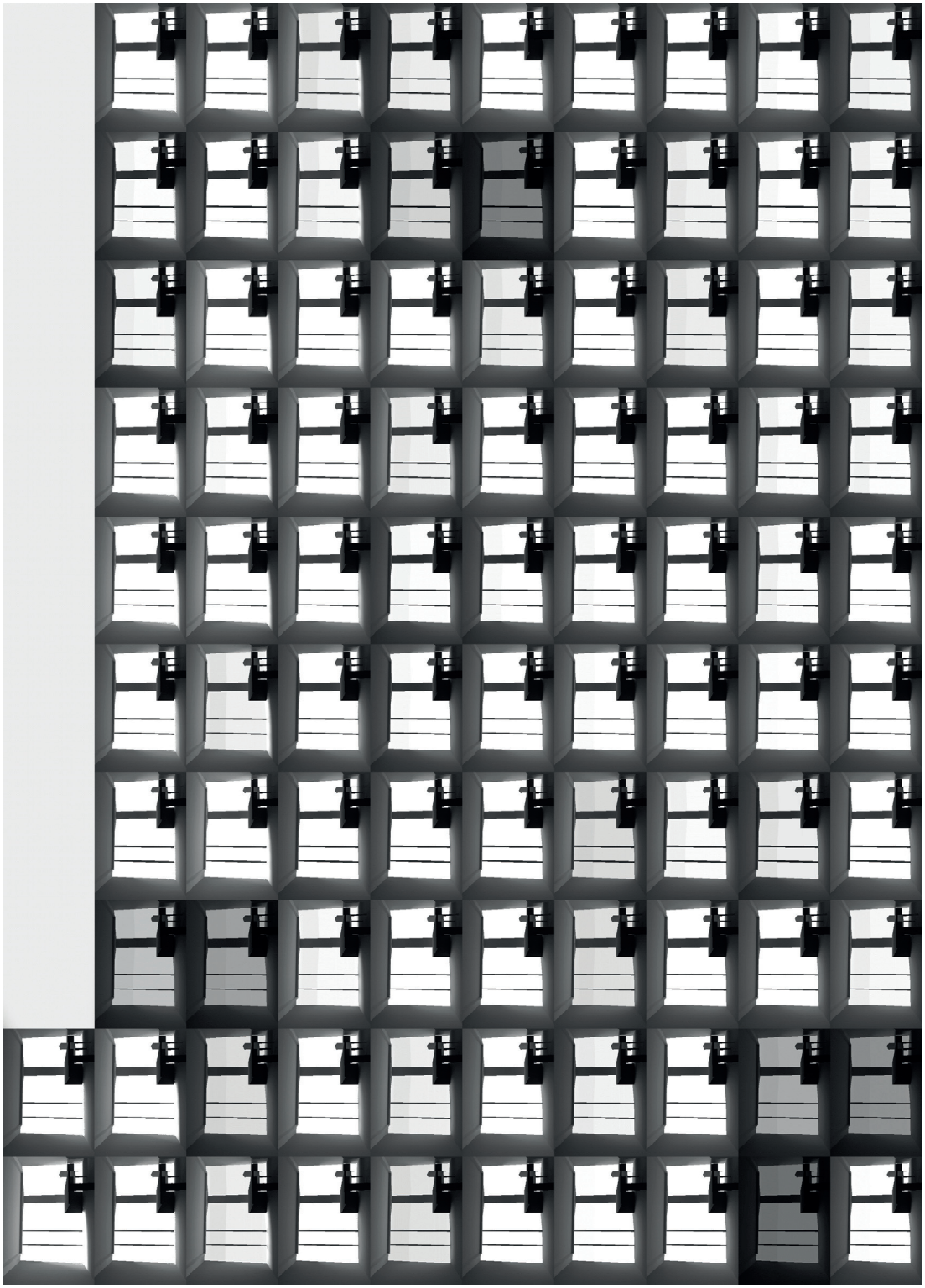

Annex 6.1 Basic considerations for architects and lighting designers

An advanced daylighting approach consisting in the use of CFS was applied in this study in order to improve the interior daylight environment in two office buildings located in a predominant clear sky location. However, the convenience of such practice is submitted to a comprehensive assessment taking into account several factors, such as the ones considered in this study. A result favourable to the use of CFS would be obtained in certain cases. Nevertheless, prior to the application of advanced daylighting strategies; basic considerations should be taken into account to achieve an improved interior daylight environment. Even if they might be contemplated as key aspects in the conception of new buildings, in practice such considerations might not be that often applied, especially in regions of predominant clear sky conditions where the use of daylight in buildings still has a potential to be exploited. Hence, few of them are mentioned here, which might be useful to assist architects and lighting designers in their decisions relative to the creation of a better interior daylight environment.

6.1.1 To improve the interior daylight distribution

A basic step toward this objective is the choice of an appropriate building orientation according to the sun course of the site, which sun's path must be taken into account first. Additionally, there are two main aspects to consider for achieving an optimal interior daylight distribution. First, the adequate selection of the glazing properties is essential to foster the daylight penetration into the room and not only in the area close to the window. A glazing transmittance above 70% improves definitely the interior illuminance distribution in the entire room. The use of tinted glazing for solar protection is an out-of-date practice; it contributes to protect the room from excessive sunlight but reduces considerably the work plane illuminance into the room, making its use inadvisable. Secondly, the reflectance properties of the interior surface materials play an important role, since some of them are more favorable than others to reflect the light. Their appropriate selection according to the recommendations (See Section 2.4) can contribute to improve the indoor illuminance distribution mainly in the zones that are distant from the window. The basic way of assessing the daylight distribution in a room is by calculating the Daylight Factor (DF) (See Section 2.4), which can be helpful to detect the room areas that receive insufficient daylight, thus would accordingly require an increased use of electric lighting. However, such assessment remains not fully satisfactory since DF calculations only take overcast sky conditions into account. For this reason, an assessment that includes all yearly sky conditions occurring in given site would be propitious (See Section 4.1). If such estimation is feasible, it might help designers to visualize the areas where the recommended work plane illuminances are more optimal across the room. As shown in this study, a convenient placement of the working spaces could be the result of assessing the frequencies of annual illuminance according to its profitabilness for visual tasks, especially for those allocated at the center and back of the room.

6.1.2 To reduce the risk of glare

Regarding daylit spaces, the visual comfort of the occupants is mainly associated to the building's architecture (orientation, shape and size of the window). In order to achieve an improved interior environment for visual comfort, the use of movable shading devices are an essential measure, especially recommended in cases where the design of the building contributes to an increased risk of glare, as observed in the case of Building B2 in the present study. Furthermore, working places can be set in order to avoid a constant direct view to potential glare sources; it is advisable to place the desk in such a way that the visual field of the occupant is not in straight view to a window.

6.1.3 To reduce the risk of overheating

Firstly, the selection of an adequate Wall to Window Ratio (WWR) is commended, as observed in the case of Building B2 in the present study; a room with a large WWR is likely to present a high risks of overheating. Such ratio is often linked to the orientation of the building and the sky conditions of the site. Additionally, taking the Solar Heat Gain Coefficient (SHGC) of the glazing into account is also advised in order to prevent overheating, especially in areas of prevailing clear sky conditions like at low latitudes. It is also recommended to consider the use of advanced glazing technologies, such as the spectrally selective glazing (e.g. low-e coated glazing) which block an important portion of the sun's heat while maintaining higher visible transmittance. In the same way, the use of Advanced Daylight Systems (which also comprises CFS), might be an effective step for suitable buildings: this study has shown its numerous advantages compared to the use of standard glazing. However, despite of all the previous recommendations, sun shadings are still required for certain cases, then use of external blinds and/or awnings can be recommended. When applicable, it is worth considering including in overhangs or light shelf in the building design (See Section 1.3).

Glossary

Global Horizontal Irradiance	GhI (W/m²)
Direct Beam Normal Irradiance	Ibn (W/m²)
Diffuse Horizontal Irradiance	Idh (W/m²)
Daylight Factor	DF (%)
Illuminance Ratio	IR (%)
Wall to Window Ratio	WWR
Useful Daylight Illuminance	UDI
Bi-directional Transmission Distribution Function	BTDF
Bi-directional Scattering Distribution Function	BSDF
High Dynamic Range Image	HDR
Computing Processing Time	CPU time
Daylight Glare Probability Index	DGP
Complex Fenestration Systems	CFS
Daylight Redirecting Film 3M brand	Film3M
CFS from TU Dortmund University	CFS1, CFS2, CFS3
Lighting Guiding Shade	LGS
Lasercut Panel	LCP
Glazing Transmittance in the visible range of the Electromagnetic Spectrum	τv
Solar Heat Gain Coefficient	SHGC

Curriculum Vitae

CHANTAL BASURTO-DÀVILA

chantal.basurto@epfl.ch

EDUCATION

1993-1998	ARCHITECT	INSTITUTO TECNOLÓGICO DE ZACATECAS MÉXICO
1997-1998	URBAN REGIONAL DESIGN SPECIALIZATION	INSTITUTO TECNOLÓGICO DE ZACATECAS MÉXICO
2005-2007	MASTER IN ARCHITECTURAL LIGHTING DESIGN (MALD)	HOCHSCHULE WISMAR, GERMANY
2006-2007	ARCHITECTURAL LIGHTING DESIGN, STAGE	PETER ANDRES, BERATENDE INGENIEURE FÜR LICHTPLANUNG, HAMBURG, GERMANY
2010-2014	PHD STUDENT	LABORATORY OF SOLAR ENERGY AND BUILDING PHYSICS (LESO-PB) EPFL, LAUSANNE, SWITZERLAND

WORK EXPERIENCE

OCTOBER 2006-MARCH 2007,	BERATUNGSLEISTUNGEN FÜR LICHTPLANUNG, HAMBURG GERMANY MASTER INTERNSHIP. ENGINEERING AND PLANNING OF DAYLIGHT AND ARTIFICIAL LIGHT.
APRIL 2001 –AUGUST 2003,	DE LA COSTA ROMADI" CONSTRUCTION -RIU JALISCO HOTELS-, NUEVO VALLARTA NAYARIT, MEXICO CONSTRUCTION FIRM RESPONSIBLE OF RIU HOTELS IN THE MEXICAN PACIFIC PROJECT'S MANAGER ASSISTANT, RESPONSIBLE OF THE CONSTRUCTION AND ARCHITECTURAL DESIGN PLANS, AND CONSTRUCTION SITE SURVEILLANCE
APRIL 1998-DECEMBRE 2000	FRANCISCO VARGAS DE LA LLATA- ARCHITECTURAL DESIGN BÜRO, ZACATECAS MÉXICO DESIGN ORIENTATED ARCHITECTURAL FIRM, MAINLY WITH COMMERCIAL AND RESIDENTIAL PROJECTS. BUILDING DESIGN PROJECT'S ASSISTANT

PROFESSIONAL QUALIFICATIONS AND SKILLS

DAYLIGHTING STRATEGIES AND ARTIFICIAL LIGHTING PLANNING, BUILDING PERFORMANCE SIMULATION, CLIMATE-BASED DAYLIGHT MODELLING
AutoCAD 2D & 3D, DiaLUX, ReLUX, RADIANCE, Energy Plus & Open Studio, EcoTect, Photosphere, Window 7, Lightsolve, Dial +
LANGUAGES SPANISH-Mother Tongue, ENGLISH-Advanced, ITALIAN-Advanced, FRENCH-Advanced, GERMAN-Basic

PUBLICATIONS

CISBAT 2011, LAUSANNE SWITZERLAND

DAYLIGHT OPTIMIZATION OF BUILDINGS AND APPLICATION OF ADVANCED DAYLIGHTING SYSTEMS IN CENTRAL MÉXICO,
BASURTO C., BORISUIT A., KÄMPF J, MÜNCH M AND SCARTEZZINI J-L

11TH RADIANCE WORKSHOP 2012, 12-14 SEPT, COPENHAGEN DENMARK

VERIFICATION OF THE COMPUTER MODELLED DAYLIGHT PROPAGATION THROUGH CFS, *BASURTO C., KÄMPF J. AND SCARTEZZINI J-L.*

CLIMA 2013, PRAGUE CZECH REPUBLIC, CONFERENCE PROCEEDINGS
VERIFICATION OF THE COMPUTER MODELLED DAYLIGHT PROPAGATION TROUGH CFS, *BASURTO C., KÄMPF J. AND SCARTEZZINI J-L.*

CISBAT 2013, LAUSANNE SWITZERLAND

SIMULATING THE DAYLIGHT PROPAGATION THROUGH CFS IN AN URBAN CONTEXT USING A VARIABLE SAMPLING SUBDIVISION SCHEME,
BASURTO C., KÄMPF J. AND SCARTEZZINI J-L.

PROFESSIONAL MEMBERSHIPS: PROFESIONAL ASSOCIATION OF LIGHTING DESIGNERS (PALD) SINCE 2005 NOWADAYS.